An investigation of the potential for silver nanoparticles to cause toxicity to human cells *in vitro*

Passapan Sriwichai

A thesis submitted in accordance with the conditions governing candidates for the degree of Doctor of Philosophy

Institute of Cellular Medicine

Newcastle University

November 2012

ABSTRACT

Engineered nanoparticles are defined as having at least one dimension between 1 to 100 nm, which are intentionally produced because of specific properties based on shape, size and surface chemistry. The small size of nanomaterials gives them specific and/or enhanced physicochemical properties compared with the same materials at the macroscale, making them of great interest for development of "new" products. Silver nanoparticles (AgNPs) are being increasingly used in consumer products such as 'stay fresh' clothing, water purification and household cleaning agents. They are released into the environment in increasing amounts and concerns have been raised about the risk of harmful impact on both the environment and human health. This research used human cells in culture as a model system to investigate the potential toxicity of AgNPs.

Early experiments used the MTT assay to define the concentrations of AgNPs and $AgNO_3$ and incubation times that caused an acceptable loss of cell viability ($\leq$ 20% loss). Using these conditions, the Comet method and phosphorylation of γH2AX determined DNA damage by the AgNPs in comparison to $AgNO_3$ on the basis of weight (μg/ml). Epigenetic changes in response to AgNPs and $AgNO_3$ were indicated by measurement of methylation of LINE-1 using pyrosequencing. The effect on oxidative stress was evaluated using a qPCR array platform followed by functional analysis of SOD1. A novel dialysis method was then developed to quantify release of Ag^+ ions from the AgNPs that were available to the cells and TEM determined cellular localisation of the AgNPs.

In conclusion, this research showed that both AgNPs and $AgNO_3$ caused DNA damage in time and dose response manners by oxidative stress mechanisms, involving inhibition of SOD1. TEM imaging of cells exposed to AgNPs indicated that they were not internalized, but bound to the cell membrane, and from here released Ag^+ ions into the cell.

ACKNOWLEDGEMENTS

I would like to gratefully and sincerely thank Dr Elaine Mutch for her guidance, patience, and understanding and most importantly her support, without this thesis would not have been possible. I would like to express my sincere thanks to Professor Faith Williams for her assistance and guidance in getting my research started on the right foot. I am also grateful Dr Christina Lye and Dr Angela Silmon for their advice, support, and encouragement throughout my PhD study.

I am particularly grateful for the assistance given by Dr Budhika Mendis, the Durham GJ Russell microscopy facility, Durham University on transmission electron microscope and energy dispersive X-ray spectroscopy. Special thanks go to Dr. Kathryn White and Tracey Davey for their valuable help in transmission electron microscope technique.

I wish to acknowledge the help provided by Dr Paul Andrew Jowey in the Western blot technique and Dr Kevin Waldron for his valuable help in dialysis and SOD1 study without his help I would not have been able to complete this thesis. I would like to express my very great appreciation to Dr Kathryn Yate for her advice, assistance, patience and encouragement during my PhD life began. My special thanks are extended to Toxicology Unit member for their assistance and understanding. I would also like to thank Professor Olaf Heidenreich, Dr Andrea Beyerle and Dr Anja Scholz for the Zeta sizer facility at Northern Institute for Cancer Research. I also thank Mr Chatchawan Singhapol for his help in the H2AX study and Dr Alexandra Groom at Human nutrition research centre for her advice and support in epigenetic study.

I am deeply indebted to Prof. Dianna Ford and Dr Simon Wilkinson for their valuable advice and support during the annual assessment.

I would like to offer my special thanks to the Royal Thai Government for granting me a scholarship.

Finally, and most importantly, I would like to express my greatly thank to my husband **Patikom** for his support, encouragement, patience and love which has enabled me to finish my thesis. My special thanks go to my mother and my older sister for their support and encouragement. I would like to dedicate this thesis to the memory of my father who passed away in 1998. I hope he would have been proud.

JOURNAL PUBLICATION AND CONFERENCE PAPERS

Sriwichai P, Williams FM, Lye C, Silmon A, Mutch E. An investigation of toxicity of silver nanoparticles to HL60 and Jurkat cells in vitro. In: Toxicology: Annual Spring Meeting of the British Toxicological Society. 2010, Edinburgh, UK; Elsevier Ireland Ltd.

Sriwichai P, Waldron K, Mutch E.The fate and toxicity of silver nanoparticles to human cells in vitro. Small 2012. In Preparation.

TABLE OF CONTENTS

TABLE OF CONTENTS (CONTINUED)

LIST OF TABLES

LIST OF FIGURES

LIST OF FIGURES (CONTINUED)

LIST OF FIGURES (CONTINUED)

LIST OF FIGURES (CONTINUED)

LIST OF FIGURES (CONTINUED)

LIST OF FIGURES (CONTINUED)

LIST OF FIGURES (CONTINUED)

LIST OF FIGURES (CONTINUED)

LIST OF FIGURES (CONTINUED)

LIST OF FIGURES (CONTINUED)

LIST OF ABBREVIATIONS

AgNPs	Silver nanoparticles
BSI	The British Standards Institution
CA	Chromosomal aberration
CBMN	Cytokinesis-block micronucleus
CCK-8	Colorimetric cell counting kit-8
CCS	Copper chaperone for superoxide dismutase
DCFHDA	Dichlorofluorescein-diacetate
DSB	DNA double strand breaks
FDA	Fluorescein diacetate
EC	EU chemical legislation Regulation
EDX	Energy-dispersive X-ray spectroscopy
ELISA	Enzyme-linked immunosorbent assay
FACS	Fluorescence-Activated Cell Sorting Analysis
FBS	Fetal bovine serum
FDA	Fluorescein diacetate
FITC	Fluorescein isothiocyanate
GPx	Glutathione peroxidase
GSH	Glutathione
GSSG	Oxidized glutathione
GSSG	Glutathione disulfide
HO-1	Hemeoxygenase-1
HR-MAS NMR	High-resolution magic angle spinning nuclear magnetic resonance spectroscopy
Laser-SNMS	Laser postionization secondary neutral mass spectrometry
LDS	Lithium dodecyl sulfate
LINE-1	Long Interspersed Nucleotide Elements
IL-8	Interleukin-8
LMPA	Low melting point agarose
MMP	Membrane potential
MTT	3-(4, 5-dimethylthiazol-2-yl)-, 5-diphenyl tetrazolium bromide
MWM	Morris water maze test
nm	Nanometer
NPs	Nanoparticles

LIST OF ABBREVIATIONS (CONTINUED)

OECD	Organization for Economic Co-operation and Development
OTM	Olive tail moment
PAGE	Polyacrylamide gel electrophoresis
PCR	Polymerase chain reaction
PDADMAC	poly-(diallyldimethyl)-ammonium-chloride
PS	Phospholipid phosphatidylserine
PI	Propidium iodide
REACH	Registration, Evaluation, Authorisation and Restriction of Chemicals
ROS	Reactive oxygen species
RT-CES	Real-time cell electronic sensing
SCGE	Single cell gel electrophoresis
SEM	Scanning electron microscopy
shRNA	Short hairpin RNA
siRNA	Small interfering RNA
SOD	Superoxide dismutases
SRs	Scavenger receptors
SPF	Specific-pathogen free
TBARS	Thiobarbituric acid reactive substance
TEM	Tranmission electron microscopy
TEMED	Tetramethylenediamine
TOF-SIMS	Time of flight secondary ion mass spectrometry
WST	Water soluble Tetrazolium

CHAPTER 1

INTRODUCTION

Chapter 1. Introduction

1.1 Nanoparticles

Definition of nanoparticles

The prefix "nano", from the Greek word "nanos" meaning a dwarf, is becoming increasingly common in scientific literature. Popularly, 'nano' is used as an adjective to describe objects, systems, or phenomena with characteristics arising from a nanometer scale structure. The nanometer (nm) is a metric unit of length and has a longstanding use in science to mean one billionth of a metre or 10^{-9} m. To put the nanoscale into perspective, Figure 1.1 illustrates where the nanoscale fits in relation to other common objects.

The British Standards Institution (BSI) has defined a nanoparticle as a discrete piece of material with one or more external dimensions in the size range from approximately 1 nm to 100 nm. If the lengths of the longest and the shortest axes of the nano-object differ significantly (typically by more than three times) the terms 'nanorod' or 'nanoplate' should be used instead of the term nanoparticle (BSI, 2007). Moreover, the European Commission recommendation of 18 October 2011 on the definition of nanomaterial addressed that 'nanomaterial' means a natural, incidental or manufactured material containing particles, in an unbound state, or as an aggregate, or as an agglomerate and where, for 50 % or more of the particles in the number size distribution, one or more external dimension is in the size range 1 nm - 100 nm (The European Commission, 2011)

It is necessary to define clearly the terms that will be used, as there remain a number of papers which discuss nanoparticles (NPs) that do not fall within the definitions that are generally accepted. In this thesis, NPs are particles with one or more dimensions in the order of 100 nm or less, as described in several papers (e.g. Buzea et al, 2007; Rai, 2009; Chen and Schuesener, 2008).

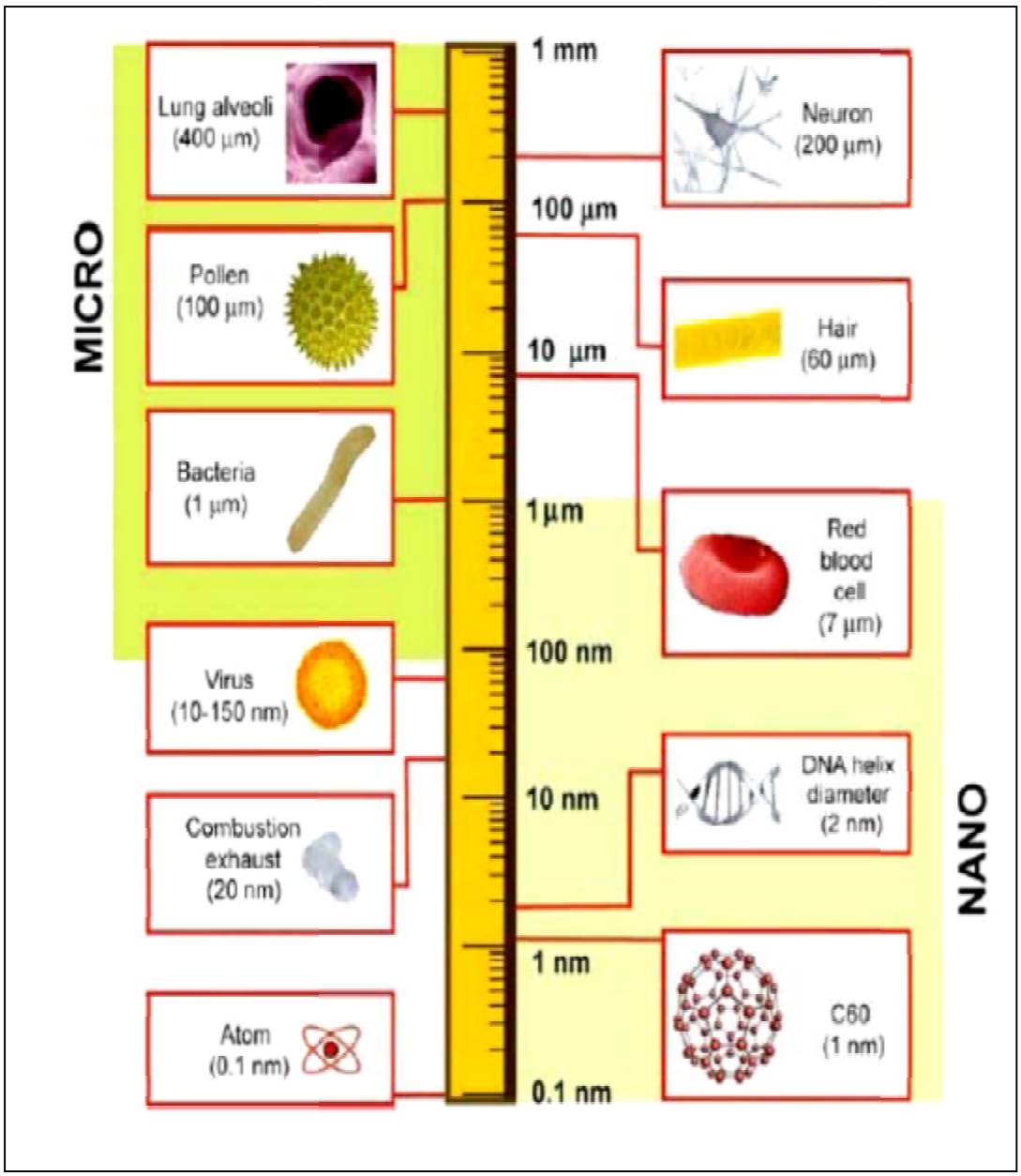

Figure1.1 The nanoscale in relation to common objects (Buzea et al, 2007).

Engineered nanoparticles

Engineered NPs are defined as poorly biodegradable particles having a diameter between 1 and 100 nm that have been intentionally engineered, produced to give specific properties based on shape, size and surface chemistry. The small size of nanomaterials gives them specific and/or enhanced physicochemical properties compared with the same materials at the macroscale, which make them of great interest for development of "new" products. For example, the features of NPs that underlie these properties and behaviour include a greatly increased surface area per unit mass, changes in the relative frequency of different surface component atoms and modified electronic characteristics. The electronic features can become quantized, leading to the so-called 'quantum effect' which can influence optical, electrical, magnetic and catalytic behaviour. The strong surface forces and Brownian motion which may be exhibited at this size range are also important as they may play a significant role in the self assembly of nanostructures.

Today, it is possible to construct particles that are aggregations of a few atoms, with sizes as small as that of proteins, smaller than cell membrane sensors. Some of them are already employed in medicine. NPs of metals such as platinum, and oxide particles of iron are used in the clinic as contrast agents in MRI or as energy vehicles for hyperthermia treatment of cancer. Other particles are employed as bacteriostatic agents (e.g. silver oxide), as a medium to aggregate particles from engine exhausts (e.g., cerium oxide NPs), while others (e.g., titanium oxide NPs) are used as a coating on glass and tiles to avoid adherence of dust.

Engineered NPs are mainly produced by three mechanisms: 1. colloidal, 2. sol-gel precipitation (wet mode), 3. mechanical milling or ablation (dry mode). A great variety of particles of different size and composition can be produced. At present, engineered NPs are used in many fields; from nanomedicine to cosmetics, from construction to agrofood, from electronics to energy power. For instance, in nanomedicine new drugs can be created to target specific biological sites or pathologies. Drugs often have limited solubility, may suffer from breakdown before they reach their target tissues, suffer poor pharmacokinetics or distribution, or may unintentionally damage healthy tissues. Nowadays, NPs have been developed to overcome these problems. In the case of NPs developed for Nanomedicine it is essential that particles are manufactured from

biocompatible materials, such as biodegradable polymers, metallic or semi-metallic ones or natural substances such as gelatin, albumin, lecithin or chitosan. The so-called active nanodrug delivery systems may utilise external energy sources such as ultrasound, light or magnetic fields to aid activation or release of the therapeutic drug at the target site. (Extracted from NNI Strategic Plan 2007, http://www.nano.gov/NNI_Strategic_Plan_2007.pdf). All these products contain NPs for many different applications and, *a priori*, it is difficult to know, and also to predict, their impact on humans and the environment.

The behaviour of manufactured NPs, should be seen in the context of the behavior of already existing naturally-occurring NPs (for example natural ammonium sulphate particles) to which the environment and humans have been exposed for millions of years. Natural NPs have been produced in many natural processes such as volcanic eruptions, forest fires, erosion and from plants and animals (flaky skin). Relatively large quantities of 'ultrafine' products are produced on incomplete combustion and irritated with human activities (often from petrol and diesel engines, industry, charcoal burning etc) which contribute to air pollution. Human activities are expected to create about 10% of the aerosols, the remaining 90% having a natural source (Taylor, 2002). Small particles suspended in the atmosphere can affect the environment and human health. For example, airborne dust particles including naturally occurring NPs and NPs produced by other processes (e.g. asbestos), are associated with dust-related lung diseases such as mesothelioma. Products containing engineered NPs are distributed on the market and commonly used in daily life. To date there is concern about the potential release to the environment of engineered NPs from a wide range of consumer products and specialist applications in fields such as medicine and environmental remediation. This concern is compounded by a lack of understanding of the impact of these materials on the environment, organisms and human health.

A number of researchers have voiced concern about possible adverse effects of NPs to man. Kirchner et al. (2005) distinguished three main causes for the toxicity of NPs following exposure to cells in culture: the chemical toxicity of the material, the small size of the NPs, and its shape. From studies with rodents, it was revealed that NPs enter the body by all exposure routes i.e. inhalation, dermal contact and ingestion, to reach the peripheral circulation (Takenaka et al, 2001; Ji et al, 2007; Oberdörster et al, 2004, 2005a,b; Chang et al 2006; Kim et al, 2008; Trop et al, 2006; Vlachou et al; 2007; Niwa

et al, 2007; Han et al 2012). Following exposure by inhalation, the nano-size of the particle has an influence on the deposition region in the lungs and potential translocation to organs (Takenaka et al, 2001; Ji et al, 2007). Furthermore, as for the potential toxicity of NPs to the reproductive system, a study by McAuliffe and Perry (2007) suggested that NPs cross the blood testes barrier and therefore there is a possibility of adverse effects on sperm cells.

1.2 Silver nanoparticles (AgNPs)

Silver has been used since ancient times for jewellery, utensils, monetary currency, dental alloys, photography, explosives, and others (Chen and Schluesener, 2008; Panyala et al, 2008). Furthermore, before the discovery of antibiotics, it was used as an antiseptic, particularly in the clearing of open wounds and burns (Larese et al, 2009). For the manufacture of AgNPs: Metallic silver is engineered into ultrafine particles via numerous methods such as spark discharging, electrochemical reduction, solution irradiation and cryochemical synthesis (Chen and Schluesener 2008). The particle size of AgNP is typically smaller than 100 nm and each particle will consist of 20 -15,000 silver atoms (Oberdörster et al. 2005 a, b; Warheit et al. 2007; Chen and Schluesener 2008). AgNPs exhibit specific physicochemical characteristics (e.g. pH-dependent partitioning to solid and dissolved particulate matter) and biological activities compared to the macro-sized metal (Lok et al. 2007; Pal et al. 2007). This effect is mainly attributed to the high surface area to mass ratio, which potentially results in high reactivity, allowing a larger amount of silver atoms to interact with their surroundings.

A recent study (Benn et al. 2008) discovered that AgNPs can leak into waste water during washing of clothing containing AgNPs, possibly disrupting useful bacteria in waste-water treatment processes or causing danger to aquatic organisms in natural water resources. According to Benn et al, some brands of socks can release 100% of AgNPs within four washings, while two other brands lost less than 1% to waste water for the same number of washings (Benn et al, 2008). Moreover, AgNPs may be released from consumer products containing AgNPs such as shirts, medical masks, toothpaste, shampoo, detergent, towels, toy teddy bears, and humidifiers, after washing in water. Four products were shown to release silver into the aqueous environment (Benn et al, 2010). AgNPs are also used in washing machines which can release silver ions (Ag^{+}ions) into waste water (Vigneshwaran et al. 2007). Several Swedish agencies,

including the Swedish Environmental Protection Agency, have protested against this application since it may result in waste water becoming contaminated with AgNPs. Recently, the United States Environmental Protection Agency decided to regulate this specific form of nanotechnology. Consequently, products containing AgNPs, such as washing machines, should be labelled antimicrobial. Nevertheless, AgNP-products are indicated as one of the fastest growing in the nanotechnology industry, with possible widespread exposure to man and the environment (Chen and Schluesener 2008). Unfortunately, large knowledge gaps exist with regard to the possible risk of exposure to these particles, in particular the long-term impact of the use of AgNPs is relatively unknown although to date a number of studies have been carried out in this area.

A selection of the most recent articles describing possible mechanisms underlying the toxicity of AgNPs, including DNA damage and epigenetic changes, are reviewed in Table 1.1.

Antibacterial properties

It has been known for a long time that silver-based compounds are useful in a wide range of bactericidal applications (Nomiya et al, 2004, Gupta et al, 1998). Moreover, silver compounds are used in medicinal treatments such as for burns and a variety of infections (e.g. treatment eye infections in newborns) (Feng et al, 2004; Dallus et al, 2011). Also, many salts of silver and silver derivatives are available commercially as antimicrobial agents (Holladay et al, 2006), but their use may result in unwanted absorption of ions such as in epidermal cells and sweat glands (Silver, 2003). A number of reports describe that the size of the AgNP is important for its antibacterial properties and AgNPs of diameter 5-32 nm have enhanced antibacterial activity (Shahverdi et al, 2007). The antibacterial activities of penicillin G, amoxicillin, erythromycin, clindamycin, and vancomycin against *Staphylococcus aureus* and *Escherichia coli* were increased in the presence of AgNPs with diameters of 1-450 nm. Antimicrobial activity of AgNPs has been reported for both Gram-negative bacteria (Baker et al, 2005; Morones et al, 2005; Panacek et al, 2006) and Gram-positive bacteria (Panacek et al. 2006). In addition to size and concentration, the antimicrobial activity of AgNPs is also influenced by shape due to increased surface area close to the target increasing the area of the release free ion, the large surface area to volume ratios (Pa et al, 2007; Wijnhovon et al, 2009).

The antimicrobial activity of silver compounds is based on the bonding of metallic ions in various biomacromolecular components. Cationic silver targets and binds to negatively charged components of proteins and nucleic acids, thereby causing structural changes and deformations in bacterial cell walls, membranes, and nucleic acids (Dias et al, 2006; Woo et al, 2008; Cavicchioli et al, 2010). Several researchers have reported that silver ions bind to DNA to block transcription and also bind to cell surface components to interrupt bacterial respiration and ATP synthesis (Batarseh, 2004; Kumar et al, 2005). Several other mechanisms for the anti-bacterial function of silver have been proposed, but non have been fully validated (Feng et al, 2000; Pandian et al, 2010)

Mechanisms of toxicity

A review of the literature has indicated that the mechanisms of underlying the toxicity of AgNP are still not fully known. In fact, in some studies AgNPs have been suggested to be non-toxic (Murali et al, 2007). However, it is known that the acute toxicity of silver and AgNPs is argyria: the most dramatic symptom of argyria is that the skin becomes blue or bluish-grey coloured. Argyria has been seen when wounds have been exposed to a large amount of silver from wound dressings, although there have been no reports of allergy to silver (Leaper, 2006).

Possible mechanisms of toxicity have been suggested by the morphological and structural changes found in bacterial cells and mammalian cell lines after treatment with AgNPs. Several studies have been carried out on the mechanisms of toxicity including AgNPs used in five commercial wound dressings (total silver content of the dressing range from13 $\mu g/cm^2$ to 934 $\mu g/cm^2$ of sample) showed that three of them caused significant cytotoxic effects on keratinocytes and fibroblast cultures *in vitro.* Wound dressing containing AgNPs in an appropriate pretreatment solution caused more than 50% the cell death after 24h exposure to keratinocytes. Acticoat ^{TM} showed 99% cell death after the dressing was delivered with water for 24h and when delivered with FBS to led 50% cell death. However, 80% of cells remained viable and when using saline as a pretreatment. Aquacel $^{®}$Ag caused cytotoxicity in all solutions, but the percent of cell death less than 50 %. Contreet$^{®}$Foam caused more than 95% of keratinocytes to be killed in all pretreatment solutions. A study of a C18-4 germ cell line; BRL 3A liver cells and PC-12 neuroendocrine cells after exposure to AgNPs revealed notably decreased mitochondrial function (Braydich-Stolle et al, 2005; Hussain et al, 2005, 2006), but the mechanism or the effect on mitochondrial function was not clarified. In the study with BRL 3A liver cells, a decrease in reduced glutathione (GSH) levels and an increase in reactive oxygen species (ROS) was found in association with mitochondrial perturbation, suggesting that oxidative stress was involved in the toxicity of AgNPs (Hussain et al, 2005). AgNPs have been reported to cause oxidative stress by interacting with thiol groups on the mitochondrial inner membrane (Almofti et al, 2003). Proteins and enzymes such as glutathione, thioredoxin, superoxide dismutases (SOD) and thioredoxin peroxidase are key components of cellular antioxidant defense pathways and play a role to neutralize ROS. Thus, AgNPs may cause an increase in

cellular ROS levels following inhibition of mitochondrial respiration followed by increased permeability of the mitochondrial membrane.

Table1.1 A selection of recent AgNP studies.

Citation	Nanoparticle size	In vitro/in vivo	Analysis method	Findings
Xu et al, 2012	5-30 nm	HeLa cells, tumour epithelial cells	- Cytokinesis-block micronucleus (CBMN) - DNA microarray and gene ontology pathway analysis	- Induced micronuclei formation at cellular level - Broad spectrum molecular responses at gene expression level - Toxicity caused by ROS and DNA damage, chromosome instability, mitosis inhibition - Inflammatory induced toxicity, signal transduction pathway and immune response pathway
Beer et al, 2012	30–50 nm	The A549 human lung carcinoma epithelial-like cell line	- MTT assay - WST-8 assay - Cell cycle analysis - Reactive oxygen species (ROS) assay - Annexin V/PI assay	- Free silver ions in AgNP play a considerable role in the toxicity
Liu et al, 2012	50–100 nm	Adult male specific-pathogen free (SPF) Wistar rats	- ROS assay - Histology analysis - Morris water maze (MWM) test - Electrophysiology recording (long-term potentiation recording)	- AgNPs induced learning and memory deficits in rats. - Possible mechanisms of AgNP neurotoxicity
Lim et al, 2012	5nm, 100nm	A human macrophage cell line (U937)	- Colorimetric cell counting kit-8 (CCK-8) - cDNA microarray - Real-time RT-PCR - ELISA - Western blot	- 5 nm AgNPs, induce IL-8 production - Hemeoxygenase-1(HO-1) - Increase expression of (HO-1), heat shock protein-70 (HSP-70) and interleukin-8 (IL-8)

-WST-8 assay= Water soluble Tetrazolium assay; WST-8= 2-(2-methoxy-4-nitrophenyl)-3-(4-nitrophenyl)-5-(2,4-disulfophenyl)-2H-tetrazolium, monosodium salt; formazan

Citation	Nanoparticle size	In vitro/in vivo	Analysis method	Findings
Song et al, 2012	40nm mPEG-SH-coated AgNPs 40 nm	Human liver cell line (HL-7702)	- MTT assay - LDH assay - Thiobarbituric acid reactive substance (TBARS) assay - GPx AssayKit - SOD Assay Kit	*AgNPs coated* - Decreased cell viability in dose- and time-dependent manner - Membrane damage - Decreased the activities of superoxide dismutase and glutathione peroxidase *AgNPs* - -Increase level of malondialdehyde, an end product of lipid peroxidation - Decrease mitochondrial membrane potential (MMP) and cause G2/M phase arrest
Singh and Ramarao, 2012	43.9 nm	- Macrophage RAW 264.7 - Macrophage J774.1 - Pulmonary epithelial (A549) - Renal epithelial (A498) - Hepatic (Hep G2) - Neuronal (Neuro 2A) cell lines	- MTT and Commassie blue (CB) assay - ROS assay - Cytokine production assay - MMP dissipation assay - Apoptosis assay	- Ag NPs are internalized via scavenger receptors (SRs) to the cytoplasm in macrophages then release Ag ions. - Ag ions interfere with normal mitochondrial function and induce apoptotic cell death. - Ag NPs induced stress pathways from ROS and cytokine production
Kang et al, 2012	7.5±2.5 nm.	Ovarian carcinoma SK-OV3 cells	- MTT assay - Western blot analysis - Flow cytometry analysis - Single-cell gel electrophoresis assay (Comet assay). - RT-PCR analysis	- Decrease in cell viability by increases in apoptosis and DNA damage - Increased the expression of heme oxygenase-1 (HO-1) in nonspecific shRNA (short hairpin RNA) expressing cells - Nrf2 knockdown cells (NRF2i) did not increase HO-1 expression - Cobalt protoporphyrin-mediated HO-1 activation in the NRF2i cells prevented AgNPs-mediated cell death - Nrf2-dependent HO-1 up-regulation plays a protective role in AgNPs induced DNA damage and consequent cell death - AgNP-mediated HO-1 induction is associated with the PI3K and p38MAPK signaling pathways

Nrf2= Nuclear factor E2-related factor-2 ; the transcription factor in human that induces the expression of gene that involved antioxidant and oxidative stress

Citation	Nanoparticle size	In vitro/in vivo	Analysis method	Findings
Kim et al, 2012	56.19±13.27 nm	- Primary cultured human periodontal ligament (PDL) cells - Human juvenile costal chondrocyte cell line C28/I2 - Squamous cell carcinoma cells from the tongue (SCC-9)	- MTT assay - Real-time cell electronic sensing (RT-CES) assays - Quantitative reverse-transcription (RT) polymerase chain reaction (PCR) analyses - Annexin V–FITC Apoptosis Detection Kit I - A luminescent Caspase-Glo 3/7 assay kit - TLR-2(The Toll-like receptor 2) siRNA or TLR-2 antibody treatment - Western blot analysis	- Induced dose-dependent effects - AgNP-mediated apoptosis was reduced after treatment with TLR-2 siRNA in both PDL cells and Chondrocytes - Functional blocking of TLR-2 with anti-TLR2 antibodies inhibited AgNP-mediated - Increased c-Jun phosphorylation, an effect that was reversed after treatment with TLR-2 siRNA - AgNP-mediated apoptosis most likely occurs via the TLR-2 pathway
Li et al, 2012	5 nm	- Human lymphoblastoid TK6 cells	- Salmonella reverse mutation assay (Ames test) - In vitro micronucleus assay - Flow cytometry	- Increased micronucleus in a dose-dependent manner - Induced micronucleus frequency - AgNPs are genotoxic toTK6 cells
Asare et al, 2012	20 nm, 200nm TiO2-NPs (21 nm)	- 8 -12 week old male 8-oxoguanine DNA glycosylase knockout mice (Ogg1−/− KO), defective in the repair of oxidated purine - The pluripotent human testicular embryonal carcinoma, NTERA-2 cl.D1 cell line (NT2)	- MTT assay - Cell death analyses by PI/Hoechst staining - Single cell gel electrophoresis (Comet assay) - Cytokine assay	- Both AgNPs more cytotoxic and cytostatic compared to TiO2-NPs - Induced apoptosis, necrosis and decreased proliferation in a concentration- and time-dependent manner. - The 200 nm AgNPs induced concentration dependent increase in DNA-strand breaks in NT2 cells.
Mukherjee et al, 2012	<100 nm	- HaCaT cells, an immortal non-cancerous human keratinocyte cell line - -HeLa cells,an epithelial adenocarcinoma cell line	- Alamar Blue, Neutral Red and Coomassie Blue assays - MTT assay - Clonogenic assay - Optical microscopic study - Reactive oxygen species (ROS) study - A commercial kit ThiolTracker™ Violet, estimate the levels of glutathione (GSH) - Adenylate kinase (AK) release assay - Apoptosis study	- Induced cytotoxicity by dose and exposure time - HeLa cells more sensitive than HaCaT cells up to their natural antioxidant levels.

Ogg1= 8-Oxoguanine-DNA glycosylase (Ogg-1)

Citation	Nanoparticle size	In vitro/in vivo	Analysis method	Findings
Flower et al, 2012	40 to 60 nm.	Human peripheral blood cells	Alkaline Comet assay	- Induced DNA damage in human peripheral blood cells
Zanette et al, 2011	25 ±7.1 nm	The human-derived keratinocyte HaCaT cell line	- MTT assay - The sulforhodamine B (SRB) assay - Propidium Iodide assay (PIA) - DAPI staining - TEM	- Reduced cell viability - No evidence of induction of necrosis - Apocynin, NADPH-oxidase inhibitor, or N(G)-monomethyl-L-argynine, nitric oxide synthase inhibitor, did not prevent NPs-induced reduction of cell viability - TEM revealed alteration of nuclear morphology but only a marginal presence of individual NPs inside the cells
Hackenberg et al, 2011	(<50 nm)	Human mesenchymal stem cells (hMSCs)	- Trypan blue exclusion test - Fluorescein diacetate (FDA) test - The alkaline single-cell micro gel electrophoresis (comet) assay - The chromosomal aberration (CA) test - The ELISA method measured the cytokines IL-6, IL-8 - Migration assay	- Induced geno- and cytotoxic effects in hMSCs at high exposure concentrations (10 µg/ml). - Subtoxic levels of AgNPs activate hMSCs and do not interfere with migration activity.
Piao et al, 2011	5-10 nm	Human Chang liver cells	- MTT assay - Phase contrast inverted microscopy - TEM - Intracellular reactive oxygen species (ROS) measurement, DCF-DA, the fluorescence of 2-,7- dichlorofluorescein - Spectrofluorometer and a flow cytometry - Detection of reduced glutathione (GSH) level by using high-resolution magic angle spinning nuclear magnetic resonance (HR-MAS NMR) spectroscopy - Colorimetric assay kit, GSH-400 - Western blot analysis - Single cell gel electrophoresis (Comet assay) - Lipid peroxidation assay	- AgNPs induced cytotoxicity than $AgNO_3$was used as a silver ion source - AgNPs caused cytotoxicity by oxidative stress-induced apoptosis and damage to cellular components.

Citation	Nanoparticle size	In vitro/in vivo	Analysis method	Findings
Piao et al, 2011 (continued)			- Protein carbonyl formation using flow cytometey - DNA fragmentation was assessed by analyzing cytoplasmic histone-associated DNA fragmentation - Mitochondrial membrane potential was analyzed using JC-1, a lipophilic cationic fluorescence dye then microscopy - Transient transfection of small interfering RNA (siRNA)	
Lee et al, 2011	<100 nm	A549 lung epithelial cells	- Formazan dye assay - Phase-contrast microscopy - LDH assay - Cell cycle analysis using fluorescence-activated cell sorting - RT-PCR	Induced strong toxicity and G2/M cell cycle arrest by a mechanism involving PKCζ downregulation
Haase et al, 2011	- Peptide-coated AgNPs of 20 nm - Peptide-coated AgNPs of 40 nm - Citrate coated - 20nm AgNPs	THP-1 cells	- WST-1 Cell Viability Assay - Fluorescence-Activated Cell Sorting (FACS) Analysis - Confocal Raman Spectroscopy - Laser-SNMS/TOF-SIMS Analyses - Laser postionization secondary neutral mass spectrometry (Laser-SNMS) - Time-offlight secondary ion mass spectrometry (TOF-SIMS) - TEM Analysis - Cell Lysates, SDS-PAGE, Immunoblot and Detection of Protein Carbonyls - Phagocytosis Assay	- Laser-SNMS/TOF-SIMS approach was introduced to visualize nanoparticles inside human cells - TOF-SIMS proved excellent to decipher and pinpoint complex biochemical changes in lipid membrane layers - Particle uptake into macrophages occurs within minutes

PKCζ=The ζ isotype of protein kinase C

Citation	Nanoparticle size	In vitro/in vivo	Analysis method	Findings
Foldbjerg et al, 2011	PVP (poly vinyl pyrrolidone) coated AgNPs 30-50 nm	The A549 human lung carcinoma epithelial-like cell line	- MTT assay - Annexin V/propidium iodide assays - Atomic absorption spectroscope - Flow cytometry	- Decreased cytotoxicity by pretreatment with the antioxidant, *N*-acetyl-cysteine and a strong correlation between the levels of ROS and mitochondrial damage or early apoptosis - DNA damage induced an increase in bulky DNA adducts shown by 32P post labeling - The level of bulky DNA adducts was strongly correlated with cellular ROS levels and could be inhibited by antioxidant pretreatment - Ag NPs are a mediator of ROS-induced genotoxicity.
Greulich et al, 2011	PVP coated AgNP 70 ± 20 nm	Human peripheral blood mononuclear cells (PBMC); monocytes and lymphocytes (T-cells)	- Phase-contrast microscopy - Focused ion beam - Scanning electron microscopy (SEM) and energy-dispersive X-ray spectroscopy (EDX) analysis - Flow cytometry - Enzyme-linked immunosorbent assay (ELISA) for the cytokine release (IL-1ra, IL-2, IL-4, IL-6, IL-8 and TNF-a) - 2′,7′-dichlorofluorescein-diacetate (DCFHDA)	- Decrease cell viability and induce oxidative stress in monocytes at concentrations of 10 µg/ml and higher - PBMC respond differentially towards AgNPs dependent on the respective subtype (monocytes or lymphocytes) - Accumulation of nanosilver in lymphocytes and monocytes - The quantity of intracellular in monocyte activation via silver ions release and subsequent ROS generation - Increased in IL-6 and IL-8 generation
Park et al, 2010	68.9 nm,	Mouse peritoneal macrophage cell, RAW264.7 cell line,	- MTT assay - The cell cycle was analyzed by measuring DNA content with the FACSCalibur system and CellQuest software - Intracellular reduced glutathione (GSH) level - Nitric oxide (NO) production quantified spectrophotometrically using Griess reagent. - Cytokine assay using an ELISA kit - RT-PCR Reverse transcription - Microscopy with a dark-field condenser	- Decreased cell viability in concentration- and time-dependent manner - Cells phagocytosed NPs and induced cytotoxicity by ionization of AgNP

Citation	Nanoparticle size	In vitro/in vivo	Analysis method	Findings
Kim et al, 2009	<10 nm	Human hematoma HepG2 cells	- Dark-field microscopy - TEM - MTT assay - Colorimetric assay - DCFH-DA - γ-H2AX, - Real time reverse transcriptase-polymerase chain reaction	- Cytotoxicity of Ag^+ ions induced oxidative stress - The expression of oxidative stress-related mRNA species was regulated differentially by AgNPs and Ag^+ ions - Induced toxicity independent of free Ag^+ ions and the mechanisms of AgNP action may be different from Ag^+ ions.
Miura and Shinohara, 2009	5–10 nm;	HeLa S3 cells	- MTT assay - Apoptosis analysis using flow cytometry - Real-time PCR	- AgNPs and $AgNO_3$ induced apoptosis in a dose dependent manner - $AgNO_3$ strongly induced apoptosis and cytotoxicity more than AgNPs - AgNPs and $AgNO_3$ induced up-regulation of the expression of stress genes, Ho-1 and mt-2A
AshaRani et al, 2009	Starch-coated AgNPs 6-20 nm	- Normal human lung fibroblast cells (IMR-90) - Human glioblastoma cells (U251)	- Cell titre blue cell viability assay - Cell cycle analysis was carried out by staining the DNA with propidium iodide (PI) followed by FACs - Annexin V–FITC for apoptosis assay - DCF-DA to detect ROS - Cytokinesis-blocked micronucleus assay (CBMN) - Alkaline Single-Cell Gel Electrophoresis (Comet Assay)	- Reduced ATP content of the cell caused damage to mitochondria and increased production of reactive oxygen species (ROS) in a dose-dependent manner - DNA damage, and cytokinesis blocked micronucleus assay (CBMN), was dose-dependent and more prominent in cancer cells - Cell cycle arrest in G2/M phase possibly due to repair of damaged DNA - No massive apoptosis or necrosis - Indicated the presence of AgNPs inside the mitochondria and nucleus - A possible mechanism of toxicity is disruption of the mitochondrial respiratory chain leading to production of ROS and interruption of ATP synthesis, which in turn causes DNA damage - Higher sensitivity of U251 cells and their arrest in G2/M phase

Citation	Nanoparticle size	In vitro/in vivo	Analysis method	Findings
Ahamed et al, 2008	25 nm	Mouse embryonic stem cells (MES)	- MTT assay - Expression of DNA repair proteins; -H2AX phosphorylation - P53 Phophorylation	- Time dependent decrease in cell viability - Increased expression of Rad51, p53 and phopho-H2AX proteins.
Cha et al, 2008	13 nm	- 7 weeks old mal balb/c mice. - Human liver cell line (Huh-7)	- MTT assay - Gutatione production; DNA content; gene expression profiling	- No cytotoxicity or change in glutathione - Altered expression patterns of genes involved in apoptosis and inflammation

1.3 Oxidative stress

Oxidative stress has specific effects on cells, including oxidative damage to proteins, lipids and DNA. Oxidative stress refers to a redox imbalance within cells usually as a result of increased intracellular reactive oxygen species (ROS) and decreased antioxidant capacity.

As mentioned earlier, the high surface area associated with AgNPs can promote the generation of ROS at a much high rate than from macro silver compounds. Consequently, the smaller the NPs, the higher the oxidative stress they may induce (Brown et al, 2001). There have been numerous studies demonstrating the induction of ROS following exposure to NPs (Karlsson et al, 2008; Papageorgiou et al, 2007; Gurr et al, 2005). In the case of AgNPs, several studies have demonstrated that AgNPs are cytotoxic (Ahamed et al, 2008; Hsin et al, 2008; Shin et al, 2007), although there is a contention about their ability to promote oxidative stress (Cha et al, 2008; Hussain et al, 2005) and a distinct lack of information on their genotoxic potential.

Cellular response to genetic damage is of particular interest to the study of cell toxicity, as this understanding allows the development of clinical treatments for carcinomas and other cytotoxic agents. The intrinsic level of DNA damage occurs spontaneously without environmental factors and as a consequence of intracellular metabolism results in changes to the nucleotide base sequence of DNA. DNA damage can also be induced by exogenous environmental factors such as radiation and numerous chemicals, which can introduce strand breaks and lesions on the phophodiester backbone.

The principal mechanism of damage in a cell is the interaction with ROS a group of molecules including free radicals (superoxide and hydroxyl) and hydrogen peroxide (Slupphaug et al, 2003). ROS are formed during a variety of normal endogenous processes and their levels are maintained by a variety of enzymes and antioxidants to give redox homeostasis (Blokhina et al, 2002). The most important of the enzymatic pathways in homeostasis is superoxide dismutaste (SOD1&2); an enzyme tasked with inactivation the highly reactive superoxide free radicals by converting them to hydrogen peroxide and water in the presence of a metal ion acting as the redox agent (Culotta et al, 2002).This could be copper, manganese, nickel or iron depending on the family of enzyme and its location in the cell; cytosolic SOD1 uses copper and zinc(Cu-Zn SOD), mitochondrial

SOD2 uses manganese and extracellular SOD favours iron (Scandalios, 2002). The enzyme works by reducing the metal ion attached to one of its subunits in one step and oxidizing it in the second step to produce oxygen and peroxide, which subsequently gets broken down by glutathione peroxidase (GPx) and catalase.
GPx is an enzyme that catalyses the reduction of hyperoxides (H_2O_2) by oxidizing glutathione in its reduced form (GSH) (Berg, 2006). The enzyme is characterized as a tetrameric glycoprotein that contains the amino acid seloncysteine, which is oxidized by hydrogen peroxide to produce selenenic acid (Day, 2008). The GSH then converts sellenenic acid back to its original form and becomes oxidized in the process, producing a molecule of oxidized glutathione (GSSG) and water. GSH reductase is responsible for converting GSSG back into its reduced form, allowing further reactions to take place (Wu et al, 2004). Catalase is another enzyme that catalyses the same hydrogen peroxide reaction; this works alongside glutathione peroxidase and is generally responsible for removing hydrogen peroxide generated within the cell. Subsequent research has found this enzyme in high numbers in the peroxisomes (Limon-Pacheco and Gonseball, 2008), supporting this idea.

According to the chemical reaction mentioned earlier, there will be oxidative defense enzymes involved in each reaction and SOD is the major defense against superoxide radicals and SOD1 is one of three superoxide dismutases responsible for destroying free superoxide radicals in the body. Functional of SOD1 is binds copper and zinc ions also bind with chaperone like copper chaperone for superoxide dismutase; CCS, specifically delivers Cu to copper/zinc superoxide dismutase and may activate copper/zinc superoxide dismutase through direct insertion of the Cu cofactor. However, non-enzymatic processes also play a key role in protection against oxidative stress. Although most of the reduced glutathione in the cell is utilized by the glutathione peroxidase enzymes, it can also form conjugates directly without the need for enzymatic catalysis. Glutathione can also be used as a conjugate for eletrophilic compounds via interactions with glutathione S-transferases, although this is not a direct protection against oxidative stress (merely against general cytotoxic agents). Antioxidants such as ascorbic acid, α- tocopherol and β-carotene are electron donors that neutralize free redicals by reduction, using any number of selenium, copper, zinc or manganese as co-factors (Harris, 1992). Fenton's reaction is the final example of a process that causes spontaneous removal of certain reaction oxygen species. It is specifically involved in the conversion of hydrogen peroxide to a hydroxyl free radical and a hydroxide ion via the oxidation of Fe2+ ions. This produces a ferric ion that

is then reduced back into Fe^{2+} via oxygen free redical, thus maintaining the supply of oxidising iron (Templeton, 2002).

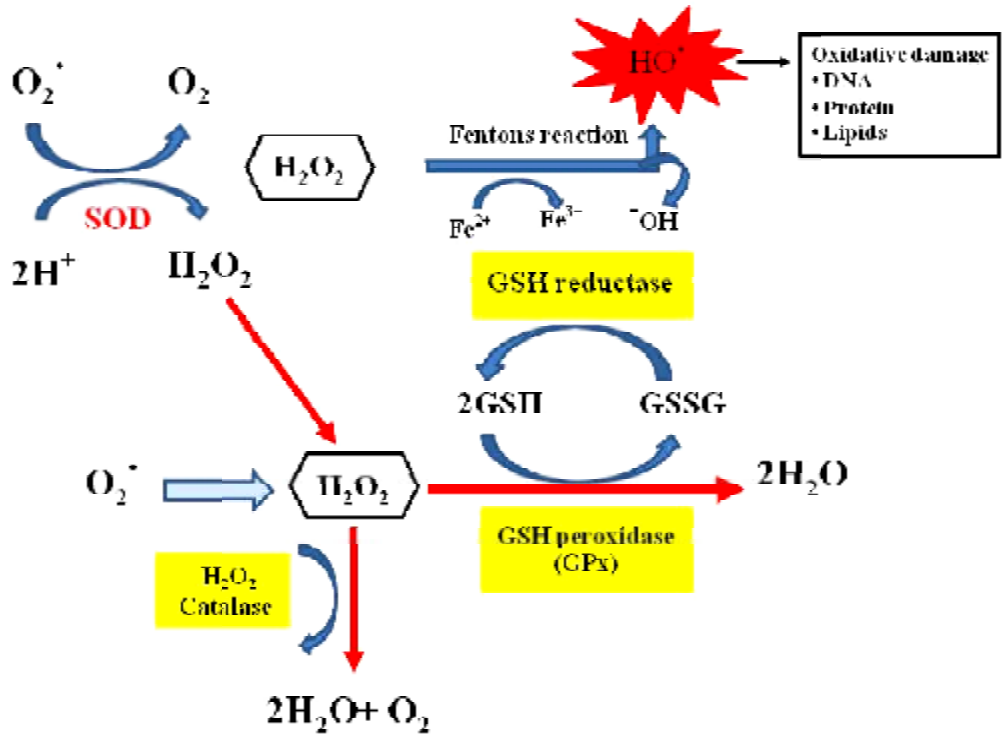

Figure 1.2 Oxidative stress pathways.

1.4 Possible mechanisms of oxidative DNA damage by AgNPs

DNA damage is an inevitable fact for a cell, and although protective mechanisms play a major role in cellular defence, repair pathways are needed to remove the damage. The identification of DNA damage during replication causes a cascade of signaling pathways and ultimately checkpoint activation, suspending the cell in a quiescent (G_0) state. In fact the identification of damage increases the synthesis of certain repair proteins so that the cell has both the time and means to repair itself, although if this is too great then the cell will sacrifice itself for the integrity of the whole organism and undergo apoptosis. The p53 mediated apoptosis in response to double strand breaks is one such example of this and involves a cascade initiated by DNA-dependent protein kinase (Gorgoulis et al, 2005). Although the apoptosis mechanism of the cell is self initiated, numerous repair mechanisms exist to allow cells to correct for DNA damage so that it had the potential to survive.

It has been reported that AgNPs can enter the body via inhalation and ingestion and possibly also by dermal penetration. Nanoparticles that penetrate the cell and subsequently reach the nucleus can directly interact with DNA or DNA-related proteins that may lead to damage to genetic material (Singh et al, 2009). It has been shown that AgNPs may enter the mitochondria and nucleus where they are directly involved in toxicity and DNA damage (Asharani et al, 2009). They cause intra-nuclear protein aggregates that can lead to inhibition of replication, transcription, and cell proliferation (Feng et al, 2000). Alternatively, DNA damage may take place through indirect mechanisms such as following increased oxidative stress (Singh et al, 2009) as described in the previous section.

1.5 Epigenetic changes

The meaning of the word “epigenetics” is in addition to changes in genetic sequence (Weinhold, 2006). Furthermore, this term has evolved to include the study of the mechanisms or pathways that maintain heritable patterns of gene expression and gene function without changing the sequence of DNA. The complete set of characteristics of epigenetic pathways in an organism is defined as the epigenome and it can be thought of as a second code that is overlaid on the DNA sequence code of the genome. As each organism has not only one single genome, it also has multiple epigenomes which may differ by cell and tissue type, and which may change over the lifetime of the organism. A number of epigenetic pathways are reported such as DNA methylation, histone modifications, nucleosome remodeling, and non-coding RNA-mediated pathways. However, apart from these four, it is likely that more will be discovered in the future. Nowadays, the most investigated pathways are DNA methylation and histone modifications. The fundamental concepts of these pathways are described below:

DNA methylation occurs when cytosine-containing nucleotides in DNA are modified by the addition of a methyl ($-CH_3$) group. Cytosine is one of the five nucleotides in the nucleic acid of DNA and RNA. A methyl group is covalently added to the fifth carbon of the cytosine ring to form 5-methyl cytosine (Figure 1.3) at the site where cytosine is linked via a phosphate to guanine. The sites rich in the CpG pattern are call CpG islands. DNA methylation is involved with regulation of cell function, and the amount of methylation may relate to the degree of repression of transcription, resulting in adverse health effects such as cancer.

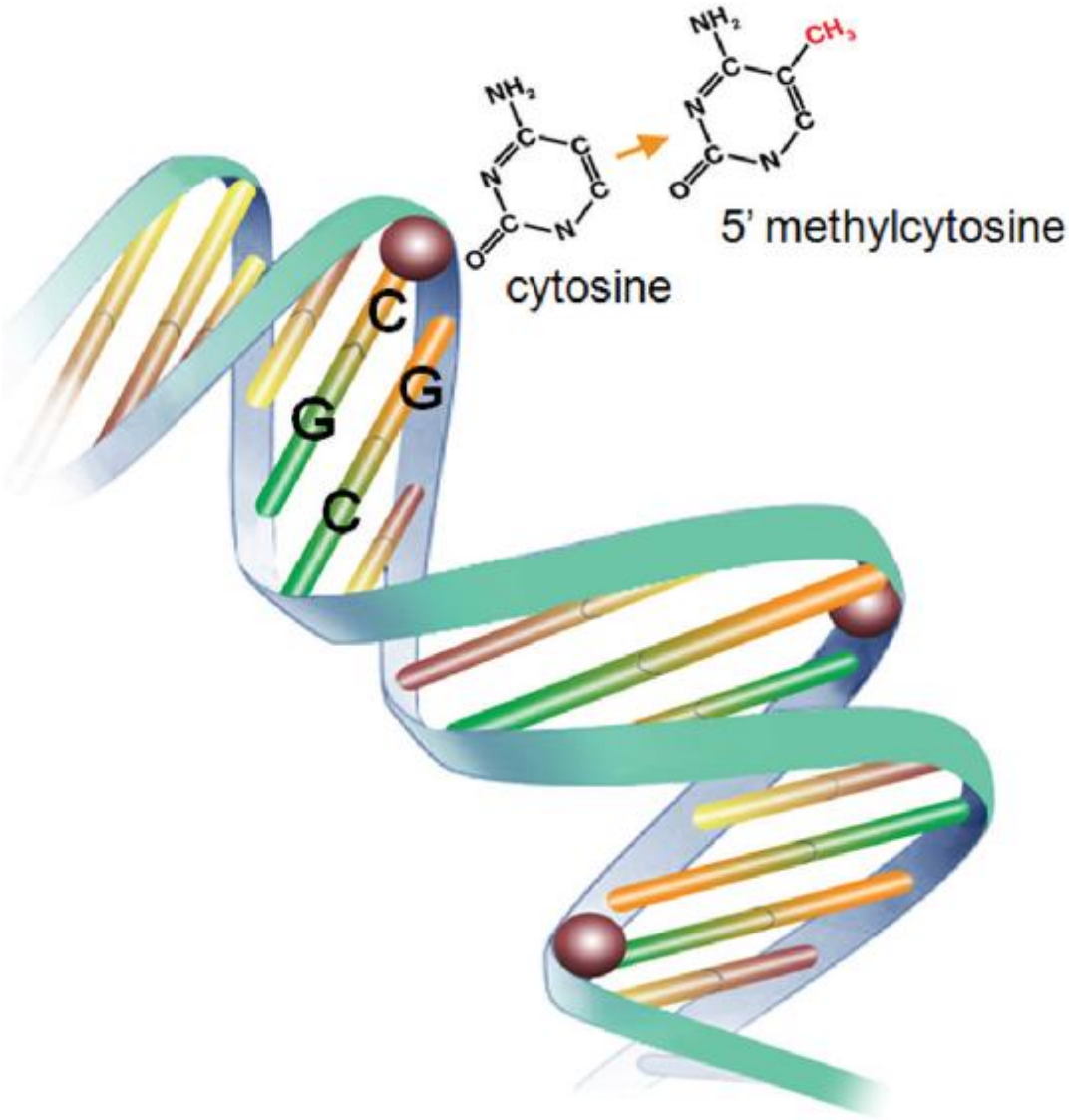

Figure 1.3 The principle of methylation and the chemical structure of cytosine when added a methyl group to the fifth carbon of the cytosine ring to form 5-methyl cytosine (Barros and Offenbacher, 2009)

Histones are globular proteins around which DNA coils to form chromatin (Figure 1.4). During gene transcription, histones play an important role in the control of how tightly or loosely chromatin is packed. This influences whether genes can be transcribed. Modification of histones occurs through enzyme-catalyzed addition or removal of certain molecules, such as methyl or acetyl groups, phosphate, or ubiquitin (Figure1.5). Improper modifications of histones cause genes to be expressed abnormally which can also lead to adverse health effects.

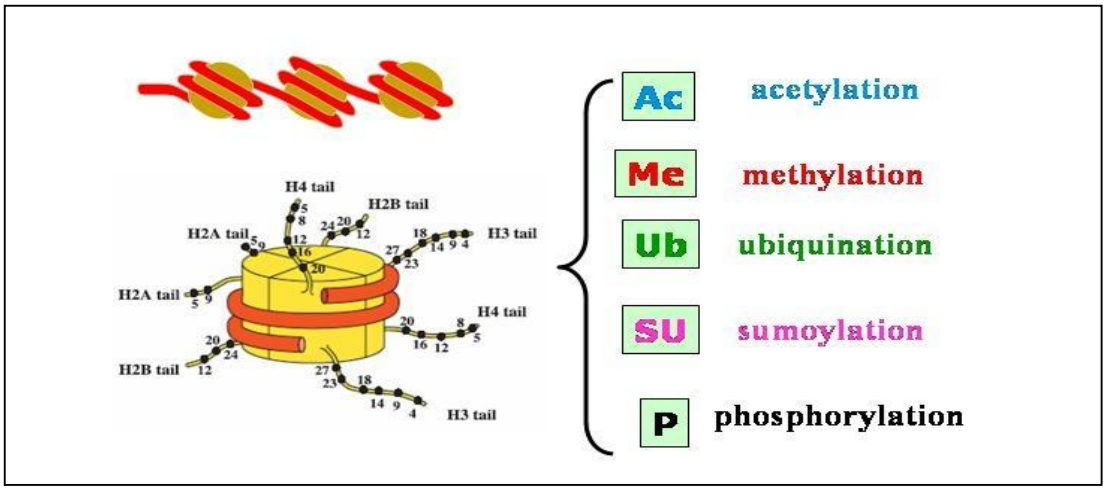

Figure 1.4 Nucleosome models and major posttranslational modications; acetylation, methylation, ubiquination, sumoylation, phosphorylation, which are important in gene expression regulation (Zheng, http://chemistry.gsu.edu/faculty/Zheng/research.html).

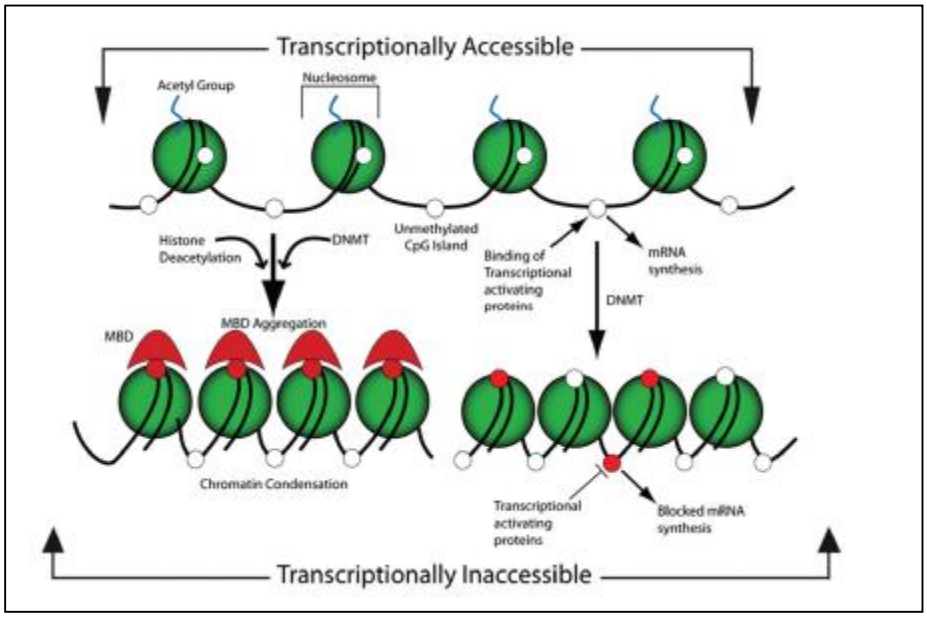

Figure 1.5 Histone modifications (Barron and Offenbacher, 2009). DNMT is DNA methyl transferase, MBD is methyl binding domain proteins.

There is increasing information that epigenetic changes play a critical role in the development of diseases, such as cancer, schizophrenia, bipolar disorder, autism and systemic lupus erythematosus (Vliet et al, 2007). Furthermore, epigenetics is recognized as a mediator of the interaction between the environment and genetics (Esteller, 2006). Factors such as the environment and diet can influence epigenetic changes. Epigenetic effects can be described as subtle and cumulative changes to DNA that may be passed on to daughter cells and progeny. There have been reports that metal nanoparticles can cause oxidative stress leading to apoptosis but this has not been investigated at the epigenomic level (Shi et al, 2004). It has been reported that cadmium telluride quantum dots induce epigenetic and genomic changes in human breast cells (MCF-7) that lead to cell death (Choi et al, 2008). Since epigenetics plays an important role in non-genotoxic adverse effects to cells that may be inherited, it is important to investigate this mechanism for AgNPs.

1.6 Cellular uptake of AgNPs

Internalisation of AgNPs influence cell function and physiology so we investigated whether the purposed influx of AgNPs in a number of cell types in order to determine the intracellular fate of particles. Possible influx of AgNPs (mechanisms) is in a number of the studied as show in figure 1.6.

The accumulation of AgNPs in macrophages has been indicated in vivo (Takenaka et al., 2001; Cho et al., 2009). The implications of accumulation of AgNPs are not fully understood but include deposition within the kerainocytes, a skin. Following exposure to silver by the oral route, it can translocate to various tissues in the body and it has been observed in fibroblasts, macrophages, nerves, and capillary walls (Wadhera and Fung 2005). Ingested silver may eventually reach the skin where it binds to metallothionein to produce the blue colour associated with argaria.

Lesniak et al (2005) reported AgNPs were taken up by epithelial cells and fibroblasts or monocytes, which was independent of cell type. The research later showed that silver dendrimer complexes and AgNPs were bound to the surface of cell membranes and also in the cytoplasm, trapped in phagocytic or endocytic vesicles. This suggests that internalization of both types of silver NP occurred through distinct mechanisms, i.e., phagocytosis and diffusion.

AshaRani et al (2009) studied the cytotoxicity and genotoxicity of starch-coated AgNPs (6-20 nm) in normal human lung fibroblast cell (IMR-90) and human glioblastoma cells (U251). The AgNPs caused disruption of the mitochondrial respiratory chain leading to production of ROS and interruption of ATP synthesis, leading to DNA damage. Uptake of AgNPs (100 μg/mL) in U251 cells analysed by TEM showed large endosomes in the cytoplasm of the cells which contained AgNPs. AgNPs were also present at the nuclear membrane, which suggested that they entered the cell through endocytosis rather than diffusion. The nuclear envelope has multiple pores with an effective diameter of 9-10 nm, through which transport of proteins takes place and, due to the small size of AgNPs, it is possible that they diffused into the nucleus through the pores.

Park et al (2010) reported the cytotoxicity of AgNPs (~70 nm) in mouse peritoneal macrophage cells (RAW264.7) after 24, 48, 72, and 96 h. After 24h, dark field microscopy indicated that the AgNPs had been ingested by viable Raw264.7 cells, possibly by phagocytosis, but they were not seen in dead cells.

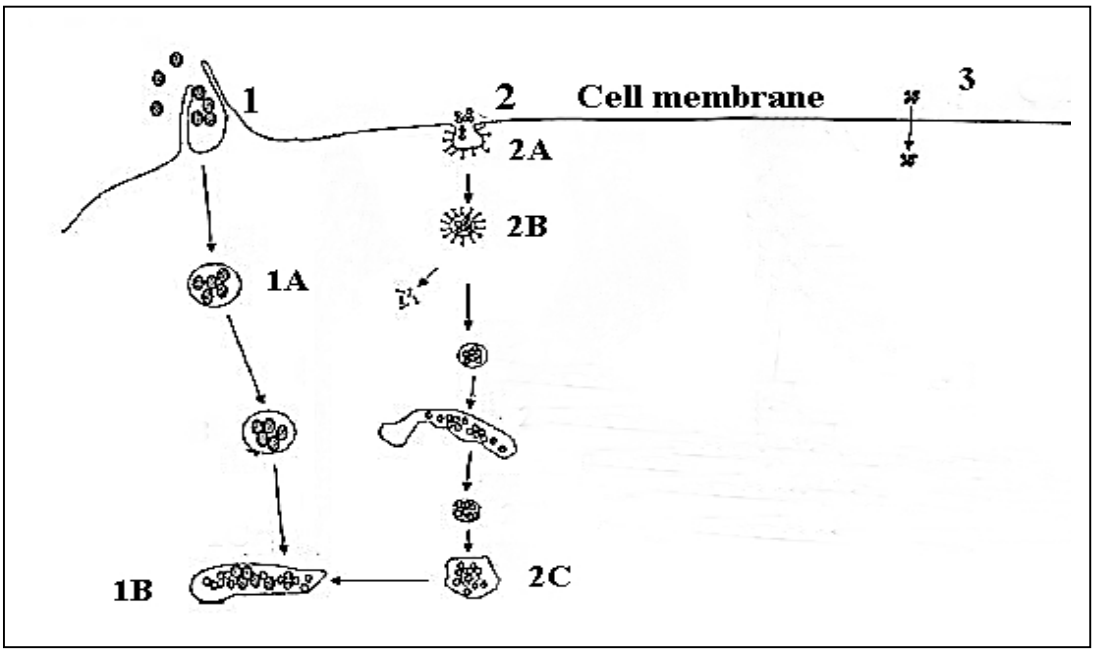

Figure 1.6 Possible pathways of cellular uptake of AgNPs through phagocytosis (1), clathrin-mediated endocytosis (2) and diffusion (3) (adapted from Unfried et al, 2007). During phagocytosis particles become engulfed via specific membrane receptors (e.g., scavenger receptors), leading to the formation of an early phagosome (1A), which subsequently matured (1B). Clathrin-mediated endocytosis is carried out at specific membrane regions, referred to as clathrin coated pits (2A). Following formation of a clathrin-coated vesicle (2B) particles are subsequently processed to late endosomes (2C). Finally, particles may translocate into cells via diffusion (3), which in contrast to all aforementioned pathways, is a non-active process.

1.7 Aims

1. To determine whether AgNPs cause DNA damage to human cells in culture. Jurkat and HL60 cells were used to represent effects in T-lymphocyes and macrophages, respectively (Figure 1.8).
2. To investigate the mechanisms underlying any DNA damage seen in the human cell lines.
3. To use TEM to image cellular uptake of AgNPs with elemental confirmation by EDX.

Firstly the cytotoxicity caused by silver nitrate compared to AgNPs, was assessed with the MTT assay. The experiments aimed to define the concentration and time parameters that would cause ≤ 20% loss of cell viability, to investigate DNA damage in the absence of cell death. Further experiments evaluated the level of apoptotic cells by the AnnexinV-PI assay and the cleavage of PARP.

DNA damage determined by the COMET assay in human Jurkat and HL60 cells in vitro was evaluated after exposure to negatively and positively charged AgNPs in comparison with silver nitrate.

In order to confirm whether the DNA damage was from single or double strand breaks the degree of phosphorylation of γH2AX that occurs mainly in response to DNA double strand breaks (DSB) was determined. The importance of altered methylation status associated with the DNA damage was determined by pyrosequencing

It was hypothesized that silver ions might induce oxidative stress in the cells therefore transcriptional changes in oxidative stress markers were measured following exposure to AgNPs and silver nitrate. To investigate the effect of silver on superoxide dismutase SOD functional activity proteins were separated by size exclusion chromatography and fractions were analysed for SOD-1 activity and for copper and silver by ICP-MS.

The second aim was to quantify the release of Ag^+ ions from AgNPs since this would give an estimate of the concentration of silver ions available to the cells to potentially induce toxicity and allow comparison of effects with those of sliver nitrate. A novel dialysis method linked with ICP-MS was developed to determine the release of Ag^+ ions from the AgNPs within the cells.

Finally the aim was to determine whether AgNPs entered the cells or whether toxicity might be due to silver ion release from the NPs.TEM was used to image localisation of the AgNPs within the cells, with elemental confirmation by EDX.

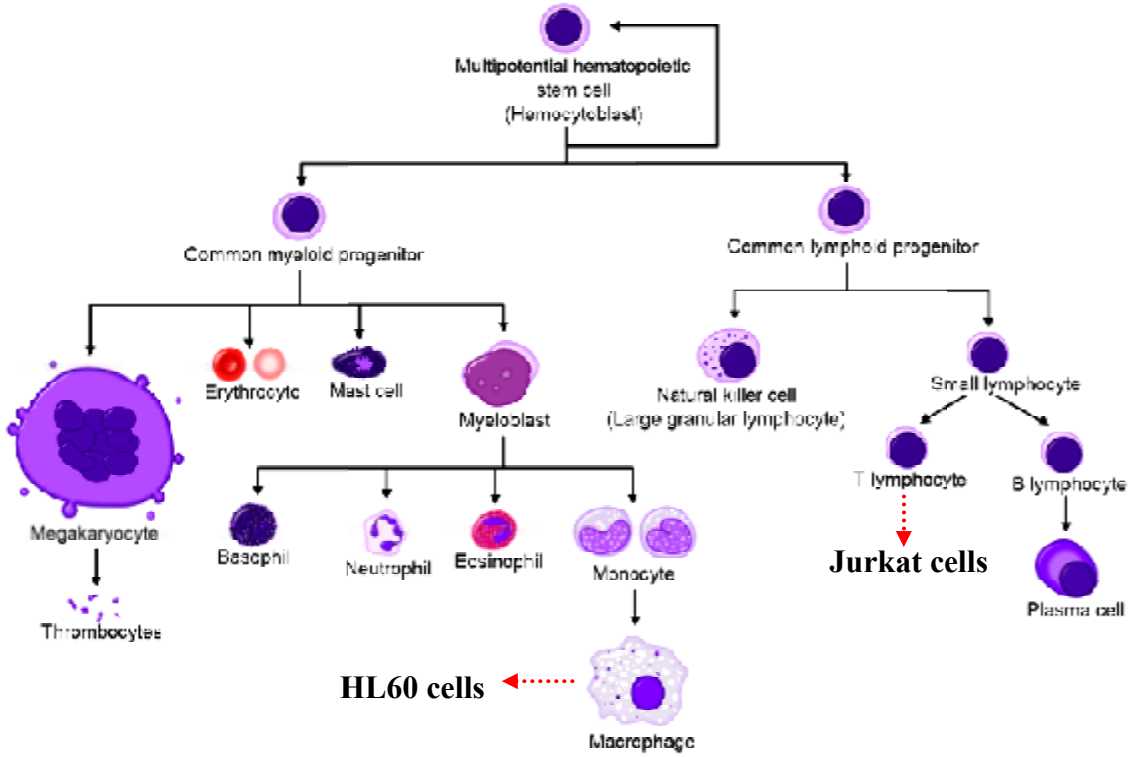

Figure 1.7 The cell lineage of HL60 and Jurkat cells. Adaped from Häggström, http://en. Wikipedia.org/wiki/Heematopoiesis#References.

CHAPTER 2

MATERIALS AND METHODS

Chapter 2. Materials and Methods

2.1 Materials

2.1.1 Human cells

All cells were grown at 37 °C in a humidified atmosphere containing 5% CO_2 /95% air.

Jurkat cells

The cells are Human T cell lymphoblasts (Jurkat). This cell line cannot carry out phagocytosis and it was derived from Jurkat Fred Hutchinson Cancer Research Centre (FHCRC). The IL-2 producing cell line was derived by incubating the cells at 41°C for 48 hours followed by a limiting dilution cloning over macrophages. Jurkats are suspension cells routinely grown in Roswell Park Memorial Institute medium: RPMI 1640 supplemented with 10% fetal bovine serum (FBS), 2mM glutamine and 10 U/ml of penicillin/streptomycin (all from Sigma). Cells were routinely cultured in T75 flasks (Corning) at a cell density of $3x10^5$ /ml - $9x10^5$ /ml until required for specific experiments.

HL60 cells

Human Caucasian promyelocytic leukaemia cell line (HL-60). It was reported that these cells can carry out phagocytosis (Gallagher et al, 1979). They were derived from peripheral blood leukocytes obtained from a 36-year-old Caucasian female with acute promyelocytic leukemia. Cultures were maintained between $1x10^5$ /ml - $9x10^5$ /ml in RPMI 1640 with 2mM glutamine and 10-20% FBS until required for specific experiments.

2.1.2 Silver nanoparticles

Type of silver nanoparticles investigated

All were purchased from NanoComposix, Inc, San Diego, America.

1. Negatively charged silver nanoparticles (diameter 10 nm)

Material: colloidal silver nanoparticles (diameter 10 nm)

Zeta potential(c): -30.2 mV

Suspension properties: suspended in 2 mM citrate buffer (**[**Na]~6 mM).

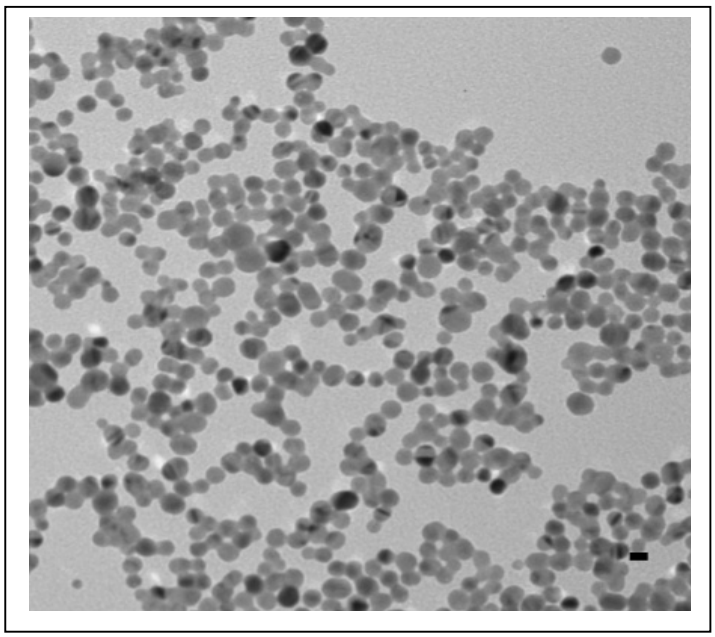

Figure 2.1 TEM image of negatively charged NPs, scale bar represent 10 nm

2. Positively charged silver nanoparticls (diameter 10 nm)

Material: positively charged colloidal silver nanoparticles (diameter 10 nm)

Surface is coated with PDADMAC[poly-(diallyldimethyl)-ammonium-chloride] to create positive surface charge.

Zeta potential: 18.7 mV

Suspension properties: suspended in 2 mM citrate buffer ([Na]~6 mM).

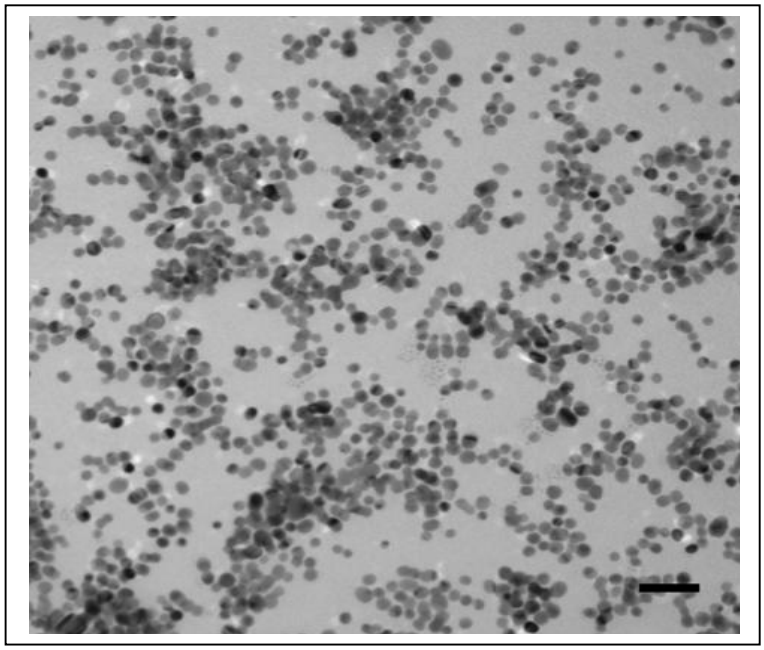

Figure 2.2 TEM image of positively charged NPs, scale bar represent 50 nm

2.2 Methods

2.2.1 *MTT assay*

The MTT [3-(4, 5-dimethylthiazol-2-yl)-, 5-diphenyl tetrazolium bromide] assay is a test that allows the measurement of cell viability/proliferation. MTT is a yellow dye that is converted to formazan, an insoluble purple compound, by the activity of intracellular dehydrogenases. The conversion is only able to take place in living cells therefore the amount of formazan produced is directly linked to the number of viable cells present. The cells are ruptured and the formazan solubilized using a solubilization solution. The absorbance of the resultant solution is read at 570nm and 690nm in a plate reader. Subtracting the 690nm value from the 570nm value gives an absorbance reading that corresponds to cell viability/proliferation (Fotakis and Timbrell, 2006).

The MTT assay was performed using a suspension of Jurkat or HL60 cells at a density of 3×10^5 /ml. One ml aliquots of this suspension were incubated with a range of silver nitrate and AgNPs concentrations (see results). Controls for the experiments were untreated cells. At the indicated time points, the cells were thoroughly re-suspended by pipetting and 100µl of this suspension was added to a 96 well plate. Ten µl of MTT dye (50µg/ml) was added to each well and cells incubated at 37°C with 5% CO_2/ 95% air for an appropriate time (see results). The cells were viewed under a light microscope to observe if formazan had accumulated inside the cell. The cells were then lysed and the formazan crystals solubilised by adding 150µl of solubilization solution (isopropanol) followed by gentle pipetting. The absorbance of the samples was then read at wavelengths of 570nm and 690nm using a multiskan spectrum microplate spectrophotometer reader and multikan spectrum software version 1.1. The 690nm value was subtracted from the value at 570nm to give an absorbance reading giving an estimate of cell proliferation/viability.

2.2.2 *Comet assay*

The Comet assay, also known as single cell gel electrophoresis (SCGE), is an electrophoresis technique which measures DNA damage in individual cells. The principle of the Comet assay is that the cell suspension is embedded in agarose on a coated microscope slide and lysed by detergents and a high salt concentration in order to expose

the DNA to the alkaline electrophoresis buffer so that the DNA unwinds from sites of strand breakage. During electrophoresis the intact/undamaged DNA head is pulled towards the anode side of the chamber. The slides are then washed with neutralizing solution and stained with a fluorescent DNA binding dye (SYBR® gold). Finally, the image of the comet cells are collected using a computerized image analysis system; Comet assay IV (Perceptive Instrument Lt).

Analysis of Comets

The diagram below shows a representative comet image (Figure 2.3). The user selects the cell to be analysed by clicking the centre of the comet head. The cell is analysed by a program called comet assay IV (IN STEM) which provides a variety of measurements, including the proportion of DNA in the head, the proportion of DNA in the tail and the length of the tail. Olive tail moment (OTM) is defined as the product of the tail length and the fraction of total DNA in the tail. Tail moment incorporates a measure of both the smallest detectable size of migrating DNA (reflected in the comet tail length) and the number of relaxed or broken pieces (represented by the intensity of DNA in the tail). A minimum of 100 cells are normally scored for each individual sample.

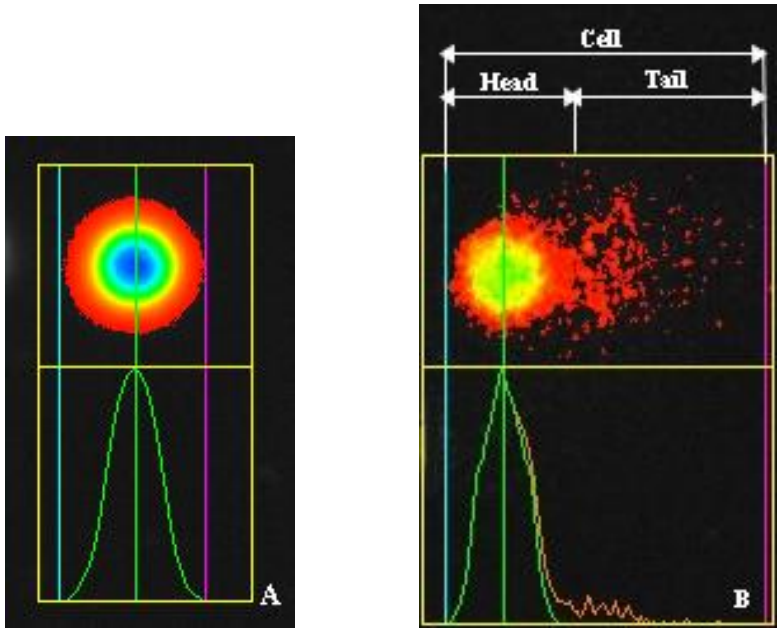

Figure 2.3 The difference between a normal cell and a damaged cell after the Comet assay. (a) shows a normal cell; (b) shows a damage cell.

All steps were performed under dim light to prevent any further DNA damage. Jurkat or HL60 cells were prepared in 6 well plates 24 hours prior to experiments. The cells were seeded at 3 x 10^5 cells/ml in RPMI containing 10 % FBS (Jurkat cells) or 20 % FBS (HL60 cells). Control consisted of untreated cells and the negative cells treated with hydrogen peroxide (50 μM) for 5 minutes. The cells were incubated with silver nitrate solution, AgNPs and appropriate controls at time and concentrations according to the experiment (see results) then centrifuged at 100 g for 5 minutes. The pellet was gently resuspended with PBS buffer to 0.5 ml. The cell suspensions were then transferred to Eppendorf tubes and placed on ice. A 2% solution of low melting point agarose (LMPA) was prepared in PBS (dissolved in a water bath at 90°C or microwaved). The LMPA was then transferred to a water bath at 37°C and allowed to equilibrate. Cell suspensions were prepared with 60 μl of cell suspension mixed with 60 μl of LMPA and dropped 60 μl onto a chilled microscope slide. Gels were spread evenly on microscope by adding a coverslip and allowed to set by placing them on an aluminum tray sat on a bed of ice. After 5 minutes, the coverslip was removed and the slides were submerged in chilled lysis buffer (2.5M NaCl, 100mM EDTA, 10mM Tris, Triton X-100 (1%v/v) and DMSO (1%v/v) pH to 10 immediately prior to use, at 0 °C for 1h. The slides were then washed in cold PBS for 15 minutes before placing in a horizontal electrophoresis tank filled with chilled alkali buffer (300mM NaOH, 200mM EDTA) for 30 minutes to allow unwinding of the DNA. After 30 minutes, electrophoresis was performed at a constant voltage of 22V and 500mA for 30 minutes. After electrophoresis the slides were washed in cold neutralization buffer (0.5M Tris pH 7.5) for 10 minutes followed by PBS for 15 minutes. DNA was then stained by adding 2 ml of SYBR gold stain (diluted 1:10000 in 1xTE buffer) to the slide for 5 minutes. Excess stain was removed and the gels were allowed to dry overnight in the dark.

2.2.3 *γH2AX foci: a DNA double strand break marker*

The method involves the use of immunofluorescence that detects the specific antigens using an antibody labeled with a fluorophore and fluorescence microscopy to view the labeled antigen.

HL60 and Jurkat cells (3x10^5 cells/ml) in RPMI were seeded in 12 wells plates and cultured for overnight. Cells were treated with silver nitrate (1 μg/ml) or AgNPs (1 μg/ml) for 4h and 24h. Etoposide (50 μM) was used as a positive control. The medium was removed by gentle centrifugation and the cells were washed with cold PBS and then

smeared onto coverslips. The cover slip was allowed to dry before being fixed with 4 % paraformaldeyhyde in PBS for 10 min at room temperature.The preparations were then washed in PBS for 5 min and then the cells were permeabilized with PBG- triton (0.2% fish skin gelatin, 0.5% bovine serum albumin in PBS and 0.5% Triton X-100) for 45 min and gently shaken at room temperature. The cells were then incubated with primary antibody (anti- phospho-Histone H2A.X (ser139), clone JBW301 (Milipore at 1:200 dilution) and then gently shaken for 2 hours at room temperature. The cells were then twice washed in PBG for 5 minutes followed by incubation with the second antibody (Alexa Fluor 594 goat anti mouse IgG (H+L), Red, Invitrogen at 1:2000 dilution) gently shaken for 1 hour at room temperature. After washing with PBS 3 times for 10 minutes, the cells were incubated in DAPI for 10 minutes before being washed 3 time times with PBS for 10 min. The cells were then mounted on coverslipes with mounting medium for fluorescence (Vectashield). Slides were examined using a fluorescence microscope (Carl Zeiss Axioplan LSM Image Browser).

2.2.4 *Western blotting*

Western blotting is a technique used to detect specific proteins in complex samples. After lysis in an appropriate buffer or a sonicator probe the proteins are denatured by adding a chemical such as lithium dodecyl sulfate (LDS) and 2-mercaptoethanol and boiled at 95 °C to ensure all proteins are denatured. After this the proteins are separated using polyacrylamide gel electrophoresis. The negatively charged protein molecules migrate through a polyacrylamide gel according to the size of the protein, so the smaller proteins migrate faster than the bigger proteins. A molecular weight marker is used to indicate the size of the proteins. The proteins are then transferred onto nitrocellulose membranes by electrophoresis. Then specific antibodies are used to detect the proteins of interest and an appropriate secondary antibody, which binds specifically to the primary antibody, is incubated with the membrane. The secondary antibody contains a conjugated tag such as horseradish peroxidase (HRP) that will bind to the primary antibody. The antibodies are visualized by adding chemiluminescent reagents to the membrane followed by exposure to X-ray film.

Preparation of Western blots

Jurkat or HL60 cells ($5x10^5$ cells/ml) were treated with either silver nitrate (1 µg/ml) or AgNPs (1 µg/ml) and incubated for 4 hours or 24 h. Etoposide (50µM) was used as a positive control. At the appropriate appointed time the medium was removed and the cells were centrifuged for 5 min at 5000 rpm and the cell pellet washed twice in cold PBS.The PBS was removed to waste and 50 µl lysis buffer (LDS Sample Buffer4x, Invitrogen) containing 5% 2-mercaptoethanol (Sigma) was added. The samples were lysed using a sonicator probe then they were heated to 95°C for 5 minutes. The protein concentration was determined by the Coomassie Protein Assay (Thermo Scienfific). Lysed sample (1 µl) was added to 19 µl of water to which 1 ml of Coomassie reagent was added. The amount of protein was then determined by reading in a spectrophotometer at 595 nm using lysis buffer to zero the samples. Absorbance readings were then compared to a standard curve of known bovine serum albumin concentrations.

Equal amounts of protein (12 µg) were separated on 4-12% bis-tris polyacrylaminde gel (Invitrogen). Molecular weight protein markers (Seeblue plus2 pre-stained standard, Invitrogen) were loaded at 8 µl at one end of the gel and 4 µl at the other side to indicate the orientation of the gel after electrophoresis. The gels were run at 165 volts for one hour and a half or until the dye at the front had reached the bottom of the gel. Proteins were then transferred to nitrocellulose membrane (Hybond C Extra, GE Healthcare).

The membrane was soaked in a small amount of Ponseau S (Sigma) solution to check the quality of transfer and protein separation and then rinsed with TBST (50mM TRIS pH 7.6, 150 mM NaCl, and 0.2 % Tween-20) for 5 min to remove the Ponseau S solution. After that the membrane was incubated in 50 ml of blocking solution (5% milk powder in TBST) for 1 hour to reduce non- specific antibody binding.

The membrane was then probed using a primary antibody of interest; these include: cleaved PARP (asp214) antibody (human specific) (Signalling Technologies), anti-GAPDH mouse mAb (6C5) (Calbiochem) and phospho-histone H2A.X (ser139) antibody (Signalling Technologies). Primary antibodies were diluted in 5 ml of blocking solution in 50 ml Falcon tubes; the dilution was 2:5,000, 1:1,000 and 2:5,000 respectively. The membrane was incubated with the primary antibody overnight before washing twice in TBST, each for 5 min. The membrane was incubated in appropriate HRP conjugated secondary antibody (1:5,000 in blocking buffer) in a 50 ml falcon tube for 30 min then washed in TBST, with several changes of a buffer over one hour. The membrane was visualized using chemiluminescence (ECL plus, GE Healthcare). After adding the ECL

reagents the membranes were sealed within plastic sheets and the images captured by a Syngene G: Box gel documentation system. Image analysis was by Gene Tools

2.2.5 *qPCR array for oxidative stress markers*

PCR array uses a set of optimized real-time PCR primer assays on 96-well plates for oxidative stress pathway among others. PCR array profiles the expression of 84 genes related to oxidative stress and real-time PCR is used to analyze expression of a focused panel of genes related to oxidative stress within the array. The array provides valuable information on the oxidative stress status of the cell after exposure to AgNPs.
Jurkat cells or HL60 cells ($5x10^5$ cells/m) in RPMI medium were treated with silver nitrate (1µg/ml) or positively charged AgNPs (1µg/ml) or negatively charged AgNPs (1µg/ml) and incubated for 24 h at 37 °C in 5% CO_2. The medium was then removed and the cells centrifuged at 3,000 rpm for 5 min. The cell pellet was washed twice in cold PBS at 3,000 rpm for 5 min. The PBS was removed and the cell pellet was extracted for RNA using the RNeasy kit (Qiagen), following the manufacturer's protocol. RNA quality and concentration was measured using a NanoDrop® ND-1000 UV-vis Spectrophotometer (Labtech). Extracted RNA was further purified using Deoxyribonuclease I, Amplification Grade (Invitrogen) and measured again. cDNA was prepared from the RNA samples (1µg) using RT^2 First Strand Kits, C-03 (SABiosciences). cDNA was then added to RT^2 qPCR Master Mix (SYBR Green) and the PCR products (25µl) were added to a 96 well RT^2 Profiler™ PCR Array Human Oxidative Stress and Antioxidant Defense plate (PAHS-065A, SABiosciences). The plate was run in an iCycler iQ real-time PCR system (Bio-Rad). The following amplification protocol was applied: after 10 min of incubation at 95 °C to activate the Hot Start DNA polymerase, 40 cycles of amplification were accomplished with (a) 15s at 95 °C for denaturation and (b) 60s at 60 °C for annealing (fluorescence detection). The PCR reactions were performed in separate 96-well plates in each group. Each PCR array profiles the expression of 84 pathway specific genes plus house keeping control marker. Gene expression data analysis was performed using the software provided by SABiosciences.

2.2.6 *Transmission electron microscopy (TEM) and energy dispersive X-ray spectroscopy (EDX)*

Jurkat cells or HL60 cells ($5x10^5$ cells/ml) were treated with silver nitrate (1µg/ml), negatively charged AgNPs (1µg/ml) or untreated cells and incubated for 10 min, 30 min and 24 h. The medium was then removed and the cells were centrifuged at 1000 rpm for 3 min. The cell pellet was fixed in 2% gluteraldehyde in sodium cacodylate buffer at 4°C for overnight and the cells were then secondary fixed in 1% osmium tetroxide for 1 h then the cells were enrobed in agarose. The cell preparations were dehydrated using 25% acetone, 50% acetone, 75% acetone for 30 min each and then 100% acetone for an hour. Cells were impregnated with 25% resin (TAAB epoxy resin kit) in acetone, 50% resin in acetone, 75% resin in acetone for an hour each and then 100% resin with a minimum of 3 changes over 24 h. The cell preparations were embedded in 100% resin in a mould at 60° C for 24 h. After polymerization, ultrathin sections (approximate 80 nm thickness) were cut using a diamond knife on a RMC MT-XL ultramicrotome. The sections were stretched using chloroform to eliminate compression and then mounted on Pioloform filmed copper grids (for samples viewed using transmission microscope) or mounted on copper grids (for samples examined using energy dispersive X-ray spectroscopy). The grid was strained with 2% aqueous uranyl acetate and lead citrate (Leica) (for samples viewed using transmission microscope). The grids were examined using a Philips CM 100 Compustage (FEI) transmission electron microscope and digital images were collected using an AMT CCD camera (Deben) (Electron Microscopy Research Services, Newcastle University). The grids were analysed using a JEOL 2100F FEG transmission electron microscope with energy dispersive X-ray spectroscopy Oxford INCAx-sight and digital images were collected using Gatan GIF tridiem (The Durham GJ Russell Microscopy Facility, Durham University).

2.2.7 Epigenetic changes

A pyrosequenzer is used to study global DNA methylation for preliminary analysis (Wright et al, 2010). Typical measurements of global methylation involve analysis within repetitive DNA sequence. Long Interspersed Nucleotide Elements (LINE-1), half a million repetitive elements in human DNA were selected for analysis of methylation in this study. The study of Wright et al (2010) showed an association between lead exposure and LINE-1 DNA methylation which may represent a biomarker of past lead

exposure. Since lead and silver are transitional elements, this part of the research aimed to measure methylation of LINE1 in order to assess global DNA methylation associated with exposure to AgNPs.

DNA extraction and bisulfite treatment

Jurkat cells or HL60 cells containing $5x10^5$ cells/ml were treated with either of silver nitrate (1 µg/ml), negatively charged AgNPs (1 µg/ml) or positively charged AgNPs (1µg/ml) and incubated for 4 h, 24 h or 48 h. Untreated cells were used as a control. At the appropriate appointed time, the medium was removed and the cells were centrifuged for 5 min at 5000 rpm, the cell pellet was then washed twice in cold PBS. Genomic DNA was extracted from samples using DNeasy blood & tissue kits (Qiagen). DNA was treated using EZ DNA Methylation-Gold™ Kit (Zymo Research Corp) according to the manufacturer's recommendations. The final elution was performed with 30µl of M-Elution Buffer.

LINE-1 PCR and pyrosequencing

Bisulfite-treated DNA was amplified by PCR using primers designed for a LINE-1 sequence. PCR was carried out using 12.5 µl of Qiagen hotstar mastermix (Qiagen) 1 pmol of the forward primer (TTTTGAGTTAGGTGTGGGATATA), 1 pmol of the biotinylated reverse primer (biotin-AAAATCAAAAAATTCCCTTTC), 1µl of bisulfite-treated genomic DNA, 3 µl of 10x reaction buffer with $MgCl_2$ (Sigma), and 6.5 µl of molecular grade water. The cycling conditions were as follows: denaturation at 95 °C for 15 min, followed by 50 cycles of denaturation at 95 °C for 15 s, annealing at 50 °C for 30 s and extension at 72 °C for 15 s followed by a final extension cycle of 72 °C for 5min. Biotin-labeled primers were used to purify the final PCR product using Sepharose beads. The PCR product was bound to Streptavidin Sepharose HP (Amersham Biosciences) and the Sepharose beads containing the immobilized PCR product were purified, washed, and denatured using 0.2 M NaOH, and washed again using the Pyrosequencing Vacuum Prep Tool (Pyrosequencing, Inc.), as recommended by the manufacturer. Then, 10 µM of the pyrosequencing primer was annealed to the purified single-stranded PCR product and pyrosequencing was performed using the PyoMark MD (Biotage) The relative 5-mC content was expressed as percentage of methylated cytosines divided by the sum of

methylated and unmethylated cytosines (5-mC/[5-mC + unmethylated cytosine] = %5-mC). Built-in controls were used to verify bisulphite conversion efficiency.

2.2.8 ICP-MS

Inductively coupled plasma mass spectrometry (ICP-MS) is an extremely sensitive technique that can measure and identify metals in the pM-nM range. ICP-MS uses quadrupole mass spectrometry for measurement of individual atomic isotopes. Inductively coupled plasma (ICP) is the method by which the sample is atomized and ionized to generate positively charged atomic ions to feed into the MS. The MS switches between a setting for each metal isotope to allow detection of specific ionic forms of the metals of interest.

Protein extraction and analysis

Jurkat cells or HL60 cells containing $5x10^5$ cells/ml were treated with either silver nitrate (1 µg/ml) or AgNPs (1 µg/ml) and incubated for 4 h or 24 h. At an appropriate time the medium was removed and the cells were centrifuged for 5 min at 5000 rpm, the cell pellet was then washed in cold PBS and kept at -80°C until analysis. Each preparation was freeze-thawed in 250 µl buffer (25mM Hepes, pH7.5). Followed by brief freezing under a stream of nitrogen for 3 min. The cells were then thawed, and vortexed vigorously. The two previous steps were repeated 3 times and then the samples were spun for 5 min at maximum speed to separate the supernatant (containing soluble proteins) from the pellet. The supernatant was removed to a clean tube. The concentration of the preparation protein was quantified by absorbance at 280 nm calibrated against protein standard. Total soluble protein preparations (100 µl) were loaded onto a high performance liquid chromatography (HPLC) size exclusion column (SW3000 matrix, Tosoh Bioscience), resolved in 5 mM Hepes pH 7.5, 50 mM NaCl. The flow rate was 0.5 ml/min and fractions were collected every minute. 300 µl of the fraction was diluted 1:10 in 2.5% nitric acid (Suprapur, Merck), containing 20 µg/L Co and 20 µg/L Pt as internal standards, for analysis by ICP-MS (Thermo Electron Corp., X-Series). Mass ions (55Mn, 59Co, 63Cu, 65Cu, 66Zn, 107Ag and 195Pt) were monitored (100 reads of 25ms each in 5 channels with 0.02 AMU separations) in triplicate measurements, and concentrations of the metal containg proteins were calculated by comparison to matrix-matched mixed-element standard solutions.

SOD 1 activity assay

Negatively stained polyacrylamide gel was used to determine Superoxide Dismutase (SOD1) activity. Aliquots (50 µl) of copper containing fractions of eluant from the HPLC size exclusion chromatography of the soluble lysates from cells exposed to AgNPs for 4h and 24 h were analysed by polyacrylamide gel electrophoresis (PAGE) on an 15% (w/v) acrylamide gel. The gel was first soaked in 30 ml of 2 mM nitroblue tetrazolium (NBT) for 15 min, briefly washed, then soaked in the dark in 30 ml 20 mM Tris 1M buffer (pH7.5) containing 30 mM tetramethylenediamine (TEMED) and $3x10^{-2}$ mM riboflavin for another 15 min. The gel was briefly washed again, and then illuminated on a light box with a dense light intensity for 15 min to initiate the photochemical reaction. All the procedures were carried out at room temperature, and the two soaking steps were shaken on a platform. The gel was scanned using an ImageJ application (NIH) immediately after the photochemical reaction.

2.2.9 *Dialysis to determine free Ag^+ ions*

Free Ag^+ ions were determined by equilibrium dialysis. The experiments used cellulose ester dialysis tubing (GeBAflex-tube Midi, 8 kDa) that had been thoroughly prewashed in distilled water. Preliminary experiments were carried out in order to determine equilibration times (~24 h) for Ag^+ ions through the membranes.

The dialysis tubes were filled with 0.8 ml of either 1µg/ml or 10µg/ml of AgNPs in growth medium containing Jurkat or HL60 cells, then sealed and placed in plastic bags containing 4 ml of each experimental solution (see results). Experiments were allowed to reach dialysis equilibrium over 4, 12, 24 and 48 h. At the appropriate time the experiment was terminated and samples (300 µl) were taken from the medium surrounding the dialysis tube for analysis. The samples were then acidified in 2.5% nitric acid (Merck) by diluting 1:10. They were analysed by ICP-MS (Thermo Electron Corp., X-Series) for silver. Cobalt (20 µg/L) was added to all samples as an internal standard to calibrate the instrument for silver. Metal concentrations were determined by comparison to matrix-matched elemental standards.

2.2.10 Detecting of apoptosis and necrosis in cells using an Annexin-V FITC kit

(Modified from Gunaratnam and Grant, www. sigmaaldrich.com/img/assets/6780/ Detectin Apoptosis.pdf.)

Apoptosis is a normal programmed process that occurs during the life cycle of the cell. The process is characterized by specific morphologic changed such as loss of plasma membrane asymmetry that is the earliest sign of the apoptosis and this is usuallly used to detect apoptosis and necrosis in cells. In apoptotic cells, phospholipid phosphatidylserine (PS) in the membrane is translocated from the inner to outer plasma membrane which allows PS to bind with Annexin V which can be conjugated to a fluorochrome and detected during apoptosis observed by microscope. While the membrane of dead and damaged cells are permeable to propidium iodied (PI) consequently late apoptosis in cells and necrosis in cells are detected both Annexin V and PI.

The AnnexinV-PI assay allows determination of healthy cells (annexin V^-, PI^-); early apoptotic cells (annexin V^+, PI^-) and necrotic cells (annexin V^-, PI^+) using the Annexin V-FITC kit (Sigma). The kit allows detection of Annexin V bound to apoptotic cells with fluorescein isothiocyante (FITC) which labels phosphatidylserine sites on the membrane surface while propidium iodide (PI) labels the DNA of necrotic cells, having permeable cell membranes. This kit allows determination by fluorescence microscopy.

Jurkat and HL60 cells ($5x10^3$ cells/ml) were exposed to a single dose of negatively charged AgNPs (1 µg/ml) (Sigma, NanoComposite) or 1 µg/ml of silver nitrate for 4 h or 24 h. At each time point the cells were washed twice times with the PBS. After that, the cells were resuspended in 1x binding buffer at a concentration of ($2x10^4$ cells/ml). 125 µl of cell suspensions were mixed with 1.25µl of Annexin V FITC Conjugate and 2.5 ml of propidium iodide solution.The cells were incubated at room temperature for exactly 10 minutes and protected from light. A 2% solution of low melting point agarose (LMPA) was prepared in PBS (dissolved in a water bath at 90°C or microwaved). The LMPA was then transferred to a water bath at 37°C and allowed to equilibrate. At an appropriate time the 60 µl of cell suspension was mixed with 60µl of LMPA and dropped 60 µl onto a chilled microscope slide. Gels were spread evenly on a microscope slide by adding a coverslip and allowing them to set by placing them on an aluminum tray sat on a bed of ice.Then they were immediately viewed with the fluoresscence microscopy.

CHAPTER 3

THE CYTOTOXICITY OF SILVER NANOPARTICLES TO HUMAN CELL IN VITRO

Chapter 3. The cytotoxicity of silve nanoparticles to human cell *in vitro*

3.1 The cytotoxic effects of silver nitrate compared to AgNPs at a single high dose

AgNPs are being increasingly used in daily life. These materials are contained in numerous consumer products and this raises concerns about the possibility of adverse effects on human health. To date, information about the toxicity these materials has still not been clarified. It is believed that bulk forms of silver have no adverse health effects to humans when they are exposed to levels producing ~ 2.3 μg/L, in blood, which have been seen in individuals with no adversed effects (Wan et al, 1991). Many studies have evaluated the acute toxic effects of AgNPs at relatively high doses but chronic toxicity at low doses should also be evaluated to reflect chronic exposure to AgNPs *in vivo*. Currently, the fate and toxicity of AgNPs is unclear and it is unknown whether it is the AgNPs that are toxic or whether toxicity results from free silver ions being released from the NPs. To evaluate this, experiments were designed so that the cells were exposed to AgNPs in parallel with $AgNO_3$ to represent exposure to AgNPs and Ag^+ ions, respectively.

In this part of the research, the toxic effects of AgNPs were investigated in HL60 and Jurkat cells in comparison to $AgNO_3$ for various exposure times. In these experiments a "high dose" represents 1 μg/ml-10 μg/ml.

The cytotoxic effects of $AgNO_3$ to Jurkat and HL60 cells in vitro

Jurkat and HL60 cells ($5x10^3$ cells/ml) were exposed to $AgNO_3$ (1, 5, 10 μg/ml) for 4, 24 and 48 h. At each time point, the cells were harvested and washed in fresh RPMI prior to analysis of cell viability using the MTT assay (see Methods, Chapter 2) This study was conducted at relatively high $AgNO_3$ concentrations to assess cytoxicity to both cell types from Ag^+ ions for up to 48 h. Cells were also exposed to a single dose of H_2O_2 (50 μM) for the same time points as an indicator of cytotoxicity from a chemical known to cause loss of cell viability by oxidative stress (positive control)

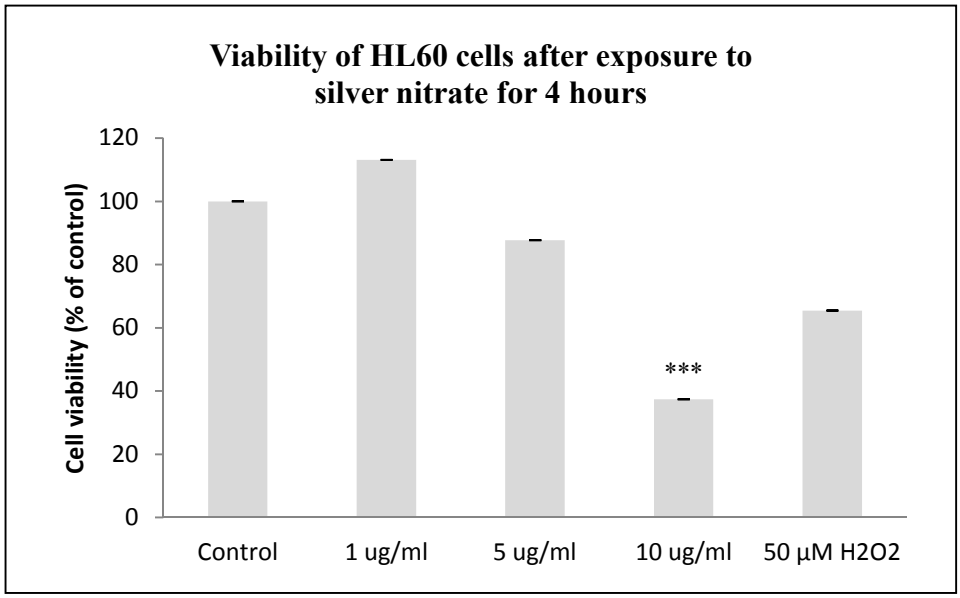

Figure 3.1 The cytotoxicity of silver nitrate to HL60 cells. Cells were exposed to 1, 5 and 10 µg/ml silver nitrate or H_2O_2 (positive control) for 4 hours. Cell viability was determined by the MTT assay. The data are expressed as the mean ±SEM of triplicate culture wells. Values are given in Appendix A (Table 1). ***P<0.001 (one way ANOVA)

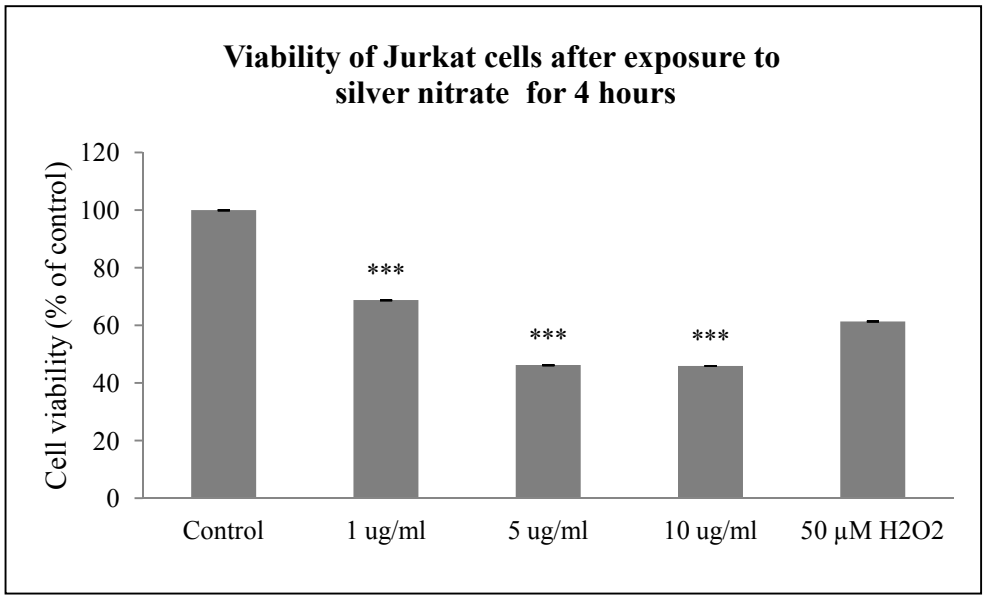

Figure 3.2 The cytotoxicity of silver nitrate to Jurkat cells. Cells were exposed to 1, 5 and 10 µg/ml silver nitrate or H_2O_2 (positive control) for 4 hours. Cell viability was determined by the MTT assay. The data are expressed as the mean ±SEM of triplicate culture wells. Values are given in Appendix A (Table 2). ***P<0.001 (one way ANOVA)

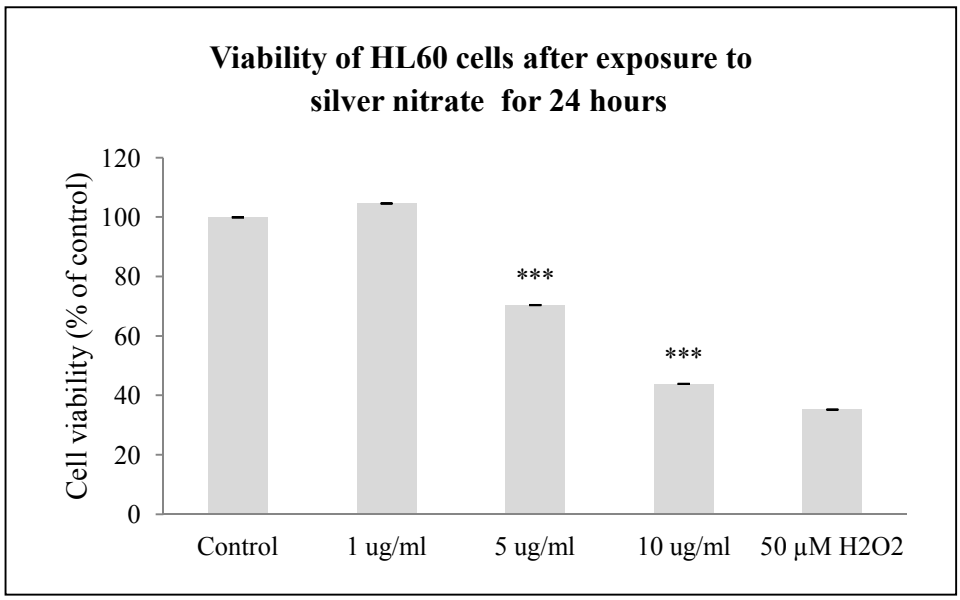

Figure 3.3 The cytotoxicity of silver nitrate to HL60 cells. Cells were exposed to 1, 5 and 10 µg/ml silver nitrate or H_2O_2 (positive control) for 24 hours. Cell viability was determined by the MTT assay. The data are expressed as the mean ±SEM of triplicate culture wells. Values are given in Appendix A (Table 1). ***P<0.001 (one way ANOVA)

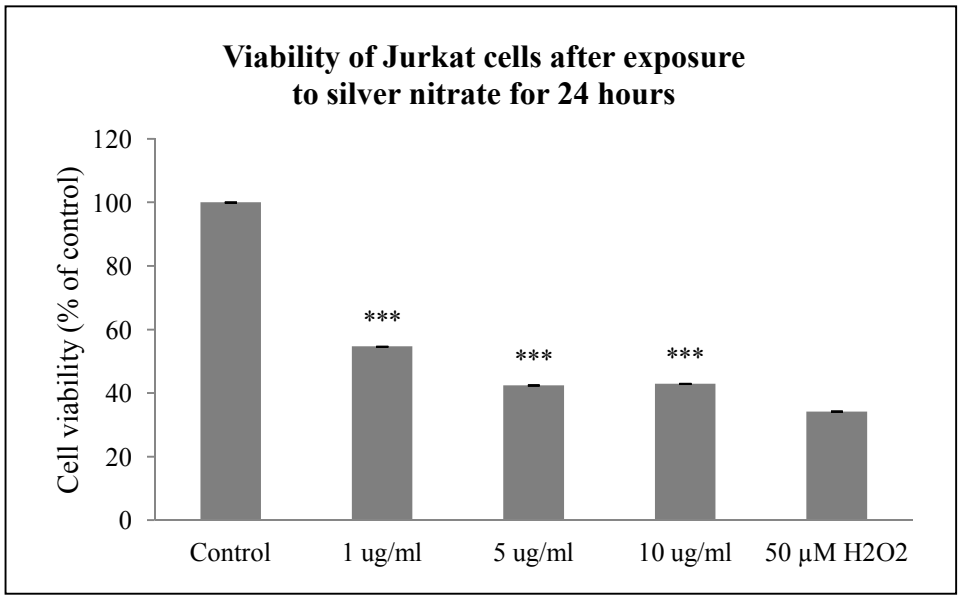

Figure 3.4 The cytotoxicity of silver nitrate to Jurkat cells. Cells were exposed to 1, 5 and 10 µg/ml silver nitrate or H_2O_2 (positive control) for 24 hours. Cell viability was determined by the MTT assay. The data are expressed as the mean ±SEM of triplicate culture wells. Values are given in Appendix A (Table 2). ***P<0.001 (one way ANOVA)

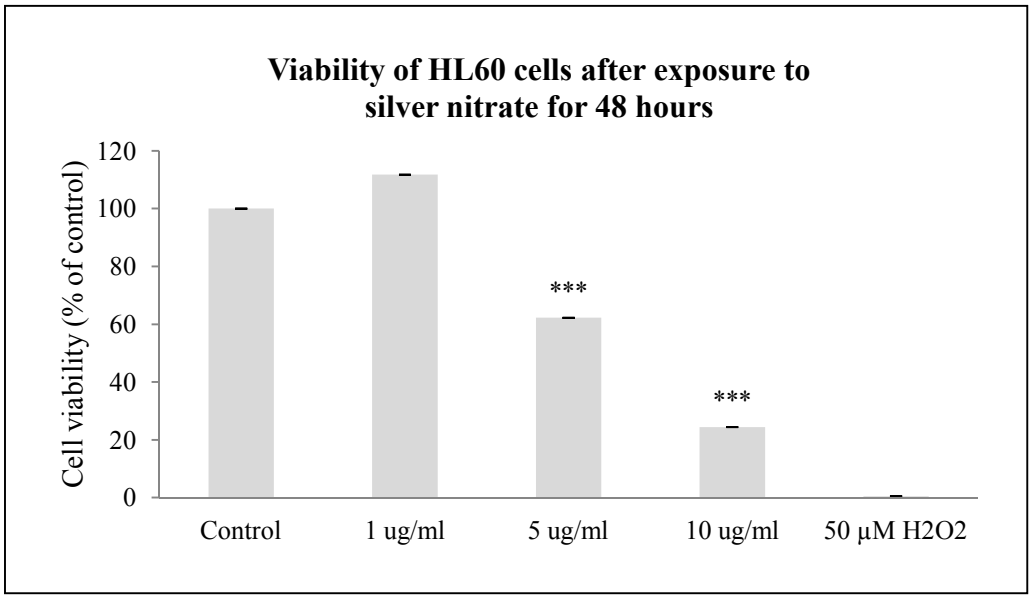

Figure 3.5 The cytotoxicity of silver nitrate to HL60 cells. Cells were exposed to 1, 5 and 10 µg/ml silver nitrate or H_2O_2 (positive control) for 48 hours. Cell viability was determined by the MTT assay. The data are expressed as the mean ±SEM of triplicate culture wells.Values are given in Appendix A (Table 1). ***P<0.001 (one way ANOVA)

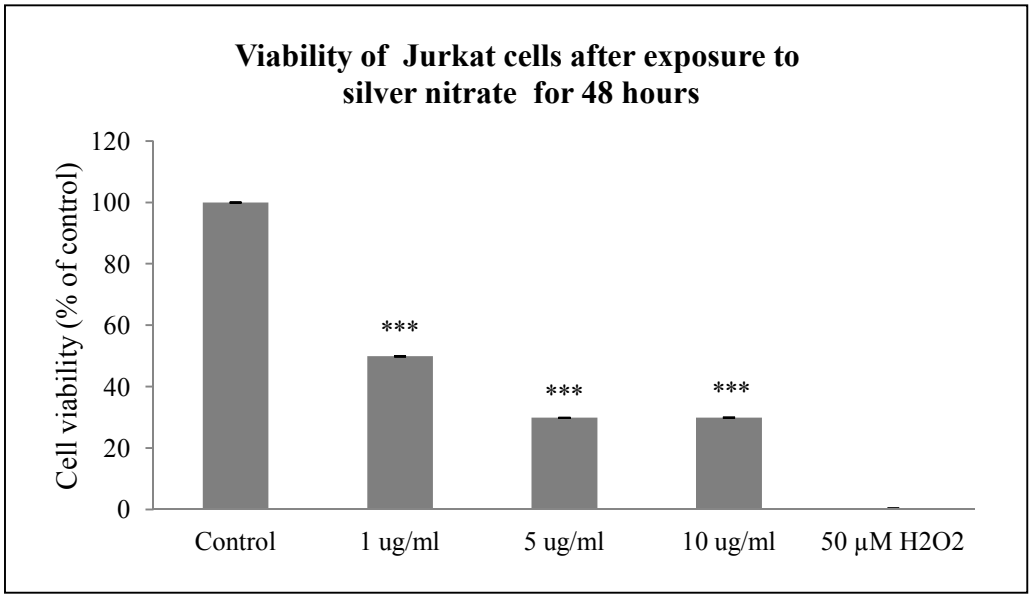

Figure 3.6 The cytotoxicity of silver nitrate to Jurkat cells. Cells were exposed to 1, 5 and 10 µg/ml silver nitrate or H_2O_2 (positive control) for 48 hours. Cell viability was determined by the MTT assay. The data are expressed as the mean ±SEM of triplicate culture wells.Values are given in Appendix A (Table 2). ***P<0.001 (one way ANOVA)

Summary of results of studies with silver nitrate at high dose (1-10 µg/ml)

- H_2O_2 caused loss of cell viability in a time dependent manner (~50% loss at 4h, 70% loss at 24h and 100% loss at 48h) which was similar in both cell types.
- $AgNO_3$ caused a dose and time dependent loss of cell viability in HL60 cells with only ~20% of cells remaining viable at the highest dose (10 µg/ml) at 48 h.
- $AgNO_3$ also caused a dose and time dependent loss of cell viability in Jurkat cells, again only ~20% of cells remained viable at 48 h following dosing with 10 µg/ml.
- $AgNO_3$ caused a greater loss of cell viability in Jurkat cells compared to HL60 cells, particularly at the lower concentrations (1 µg/ml and 5 µg/ml).
- At the lowest dose of $AgNO_3$ (1µg/ml), there was a suggestion of increased proliferation of HL60 cells of all time points, but this did not reach significance.

The cytotoxicity of negatively charged AgNPs to Jurkat and HL60 cells in vitro

Jurkat and HL60 cells ($5x10^3$ cells/ml) were exposed to a single dose of negatively charged AgNPs (1, 5, 10 μg/ml) for 4, 24 and 48 h. As for the previous experiment using $AgNO_3$, at each time point the cells were harvested and taken for viability analysis using the MTT assay (see Methods, Chapter 2). The cells were exposed to the AgNPs at the same concentrations as $AgNO_3$ on the basis of weight (μg/ml). Again, H_2O_2 (50 μM for 4, 24, 48 h) was used as the positive control.

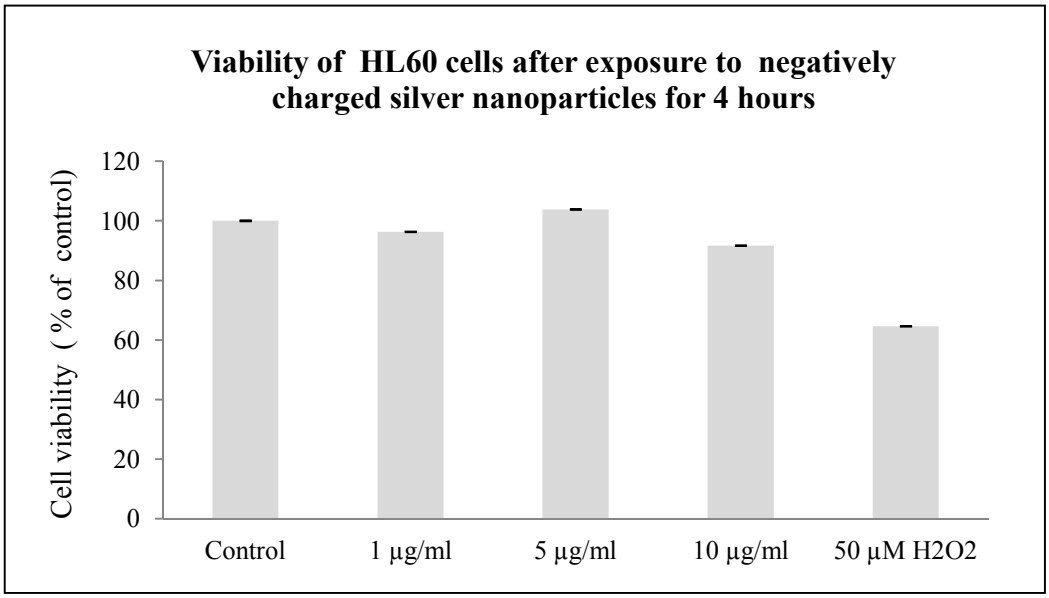

Figure 3.7 The cytotoxicity of negatively charged AgNPs to HL60 cells. Cells were exposed to 1, 5 and 10 µg/ml silver nitrate or H_2O_2 (positive control) for 4 hours. Cell viability was determined by the MTT assay. The data are expressed as the mean ±SEM of triplicate culture wells.Values are given in Appendix A (Table 3).

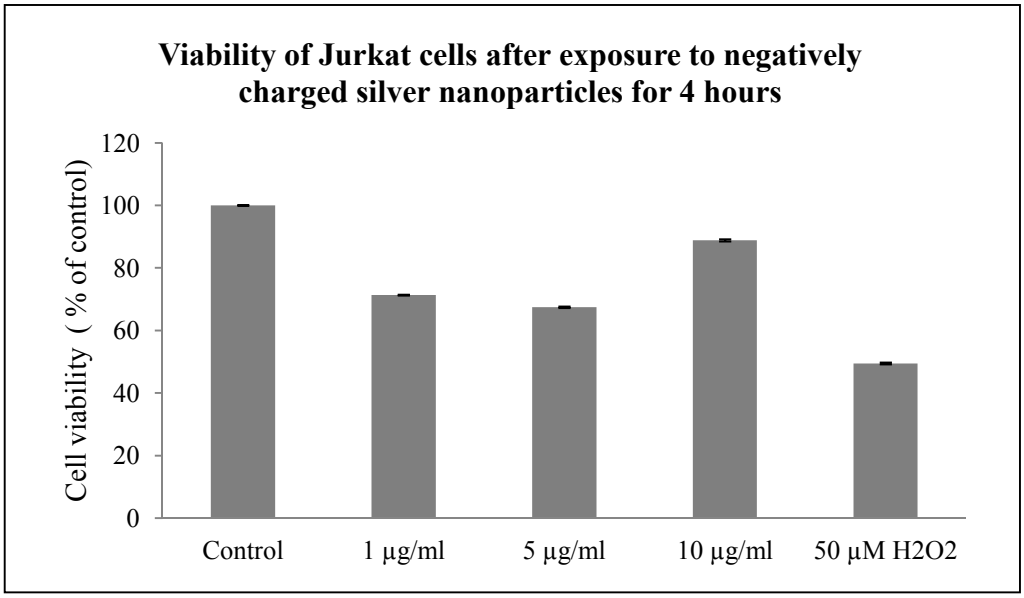

Figure 3.8 The cytotoxicity of negatively charged AgNPs to Jurkat cells. Cells were exposed to 1, 5 and 10 µg/ml silver nitrate or H_2O_2 (positive control) for 4 hours. Cell viability was determined by the MTT assay. The data are expressed as the mean ±SEM of triplicate culture wells.Values are given in Appendix A (Table 4).

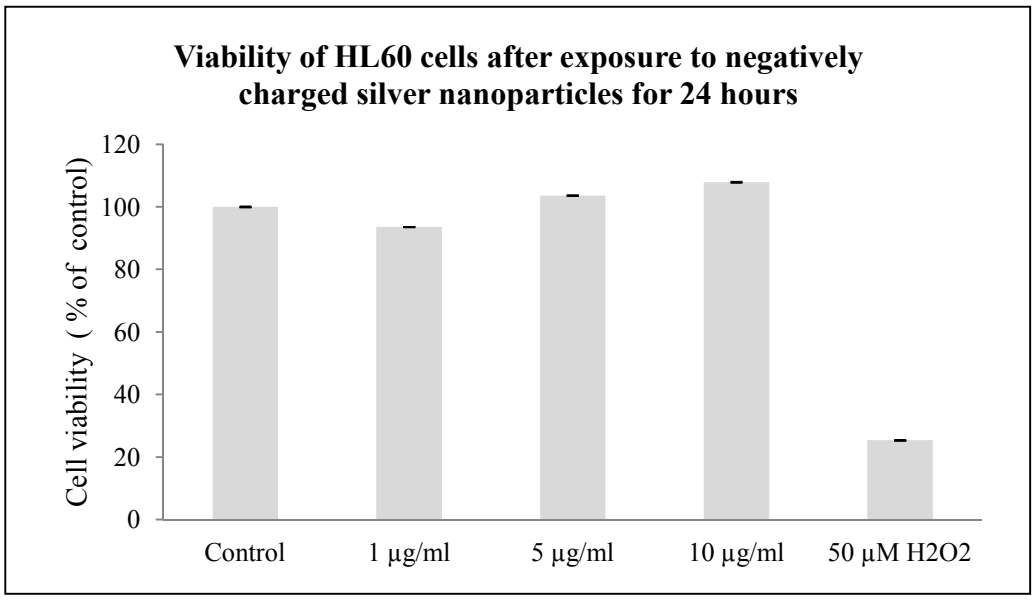

Figure 3.9 The cytotoxicity of negatively charged AgNPs to HL60 cells. Cells were exposed to 1, 5 and 10 µg/ml silver nitrate or H_2O_2 (positive control) for 24 hours. Cell viability was determined by the MTT assay. The data are expressed as the mean ±SEM of triplicate culture wells.Values are given in Appendix A (Table 3).

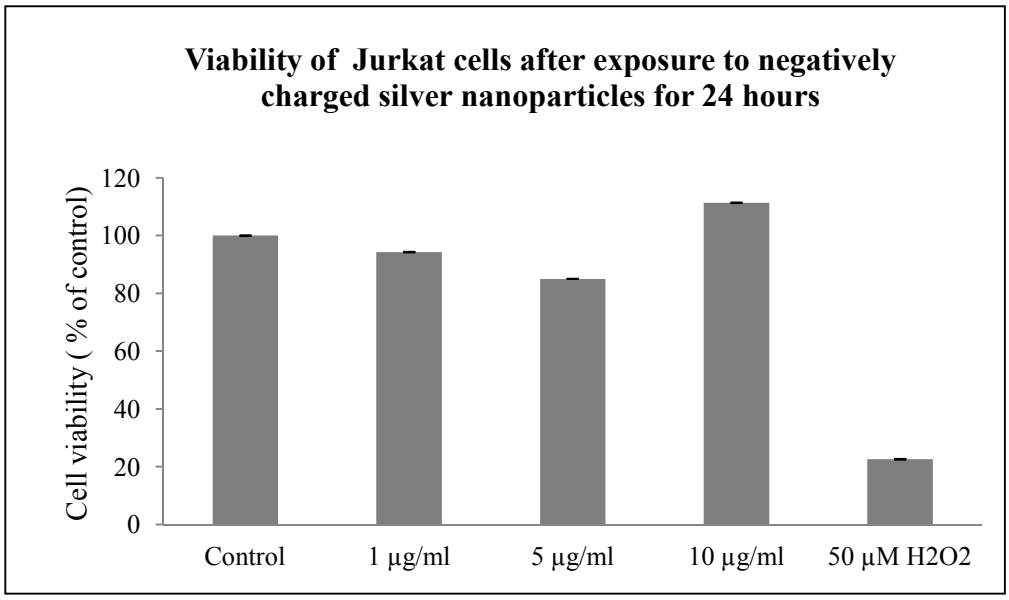

Figure 3.10 The cytotoxicity of negatively charged AgNPs to Jurkat cells. Cells were exposed to 1, 5 and 10 µg/ml silver nitrate or H_2O_2 (positive control) for 24 hours. Cell viability was determined by the MTT assay. The data are expressed as the mean ±SEM of triplicate culture wells.Values are given in Appendix A (Table 4).

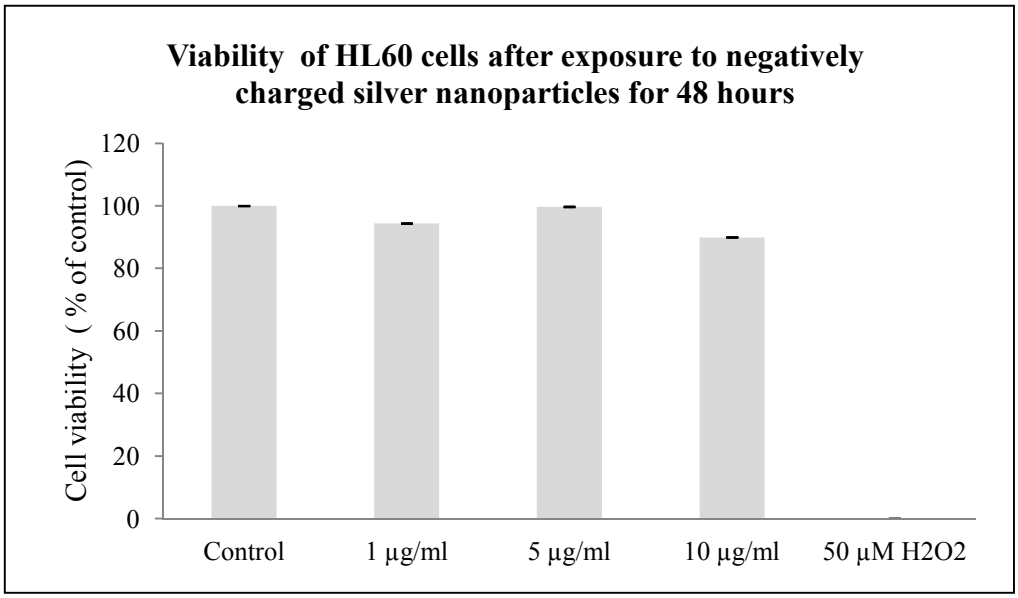

Figure 3.11 The cytotoxicity of negatively charged AgNPs to HL60 cells. Cells were exposed to 1, 5 and 10 µg/ml silver nitrate or H_2O_2 (positive control) for 48 hours. Cell viability was determined by the MTT assay. The data are expressed as the mean ±SEM of triplicate culture wells.Values are given in Appendix A (Table 3).

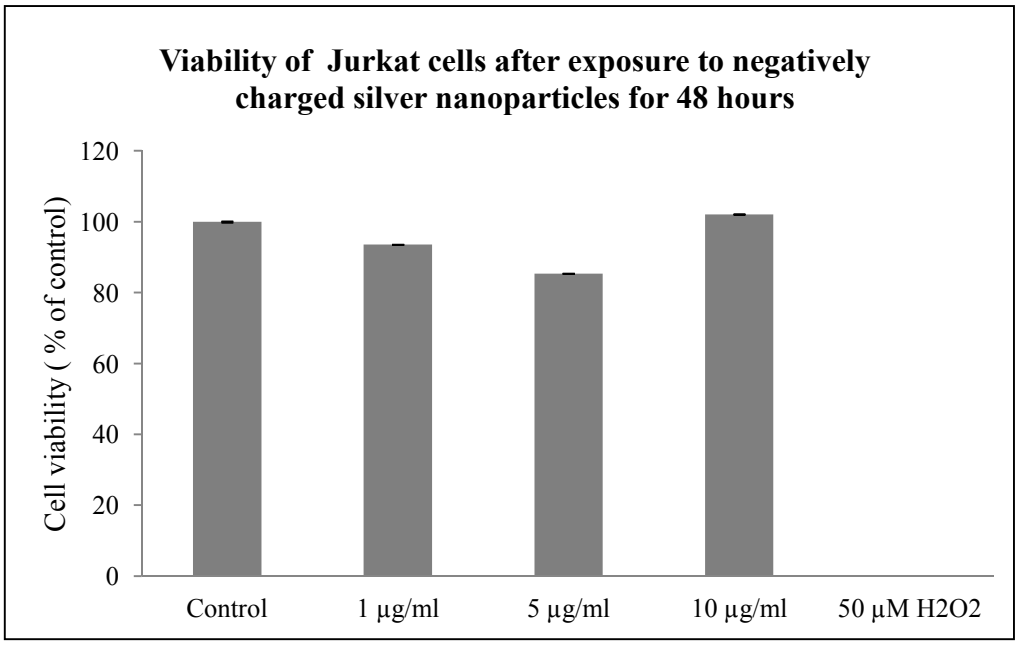

Figure 3.12 The cytotoxicity of negatively charged AgNPs to Jurkat cells. Cells were exposed to 1, 5 and 10 µg/ml silver nitrate or H_2O_2 (positive control) for 24 hours. Cell viability was determined by the MTT assay. The data are expressed as the mean ±SEM of triplicate culture wells.Values are given in Appendix A (Table 4).

Summary of results of studies with negatively charged AgNPs at high dose (1-10 µg/ml)

- H_2O_2 caused loss of cell viability with a profile that was similar to the $AgNO_3$ experiments.
- Negatively charged AgNPs caused only a small decrease in cell viability in HL60s.
- For Jurkat cells, negatively charged AgNPs caused about ~ 30% decrease in cell viability at 4h for the two lower doses (1 µg/ml and 5 µg/ml), while the highest dose had little effect. At later time points (24h and 48h), there was less effect on cell viability compared to that seen at 4 h.
- In contrast to $AgNO_3$, negatively charged AgNPs did not cause increased proliferation in HL60 cells.

The cytotoxicity of positively charged AgNPs to Jurkat and HL60 cells in vitro

Jurkat and HL60 cells ($5x10^3$ cells/ml) were exposed to a single dose of positively charged AgNPs (1, 5, 10 μg/ml) for 4, 24 and 48 h in parallel with the previous experiment with negatively charged AgNPs. As before, at each time point the cells were harvested and taken for analysis of cell viability using the MTT assay (see Methods, Chapter 2) Again, H_2O_2 (50 μM for 4, 24, 48 h) was used as the positive control.

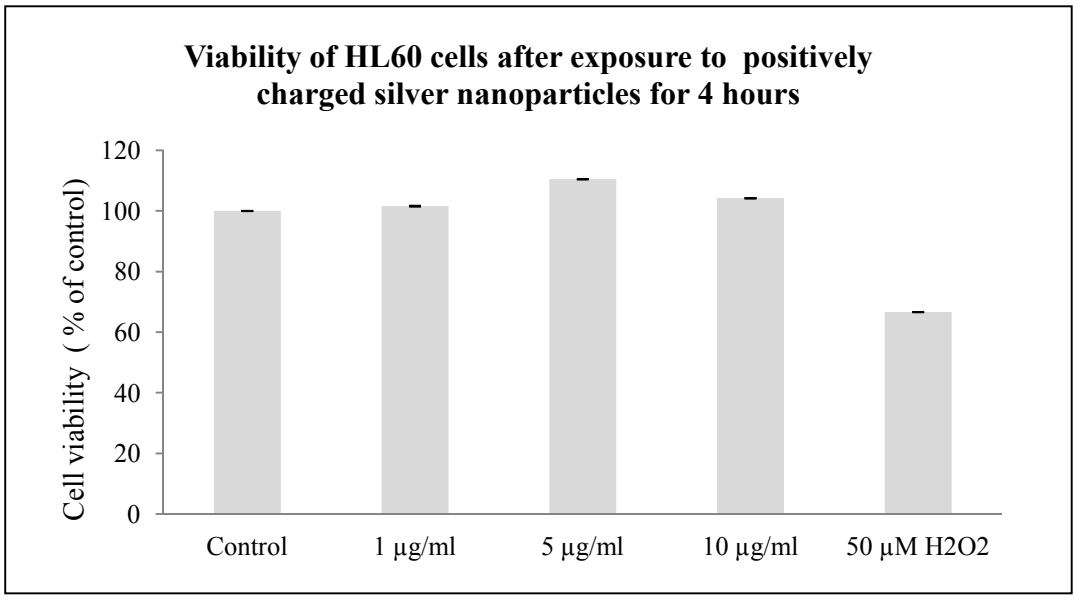

Figure 3.13 The cytotoxicity of positively charged AgNPs to HL60 cells. Cells were exposed to 1, 5 and 10 µg/ml silver nitrate or H_2O_2 (positive control) for 4 hours. Cell viability was determined by the MTT assay. The data are expressed as the mean ±SEM of triplicate culture wells.Values are given in Appendix A (Table 5).

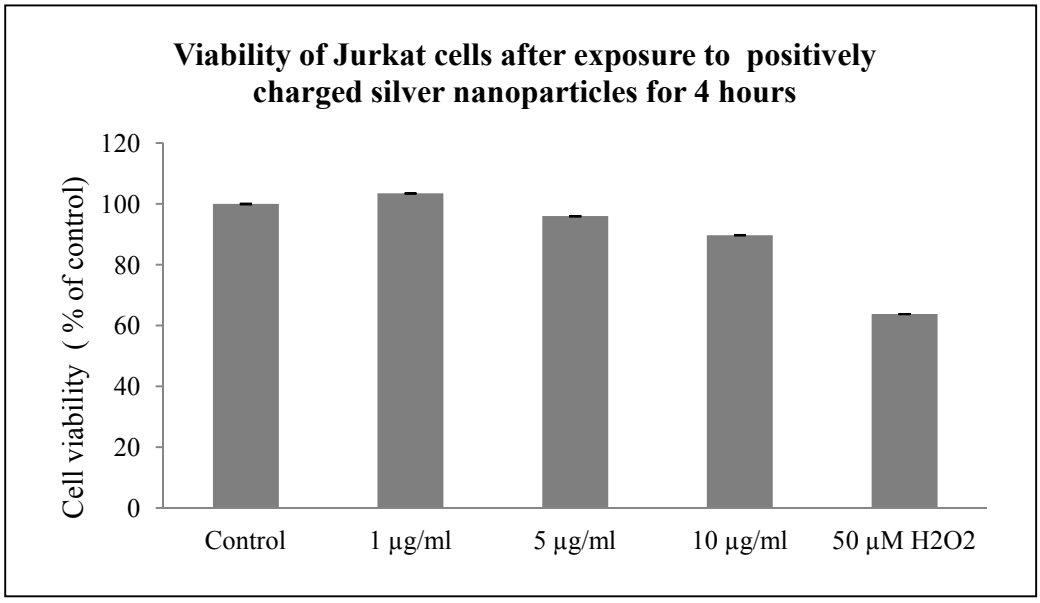

Figure 3.14 The cytotoxicity of positively charged AgNPs to Jurkat cells. Cells were exposed to 1, 5 and 10 µg/ml silver nitrate or H_2O_2 (positive control) for 4 hours. Cell viability was determined by the MTT assay. The data are expressed as the mean ±SEM of triplicate culture wells.Values are given in Appendix A (Table 6).

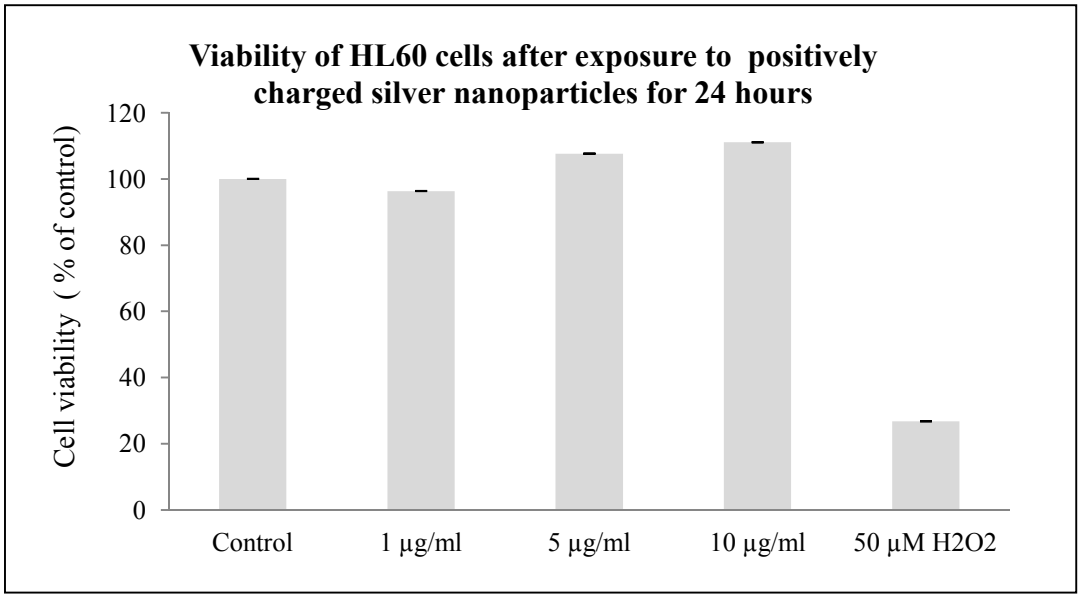

Figure 3.15 The cytotoxicity of positively charged AgNPs to HL60 cells. Cells were exposed to 1, 5 and 10 µg/ml silver nitrate or H_2O_2 (positive control) for 24 hours. Cell viability was determined by the MTT assay. The data are expressed as the mean ±SEM of triplicate culture wells.Values are given in Appendix A (Table 5).

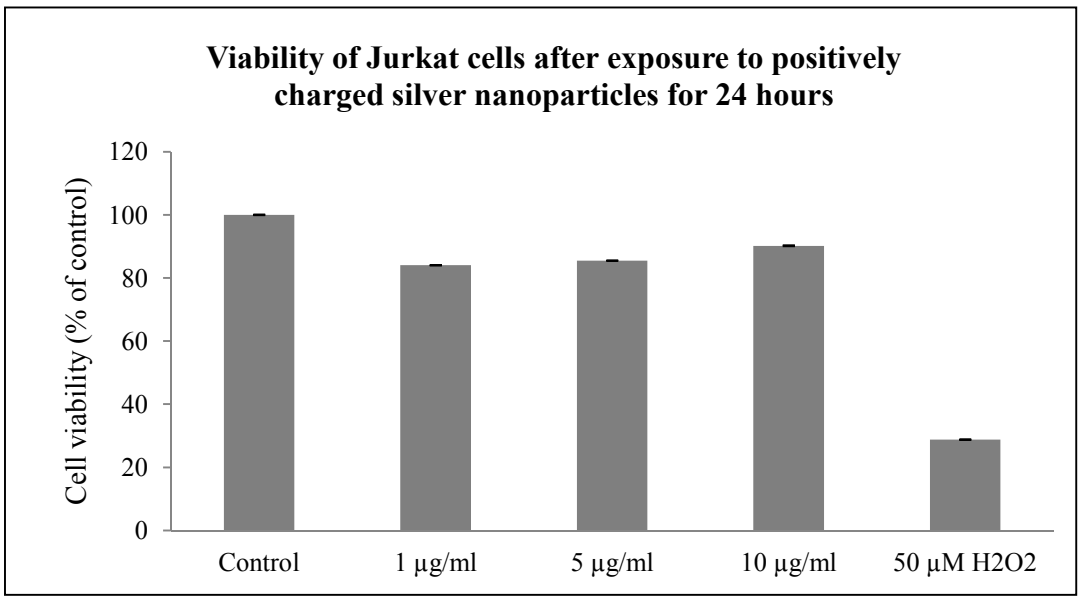

Figure 3.16 The cytotoxicity of positively charged AgNPs to Jurkat cells. Cells were exposed to 1, 5 and 10 µg/ml silver nitrate or H_2O_2 (positive control) for 24 hours. Cell viability was determined by the MTT assay. The data are expressed as the mean ±SEM of triplicate culture wells.Values are given in Appendix A (Table 6).

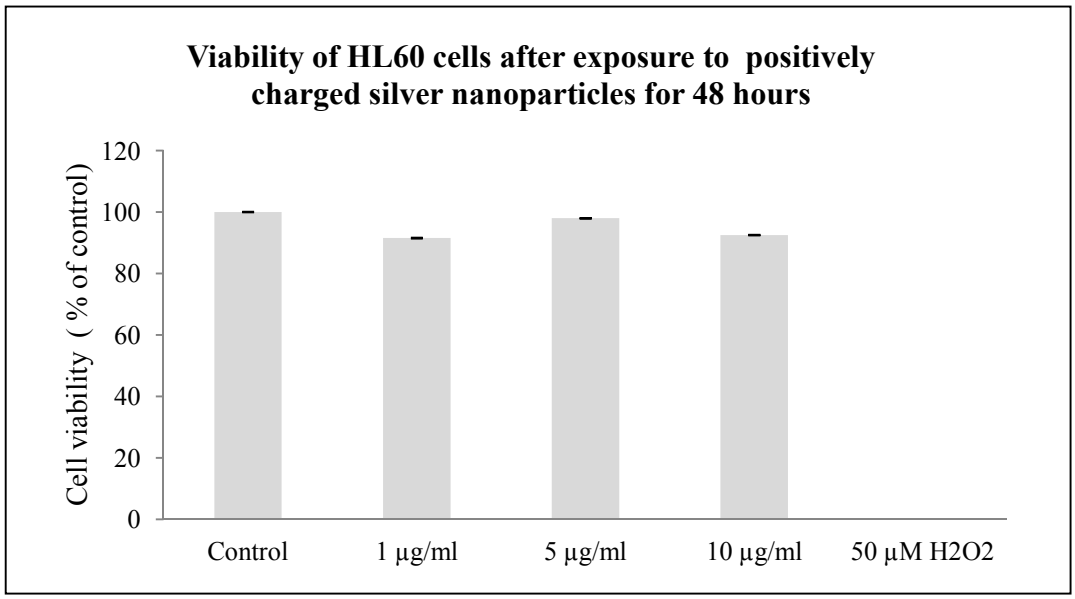

Figure 3.17 The cytotoxicity of positively charged AgNPs to HL60 cells. Cells were exposed to 1, 5 and 10 µg/ml silver nitrate or H_2O_2 (positive control) for 48 hours. Cell viability was determined by the MTT assay. The data are expressed as the mean ±SEM of triplicate culture wells.Values are given in Appendix A (Table 5).

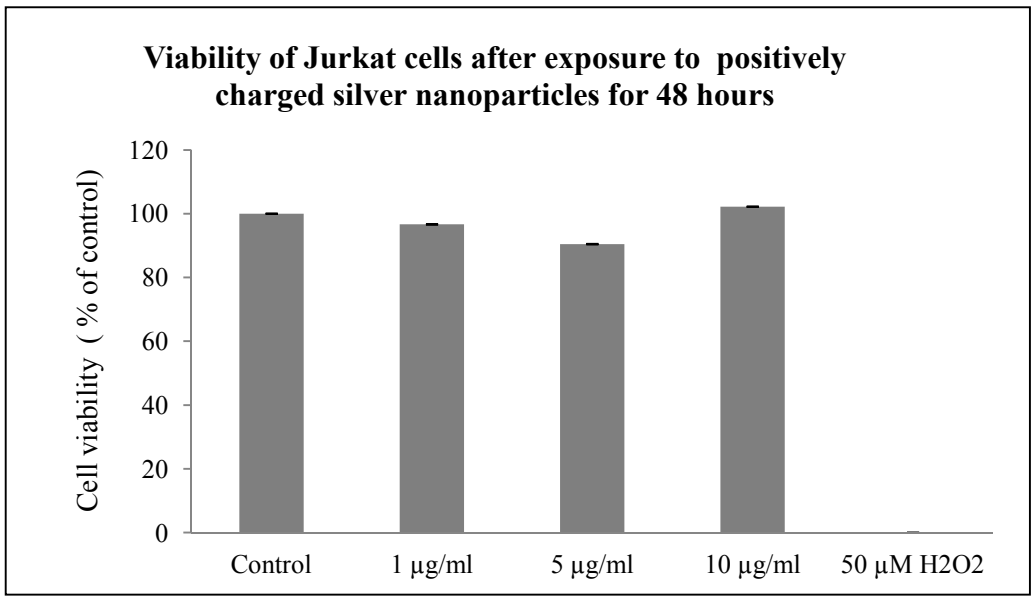

Figure 3.18 The cytotoxicity of positively charged AgNPs to Jurkat cells. Cells were exposed to 1, 5 and 10 µg/ml silver nitrate or H_2O_2 (positive control) for 48 hours. Cell viability was determined by the MTT assay. The data are expressed as the mean ±SEM of triplicate culture wells.Values are given in Appendix A (Table 6).

Summary of results of studies with positively charged AgNPs at high dose (1-10 µg/ml)

- H_2O_2 caused loss of cell viability in both cell types with a similar profile to that seen previously.
- Positively charged AgNPs caused little loss of cell viability to either Jurkats or HL60 cells at all doses and time points.
- In contrast to $AgNO_3$, the positively charged AgNPs (1µg/ml) did not increase proliferation in HL60 cells.

3.2 The effects of silver nitrate compared to AgNPs at a single low dose.

The cytotoxic effects of $AgNO_3$ compared to AgNPs at a single low dose

In the previous section of the research, relatively high doses (1-10 μg/ml) of $AgNO_3$ and AgNPs were used to establish the concentrations at which the elements caused loss of cell viability. In this set of experiments lower doses of $AgNO_3$ and AgNPs were used to establish the concentrations and time points when minimal loss of cell viability occurred. In these experiments "low dose" represents 0.01-1 μg/ml.

Jurkat and HL60 cells ($5x10^3$ cells/ml) were exposed to a single dose of $AgNO_3$ or the two types of AgNPs (0.01, 0.1, 0.5, 1 μg/ml) for 4, 24 and 48 h. As before, at each time point the cells were harvested and taken for analysis of cell viability using the MTT assay (see Methods, Chapter 2) Again, H_2O_2 (50 μM for 4, 24, 48 h) was used as the positive control.

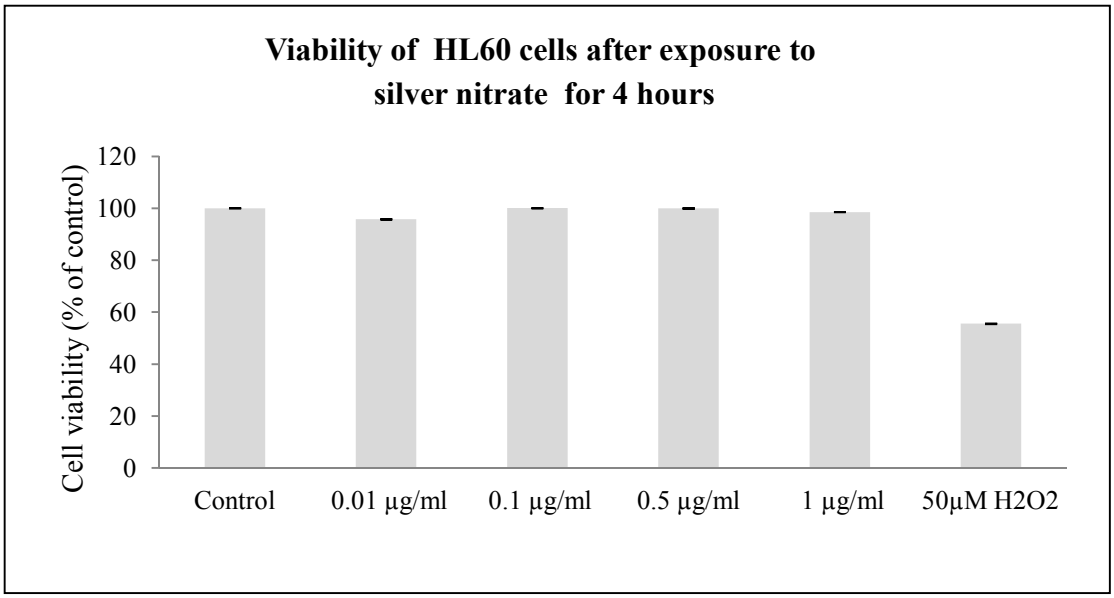

Figure 3.19 The cytotoxicity of silver nitrate to HL60 cells. Cells were exposed to 0.01, 0.1, 0.5 and 1 µg/ml silver nitrate or H_2O_2 (positive control) for 4 hours. Cell viability was determined by the MTT assay. The data are expressed as the mean ±SEM of triplicate culture wells.Values are given in Appendix A (Table 7).

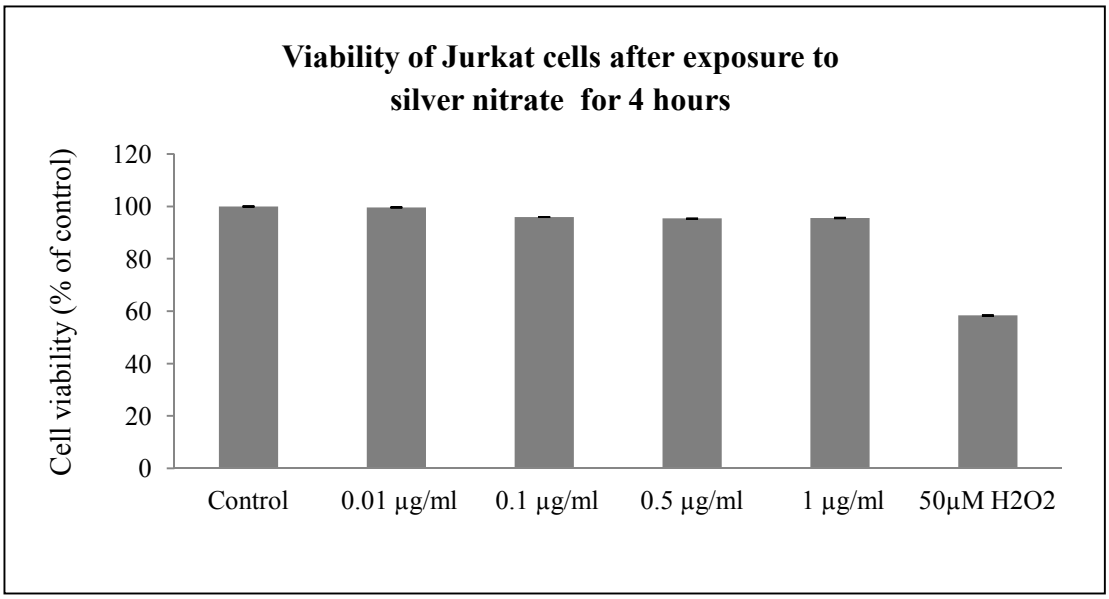

Figure 3.20 The cytotoxicity of silver nitrate to Jurkat cells. Cells were exposed to 0.01, 0.1, 0.5 and 1 µg/ml silver nitrate or H_2O_2 (positive control) for 4 hours. Cell viability was determined by the MTT assay. The data are expressed as the mean ±SEM of triplicate culture wells.Values are given in Appendix A (Table 8).

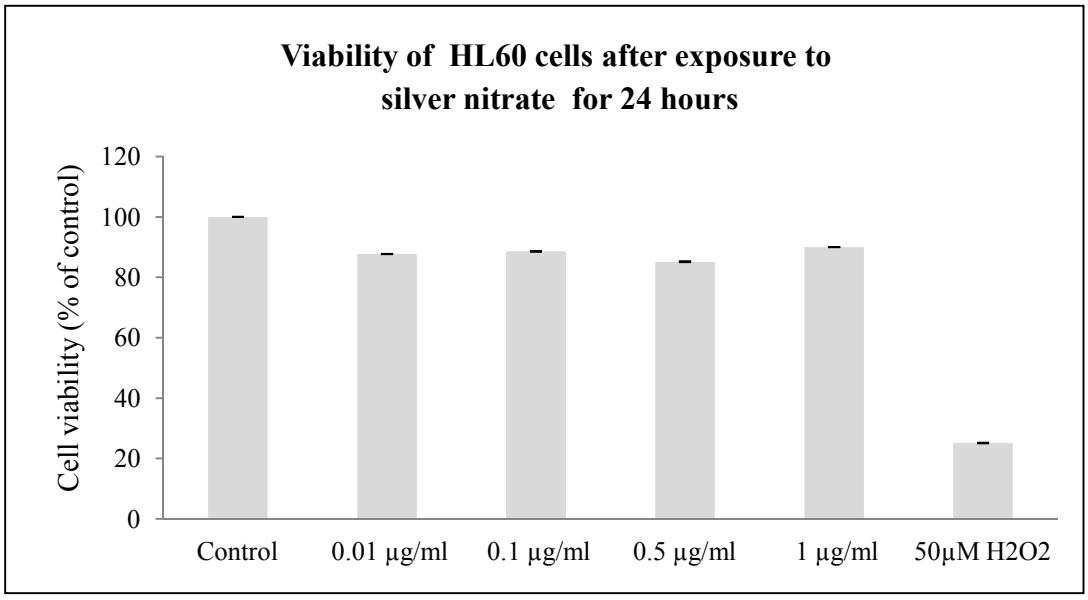

Figure 3.21 The cytotoxicity of silver nitrate to HL60 cells. Cells were exposed to 0.01, 0.1, 0.5 and 1 µg/ml silver nitrate or H_2O_2 (positive control) for 24 hours. Cell viability was determined by the MTT assay. The data are expressed as the mean ±SEM of triplicate culture wells.Values are given in Appendix A (Table 7).

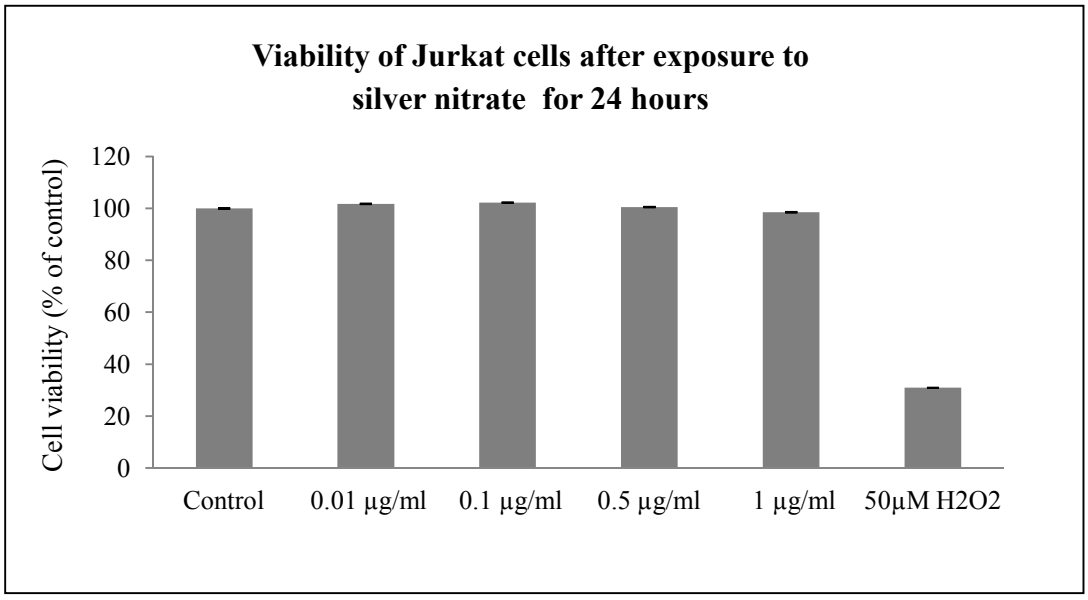

Figure 3.22 The cytotoxicity of silver nitrate to Jurkat cells. Cells were exposed to 0.01, 0.1, 0.5 and 1 µg/ml silver nitrate or H_2O_2 (positive control) for 24 hours. Cell viability was determined by the MTT assay. The data are expressed as the mean ±SEM of triplicate culture wells.Values are given in Appendix A (Table 8).

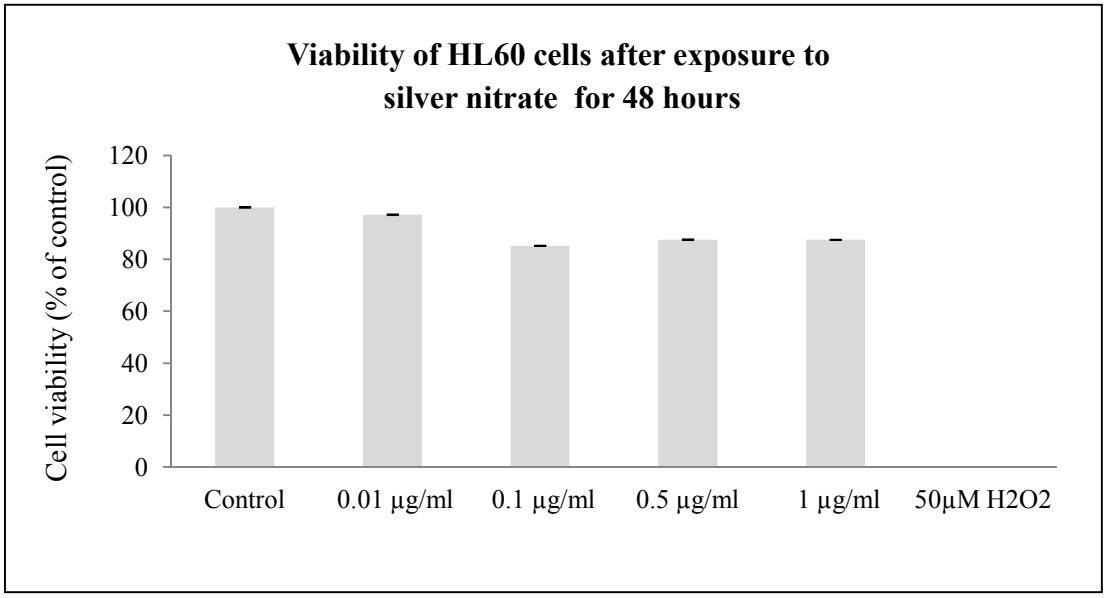

Figure 3.23 The cytotoxicity of silver nitrate to HL60 cells. Cells were exposed to 0.01, 0.1, 0.5 and 1 µg/ml silver nitrate or H_2O_2 (positive control) for 48 hours. Cell viability was determined by the MTT assay. The data are expressed as the mean ±SEM of triplicate culture wells.Values are given in Appendix A (Table 7).

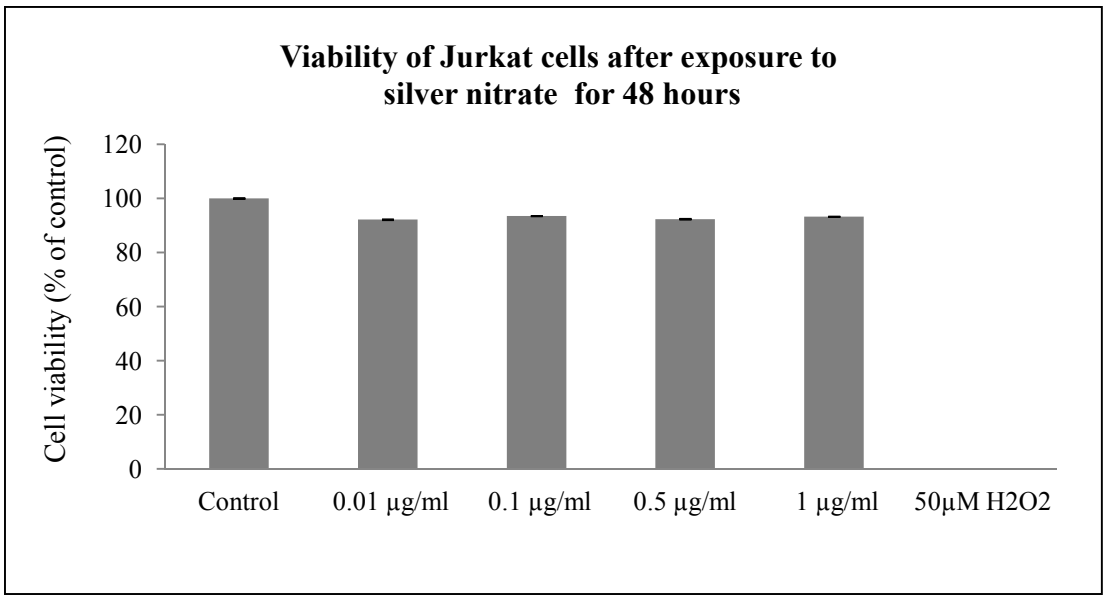

Figure 3.24 The cytotoxicity of silver nitrate to Jurkat cells. Cells were exposed to 0.01, 0.1, 0.5 and 1 µg/ml silver nitrate or H_2O_2 (positive control) for 48 hours. Cell viability was determined by the MTT assay. The data are expressed as the mean ±SEM of triplicate culture wells.Values are given in Appendix A (Table 8).

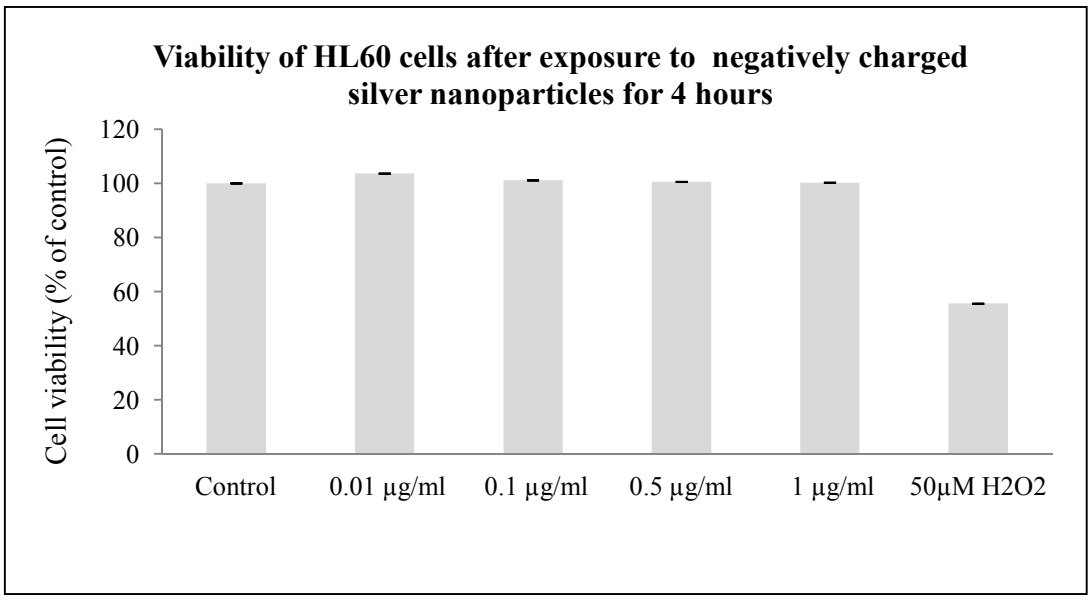

Figure 3.25 The cytotoxicity of negatively charged AgNPs to HL60 cells. Cells were exposed to 0.01, 0.1, 0.5 and 1 µg/ml silver nitrate or H_2O_2 (positive control) for 4 hours. Cell viability was determined by the MTT assay. The data are expressed as the mean ±SEM of triplicate culture wells.Values are given in Appendix A (Table 9).

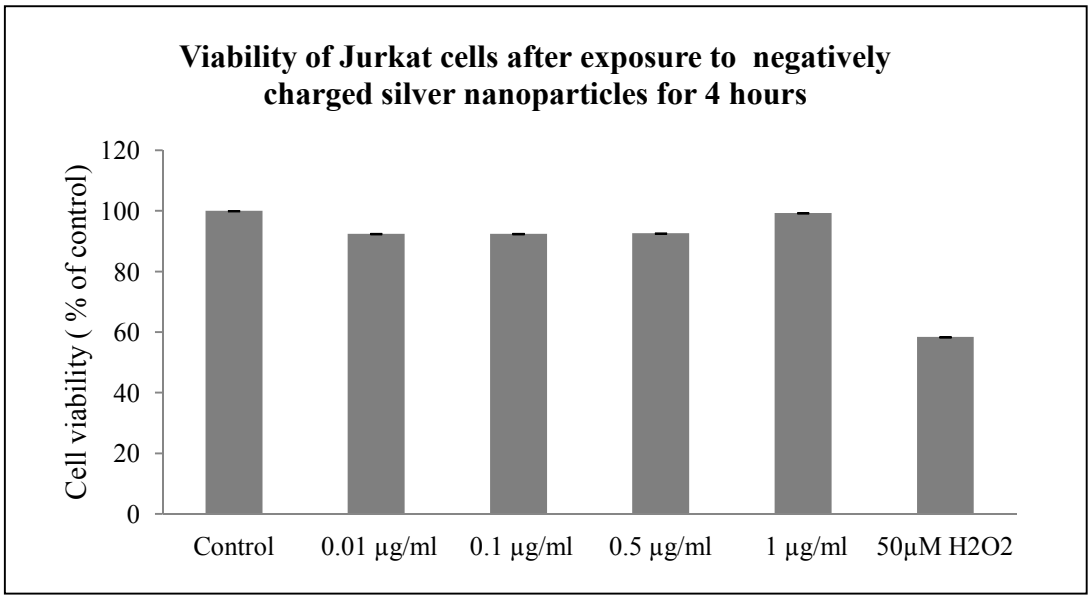

Figure 3.26 The cytotoxicity of negatively charged AgNPs to Jurkat cells. Cells were exposed to 0.01, 0.1, 0.5 and 1 µg/ml silver nitrate or H_2O_2 (positive control) for 4 hours. Cell viability was determined by the MTT assay. The data are expressed as the mean ±SEM of triplicate culture wells.Values are given in Appendix A (Table 10).

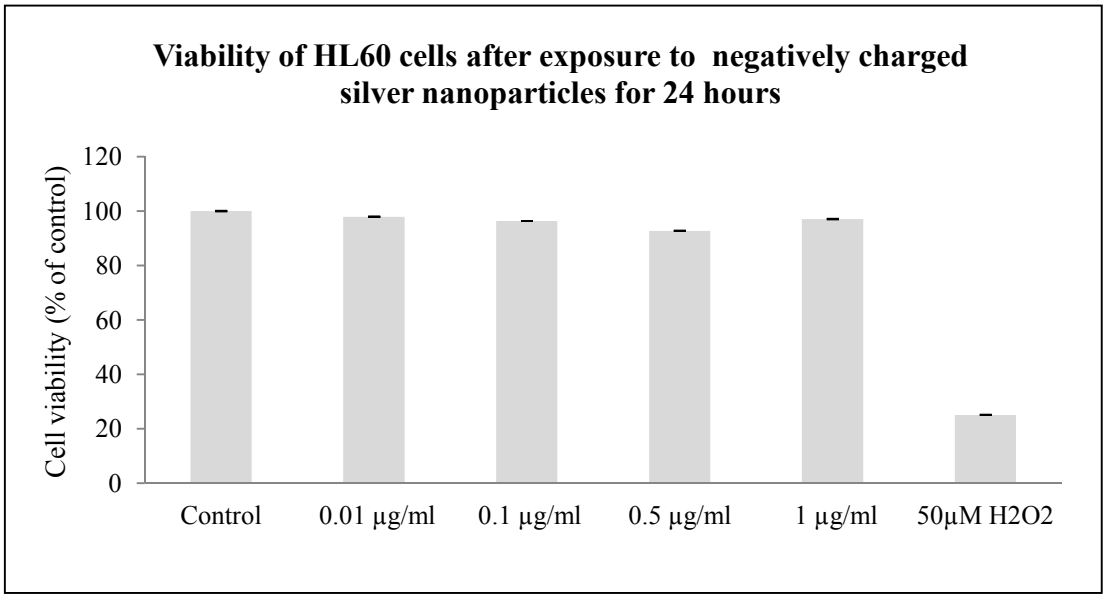

Figure 3.27 The cytotoxicity of negatively charged AgNPs to HL60 cells. Cells were exposed to 0.01, 0.1, 0.5 and 1 µg/ml silver nitrate or H_2O_2 (positive control) for 24 hours. Cell viability was determined by the MTT assay. The data are expressed as the mean ±SEM of triplicate culture wells.Values are given in Appendix A (Table 9).

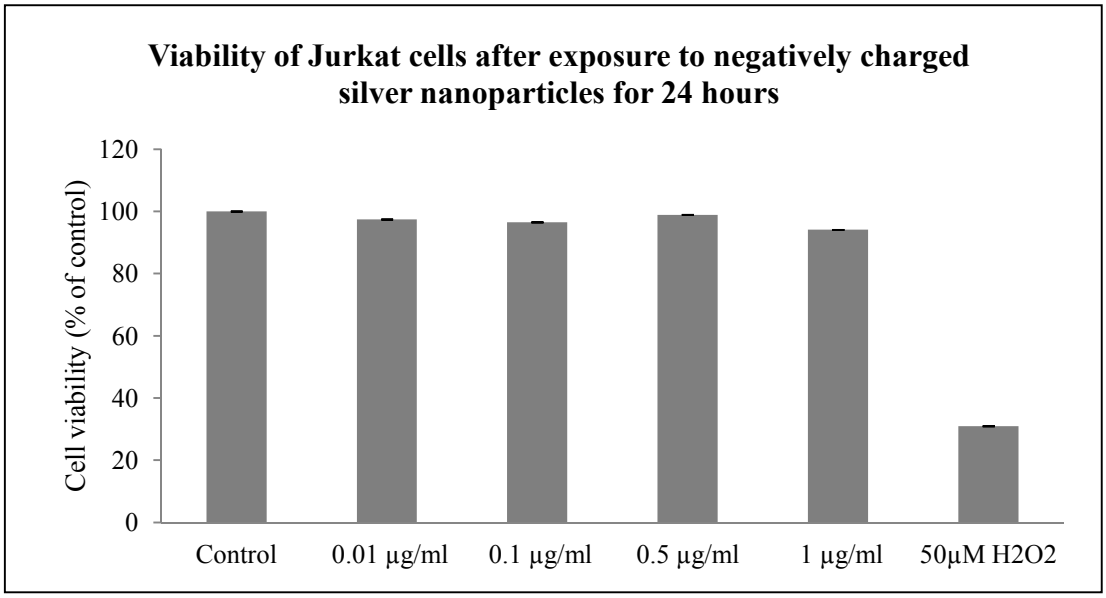

Figure 3.28 The cytotoxicity of negatively charged AgNPs to Jurkat cells. Cells were exposed to 0.01, 0.1, 0.5 and 1 µg/ml silver nitrate or H_2O_2 (positive control) for 24 hours. Cell viability was determined by the MTT assay. The data are expressed as the mean ±SEM of triplicate culture wells.Values are given in Appendix A (Table 10).

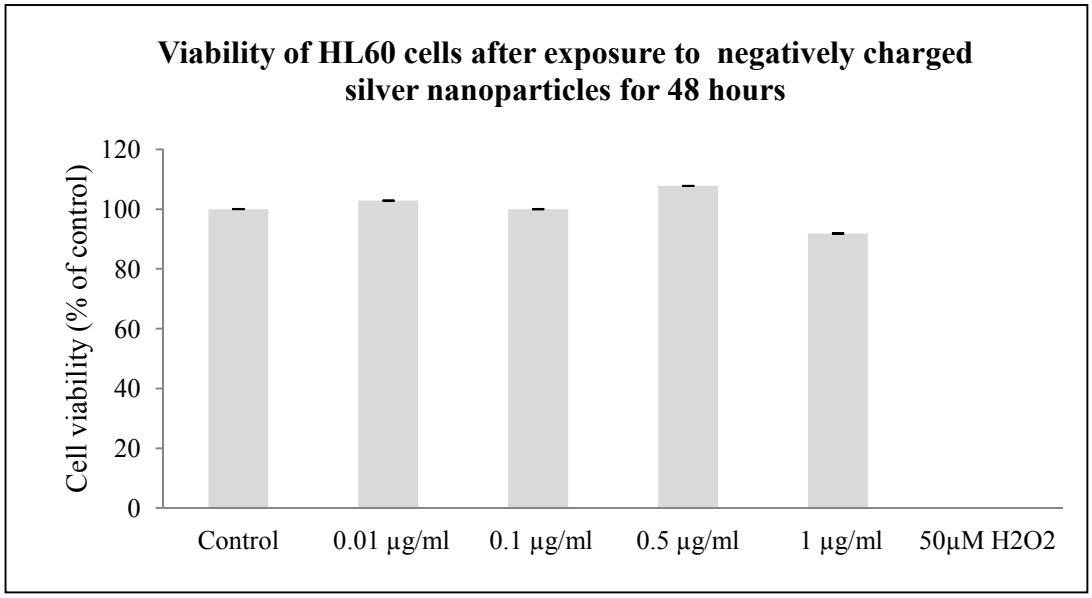

Figure 3.29 The cytotoxicity of negatively charged AgNPs to HL60 cells. Cells were exposed to 0.01, 0.1, 0.5 and 1 µg/ml silver nitrate or H_2O_2 (positive control) for 48 hours. Cell viability was determined by the MTT assay. The data are expressed as the mean ±SEM of triplicate culture wells.Values are given in Appendix A (Table 9).

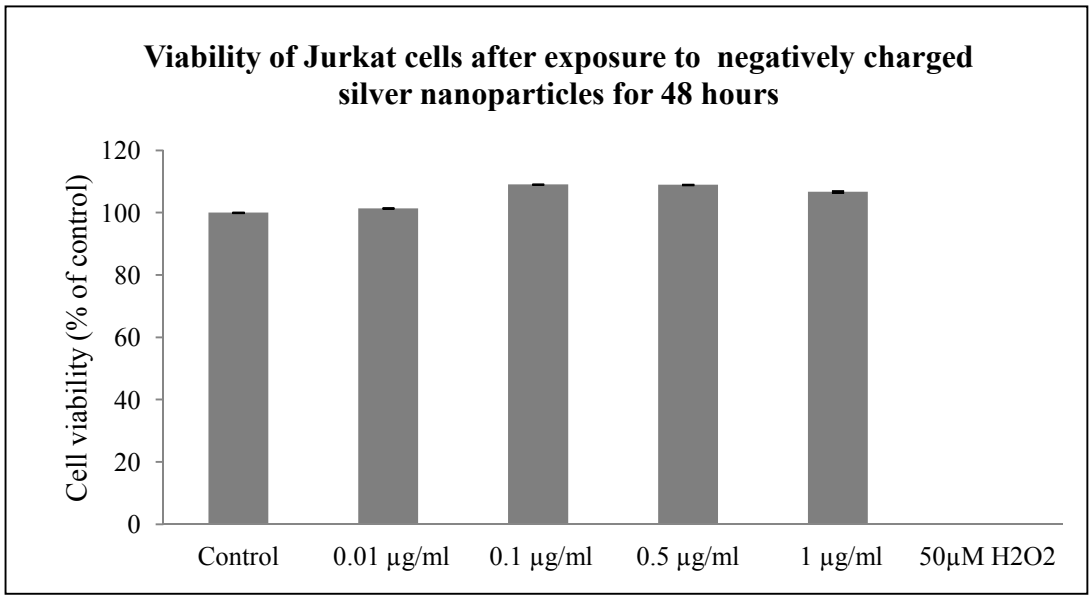

Figure 3.30 The cytotoxicity of negatively charged AgNPs to Jurkat cells. Cells were exposed to 0.01, 0.1, 0.5 and 1 µg/ml silver nitrate or H_2O_2 (positive control) for 48 hours. Cell viability was determined by the MTT assay. The data are expressed as the mean ±SEM of triplicate culture wells.Values are given in Appendix A (Table 10).

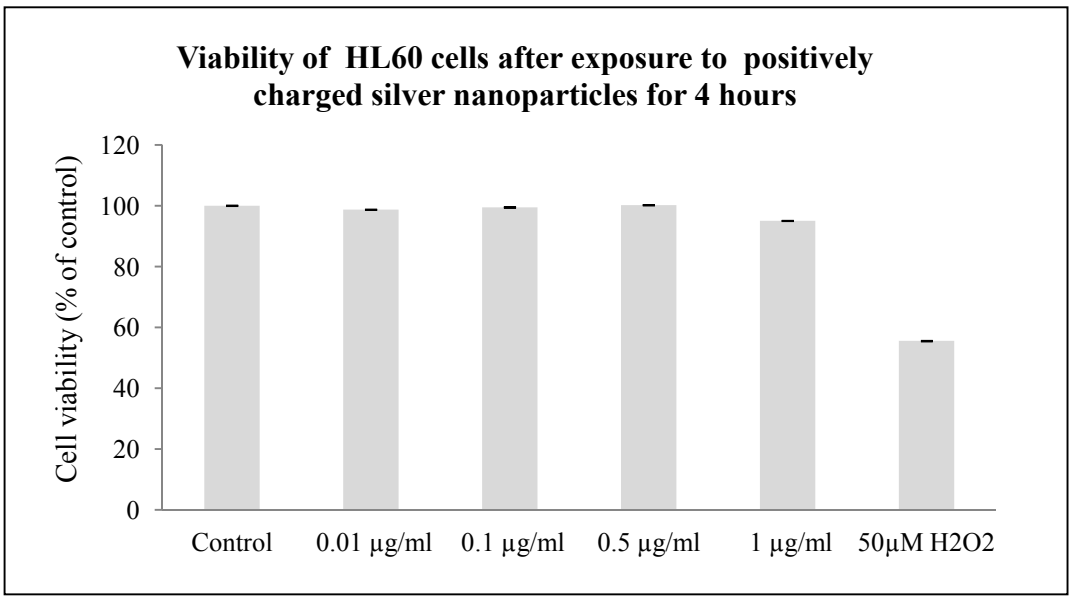

Figure 3.31 The cytotoxicity of positively charged AgNPs to HL60 cells. Cells were exposed to 0.01, 0.1, 0.5 and 1 µg/ml silver nitrate or H_2O_2 (positive control) for 4 hours. Cell viability was determined by the MTT assay. The data are expressed as the mean ±SEM of triplicate culture wells.Values are given in Appendix A (Table 11).

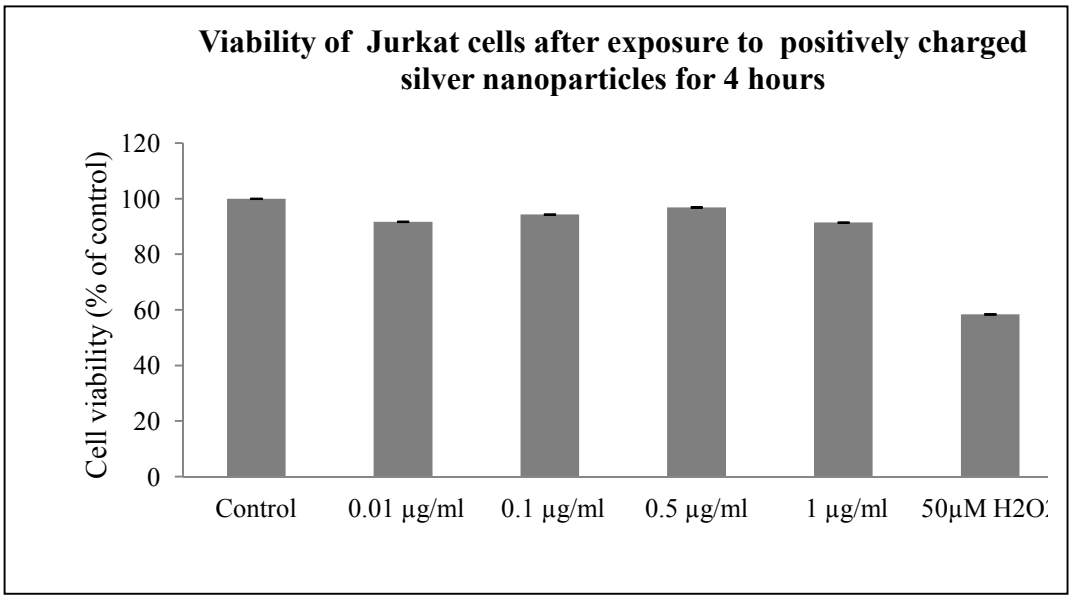

Figure 3.32 The cytotoxicity of positively charged AgNPs to Jurkat cells. Cells were exposed to 0.01, 0.1, 0.5 and 1 µg/ml silver nitrate or H_2O_2 (positive control) for 4 hours. Cell viability was determined by the MTT assay. The data are expressed as the mean ±SEM of triplicate culture wells.Values are given in Appendix A (Table 12).

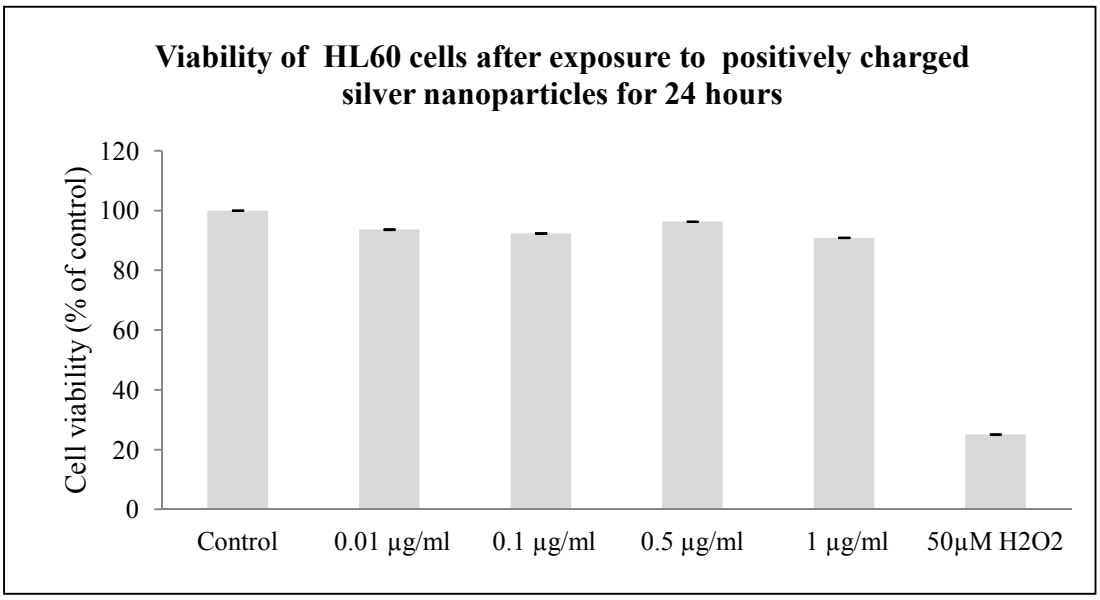

Figure 3.33 The cytotoxicity of positively charged AgNPs to HL60 cells. Cells were exposed to 0.01, 0.1, 0.5 and 1 µg/ml silver nitrate or H_2O_2 (positive control) for 24 hours. Cell viability was determined by the MTT assay. The data are expressed as the mean ±SEM of triplicate culture wells.Values are given in Appendix A (Table 11).

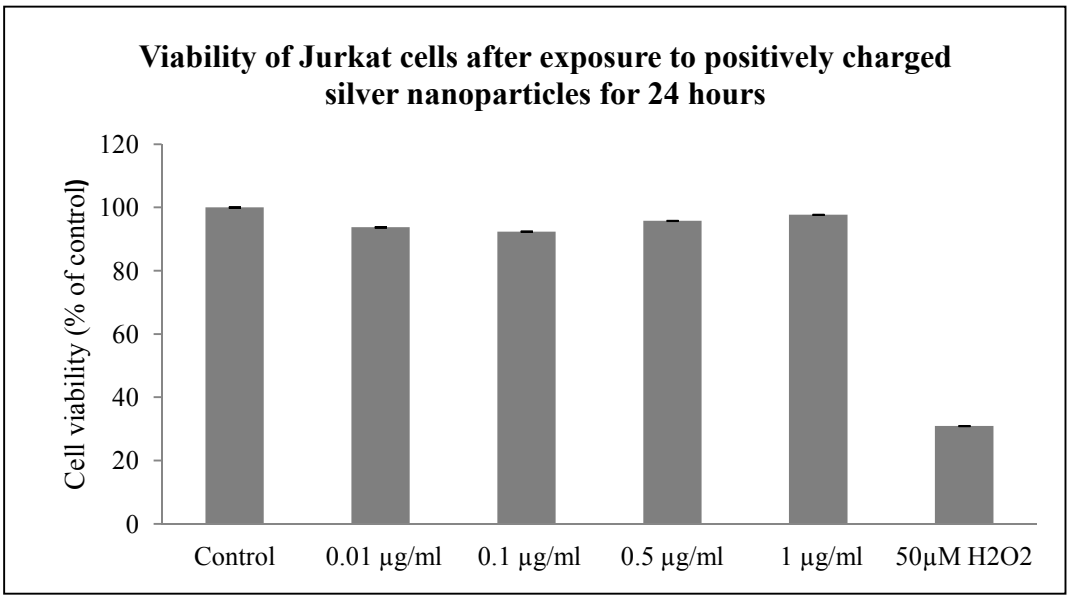

Figure 3.34 The cytotoxicity of positively charged AgNPs to Jurkat cells. Cells were exposed to 0.01, 0.1, 0.5 and 1 µg/ml silver nitrate or H_2O_2 (positive control) for 24 hours. Cell viability was determined by the MTT assay. The data are expressed as the mean ±SEM of triplicate culture wells.Values are given in Appendix A (Table 12).

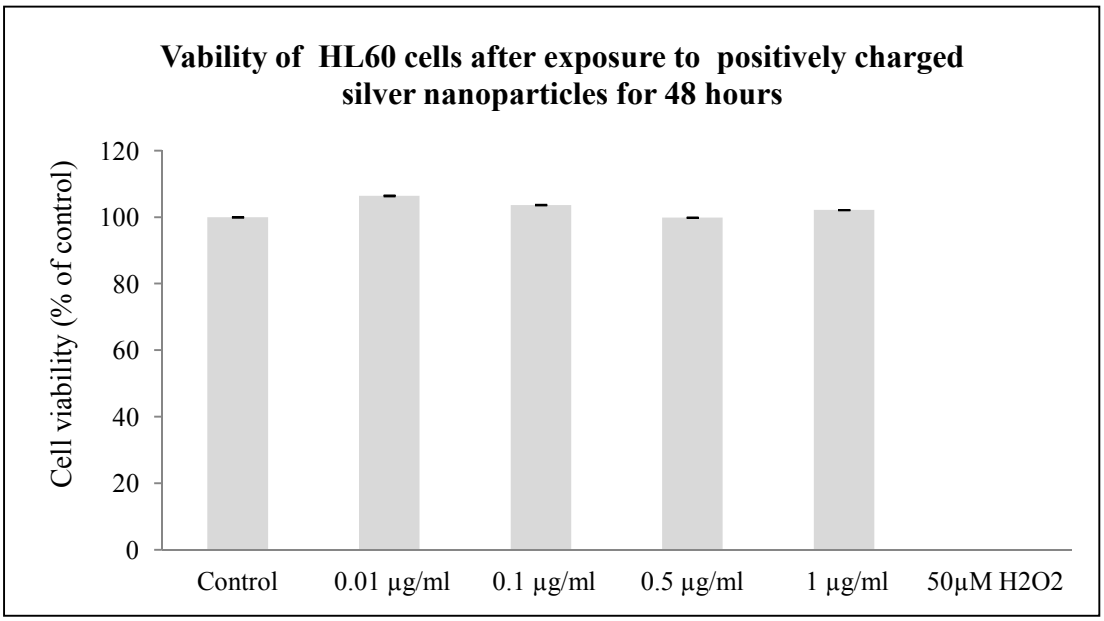

Figure 3.35 The cytotoxicity of positively charged AgNPs to HL60 cells. Cells were exposed to 0.01, 0.1, 0.5 and 1 µg/ml silver nitrate or H_2O_2 (positive control) for 48 hours. Cell viability was determined by the MTT assay. The data are expressed as the mean ±SEM of triplicate culture wells.Values are given in Appendix A (Table 11).

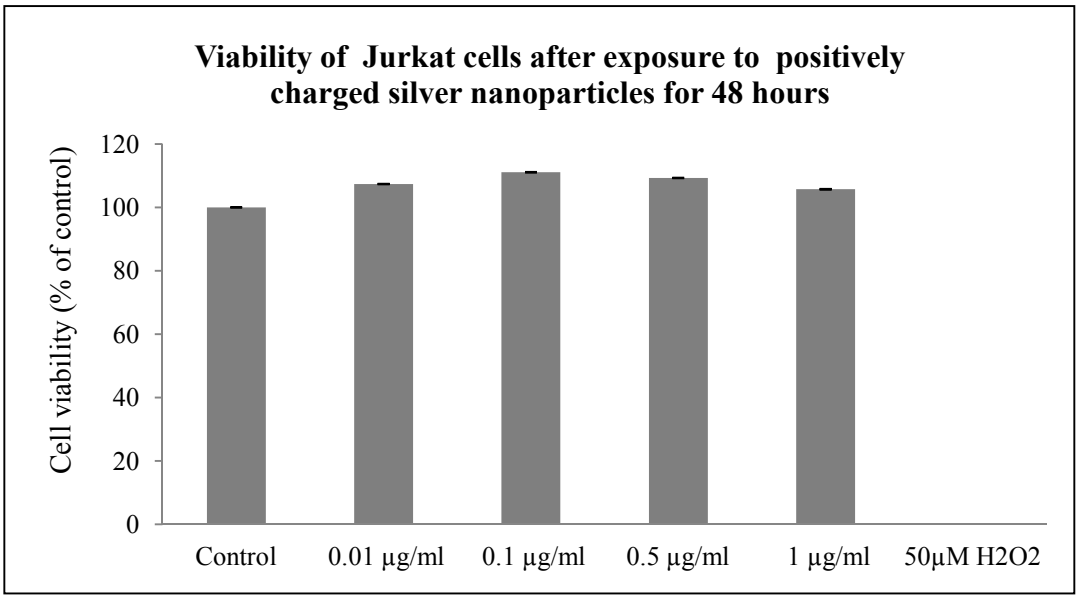

Figure 3.36 The cytotoxicity of positively charged AgNPs to Jurkat cells. Cells were exposed to 0.01, 0.1, 0.5 and 1 µg/ml silver nitrate or H_2O_2 (positive control) for 48 hours. Cell viability was determined by the MTT assay. The data are expressed as the mean ±SEM of triplicate culture wells.Values are given in Appendix A (Table 12).

Summary of results of studies with silver nitrate, negatively charged AgNPs and positively charged AgNPs at low dose (0.01-1 µg/ml)

- Again, H_2O_2 was seen to cause a dose and time dependent loss of cell viability with a similar profile to previous experiments.
- At all the lower concentrations of $AgNO_3$ and AgNPs used there was no significant loss of cell viability in either cell type and at any time point.
- There was a suggestion of increased proliferation (p=n.s) in both cell types, particularly at the longer time points.
- These experiments established time and concentration parameters which would cause minimal cytotoxicity. These incubation conditions would be used in later studies to measure other forms of toxicity (DNA damage; oxidative stress; epigenetic changes), knowing that the effects measured would not be greatly influenced by loss of cell viability.

3.3 Apoptosis and necrosis caused by silver nitrate and AgNPs

The AnnexinV-PI assay allows determination of healthy cells (annexin V^-, PI^-); apoptotic cells (annexin V^+, PI^-) and necrotic cells (annexin V^-, PI^+) using the Annexin V-FITC kit (Sigma). The kit allows detection of Annexin V bound to apoptotic cells with fluorescein isothiocyanate (FITC) which labels phosphatidylserine sites on the membrane surface while propidium iodide (PI) labels the DNA of necrotic cells, having permeable cell membranes. This kit allows determination by fluorescence microscopy.

Jurkat and HL60 cells ($5x10^3$ cells/ml) were exposed to a single dose of negatively charged AgNPs (1 μg/ml) (Sigma, NanoComposite) or 1 μg/ml of silver nitrate for 4 or 24 h. At each time point the cells were harvested and taken for analysis of apoptotic cells and necrotic cells using the Annexin V-FITC kit (see Methods, Chapter 2). The apoptotic cell and nectrotic cell as show in figure (3.37 and 3.38).

Table 3.1 Apoptosis and necrosis in HL60 and Jurkat cells from exposure to $AgNO_3$ or negatively charged AgNPs for 4 or 24 hours, (n=1). Cell count=1,000 cells.

Treatments	**Apoptotic cells (%)**		**Necrotic cells (%)**	
	4h	**24h**	**4h**	**24h**
HL60 cells- control	0.4	0.5	0.3	0.4
HL60 cells+1 µg/ml $AgNO_3$	0.6	0.7	0.8	1.1
HL60 cells+1 µg/ml AgNPs-Sigma	0.5	0.6	0.5	0.9
HL60 cells+ 1 µg/ml AgNPs-NC	0.6	0.8	0.4	0.4
Jurkat cells- control	0.4	0.5	0.5	0.6
Jurkat cells+ 1 µg/ml $AgNO_3$	1.1	2.2	1.1	1.1
Jurkat cells+1 µg/ml AgNPs-Sigma	0.7	0.8	1.0	1.1
Jurkat cells + 1 µg/ml AgNPs-NC	0.4	0.7	0.9	1.0

AgNPs-NC= Negatively charged AgNPs supplied by NanoComposix

AgNPs-Sigma= Negatively charged AgNPs supplied by Sigma

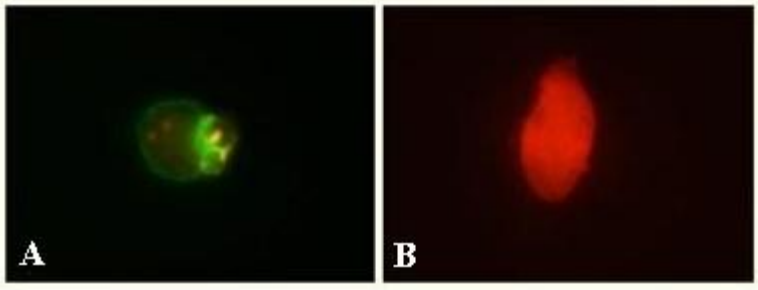

Figure 3.37 HL60 cells after $AgNO_3$ (1 µg/ml) for 24h. The cells were stained with FITC-labeled Annexin V and propidium iodide. The figures are fluorescent microscope images of HL60 cells showing an apoptotic cell (annexin V^+/PI-) (A); and a necrotic cell (annexin V^-/PI^+) (B)

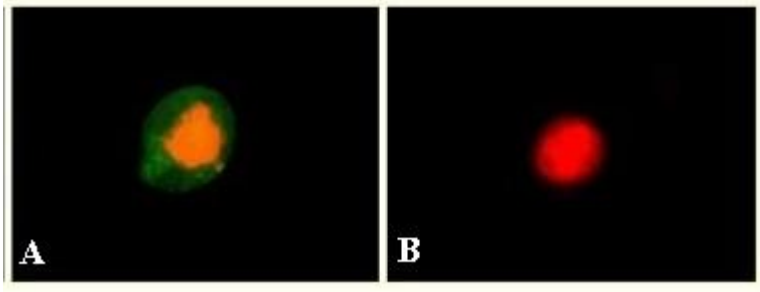

Figure 3.38 Jurkat cells after $AgNO_3$ (1 µg/ml) for 24h. The cells were stained with FITC-labeled Annexin V and propidium iodide. The figures are fluorescent microscope images of Jurkat cells showing an apoptotic cell (annexin V^+/PI^-) (A); and a necrotic cell (annexin V^-/PI^+) (B)

Summary of results of studies of apoptosis and necrosis caused by silver nitrate and AgNPs

- Treatment with $AgNO_3$ or negatively charged AgNPs (1 µg/ml) for 4 h or 24 h did not significantly increase apoptotic or necrotic events, although there was a suggestion that Jurkats were more sensitive to this than HL60s (table 3.1).
- The level of apoptotic and necrotic cells following treatment with AgNPs or $AgNO_3$were low and similar to the control cell. This indicated that apoptosis was not induced .

3.4 Discussion

In this part of the research, the MTT assay was used to investigate the level of cytotoxicity caused by silver nitrate compared to AgNPs in HL60 and Jurkat cells at time points up to 48 h. The experiments aimed to define the concentration and time parameters that would cause ≤ 20% loss of cell viability, which was considered to be an acceptable level of toxicity. These incubation conditions were to be used in subsequent studies of DNA damage, oxidative stress and epigenetic changes, knowing that the effects would not be greatly influenced by loss of cell viability.

H_2O_2 proved to be a consistent control for the experiment. It caused a time dependent decrease in cell viability that had a similar profile in Jurkat and HL60 cells, and Jurkats were more sensitive to cytotoxicity than HL60s. H_2O_2 causes DNA damage by oxidative stress mechanisms since it can easily cross cellular membranes using water channels (aquapores) (Henzler and Steuldle, 2000). H_2O_2 causes a spectrum of DNA lesions, mainly single strand breaks (SSBs), in parallel with cytotoxicity, repair or cell death. The damage results from production of $^{\bullet}OH$ radicals via the Fenton's reaction in the presence of transition metals such as ferrous ions, Fe^{2+} (Lee et al, 2002). However, the profile of cytotoxicity, repair or cell death by hydrogen peroxide will differ considerably to that from a chemical which is less rapidly detoxified, such as silver.

These data showed that $AgNO_3$was more toxic to Jurkat cells than HL60s, with only about 20% of Jurkat cells remaining viable at the highest dose after 48h. Ag^+ ions would be released from $AgNO_3$ under aqueous conditions and it is intriguing that Jurkat cells appeared to be much more sensitive to loss of viability and/or reduced proliferation compared to HL60s. It is possible that HL60 cells (derived from immortalized macrophages/monocytes) are more efficient at detoxifying Ag+ ions than Jurkat cells (immortalized T-lymphocytes). Studies have shown that the MRPI-GS-X efflux pump is involved in removing toxic metal complexes, such as glutathione-As and glutathione-Cd, from macrophages (Leslie et al 2004; Li et al, 1996). Ag^+ ions are known to accumulate as non toxic deposits of Ag-sulphur in lysosome-like organelles within the cell, which limits toxicity. Ag+ ions also bind avidly to SH-groups (e.g. in cysteine) present in proteins such as cysteine-rich metallothionein (Lansdown, 2006), which is highly up regulated in tissues exposed to various metals (Lansdown, 2001), thus limiting toxicity.

However, when these defense mechanisms become overwhelmed by higher concentrations of Ag^+ ions toxic events, such as DNA damage and cell death, will occur.

These experiments also showed that negatively charged AgNPs (but not positively charged ones) caused greater loss of cell viability to Jurkat cells than HL60s. It has been reported that the interaction of proteins with AgNPs could potentially affect the entry and intracellular localization of NPs within cells, and thus their toxicity (Cedervall et al, 2007). Moreover, Johnston et al (2010) highlighted that the presence of serum in tissue culture medium can cause a reduction in the size of NP aggregates. Similarly, negatively charged polystyrene bead NPs interacted differently with HepG2 cells compared to primary rat hepatocytes that were suspended in culture medium containing FCS, compared to culture medium without FCS (Johnston et al, 2010). The authors hypothesized that the higher the serum concentration in the medium, the lower the toxicity. It is plausible therefore, that the higher toxicity of negatively charged AgNPs to Jurkats compared to HL60 may have been influenced by the relatively lower FBS concentration in Jurkats (10% in Jurkats and 20% in HL60s).

On a weight basis, $AgNO_3$ caused a much greater loss of cell viability than negatively or positively charged AgNPs, suggesting that release of Ag^+ions into the cell from AgNPs was less than the respective $AgNO_3$ concentration. In these experiments, the cells were known to be exposed to 0.06 μM-58.9 μM of Ag^+ions from $AgNO_3$ (0.01-10 μg/ml). However, at this stage of the research the concentration of Ag^+ ions available to the cells from AgNPs could not be calculated as analysis of the AgNPs by ICP-MS requires acid digestion, with release of Ag^+ ions. Later experiments used a novel dialysis technique to determine the concentration of Ag^+ions available to the cells from the AgNP dose (Xu et al, 2010).

CHAPTER 4

DNA DAMAGE BY SILVER NANOPARTICLES

Chapter 4. DNA damage by silver nanoparticles

4.1 DNA damage by silver nitrate and AgNPs at 4h post dose

The data contained in chapter 3 showed that concentrations of $AgNO_3 \geq 1$ μg/ml caused an unacceptably high loss of viability to both HL60 and Jurkat cells at 24h and 48h. Therefore, in this chapter both cell types were exposed to $AgNO_3$ (0.1, 1, 5 μg/ml) for only 4h when viability was known to be ≥ 80% in HL60s, although viability was only about 50% in Jurkats at the higher concentration. Conversely, positively charged AgNPs (0.01-10 μg/ml) had been shown to have little effect on viability for up to 48h, although negatively charged ones caused ~40% to reduction in viability of Jurkats at the higher concentration.

In this part of the research DNA damage was measured in HL60 and Jurkat cells following exposure to silver nitrate or AgNPs using conditions that did not cause marked loss of cell viability. Jurkat and HL60 cells ($5x10^3$ cells/ml) were exposed to $AgNO_3$ or the AgNPs (0.1, 1, 5 μg/ml) when the cells were harvested and washed in fresh RPMI prior to analysis of DNA damage using the Comet assay (see Methods, Chapter 2). Cells were also exposed to H_2O_2 (50 μM, 5 min) a chemical known to cause DNA damage by oxidative stress (positive control). 200 cells per parameter were scored and the experiment was performed on one occasion.

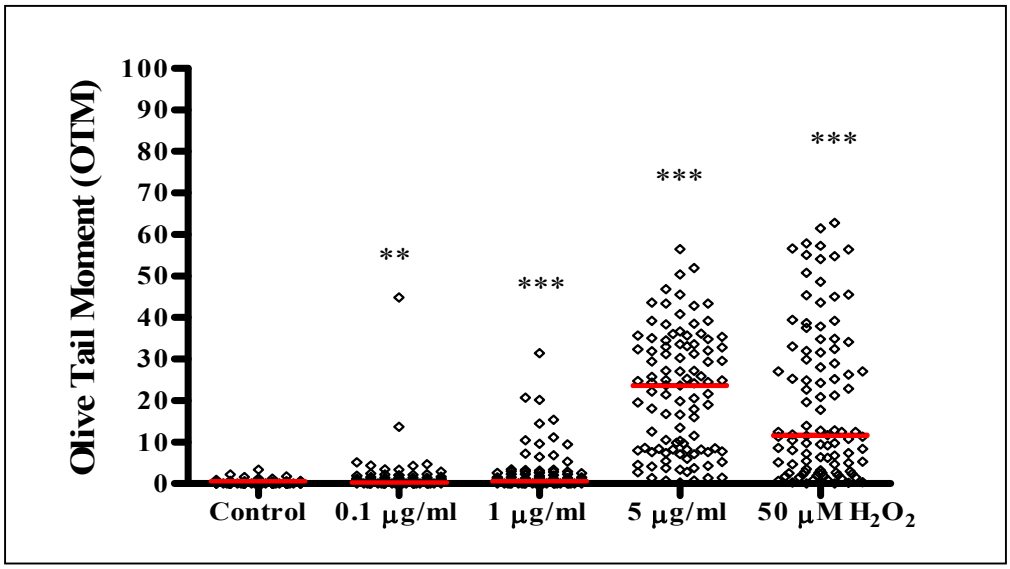

Figure 4.1 The effect of silver nitrate on DNA damage in HL60 cells. Cells were exposed to different concentrations of silver nitrate or H_2O_2 (positive control) for 4h. DNA damage was determined by the Comet assay. The red lines represent the median. Values are given in table 4.1. ** $p<0.01$, *** $p<0.001$, compared to control (Kruskal-Wallis analysis with Dunn's post-hoc test).

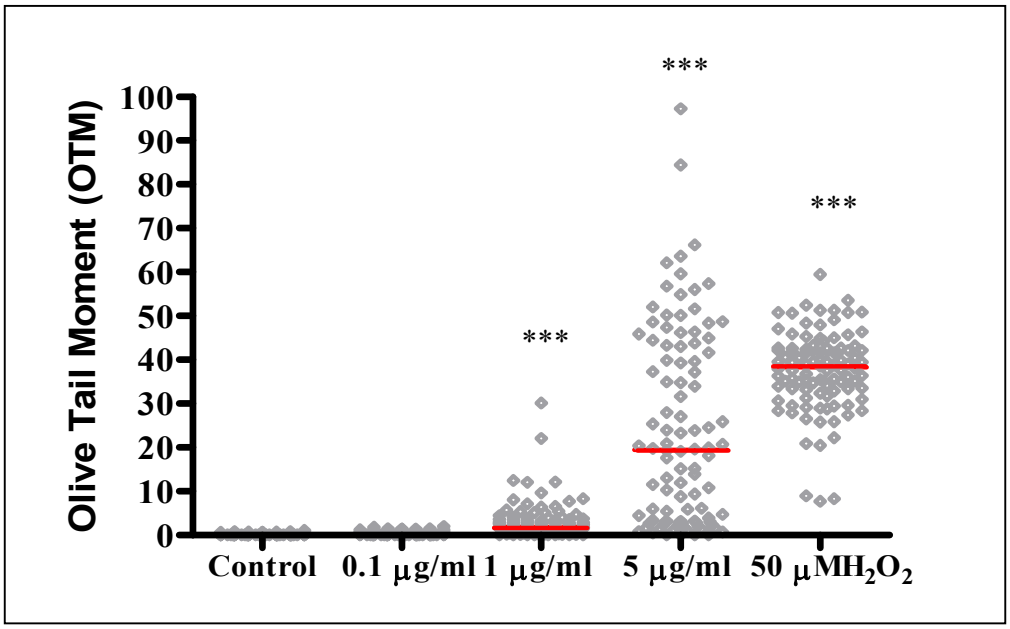

Figure 4.2 The effect of silver nitrate on DNA damage in Jurkat cells. Cells were exposed to different concentrations of silver nitrate or H_2O_2 (positive control) for 4h. DNA damage was determined by the Comet assay. The red lines represent the median. Values are given in table 4.1. *** $p<0.001$, compared to control (Kruskal-Wallis analysis with Dunn's post-hoc test).

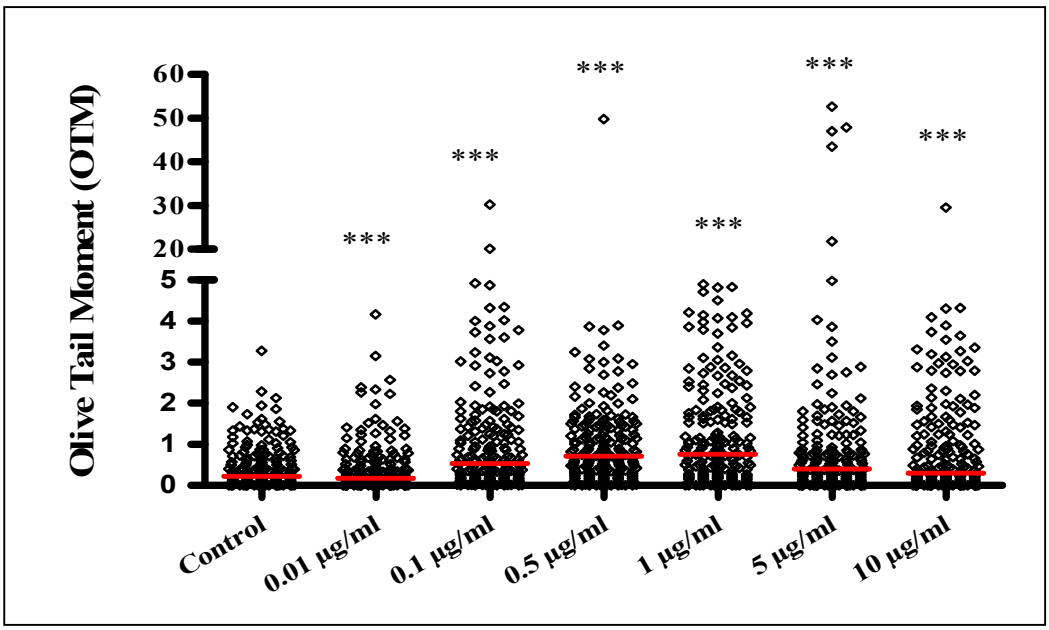

Figure 4.3 The effect of negatively charged AgNPs on DNA damage in HL60 cells. Cells were exposed to different concentrations of negatively charged AgNPs for 4h. DNA damage was determined by the Comet assay. The red lines represent the median. Values are given in table 4.1. *** $p<0.001$, compared to control (Kruskal-Wallis analysis with Dunn's post-hoc test).

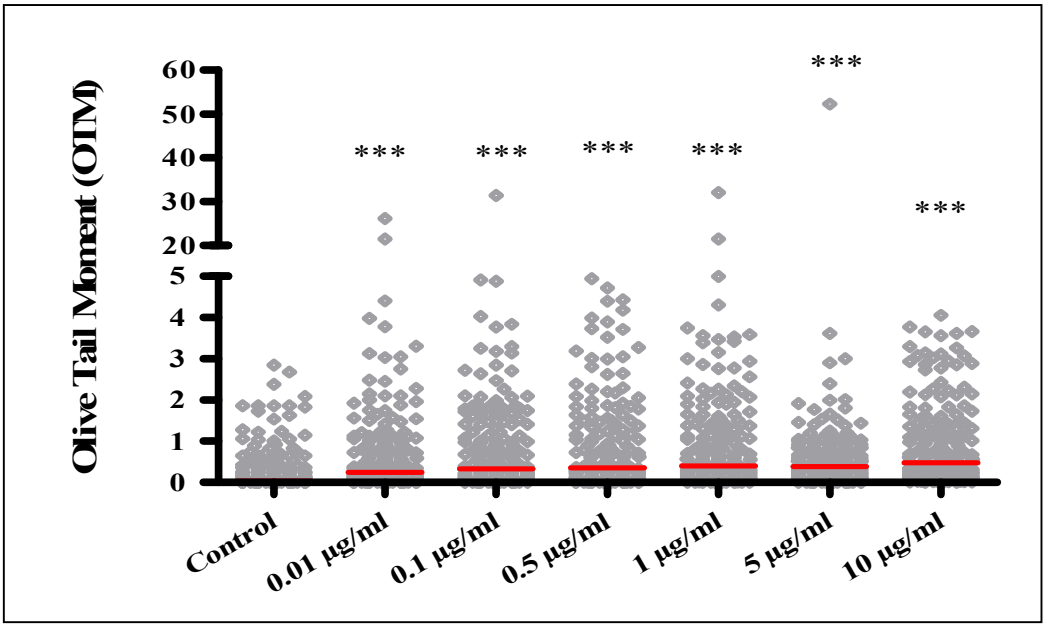

Figure 4.4 The effect of negatively charged AgNPs on DNA damage in Jurkat cells. Cells were exposed to different concentrations of negatively charged AgNPs for 4h. DNA damage was determined by the Comet assay. The red lines represent the median.Values are given in table 4.1. *** $p<0.001$, compared to control (Kruskal-Wallis analysis with Dunn's post-hoc test).

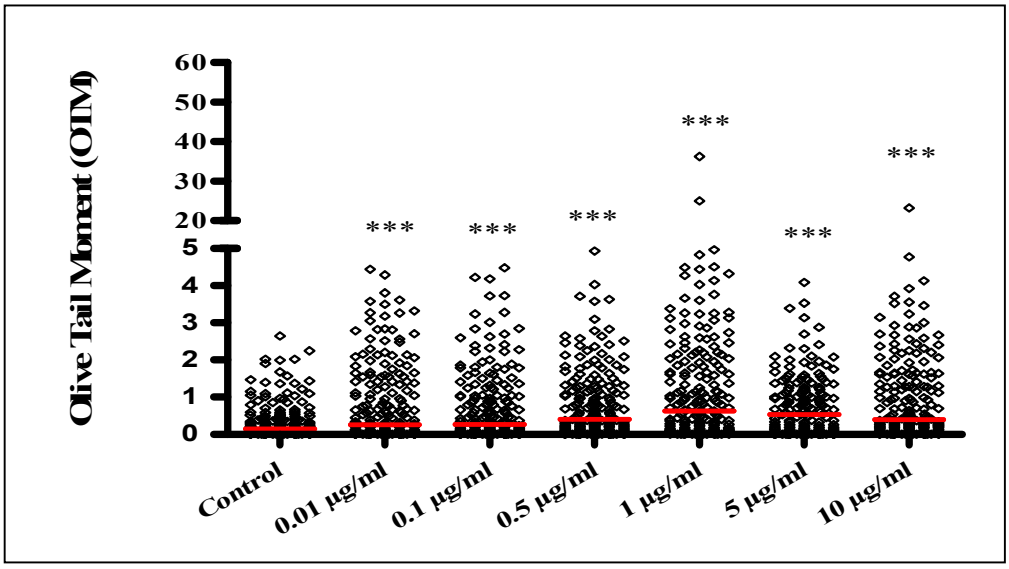

Figure 4.5 The effect of positively charged AgNPs on DNA damage in HL60 cells. Cells were exposed to different concentrations of positively charged AgNPs for 4h. DNA damage was determined by the Comet assay. The red lines represent the median. Values are given in table 4.1. *** $p<0.001$, compared to control (Kruskal-Wallis analysis with Dunn's post-hoc test).

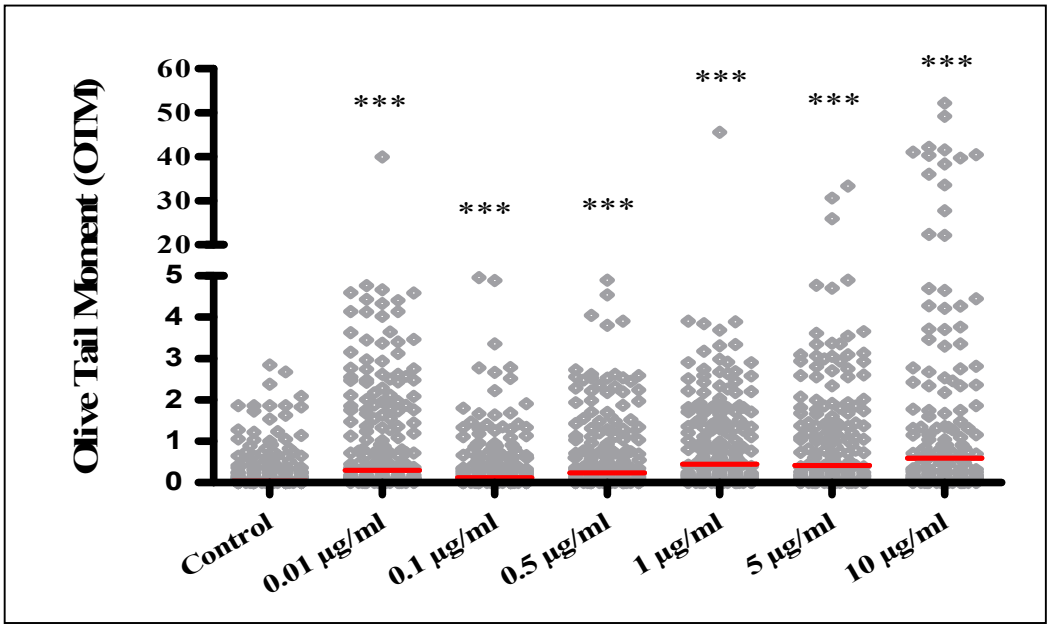

Figure 4.6 The effect of positively charged AgNPs on DNA damage in Jurkat cells. Cells were exposed to different concentrations of positively charged AgNPs for 4h. DNA damage was determined by the Comet assay. The red lines represent the median. Values are given in table 4.1. ** $p<0.01$, *** $p<0.001$, compared to control (Kruskal-Wallis analysis with Dunn's post-hoc test).

Summary of results of studies of DNA damage by silver nitrate compared to AgNPs (negatively and positively charged) at 4h post dose

The Mann Whitney U test was used to compare the DNA damage in HL60 cells with Jurkat cells (Table 4.1).

- H_2O_2 caused DNA damage to both HL60 and Jurkats at 4 h, but the damage was significantly higher in Jurkats ($p<0.001$) compared to HL60s.

- $AgNO_3$ caused DNA damage to HL60 and Jurkat cells at 4 h in a dose response manner.
- The damage was generally higher in Jurkats compared to HL60s for exposure to $AgNO_3$ (1 μg/ml, $p<0.001$; 5μg/ml, p=ns)

- Negatively charged AgNPs caused DNA damage to both cell types at 4 h for all concentrations tested and the profiles of damage appeared to be dose dependent.
- DNA damage by negatively charged AgNPs was generally higher in HL60 cells compared to Jurkats (0.1 μg/ml, $p<0.01$; 0.5 μg/ml, $p<0.01$; 1 μg/ml, $p<0.01$)

- Positively charged AgNPs caused DNA damage to both cell types at 4h for all concentrations tested and, in general, the profiles of DNA damage were dose dependent.
- The level of DNA damage by positively charged AgNPs was often higher in HL60 cells compared to Jurkats at the lower concentrations, but this was not consistant.

- On a weight basis, DNA damage was much higher from exposure to $AgNO_3$ compared to AgNPs. This was the case for both cell types.

Table 4.1 DNA damage (Olive Tail Moment, O.T.M) determined for Jurkat and HL60 cells exposed to $AgNO_3$, negatively charged AgNPs or positively charged AgNPs for 4h. * $p<0.05$, ** $p<0.01$, *** $p<0.001$(Mann Whitney U test comparing HL60 with Jurkat cells)

Treatment	Median		P value
	HL60 cells	Jurkat cells	
$AgNO_3$			
0.1 µg/ml	0.40	0.13	0.01
1 µg/ml	0.61	1.85	0.001
5 µg/ml	23.68	19.44	ns
Negatively charged AgNPs			
0.01 µg/ml	0.19	0.26	0.05
0.1 µg/ml	0.54	0.34	0.01
0.5 µg/ml	0.72	0.35	0.01
1 µg/ml	0.77	0.40	0.01
5 µg/ml	0.40	0.39	ns
10 µg/ml	0.31	0.48	0.01
Positively charged AgNPs			
0.01 µg/ml	0.26	0.31	ns
0.1 µg/ml	0.28	0.13	0.01
0.5 µg/ml	0.41	0.23	0.05
1 µg/ml	0.64	0.45	ns
5 µg/ml	0.53	0.42	ns
10 µg/ml	0.39	0.59	0.05
50µMH_2O_2	11.78	38.26	0.001

ns= not significant, ($p>0.05$).

4.2 DNA damage by silver nitrate, negatively charged or positively charged AgNPs (0.01-1 µg/ml): time course

DNA damage by silver nitrate (0.01-1 µg/ml): time course.

In this set of experiments, Jurkat and HL60 cells were exposed to lower concentrations of $AgNO_3$ (0.01-1 µg/ml) compared to the study in 4.1, so that DNA damage could be measured up to 48 h when cell viability was always ≥ 80% (See section 3.1).

Jurkat and HL60 cells ($5x10^3$ cells/ml) were exposed to a single dose of $AgNO_3$ (0.01, 0.1, 0.5, 1 µg/ml) for 4, 24 and 48 h. As before, at each time point the cells were harvested and taken for analysis of DNA damage using the Comet assay (see Methods, Chapter 2).

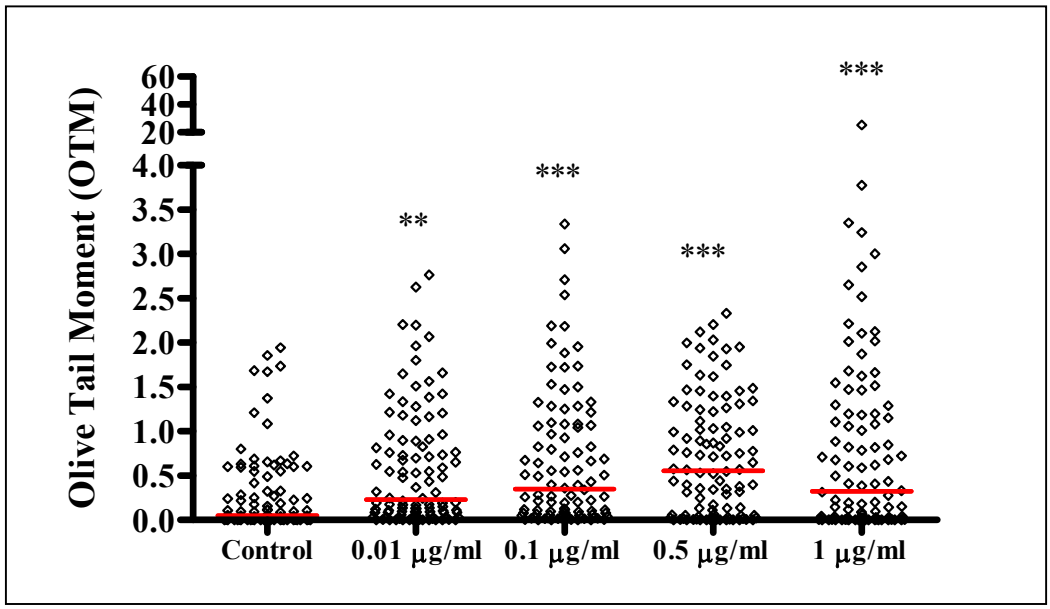

Figure 4.7 The effect of silver nitrate on DNA damage in HL60 cells. Cells were exposed to different concentrations of silver nitrate for 4h. DNA damage was determined by the Comet assay. The red lines represent the median. Values are given in table 4.2.
** p<0.01, *** p<0.001, compared to control (Kruskal-Wallis analysis with Dunn's post-hoc test).

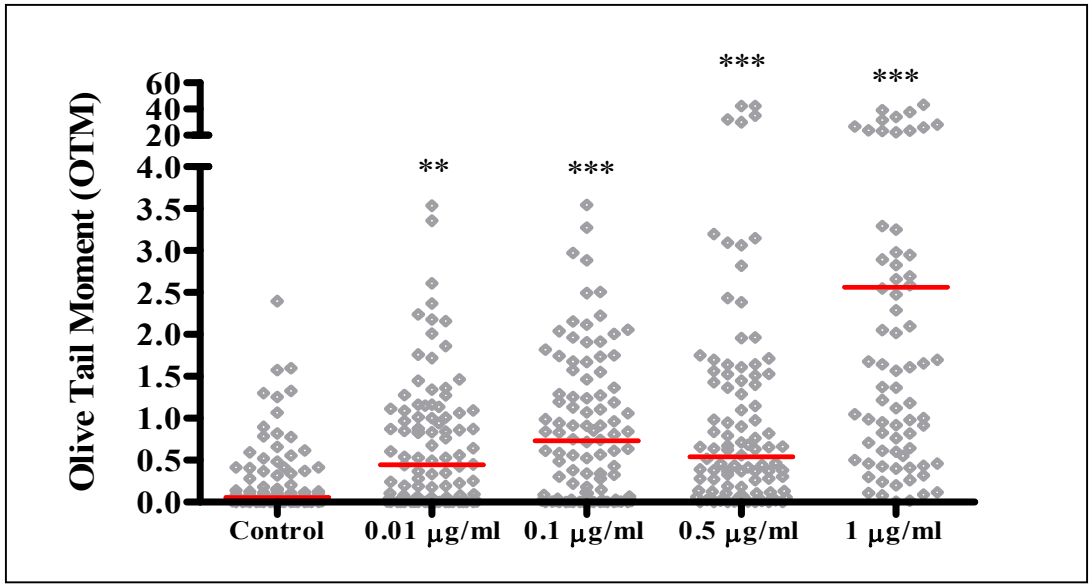

Figure 4.8 The effect of silver nitrate on DNA damage in Jurkat cells. Cells were exposed to different concentrations of silver nitrate for 4h. DNA damage was determined by the Comet assay. The red lines represent the median. Values are given in table 4.2.
** p<0.01, *** p<0.001, compared to control (Kruskal-Wallis analysis with Dunn's post-hoc test).

.

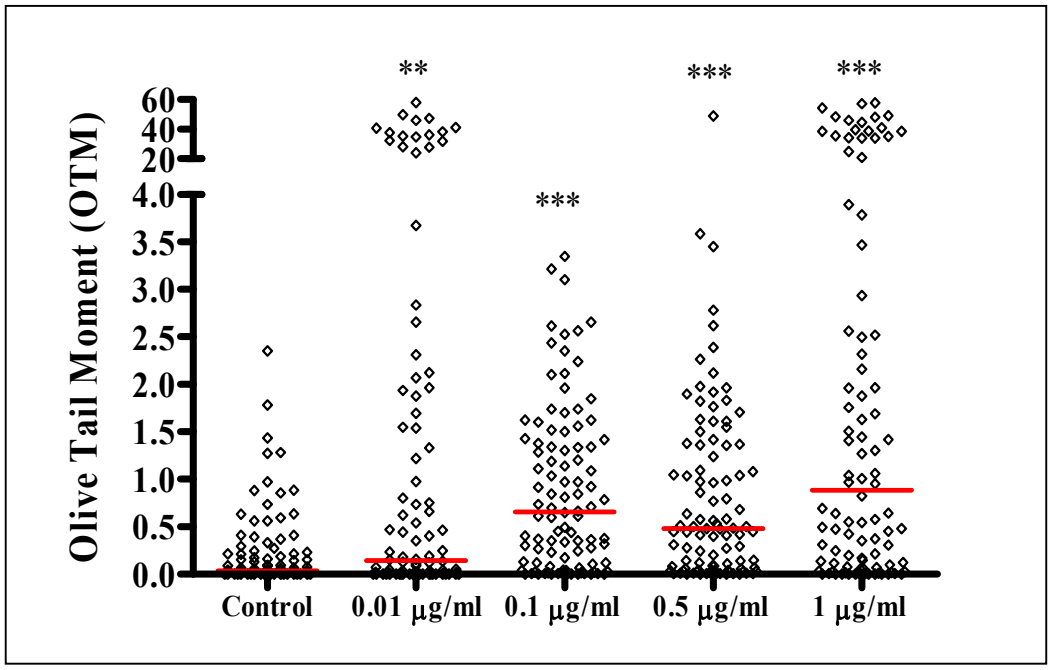

Figure 4.9 The effect of silver nitrate on DNA damage in HL60 cells. Cells were exposed to different concentrations of silver nitrate for 24h. DNA damage was determined by the Comet assay. The red lines represent the median. Values are given in table 4.2. ** $p<0.01$, *** $p<0.001$, compared to control (Kruskal-Wallis analysis with Dunn's post-hoc test).

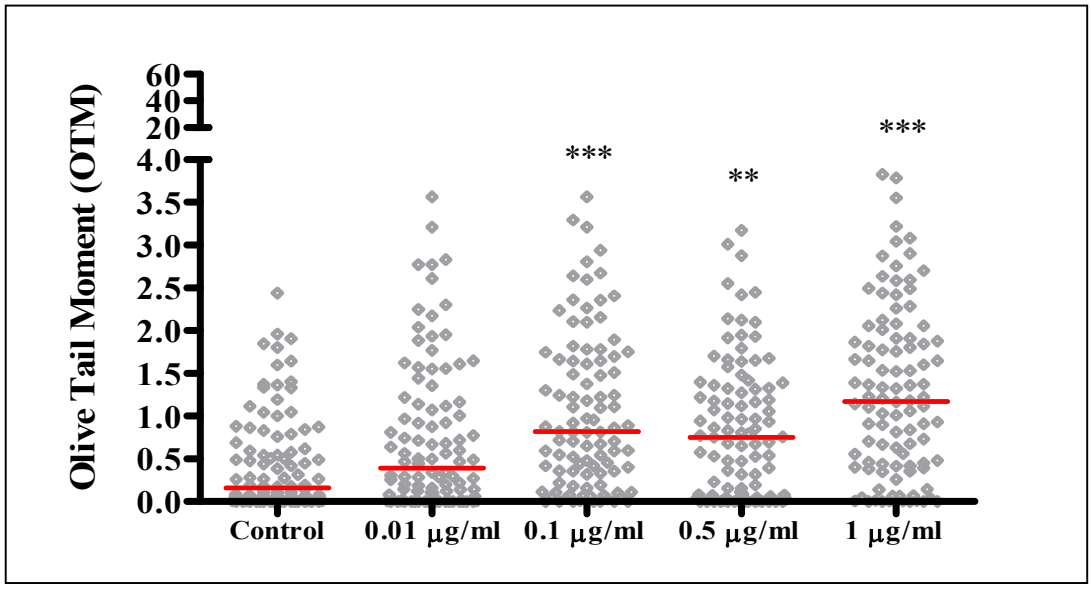

Figure 4.10 The effect of silver nitrate on DNA damage in Jurkat cells. Cells were exposed to different concentrations of silver nitrate for 24h. DNA damage was determined by the Comet assay. The red lines represent the median. Values are given in table 4.2. ** $p<0.01$, *** $p<0.001$, compared to control (Kruskal-Wallis analysis with Dunn's post-hoc test).

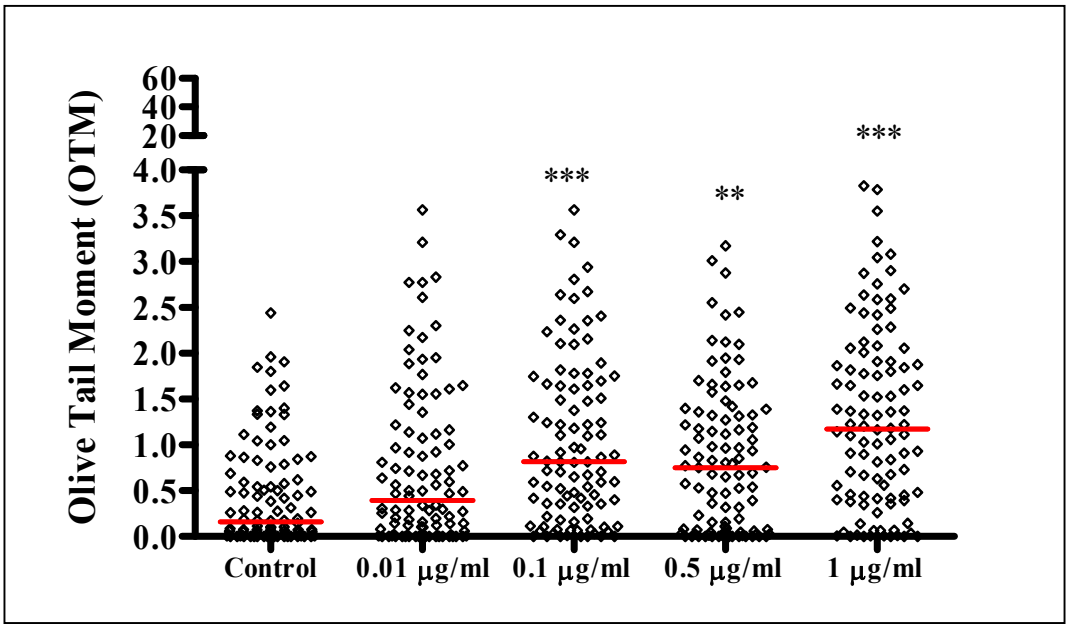

Figure 4.11 The effect of silver nitrate on DNA damage in HL60 cells. Cells were exposed to different concentrations of silver nitrate for 48h. DNA damage was determined by the Comet assay. The red lines represent the median. Values are given in table 4.2. *** $p<0.001$, compared to control (Kruskal-Wallis analysis with Dunn's post-hoc test).

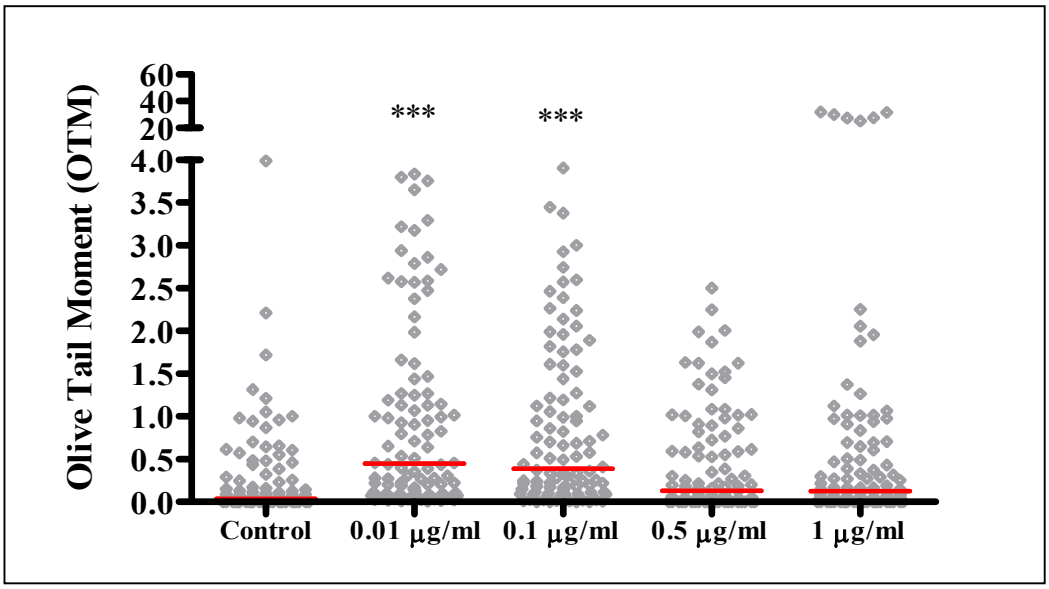

Figure 4.12 The effect of silver nitrate on DNA damage in Jurkat cells. Cells were exposed to different concentrations of silver nitrate for 48 h. DNA damage was determined by the Comet assay. The red lines represent the median. Values are given in table 4.2. ** $p<0.01$, *** $p<0.001$, compared to control (Kruskal-Wallis analysis with Dunn's post-hoc test).

Summary of results of studies of DNA damage by silver nitrate, negatively charged or positively charged AgNPs (0.01-1 µg/ml): time course

The Mann Whitney U test was used to compare the DNA damage in HL60 cells with Jurkats (Table 4.2)

- $AgNO_3$ caused significant DNA damage to both cell types in a dose response manner at 4 h and 24 h post dose.
- At 4h and 24 h, the DNA damage was higher in Jurkats than HL60 at all concentrations, although this did not quite reach statistical significance in some cases.
- At 48 h, the damaged was no longer higher in Jurkats compared to HL60s, which may reflect loss to the system of the most damaged Jurkats.

Table 4.2 DNA damage (Olive Tail Moment, O.T.M) determined for Jurkat and HL60 cells exposed to $AgNO_3$ for 4h, 24 h and 48h. *** $p<0.001$(Mann Whitney U test comparing HL60 with Jurkat cells)

Time	Treatment	Median		P value
		HL60 cells	Jurkat cells	
4h	**$AgNO_3$**			
	0.01 µg/ml	0.231	0.448	n.s
	0.1 µg/ml	0.349	0.730	n.s
	0.5 µg/ml	0.556	0.540	n.s
	1 µg/ml	0.324	2.565	0.001
24h	**$AgNO_3$**			
	0.01 µg/ml	0.144	0.395	n.s
	0.1 µg/ml	0.655	0.819	n.s
	0.5 µg/ml	0.479	0.753	n.s
	1 µg/ml	0.887	1.175	n.s
48h	**$AgNO_3$**			
	0.01 µg/ml	0.395	0.448	n.s
	0.1 µg/ml	0.819	0.391	n.s
	0.5 µg/ml	0.753	0.131	n.s
	1 µg/ml	1.175	0.128	0.001

n.s= not significant, ($p>0.05$)

DNA damage by negatively charged and positively charged AgNPs (0.01-1 µg/ml): time course.

In this set of experiments, Jurkat and HL60 cells were exposed to negatively charged or positively charged AgNPs using the same concentrations and time points as in the $AgNO_3$ study (previous section). The aim of this study was to compare the profile and level of DNA damaged caused by $AgNO_3$ with the two types of AgNPs.

Jurkat and HL60 cells were exposed to a single dose of negatively charged AgNPs or positively charged AgNPs (0.01, 0.1, 0. 5, 1 µg/ml) for 4, 24 and 48 h. As for the previous experiment, at each time point the cells were harvested and taken for DNA damage analysis using the Comet assay (see Methods, Chapter 2). The cells were exposed to the AgNPs at the same concentration as $AgNO_3$ on the basis of weight (µg/ml).

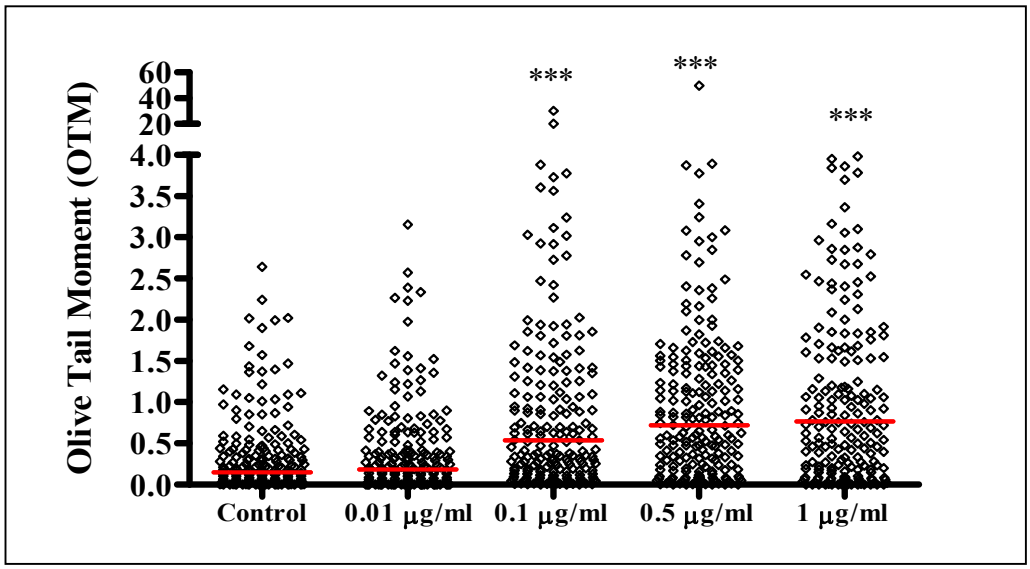

Figure 4.13 The effect of negatively charged AgNPs on DNA damage in HL60 cells. Cells were exposed to different concentrations of negatively charged AgNPs for 4h. DNA damage was determined by the Comet assay. The red lines represent the median. Values are given in table 4.3. *** $p<0.001$, compared to control (Kruskal-Wallis analysis with Dunn's post-hoc test).

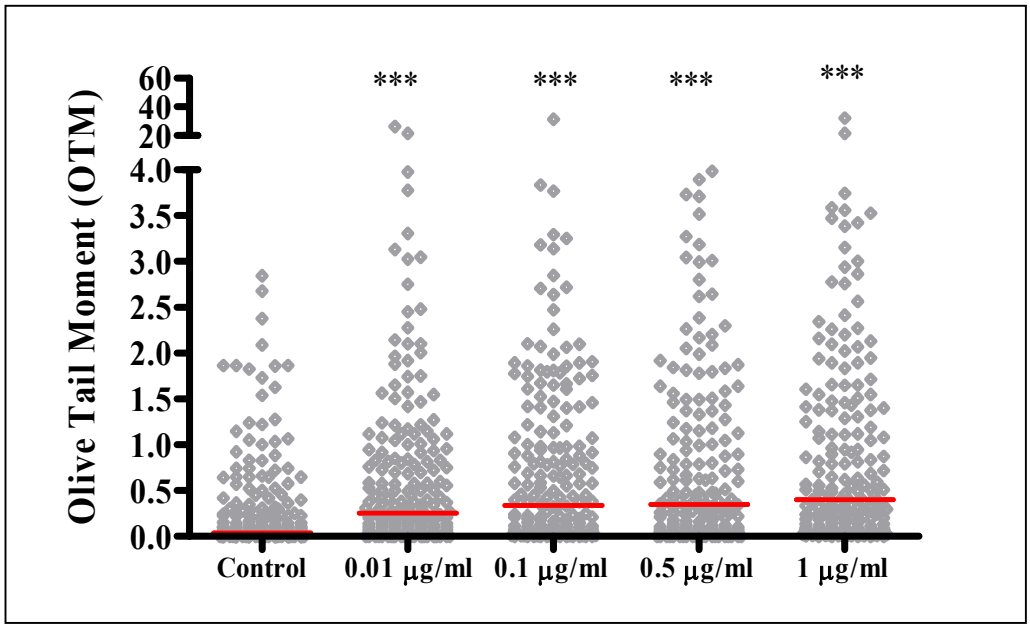

Figure 4.14 The effect of negatively charged AgNPs on DNA damage in Jurkat cells. Cells were exposed to different concentrations of negatively charged AgNPs for 4h. DNA damage was determined by the Comet assay. The red lines represent the median. Values are given in table 4.3. *** $p<0.001$, compared to control (Kruskal-Wallis analysis with Dunn's post-hoc test).

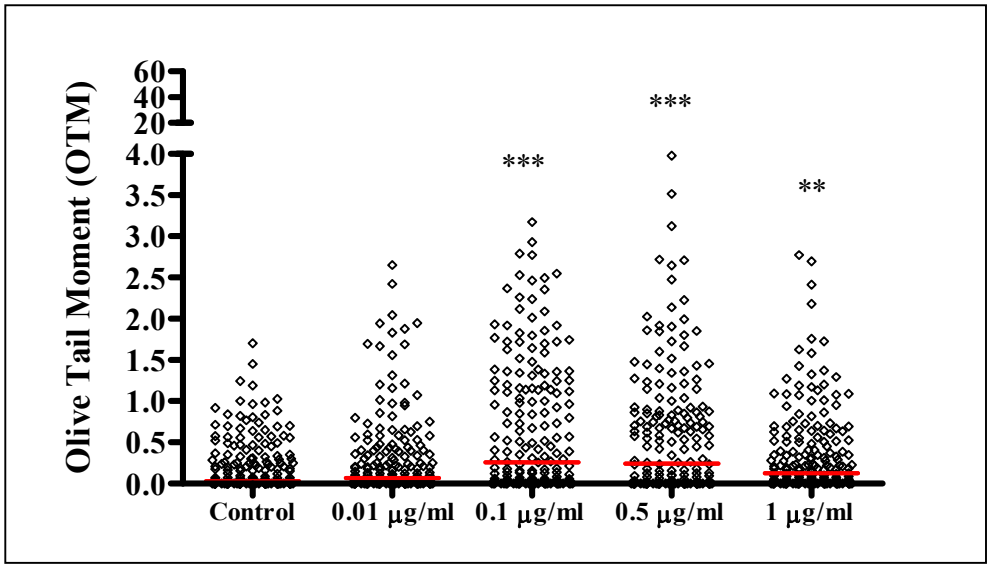

Figure 4.15 The effect of negatively charged AgNPs on DNA damage in HL60 cells. Cells were exposed to different concentrations of negatively charged AgNPs for 24h. DNA damage was determined by the Comet assay. The red lines represent the median. Values are given in table 4.3. ** $p<0.01$, *** $p<0.001$, compared to control (Kruskal-Wallis analysis with Dunn's post-hoc test).

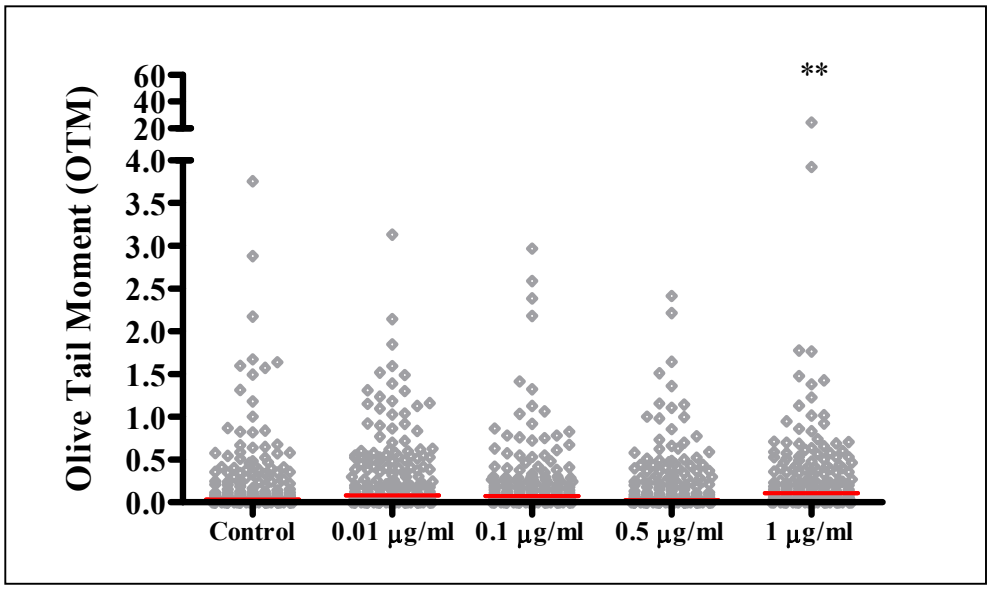

Figure 4.16 The effect of negatively charged AgNPs on DNA damage in Jurkat cells. Cells were exposed to different concentrations of negatively charged AgNPs for 24h. DNA damage was determined by the Comet assay. The red lines represent the median. Values are given in table 4.3. ** $p<0.01$, compared to control (Kruskal-Wallis analysis with Dunn's post-hoc test).

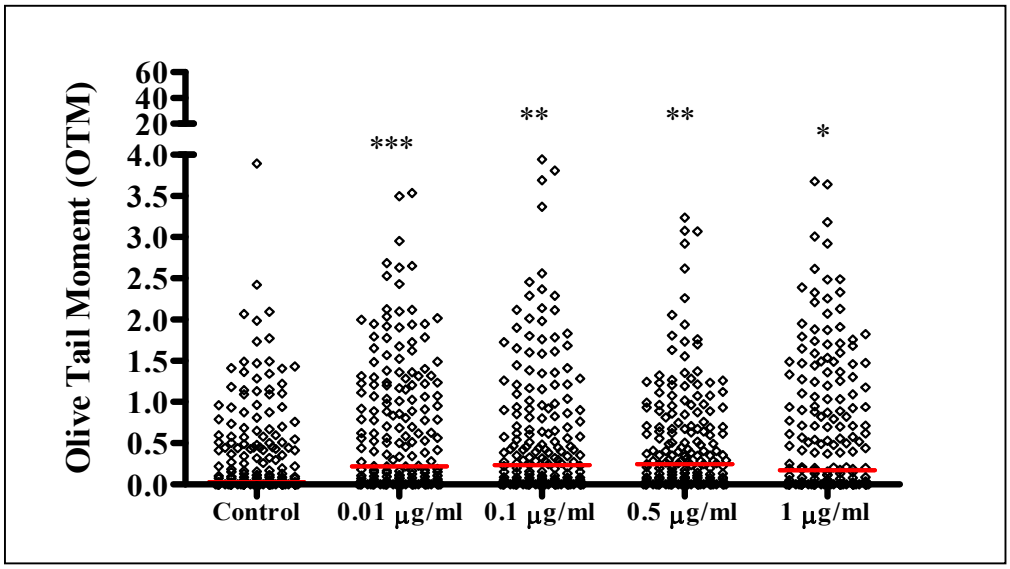

Figure 4.17 The effect of negatively charged AgNPs on DNA damage in HL60 cells. Cells were exposed to different concentrations of negatively charged AgNPs for 48h. DNA damage was determined by the Comet assay. The red lines represent the median. Values are given in table 4.3. * $p<0.05$, ** $p<0.01$, *** $p<0.001$, compared to control (Kruskal-Wallis analysis with Dunn's post-hoc test).

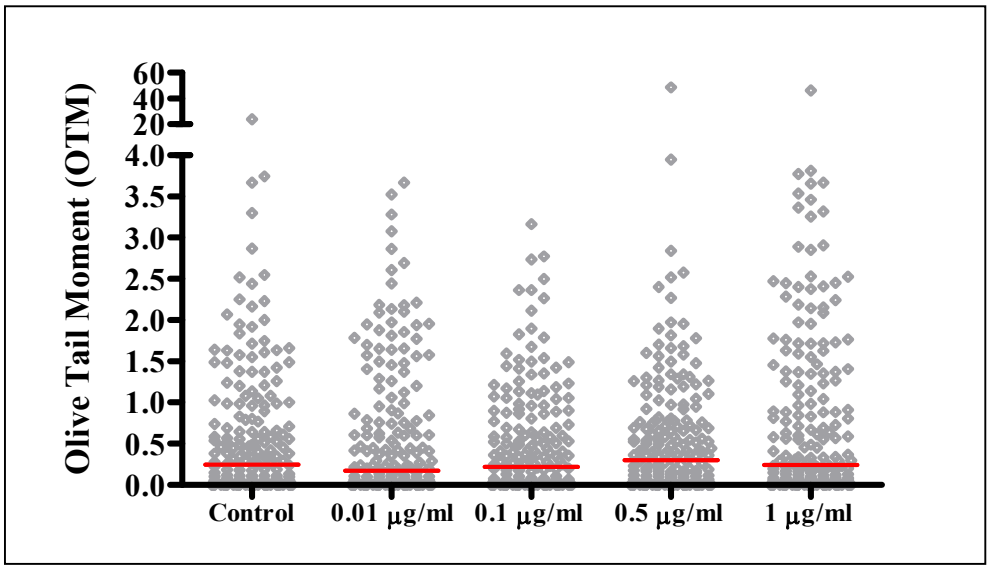

Figure 4.18 The effect of negatively charged AgNPs on DNA damage in Jurkat cells. Cells were exposed to different concentrations of negatively charged AgNPs for 48h. DNA damage was determined by the Comet assay. The red lines represent the median. Values are given in table 4.3.

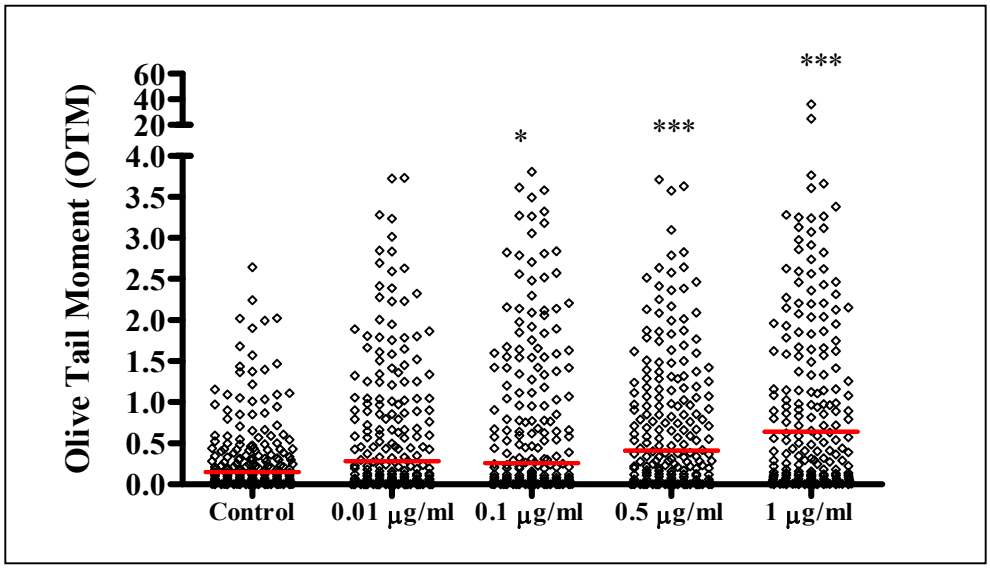

Figure 4.19 The effect of positively charged AgNPs on DNA damage in HL60 cells. Cells were exposed to different concentrations of positively charged AgNPs for 4h. DNA damage was determined by the Comet assay. The red lines represent the median. Values are given in table 4.3. * $p<0.05$, *** $p<0.001$, compared to control (Kruskal-Wallis analysis with Dunn's post-hoc test).

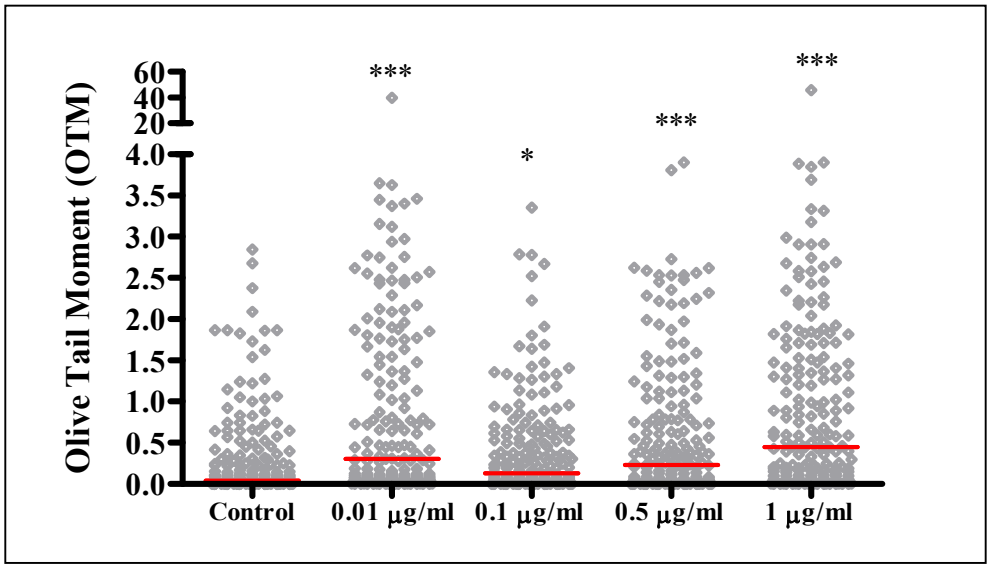

Figure 4.20 The effect of positvely charged AgNPs on DNA damage in Jurkat cells. Cells were exposed to different concentrations of positively charged AgNPs for 4h. DNA damage was determined by the Comet assay. The red lines represent the median. Values are given in table 4.3. * $p<0.05$, *** $p<0.001$, compared to control (Kruskal-Wallis analysis with Dunn's post-hoc test).

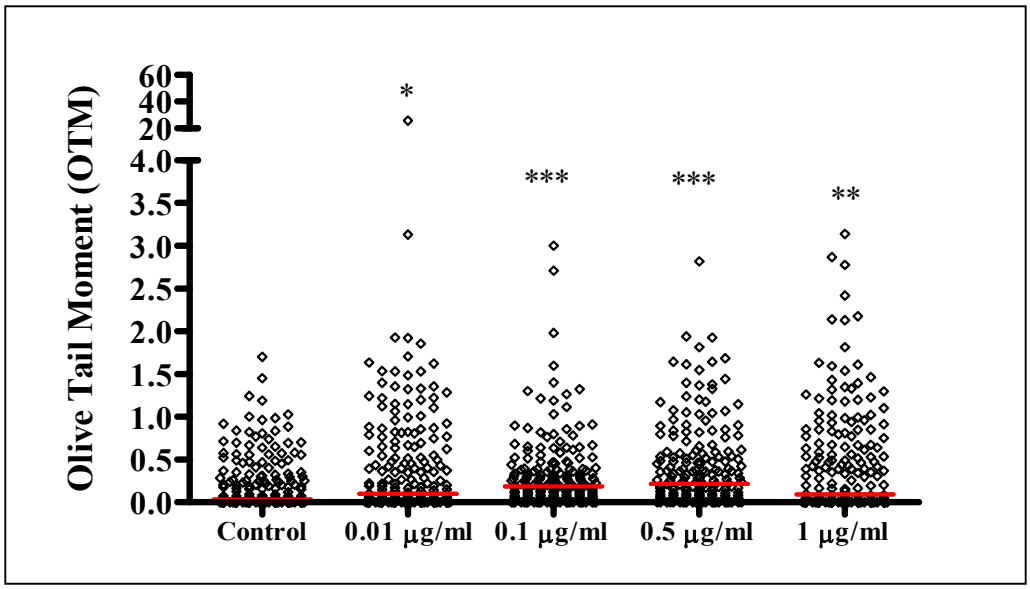

Figure 4.21 The effect of positively charged AgNPs on DNA damage in HL60 cells. Cells were exposed to different concentrations of positively charged AgNPs for 24h. DNA damage was determined by the Comet assay. The red lines represent the median. Values are given in table 4.3. * $p<0.05$, ** $p<0.01$, *** $p<0.001$, compared to control (Kruskal-Wallis analysis with Dunn's post-hoc test).

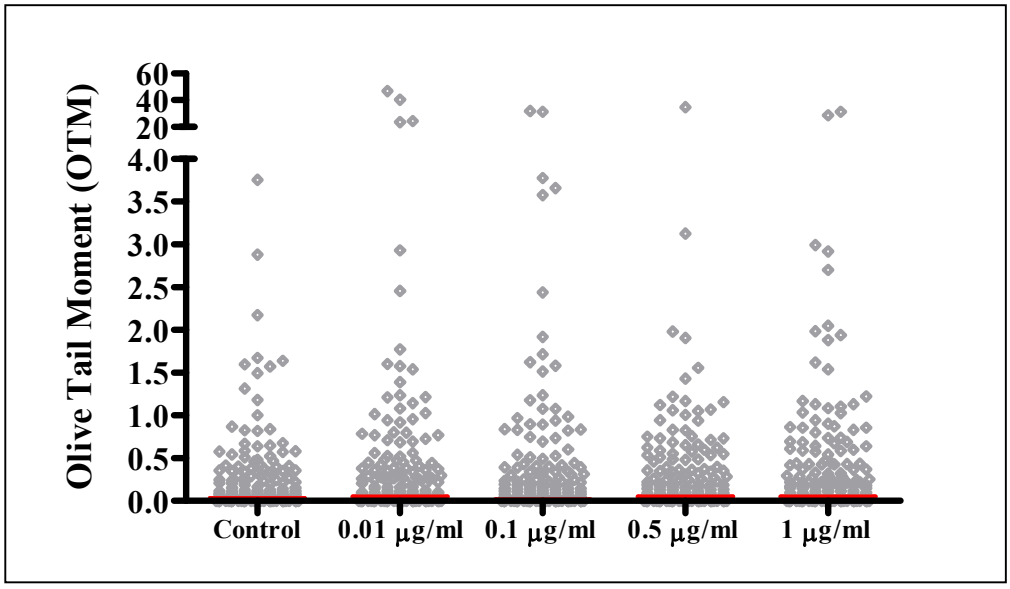

Figure 4.22 The effect of positvely charged AgNPs on DNA damage in Jurkat cells. Cells were exposed to different concentrations of positively charged AgNPs for 24h. DNA damage was determined by the Comet assay. The red lines represent the median. Values are given in table 4.3.

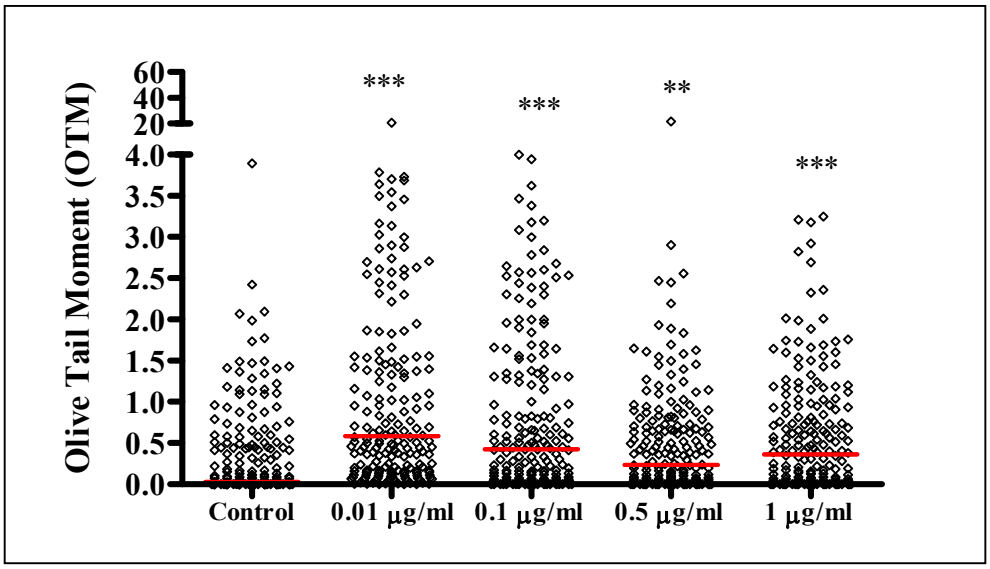

Figure 4.23 The effect of positively charged AgNPs on DNA damage in HL60 cells. Cells were exposed to different concentrations of positively charged AgNPs for 48h. DNA damage was determined by the Comet assay. The red lines represent the median. Values are given in table 4.3. ** $p<0.01$, *** $p<0.001$, compared to control (Kruskal-Wallis analysis with Dunn's post-hoc test).

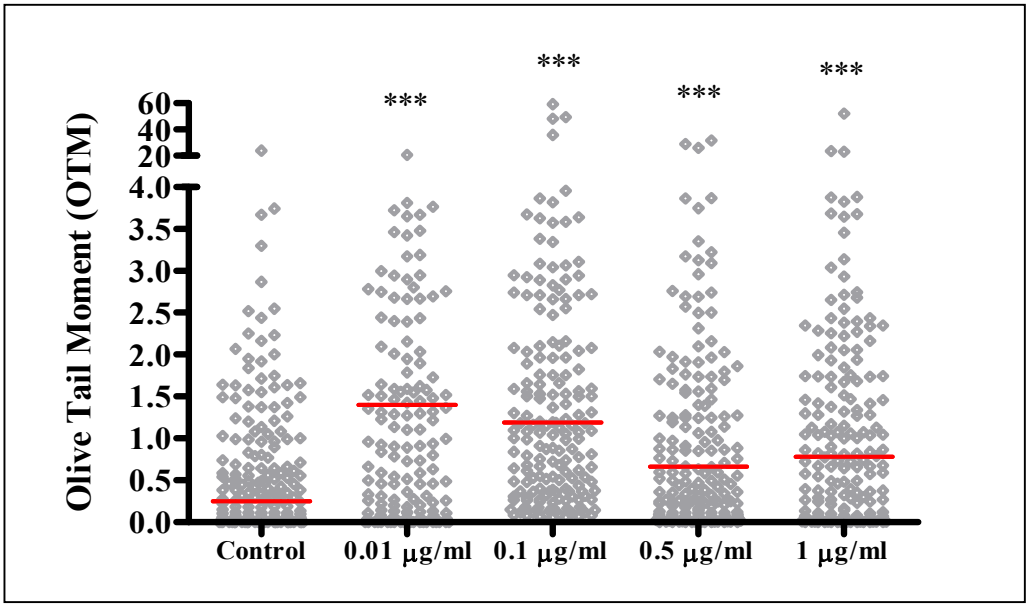

Figure 4.24 The effect of positvely charged AgNPs on DNA damage in Jurkat cells. Cells were exposed to different concentrations of positively charged AgNPs for 48h. DNA damage was determined by the Comet assay. The red lines represent the median. Values are given in table 4.3. *** $p<0.001$, compared to control (Kruskal-Wallis analysis with Dunn's post-hoc test).

Summary of results of studies of DNA damage by negatively charged and positively charged AgNPs (0.01-1 µg/ml): time course

The Mann Whitney U test was used to compare the DNA damage in HL60 cells with Jurkat cells (Table 4.3)

- Negatively charged AgNPs caused significant DNA damage to both cell types in a dose response manner.
- For negatively charged AgNPs, DNA damage was higher in HL60s compared to Jurkats at the earlier time points but this effect was lost by 48 h post dose.

- Positively charged AgNPs also caused significant DNA damage to both cell types in a dose response manner.
- For positively charged AgNPs, the damage was also higher in HL60s compared to Jurkats at the earlier time points, but this effect was also lost by 48 h post dose.

Table 4.3 DNA damage (Olive Tail Moment, O.T.M) determined for Jurkat and HL60 cells exposed to negatively charged AgNPs and positively charged AgNPs for 4h, 24h and 48h * p<0.05, ** p<0.01, *** p<0.001(Mann Whitney U test comparing HL60 with Jurkat cells)

Time	Treatment	Median		P value
		HL60 cells	Jurkat cells	
	Negatively charged AgNPs			
4h	0.01 µg/ml	0.19	0.22	n.s
	0.1 µg/ml	0.54	0.34	0.01
	0.5 µg/ml	0.72	0.35	0.01
	1 µg/ml	0.77	0.40	0.01
24h	0.01 µg/ml	0.07	0.08	n.s
	0.1 µg/ml	0.26	0.07	0.001
	0.5 µg/ml	0.25	0.03	0.001
	1 µg/ml	0.13	0.11	n.s
48h	0.01 µg/ml	0.22	0.17	n.s.
	0.1 µg/ml	0.23	0.22	n.s.
	0.5 µg/ml	0.25	0.30	n.s.
	1 µg/ml	0.17	0.24	0.001
	Positively charged AgNPs			
4h	0.01 µg/ml	0.28	0.31	n.s.
	0.1 µg/ml	0.26	0.13	0.01
	0.5 µg/ml	0.41	0.23	0.5
	1 µg/ml	0.64	0.45	n.s.
24h	0.01 µg/ml	0.10	0.05	n.s.
	0.1 µg/ml	0.18	0.02	0.001
	0.5 µg/ml	0.21	0.05	0.001
	1 µg/ml	0.09	0.05	n.s
48h	0.01 µg/ml	0.58	1.40	0.01
	0.1 µg/ml	0.43	1.19	0.001
	0.5 µg/ml	0.24	0.66	0.001
	1 µg/ml	0.37	0.78	0.001

ns= not significant**,** (p>0.05)

4.3 γH2AX foci

In these experiments, the nature of the DNA damage seen using the Comet method was further investigated. Here, phosphorylation of a subtype of histone H2A, (H2AX, at Ser 139) was determined since this occurs in response to DNA double strand breaks (DSB). Double strand breaks occur when two complementary strands of the double helix of DNA are damaged simultaneously.

The aim of this study was to investigate whether $AgNO_3$ or the two types of AgNPs caused DSBs in Jurkats or HL60 cells. Jurkat and HL60 cells ($5x10^3$ cells/ml) were exposed to a single dose of negatively or positively charged AgNPs or $AgNO_3$ for 4 and 24 h. At each time point the cells were harvested and taken for DSBs analysis using γH2AX immunofluorescence (see Methods, Chapter 2). Cells were inspected for γH2AX foci which stained red. Each field 100 cells were determined for γH2AX foci. Cells were also exposed to a single dose of etoposide (50 μM) at the same time points as a positive control for the assay. Again, the cells were exposed to the AgNPs at the same concentration as $AgNO_3$ on the basis of weight (μg/ml).

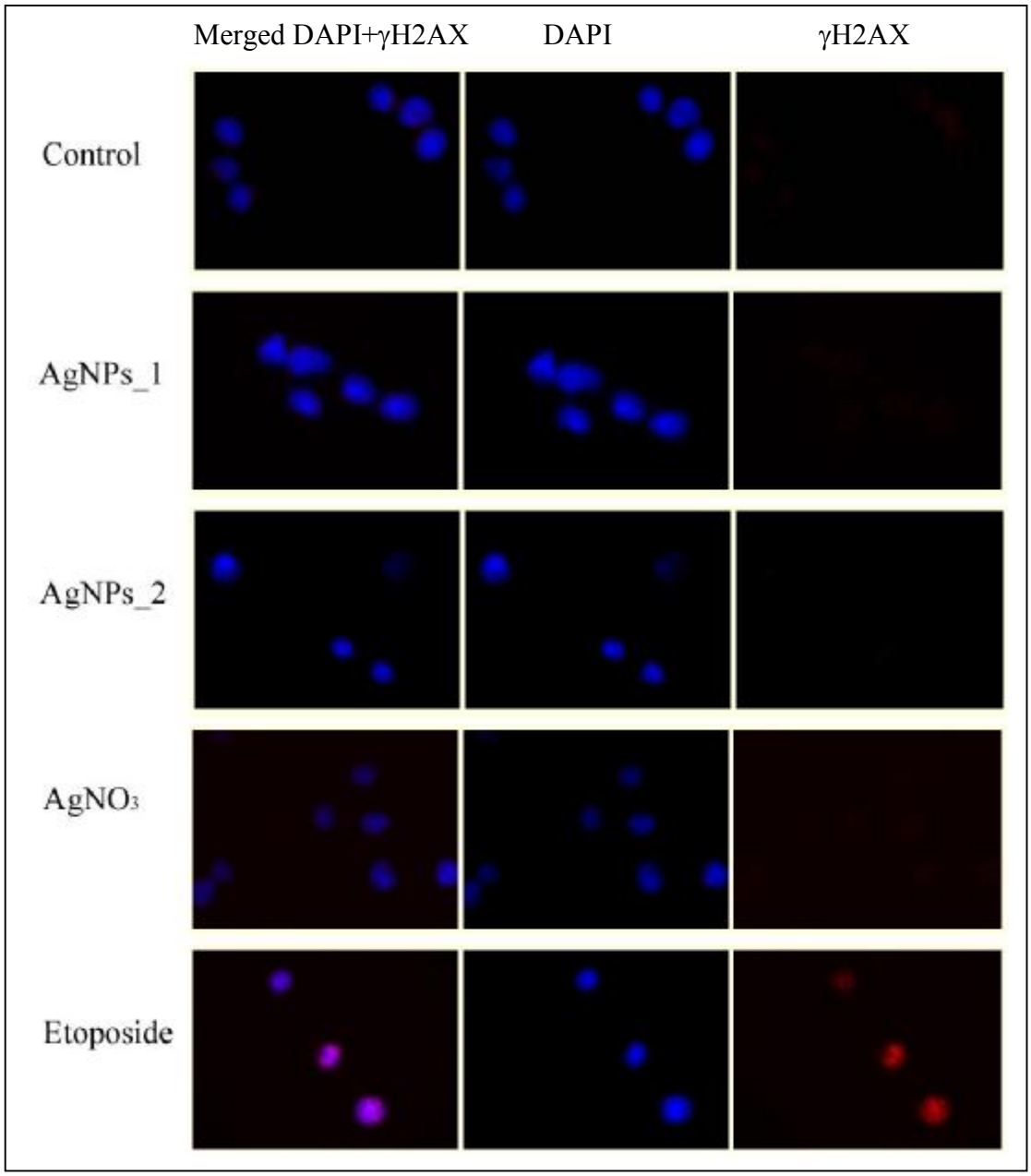

Figure 4.25 Immunofluorescence of phosphorylated γH2AX in HL60 cells after a 4h exposure to 1 μg/ml of negatively charged AgNPs (NanoComposite) (AgNP_1), negatively charged AgNPs (Sigma) (AgNP_2) or $AgNO_3$. Etoposide (50μM) for 4h was the positive control. Nuclear DNA was counterstained with DAPI (blue) and γH2AX (red).

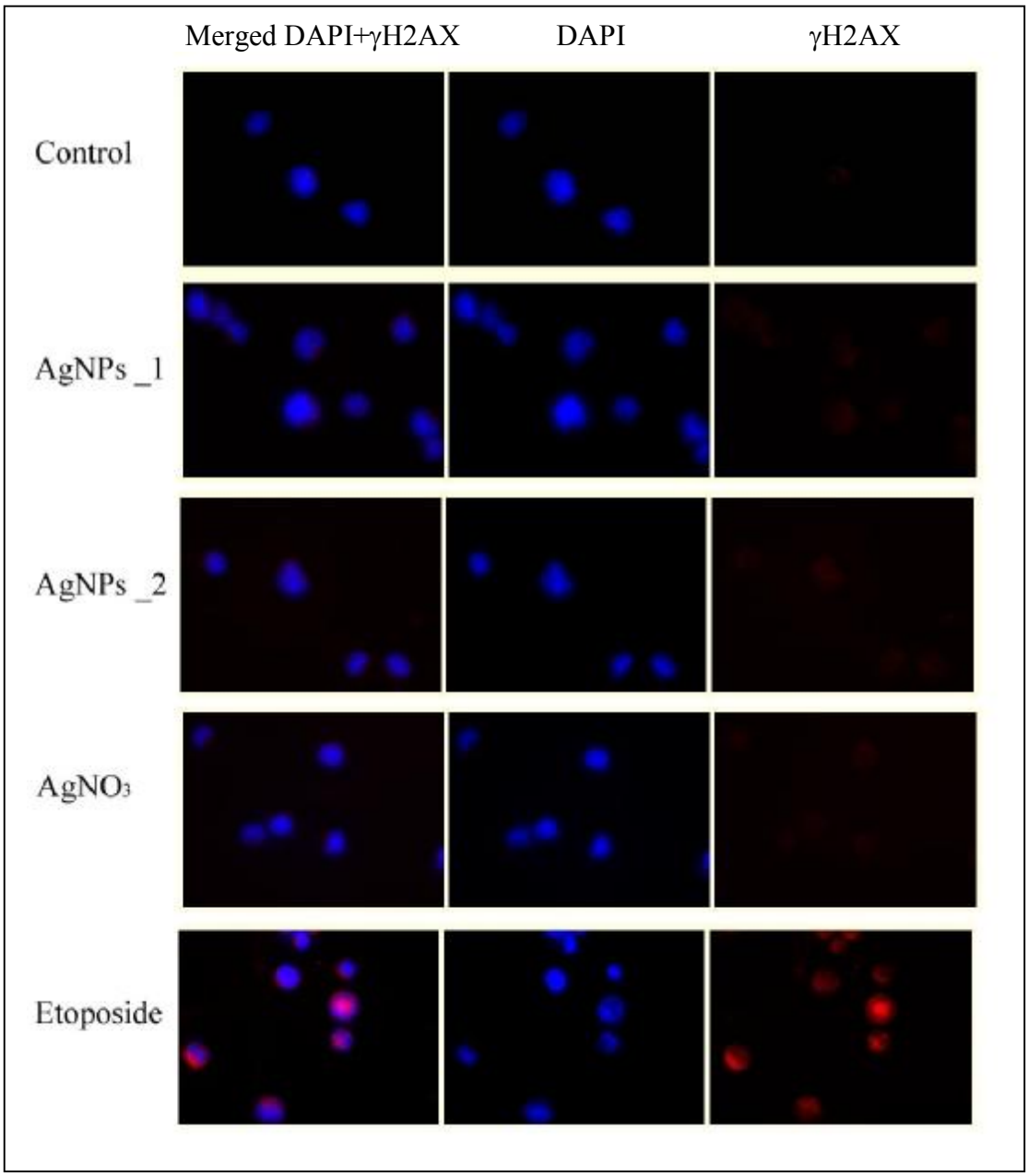

Figure 4.26 Immunofluorescence of phosphorylated γH2AX in HL60 cells after a 24h exposure to 1 μg/ml of negatively charged AgNPs (NanoComposite) (AgNP_1), negatively charged AgNPs (Sigma) (AgNP_2) or $AgNO_3$. Etoposide (50μM) for 4h was the positive control. Nuclear DNA was counterstained with DAPI (blue) and γH2AX (red).

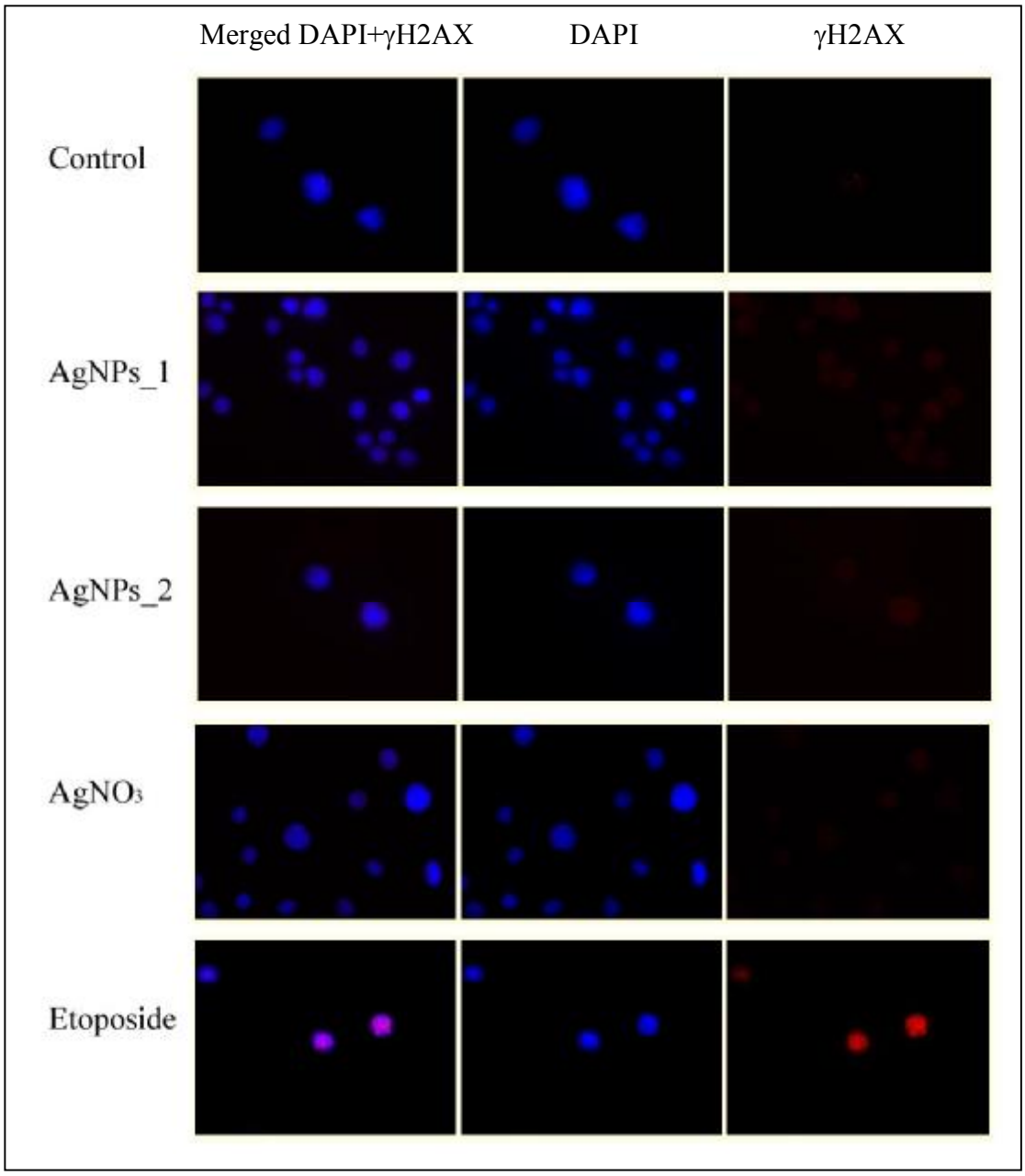

Figure 4.27 Immunofluorescence of phosphorylated γH2AX in Jurkat cells after a 4h exposure to 1 μg/ml of negatively charged AgNPs (NanoComposite) (AgNP_1), negatively charged AgNPs (Sigma) (AgNP_2) or $AgNO_3$. Etoposide (50μM) for 4h was the positive control. Nuclear DNA was counterstained with DAPI (blue) and γH2AX (red).

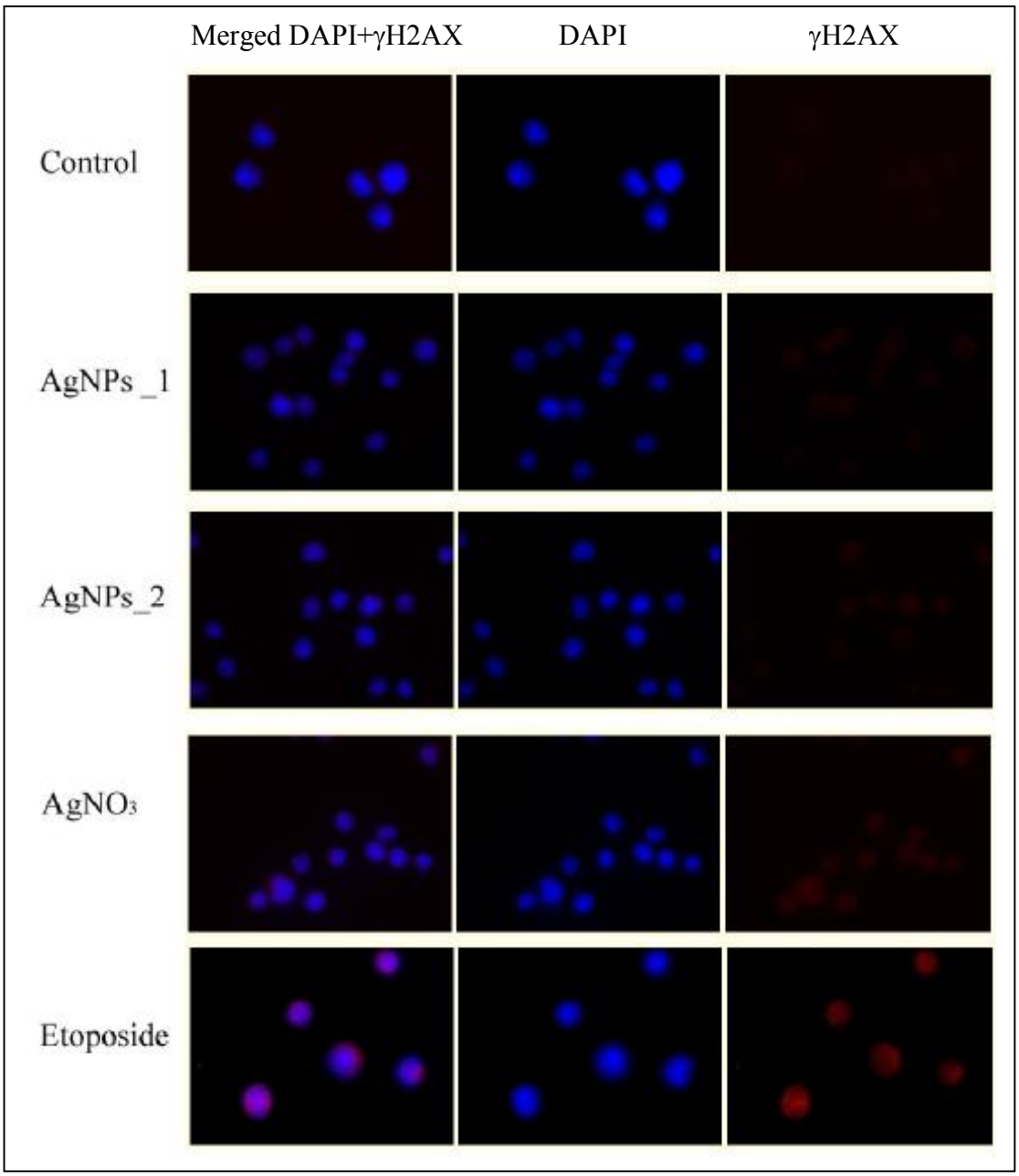

Figure 4.28 Immunofluorescence of phosphorylated γH2AX in Jurkat cells after a 24h exposure to 1 μg/ml of negatively charged AgNPs (NanoComposite) (AgNP_1), negatively charged AgNPs (Sigma) (AgNP_2) or $AgNO_3$. Etoposide (50μM) for 4h was the positive control. Nuclear DNA was counterstained with DAPI (blue) and γH2AX (red).

Summary of results of studies of γH2AX foci

- As expected, etoptoside (positive control) showed a high level of phosphorylation of γH2AX after incubation of HL60 or Jurkat cells for 4h and 24 h.
- Neither type of AgNPs or $AgNO_3$ caused phosphorylation of γH2AX in HL60s at 4h (Figure 4.25) or 24h (Figure 4.26).
- Similarly, there was no phosphorylation of γH2AX in Jurkats by either the AgNPs or $AgNO_3$ at 4h (figure 4.27) or 24h (Figure 4.28).

4.4 Western blot analysis for phosphorylated H2AX (γH2AX) and cleaved PARP

To help confirm that the AgNPs and $AgNO_3$ do not cause DNA damage by a mechanism involving double strand breaks, phosphorylation of the γH2AX protein was determined by Western blot analysis. In parallel poly(ADP-ribose) polymerase (PARP) was determined as a marker of apoptosis to support immunofluorescence studies as as abolition of PARP activity by caspase cleavage is a marker of apoptosis. GAPDH was measured as a loading control. Etoposide, an anti cancer drug is classically used as the positive control for H2AX as it inhibits topoisomerase II (topoII) which is an enzyme that unwinds DNA by making transient double -stranded breaks and indicated apoptosis.

Jurkat and HL60 cells ($5x10^3$ cells/ml) were exposed to a single dose of the two types of AgNPs or $AgNO_3$, as in the previous experiment. At each time point the cells were harvested and taken for Western blot analysis (see Methods, Chapter 2). Cells were also exposed to a single dose of etoposide (50 μM) (positive control).

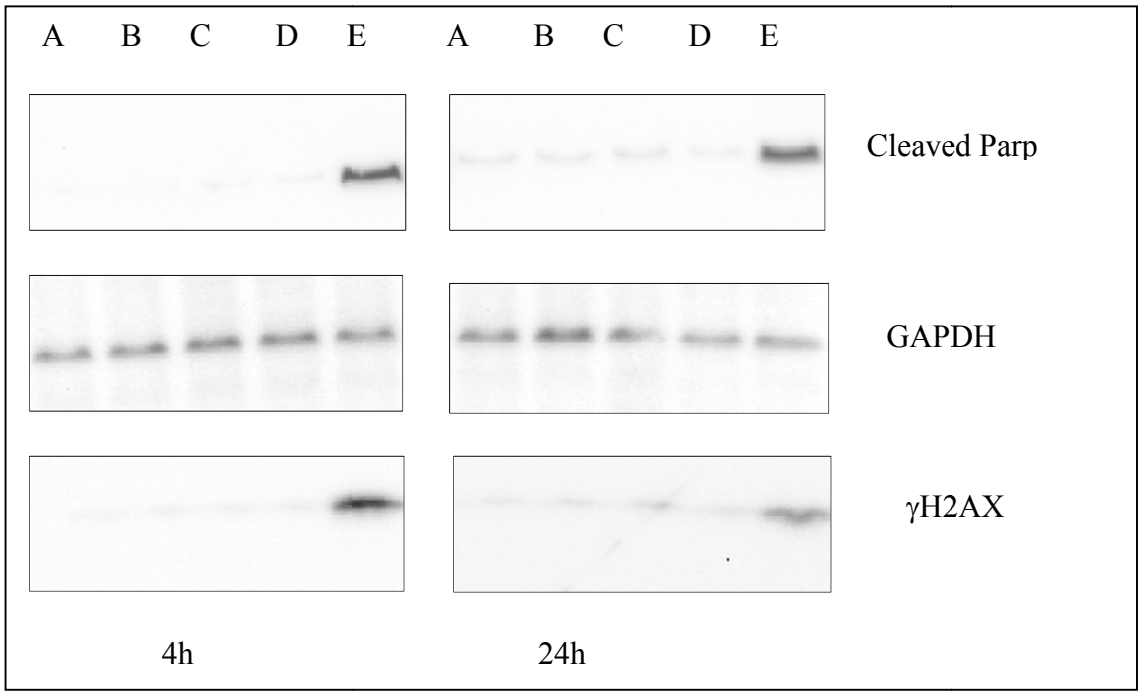

Figure 4.29 Western blot of HL60 cells after 24 h exposure to 1 µg/ml of negatively charged AgNPs (NanoComposite) (B) negatively changed AgNPs (Sigma) (C) $AgNO_3$ (D) or etoposide (50µM) (E). Control cells (no AgNPs or $AgNO_3$) are in lane A.

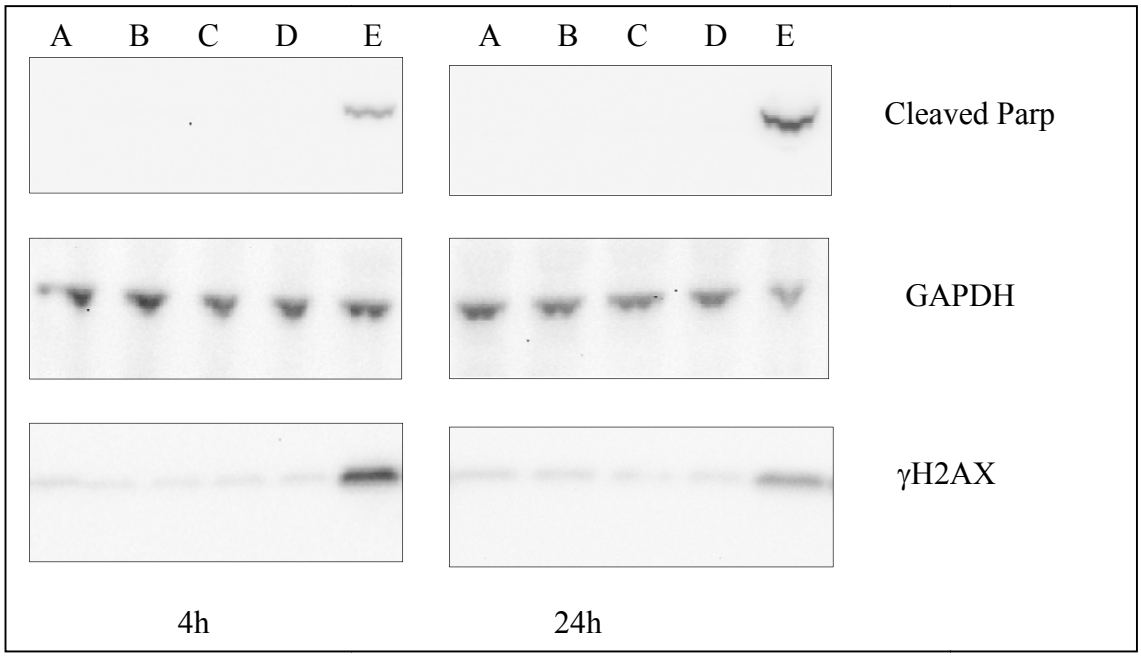

Figure 4.30 Western blot of Jurkat cells after 24 h exposure to 1 µg/ml of negatively charged AgNPs (NanoComposite) (B) negatively changed AgNPs (Sigma) (C) $AgNO_3$ (D) or etoposide (50µM) (E). Control cells (no AgNPs or $AgNO_3$) are in lane A.

Summary of results of studies of western blot analysis for phosphorylated H2AX (γH2AX) and cleaved PARP

- Western blot analysis confirmed that etoposide (positive control) phosphorylated the γH2AX protein.
- Neither AgNPs or $AgNO_3$ phosphorylated γH2AX in either cell type corroborating that these compounds do not damage DNA by a mechanism involving DSBs.
- Cleaved PARP was not detected in cells treated with AgNPs or silver nitrate confirming that at the 1 ug/ml dose as indicated by immunoflourescence assay and high cell viabilitythe level of apoptosis was too low to be detected although DNA damage was observed

4.5 DNA methylation - global methylation (epigenetics)

In this study, the methylation status of long interspersed nucleotide elements (LINE-1) was measured in Jurkat and HL60 cells after dosing with positively or negatively charged AgNPs or $AgNO_3$ at 1 µg/ml for 24 h.
Jurkat or HL60 cells ($5x10^3$ cells/ml) were exposed to a single 1 µg/ml dose of the two types of AgNPs or $AgNO_3$ for 24 h. The cells were then harvested and taken for methylation analysis using pyrosequencing (see Methods, Chapter 2). Untreated cells were used as the control.

The results from the pyrosequencing data showed that LINE-1 methylation was similar for $AgNO_3$, negatively charged AgNPs or positively charged AgNPs, compared to control (Figure 4.31).

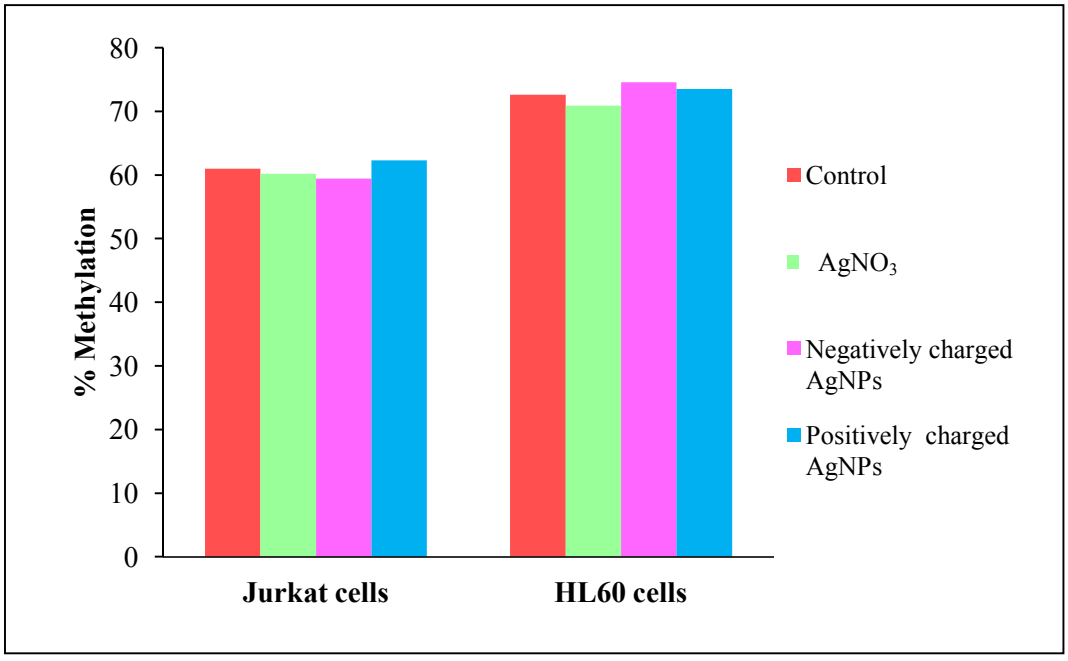

Figure 4.31 Methylation of LINE-1 in Jurkat and HL60 cells after 24 h exposure to 1 µg/ml of negatively or positively charged AgNPs or $AgNO_3$ (n=1).

4.6 Discussion

In this section, DNA damage by $AgNO_3$ and both types of AgNPs was investigated in HL60 and Jurkat cells. The studies mainly focused on measurement of DNA damage by the Comet method using incubation time and concentration parameters with pre-determined levels of cytotoxicity. Other data contained in this chapter indicated that DNA damage by double strand break mechanisms did not greatly influence the damage seen by the Comet method, and preliminary evidence was obtained that neither $AgNO_3$ nor AgNPs cause changes in global methylation.

The Comet data demonstrated that Jurkats were much more sensitive than HL60s to DNA damage by H_2O_2, the positive control for DNA damage. The damage was also significantly higher in Jurkats following exposure to $AgNO_3$. However, it is difficult to know whether the damage seen at the higher concentrations of $AgNO_3$ reflected cells entering apoptosis in parallel with DNA fragmentation, since there was about 50% loss of cell viability at these concentrations. It is also possible that the most damaged Jurkats had been completely destroyed during apoptosis or necrosis and had left the system. In chapter 3, attempts had been made to define the number of cells in apoptosis/necrosis using an Annexin V-FITC/PI kit following exposure to the elements at 1 μg/ml. These data showed that few cells were in apoptosis using these conditions, but further studies are necessary to fully define the percentage of cells in apoptosis/necrosis with DNA damage compared to healthy cells with DNA damaged caused by $AgNO_3$.

Interpretation of the data is much more complicated for cells exposed to the AgNPs. Despite much research in the area, it remains unknown whether AgNPs enter the cell to cause toxicity by releasing Ag^+ions internally, or if the AgNPs remain outside the cell, perhaps bound to thiol-containing proteins on the cell membrane, and from there release Ag^+ions that are taken up by the cell. Sllebo et al (2007) suggested that association of AgNPs with cell membranes can cause physical damage (e.g. pitting) facilitating influx of the NPs. Foulkes (2000) stated that the high affinity of non essential metals for proteins makes it unlikely that their ions, except very transiently, can exist free in biological systems. Nonetheless, the data contained in this chapter reports significant amounts of DNA damage from both types of AgNPs, which was higher in HL60 cells compared to Jurkats, at least at early time points.

In the next chapter, a novel dialysis method was used to determine the concentration of Ag+ions released from the AgNPs, which were available to the cells.

CHAPTER 5

OXIDATIVE STRESS RESPONSE OF THE CELL FROM EXPOSURE TO SILVER

Chapter 5. Oxidative stress response of the cell from exposure to silver

5.1 Equilibrium dialysis to measure silver $^{+}$ions released from AgNPs

In all the previous studies, the toxic effects of AgNPs were compared to that of $AgNO_3$ following dosing at equivalent concentrations on the basis of weight (µg/ml). The aim of this section of the research was to quantify the release of Ag^+ ions from AgNPs since this would give an estimate of the concentration of ions available to the cells.
The release of Ag^+ ions from negatively charged AgNPs was determined by equilibrium dialysis. The experiments used cellulose ester dialysis tubing (GeBAflex-tube Midi,8 kDa), which was filled with water or RPMI+FBS containing negatively charged AgNPs (NanoComposite) at concentrations of 1µg/ml or 10µg/ml. The tubes were then sealed and inserted into plastic bags containing 4 ml of water or RPMI+FBS, respectively. The samples were incubated at 37 °C for 4, 12, 24 or 48h when 300 µl of water or RPMI+FBS was taken from the bag for trace metal analysis by ICP-MS (Fig 5.2) (see Methods, Chapter 2).

The concentration of Ag^+ ions in the samples was determined by comparison to a standard curve of $AgNO_3$ (Figure 5.1)

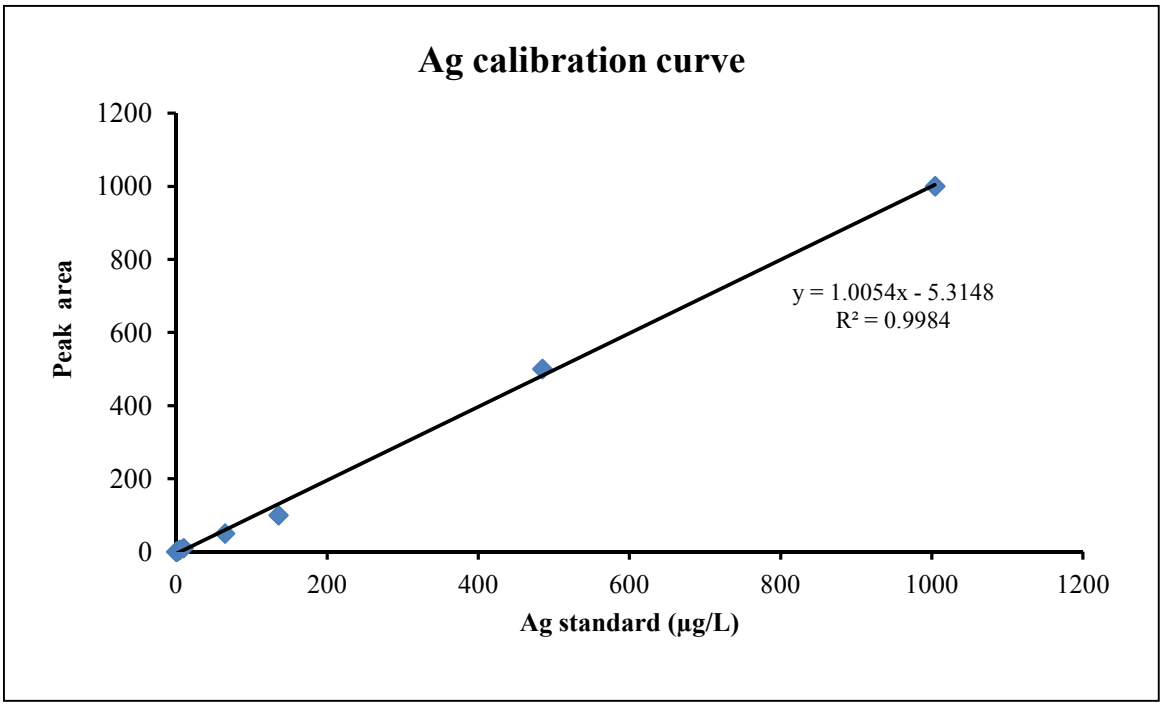

Figure 5.1 A typical calibration curve for silver determined by ICP-MS.

The release of Ag+ ions from negatively charged AgNPs in different media.

Negatively charged AgNPs were placed in the dialysis tube and put into plastic bags containing the same medium i.e. water, Jurkat medium (RPMI containing 10% FBS) or HL60 medium (RPMI containing 20% FBS) (Figure 5.2). At 4, 12, 24 and 48 h after incubation at 37°C, samples were taken from the plastic bag for analysis of Ag^{+} ions by ICP-MS.

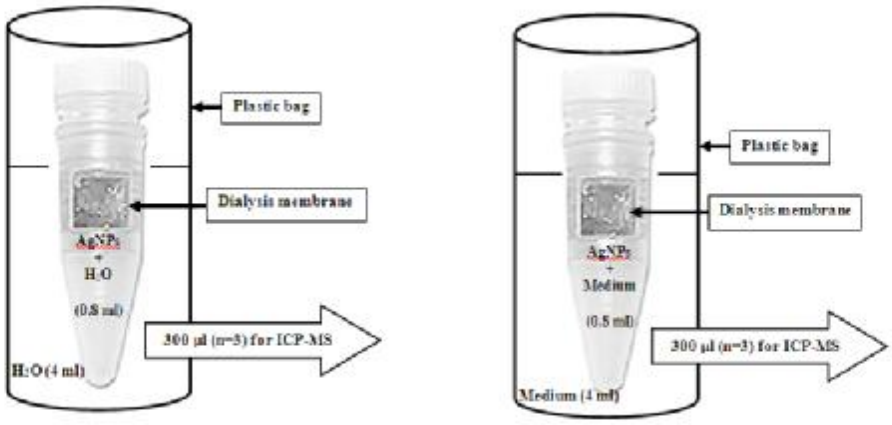

Figure 5.2 A diagram of the dialysis experiment to determine the release of Ag^{+} ions from AgNPs in different media.

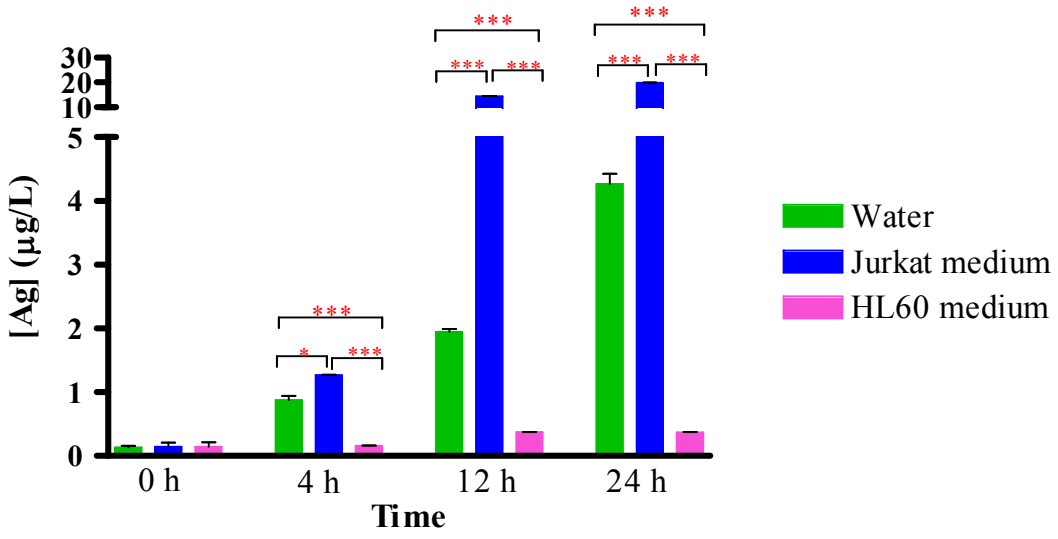

Figure 5.3 The concentration of silver released from negatively charged AgNPs (1µg/ml) in different medium.The X axis represents time. The Y axis represents the concentration of silver detected by ICP-MS. The data are the mean ±SEM (n=3). * $p<0.5$, *** $p<0.001$ different media were compared at each time point (Students t-test).

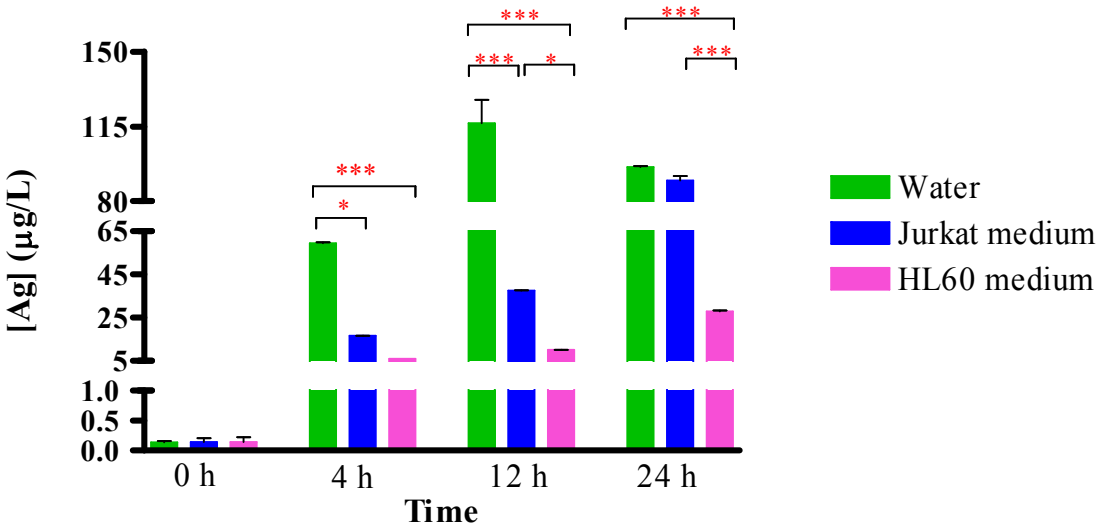

Figure 5.4 The concentration of silver released from negatively charged AgNPs (10 µg/ml) in different medium. The X axis represents time. The Y axis represents the concentration of silver detected by ICP-MS. The data are the mean ±SEM (n=3). * $p<0.5$, *** $p<0.001$ different media were compared at each time point (Students t-test).

Summary of results of studies of equilibrium dialysis to measure silver $^{+}$ions released from AgNPs

- There were significantly fewer Ag^{+} ions released from AgNPs (1 µg/ml) in HL60 medium compared to water at all time points ($p<0.001$).
- There were significantly more Ag^{+} ions released from the AgNPs (1 µg/ml) in Jurkat medium compared to water at all time points ($p<0.001$) excepted at 4h ($p<0.01$).
- There were significantly more Ag^{+} ions released from the AgNPs (1 µg/ml) in Jurkat medium compared to HL60 medium at all time points ($p<0.001$).

- For the higher dose of AgNPs (10 µg/ml), there were more Ag^{+} ions released from water compared to both Jurkat and HL60 medium.
- As seen for the lower AgNPs concentration (1 µg/ml), there were more Ag^{+} ions released from 10 µg/ml in Jurkat medium compared to HL60, although this was not so apparent as at 1 µg/ml.

The release of Ag+ ions from negatively charged AgNPs in the presence of Jurkat or HL60 cells.

Negatively charged AgNPs were placed in the dialysis tube and put into plastic bags containing the same medium Jurkat medium (containing 10% FBS) or HL60 medium (RPMI containing 20% FBS) in the presence of cells ($4x10^5$ cells/ml) (Figure 5.5). At 4, 12, 24 and 48 h after incubation at 37°C, samples were taken from the plastic bag for analysis of Ag^+ ions by ICP-MS.

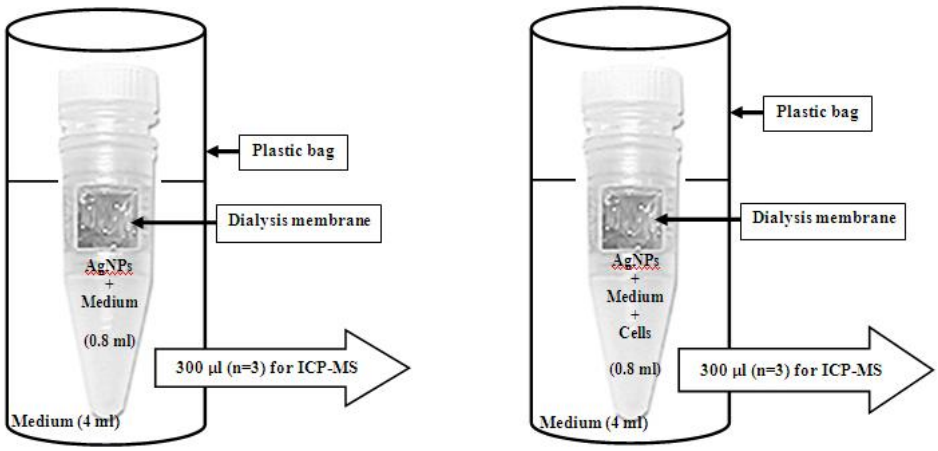

Figure 5.5 A diagram of the dialysis experiment to determine the release of Ag^+ ions from AgNPs in the presence of Jurkat or HL60 cells.

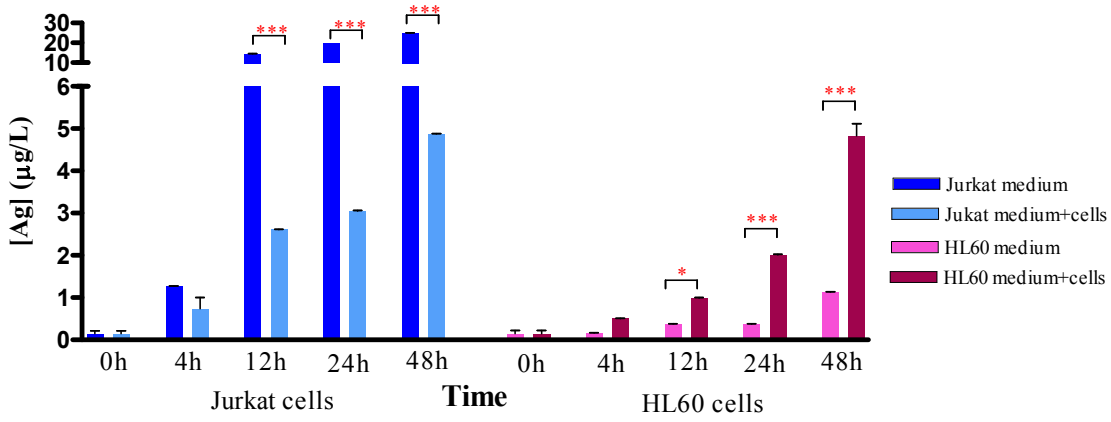

Figure 5.6 The concentration of silver released from negatively charged AgNPs (1 µg/ml) in the presence of Jurkat or HL60 cells. The X axis represents time. The Y axis represents the concentration of silver detected by ICP-MS. The data are the mean ±SEM (n=3). * $p<0.5$, *** $p<0.001$ medium containing cells compared with medium alone at each time point (Students t-test).

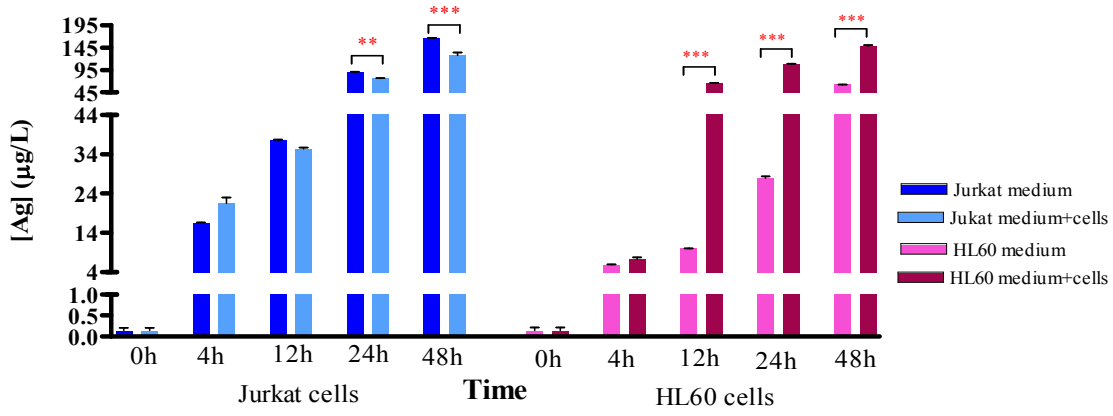

Figure 5.7 The concentration of silver released from negatively charged AgNPs (10 µg/ml) in the presence of Jurkat or HL60 cells. The X axis represents time. The Y axis represents the concentration of silver detected by ICP-MS. The data are the mean ±SEM (n=3). ** $p<0.01$, *** $p<0.001$ medium containing cells compared with medium alone at each time point (Students t-test).

Summary of results of studies of the release of Ag+ ions from negatively charged AgNPs in the presence of Jurkat or HL60 cells

Negatively charged AgNPs (1µg/ml)

- There were significantly less Ag^+ ions released from Jurkat medium with cells compared to Jurkat medium lone, at all time points.
- Conversely, there were significantly more Ag^+ ions released from HL60 medium with cells compared to HL60 medium alone, at all time points.
- At all time points, more Ag^+ ions were released from AgNPs in Jurkat medium compared to HL60 medium.
- Of importance, the amount of Ag^+ ions released from AgNPs (1µg/ml) in the presence of cells was similar for Jurkats and HL60s, particularly at 24h (the focus of most experiments).

Negatively charged AgNPs (10µg/ml)

- There were significantly less Ag^+ ions released from AgNPs in Jurkat medium with Jurkats compared to those released from Jurkat medium alone.
- Conversely, there were a significantly more Ag^+ ions released from AgNPs in HL60 medium with cells compared to those released from HL60 medium alone.

Conclusions

The release of Ag+ ions from negatively charged AgNPs appeared to be dependent on the following factors:-

1. Composition of the tissue culture medium (probably the % of FBS). The FBS in the culture medium can bind the Ag^{+} ions. The surface of the FBS molecule is negatively to can bind the silver ion and this might help to protect from agglomeration of the NPs suspended in the medium (Johnson, 2010). It has been reported that the interaction of proteins with AgNPs could potentially affect the entry and intracellular localization of NPs within cells, and thus their toxicity (Cedervall et al, 2007). The authors hypothesized that the higher the serum concentration in the medium, the lower the toxicity. It is plausible therefore, that the higher toxicity of negatively charged AgNPs to Jurkats compared to HL60 may have been influenced by the relatively lower FBS concentration in Jurkats (10% in Jurkats and 20% in HL60s).
2. The type of cell (Jurkat or HL60). Jurkat and HL60 cells were used to represent effects in T-lymphocyes and macrophages respectively. Human T-cell lymphoblasts (represented by the Jurkat cell line) cannot carry out phagocytosis while it was reported that HL60 cells can carry out phagocytosis (Gallagher et al, 1979).It is possible that the different of cell type might influence the uptake intracellularly and the toxicity response.
3. The concentration of AgNPs (1µg/ml compared to 10µg/ml). Increasing in the concentration that refers to increasing of the number of the AgNPs. According to the smaller size of the particles but have larger surface –volume ratio consequently influence to the ability of releasing of Ag+. in our studies below.
4. Time of incubation. The longer exposure time to AgNPs increased the exposure to Ag+ ion that release from AgNPs.

5.2 qPCR array analysis of oxidative stress genes

The earlier studies had reported DNA damage from $AgNO_3$ and AgNPs using the Comet method, which is generally accepted to be a measure of oxidative damage. Evidence that the damage seen resulted from an oxidative stress mechanism was supported by negative results for γH2AX phosphorylation (chapter 4) and global methylation (chapter 4).

The aim of this part of the research was to further investigate whether oxidative stress caused the DNA damage seen earlier. RT^2 Profiler™ PCR Array Human Oxidative Stress and Antioxidant Defense plates (PAHS-065A) (SAbiosciences) were used for quantitative PCR (qPCR) array analyses. Each array contained a panel of 84 primer sets for 84 individual genes related to oxidative stress with housekeeping genes to stardardise the method (Appendix B). Jurkat or HL60 cells ($5x10^5$ cells/ml) were exposed to $AgNO_3$ (1 μg/ml) or the AgNPs (1 μg/ml) for 24h when the cells were harvested and washed in fresh RPMI prior to qPCR array analyses using a qPCR Array system (see Methods, Chapter 2).

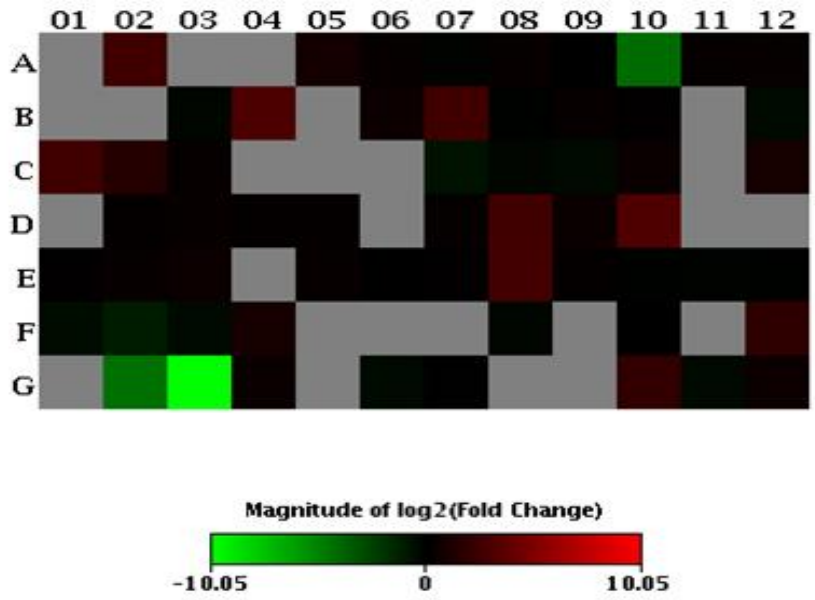

Figure 5.8 A heat map showing modulated genes (up-regulated or down-regulated) after treatment of HL60 cells with $AgNO_3$ compared to untreated cells. Genes shown in red are up-regulated and those in green are down-regulated in comparison to control. Table 5.1 gives the identity of the genes that were up regulated or down regulated ≥ 4 fold.

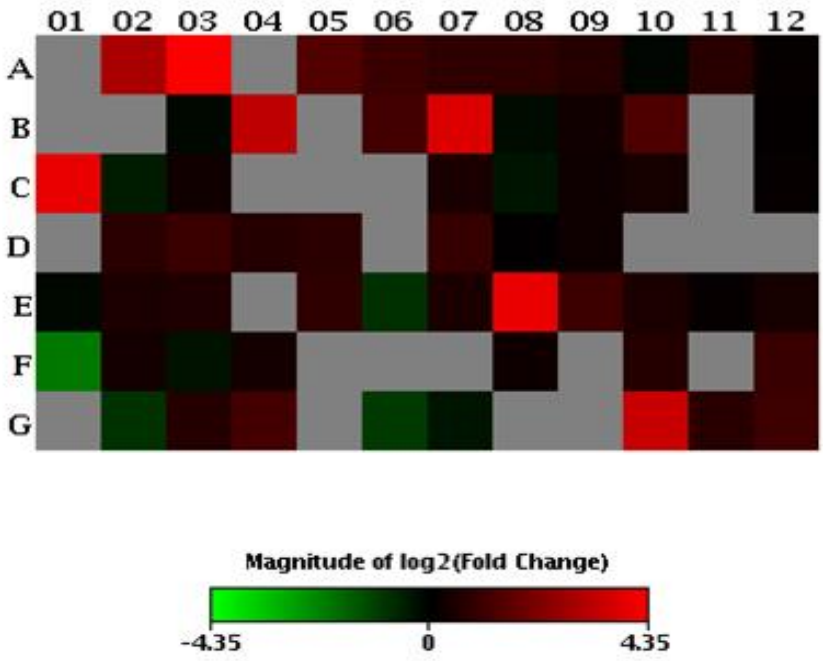

Figure 5.9 A heat map showing modulated genes (up-regulated or down-regulated) after treatment of HL60 cells with negatively charged AgNPs compared to untreated cells. Genes shown in red are up-regulated and those in green are down-regulated in comparison to control. Table 5.1 gives the identity of the genes that were up regulated or down regulated ≥ 4 fold.

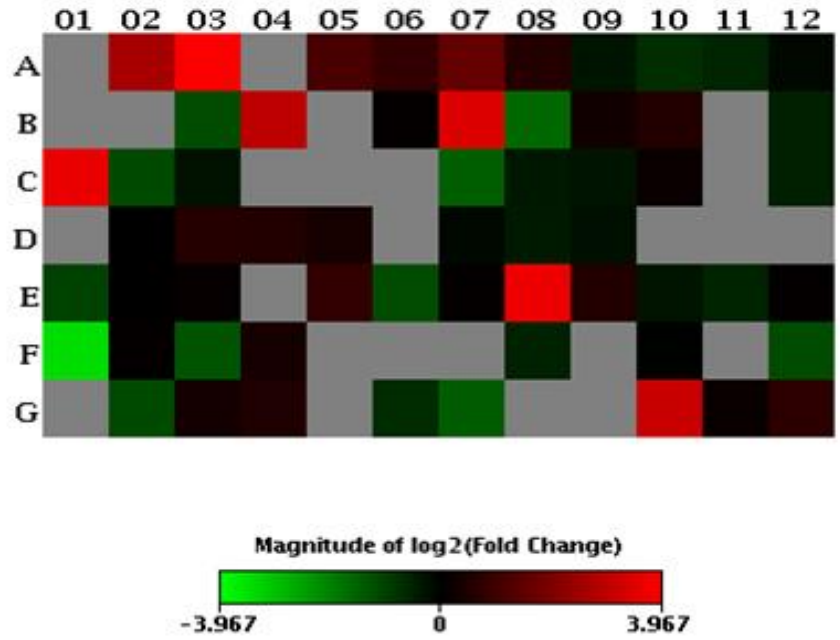

Figure 5.10 A heat map showing modulated genes (up-regulated or down-regulated) after treatment of HL60 cells with positively charged AgNPs compared to untreated cells. Genes shown in red are up-regulated and those in green are down-regulated in comparison to control. Table 5.1 gives the identity of the genes that were up regulated or down regulated ≥ 4 fold.

Table 5.1 A summary of genes involved in regulation of oxidative stress giving ≥ 4 fold change (up or down fold regulation) after treatment of HL60 cells with $AgNO_3$, negatively charged AgNPs or positively charged AgNPs (1 µg/ml) for 24 hours. Values are for one experiment.

Description	Gene symbol	Silver nitrate	Negatively charged AgNPs	Positively charged AgNPs
Arachidonate 12-lipoxygenase	ALOX12	5.86	7.57	6.13
Angiopoietin-like 7	ANGPTL7	-	20.39	15.63
Copper chaperone for superoxide dismutase	CCS	-19.03	-	-
Dual oxidase 1	DUOX1	8.06	9.51	7.71
Epoxide hydrolase 2, cytoplasmic	EPHX2	5.74	13.36	10.83
Glutathione peroxidase 2 (gastrointestinal)	GPX2	5.78	15.78	12.79
Neutrophil cytosolic factor 1	NCF1	5.7	-	-
Non-metastatic cells 5, protein expressed in (nucleoside-diphosphate kinase)	NME5	8.51	-	-
Peroxiredoxin 2	PRDX2	5.94	16.22	13.15
Phosphatidylinositol-3,4,5-trisphosphate-dependent Rac exchange factor 1	PREX1	-	-4.17	-11.03
Sirtuin (silent mating type information regulation 2 homolog) 2 (S. cerevisiae)	SIRT2	-21.26	-	-
Superoxide dismutase 1, soluble	SOD1	-1060.11	-	-
Thioredoxin domain containing 2 (spermatozoa)	TXNDC2	4	10.93	8.86

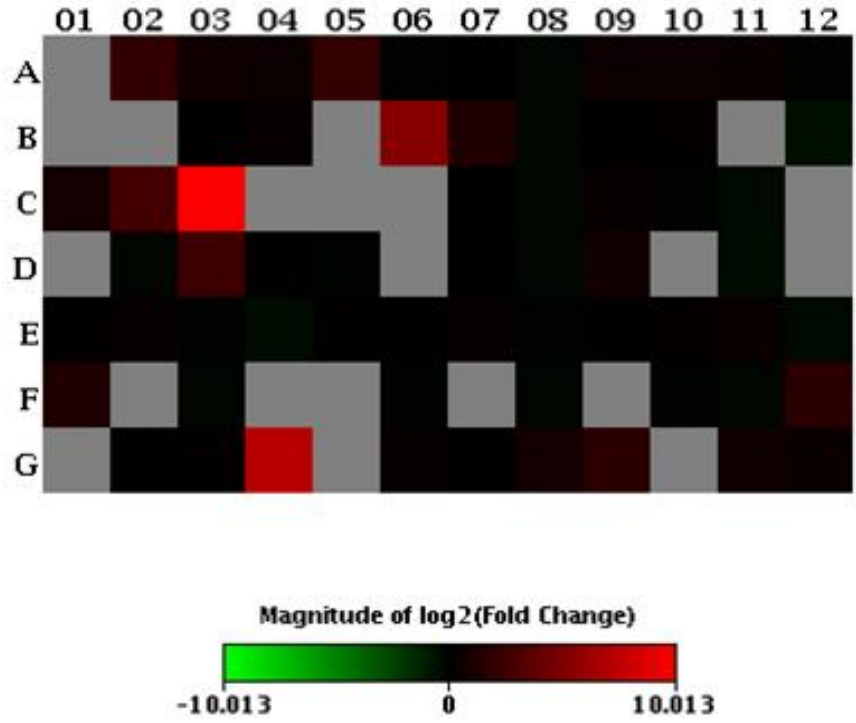

Figure 5.11 A heat map showing modulated genes (up-regulated or down-regulated) after treatment of Jukat cells with $AgNO_3$ compared to untreated cells. Genes shown in red are up-regulated and those in green are down-regulated in comparison to control. Table 5.2 gives the identity of the genes that were up regulated or down regulated ≥ 4 fold.

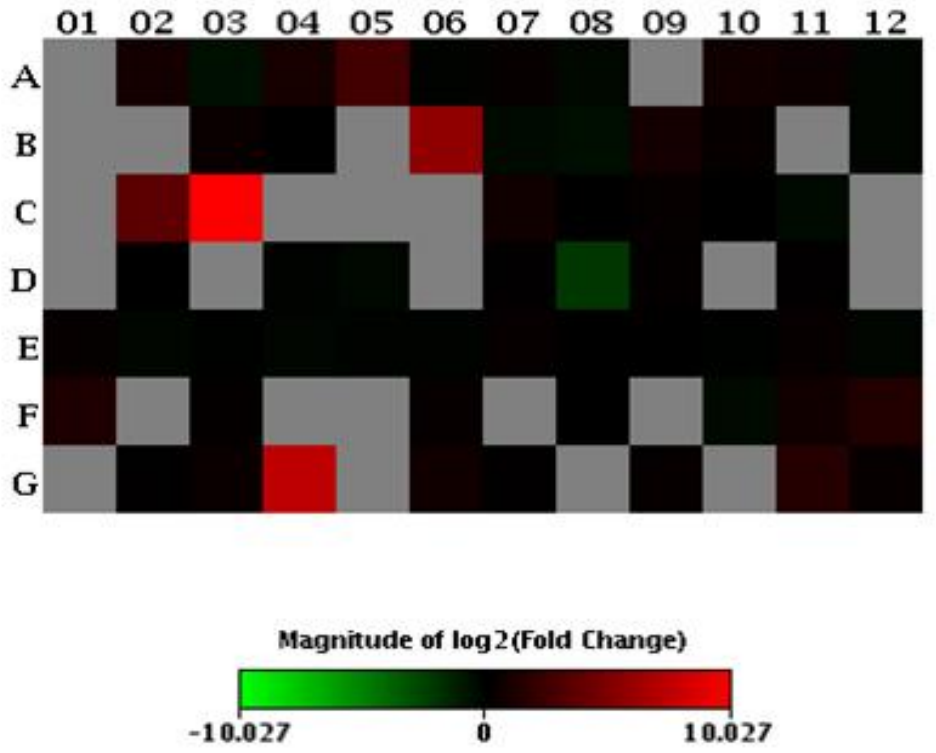

Figure 5.12 A heat map showing modulated genes (up-regulated or down-regulated) after treatment of Jukat cells with negatively charged AgNPs compared to untreated cells. Genes shown in red are up-regulated and those in green are down-regulated in comparison to control. Table 5.2 gives the identity of the genes that were up regulated or down regulated ≥ 4 fold.

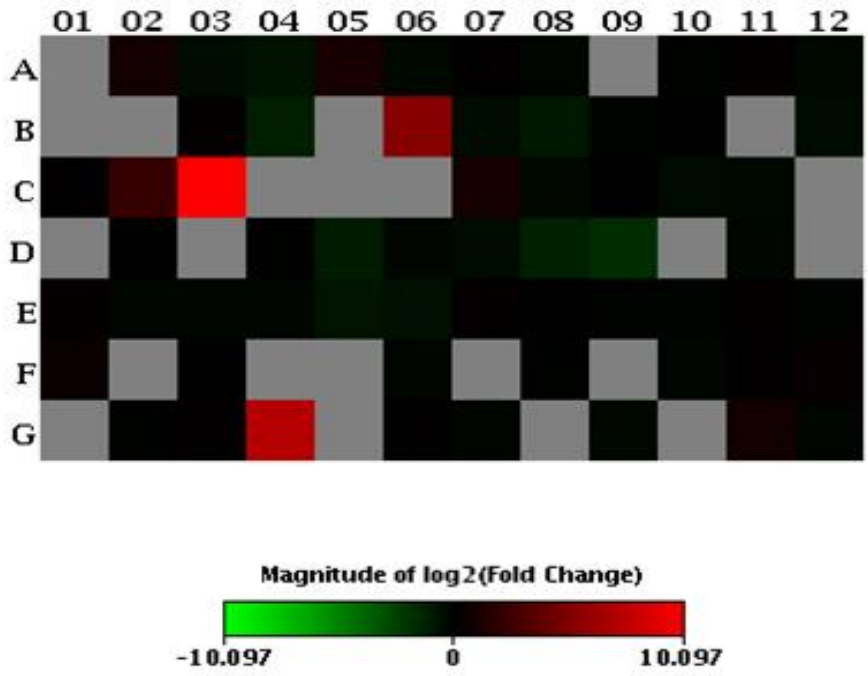

Figure 5.13 A heat map showing modulated genes (up-regulated or down-regulated) after treatment of Jukat cells with positively charged AgNPs compared to untreated cells. Genes shown in red are up-regulated and those in green are down-regulated in comparison to control. Table 5.2 gives the identity of the genes that were up regulated or down regulated ≥ 4 fold.

Table 5.2 A summary of genes involved in regulation of oxidative stress giving ≥ 4 fold change (up or down fold regulation) after treatment of Jurkat cells with $AgNO_3$, negatively charged AgNPs or positively charged AgNPs (1 µg/ml) for 24 hours. Values are for one experiment.

Description	Gene symbol	Silver nitrate	Negatively charged AgNPs	Positively charged AgNPs
Apolipoprotein E	APOE	4.09	6.18	-
Dual specificity phosphatase 1	DUSP1	40.32	52.59	41.55
Glutathione peroxidase 3 (plasma)	GPX3	6.33	12.44	4.46
Glutathione peroxidase 4 (phospholipid hydroperoxidase)	GPX4	1033.51	1043.1	1094.96
Myeloperoxidase	MPO	5.18	-	-
Neutrophil cytosolic factor 1	NCF1	-	-4.39	-
Superoxide dismutase 2, mitochondrial	SOD2	161.27	179.35	143.68

Summary of results of studies of qPCR array analysis of oxidative stress genes

HL60s

- Down regulation of copper chaperone for superoxide dismutase (CCS) by $AgNO_3$ but not the AgNPs.
- Upregulation of epoxide hydrolase 2 by $AgNO_3$ and both AgNPs.
- Upregulation of glutathione peroxidase 2 by $AgNO_3$ and both AgNPs.
- Upregulation of peroxiredoxin 2 by $AgNO_3$ and both AgNPs.
- Down regulation of superoxide dismutase 1 by $AgNO_3$, but not the AgNPs.
- Upregulation of thioredoxin domain containing 2 by $AgNO_3$ and both AgNPs.

Jurkats

- Upregulation of dual specificity phosphatase 1 by $AgNO_3$ and both AgNPs.
- Upregulation of glutathione peroxidase 3 by $AgNO_3$ and both AgNPs.
- Upregulation of glutathione peroxidase 4 by $AgNO_3$ and both AgNPs.
- Upregulation of superoxide dismutase 2 by $AgNO_3$ and both AgNPs.

5.3 Inhibition of soluble superoxide dismutase (SOD1) function by AgNPs

The qPCR data in chapter 5.2 had shown up- and down- regulation of several oxidative stress genes following exposure to $AgNO_3$ or the AgNPs. The transcriptional changes were more evident in Jurkats than HL60s, particularly when they were exposed to $AgNO_3$ for 24h. In this chapter inhibition of the function of SOD1 (soluble superoxide dismutase) was investigated in Jurkats and HL60s following exposure to $AgNO_3$ or negatively charged AgNPs.

20 ml of Jurkat cells or HL60 cells ($5x10^5$ cells/ml) were treated with negatively charged AgNPs (1 µg/ml) and incubated for 4 h or 24 h.The cells were then harvested and the protein extracted for analysis by size exclusion HPLC and fractions collected very minute 300 µl of each fraction was diluted 1:10 in 2.5% nitric acid (Suprapur, Merck), containing 20 µg/L of Co and 20 µg/L of Pt as internal standards, for analysis by ICP-MS (Thermo Electron Corp., X-Series). Mass ions (55Mn, 59Co, 63Cu, 65Cu, 66Zn, 107Ag and 195Pt) were monitored (100 reads of 25ms each in 5 channels with 0.02 AMU separations) in triplicate and concentrations of the metals of interest calculated by comparison to matrix-matched mixed-element standard solutions. (see Methods, Chapter 2).

SOD1 activity assay

A negatively stained polyacrylamide gel (PAGE) was used to determine SOD1 activity. Aliquots (50µl) of copper-containing fractions of eluants from the HPLC size exclusion chromatograpy of soluble lysates from Jurkat and HL60 were resolved by negatively PAGE and stained for SOD1 activity with tetramethylbenzidine (TMBZ)/riboflavin. (see Methods, Chapter 2).

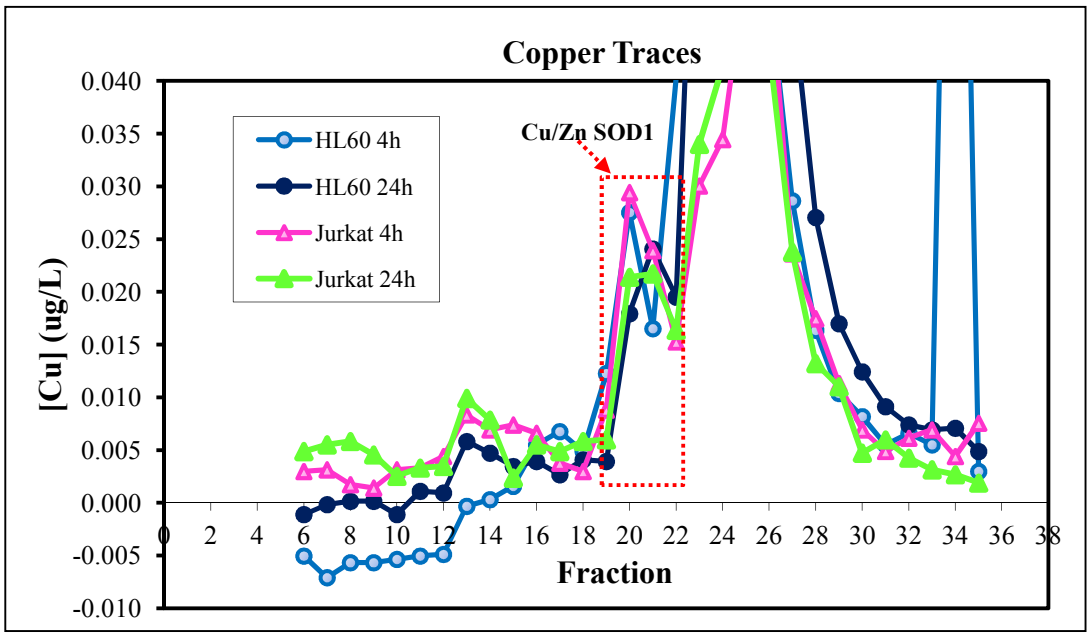

Figure 5.14 Size exclusion chromatography of HL60 and Jurkat cells exposed to negatively charged AgNPs (1µg/ml) for 4h or 24 h. SOD-1 (detected by activity PAGE) eluted in fractions 19-22. A peak in copper concentration was associated with fractions 19-22 indicating the Cu/Zn-SOD1.

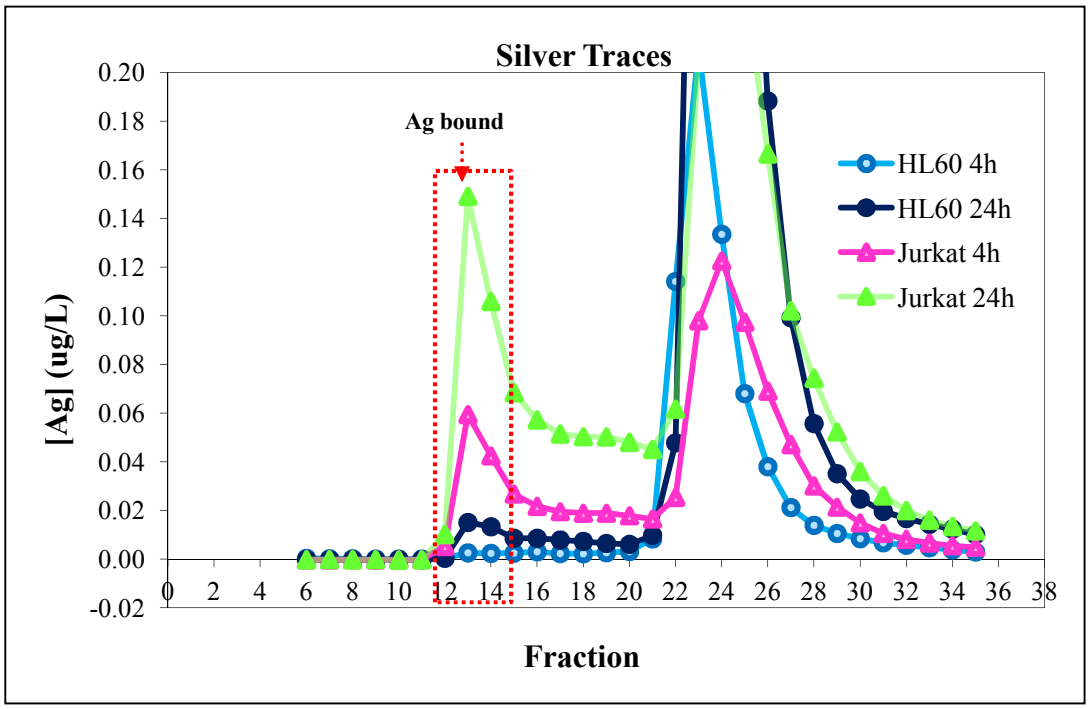

Figure 5.15 Size exclusion chromatography of HL60 and Jurkat cells exposed to negatively charged AgNPs (1µg/ml) for 4h or 24 h. A peak of silver was associated with fractions 12-15 showing the appearance of bound silver and no peak at (fraction 19-22) for Jurkat but not HL60 cells.

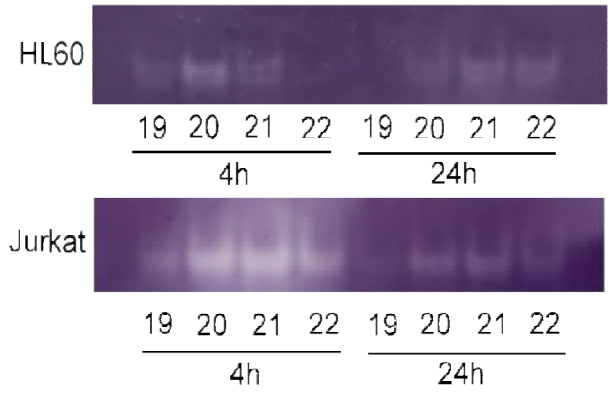

Figure 5.16 A negatively stained PAGE gel showing SOD1 activity. The lanes represent fractions 19-22 collected from the size exclusion HPLC at 4 and 24 hours. The activity gel shows decreased SOD1 activity associated with Cu eluted in fractions 19-22 for Jurkats at 24h compared to activity at 4h. For HL60s, activity was similar at 4h and 24h and similar to the level for Jurkats at 24h.

Table 5.3 The amount of copper as an indicator the level of the changes in the Cu/Zn-SOD1in fraction 19-22 of HL60 and Jurkat cells exposed to negatively charged AgNPs (1µg/ml) for 4h or 24 h from size exclusion chromatography. The data are the mean (n=3). Comparing between cell types and time (ANOVA).

Cell type	**Mean of concentration of copper (µg/L)**		**P value**
	4h	**24h**	
HL60	0.0703	0.0536	n.s
Jurkat	0.0654	0.0543	n.s
P value	n.s	n.s	

Results of studies of Inhibition of soluble superoxide dismutase (SOD1) function by AgNPs

- The size exclusion chromatography experiments showed that the level of Cu that assosicate with SOD1 was reduced in both Jurkats and HL60 following dosing with negatively charged AgNPs for 24 h compared to 4h (Figure 5.14; table 5.3).

- For Jurkats, the appearance of silver assosicate with Zn (fraction 12-15) in parallel with decreased Cu/Zn SOD1 activity suggested that the copper moiety of SOD1 had been displaced by silver (Figure 5.15).
- For HL60s, although SOD1 activity was decreased by silver at both time points, (Figure 5.16) this did not result in the appearance of an Ag+Zn containing protein in fractions 12-15, perhaps suggesting inhibition of SOD1 by a mechanism other than displacement of copper (Figure 5.15).
- For HL60s, SOD1 levels at 4h and 24h post dose were similar to level in Jurkats at 24h (Figure 5.16; table 5.3).

5.4 Discussion

In this section, a novel dialysis method was developed to determine release of Ag^+ ions from the AgNPs. It was envisaged that this experiment would allow an estimation of the amount of toxic Ag^+ ions available to the cells from the AgNPs. As discussed in chapter 4.6, it was expected that Ag^+ ions would easily enter the cells via transition pores although the experiments in this section did not take the research far enough to clarify whether the AgNPs themselves were uptaken by the cells. Focusing on a dose of negatively charged AgNPs (1 μg/ml) for 24h, it was shown in the dialysis experiments that Jurkats and HL60s were exposed to similar amounts of Ag^+ ions. The concentration of Ag^+ ions available to cells from the AgNPs (1μg/ml) at 24 h was about 3 μg/L (i.e. 0.03 μM), compared to 6 μM from $AgNO_3$ (1μg/ml). Therefore, the cells were exposed to about 200 fold more Ag^+ ions from 1μg/ml of $AgNO_3$ compared to 1μg/ml of AgNPs.

The experiments in chapter 5 also measured transcriptional changes in oxidative stress markers from exposure to 1μg/ml $AgNO_3$ (6μM Ag^+ ions) or 1μg/ml AgNPs (0.03 μM Ag^+ ions) at 24 h. It is intriguing that Jurkats showed more evidence of oxidative stress compared to HL60s from the AgNPs, given that 0.03 μM Ag^+ ions was available to both cell types. Indeed, two important oxidative stress genes, glutathione peroxidase 4 and superoxide dismutase 2, were highly upregulated in Jurkats in response to both $AgNO_3$ and AgNPs. For HL60s, the copper chaperone for SOD1(CCS) and SOD1 itself were highly down regulated by $AgNO_3$, but not AgNPs. Epoxide hydrolase and glutathione peroxidase (GPx) were moderately upregulated in HL60s in response to oxidative stress by $AgNO_3$ and AgNPs.

Oxidative stress is a state of redox disequilibrium in which ROS production overwhelms the antioxidant defense capacity of the cell, thereby leading to adverse biological consequences. One of the major events in a cell undergoing oxidative stress is a reduction in reduced glutathione (GSH) levels, which becomes oxidized to glutathione disulfide (GSSG). This event triggers cellular responses which, at least initially and at relatively low doses of the toxin, will serve to protect the cell (Xia et al, 2006). In Jurkats, GPx and mitochondrial superoxide dismutase (Mn-SOD2), were highly up regulated in response to oxidative stress from both $AgNO_3$ and the AgNPs. If transcriptional upregulation resulted in an increase in expression of GPx and SOD2, the

effect would be to limit the extent of, for example, oxidative DNA damage to the cell. However, the effect of upregulation of the two oxidative stress defense enzymes, GPx and SOD2, on reducing oxidative stress would have been greatly counteracted by the functional inhibition seen of the highly abundant soluble Cu/Zn-SOD1. The size exclusion chromatography study indicated that silver displaced the copper on SOD1 in Jurkats, which would inhibit the enzyme (Waldron et al, 2009). At higher levels of exposure to Ag^+ ions, the oxidative stress defense mechanisms would become overwhelmed, leading to cytotoxicity, oxidative damage to DNA and release of pro-apoptotic factors with removal of Jurkats from the system, as described in Chapter 4, and reported by others (e.g. Cha et al, 2008)

The data are much more difficult to interpret for HL60s, a human macrophage cell line. In contrast to Jurkats (a T-lymphocyte cell line), exposure of HL60s to the AgNPs did not elicit a high degree of upregulation of the oxidative stress markers (although there was moderate upregulation of epoxide hydrolase and GPx). Of importance, both the copper chaperone for SOD1 (CCS) and SOD1 itself were very highly downregulated in HL60s by $AgNO_3$, but not by the AgNPs. It is noteworthy that SOD1 obtains its copper co-factor via the metallo-chaperone CCS, which delivers it by specifically docking into the SOD1 active site (Rae et al, 1999). It seems possible that Ag+ ions were able to inhibit CCS, perhaps by binding to cysteines present at the metal binding site (Eissea et al, 2000), thereby inhibiting SOD1. This hypothesis requires further study, but it is corroborated here by preliminary evidence of functional inhibition of SOD1 by Ag^+ions in HL60s, even at early time points, and without an increase in the Ag/Zn-SOD1 protein.

In Chapter 6, TEM imaging of Jurkats and HL60s was carried out following exposure to AgNPs to investigate their localization within the cells.

CHAPTER 6

UPTAKE OF SILVER NANOPARTICLES INTO CELLS IN CULTURE

Chapter 6. Uptake of silver nanoparticles into cells in culture

6.1 Uptake of AgNPs into cells in culture

The data presented in the previous chapters show that, depending on the concentration and time of exposure, $AgNO_3$ and AgNPs can cause cytotoxicity, DNA damage and oxidative stress to human cells in culture. The dialysis experiments had indicated the amount of toxic Ag+ ions released from the AgNPs which were available to the cells. In this chapter, TEM was used to image localisation of the AgNPs within the cells, with elemental confirmation by EDX that the purported AgNPs actually contained silver.

Jurkat and HL60 cells ($5x10^5$ cells/ml) were exposed to $AgNO_3$, positively charged AgNPs or negatively charged AgNPs (1 µg/ml, 10 µg/ml or 50 µg/ml) for up to 24h when the cells were harvested and prepared for imaging by TEM and elemental analysis by EDX (see Methods, Chapter 2).

Uptake of positively charged AgNPs by HL60 cells

HL60 cells were exposed to positively charged AgNPs or $AgNO_3$ (1 μg/ml) for 24h in order to indicate localisation of the NPs within the cell by TEM with confirmation by EDX. In this study the cells were fixed using glutaraldehyde in sodium cacodylate buffer and secondary fixing using osmium tetroxides followed by staining with uranyl acetate and lead citrate (see Methods, Chapter 2)

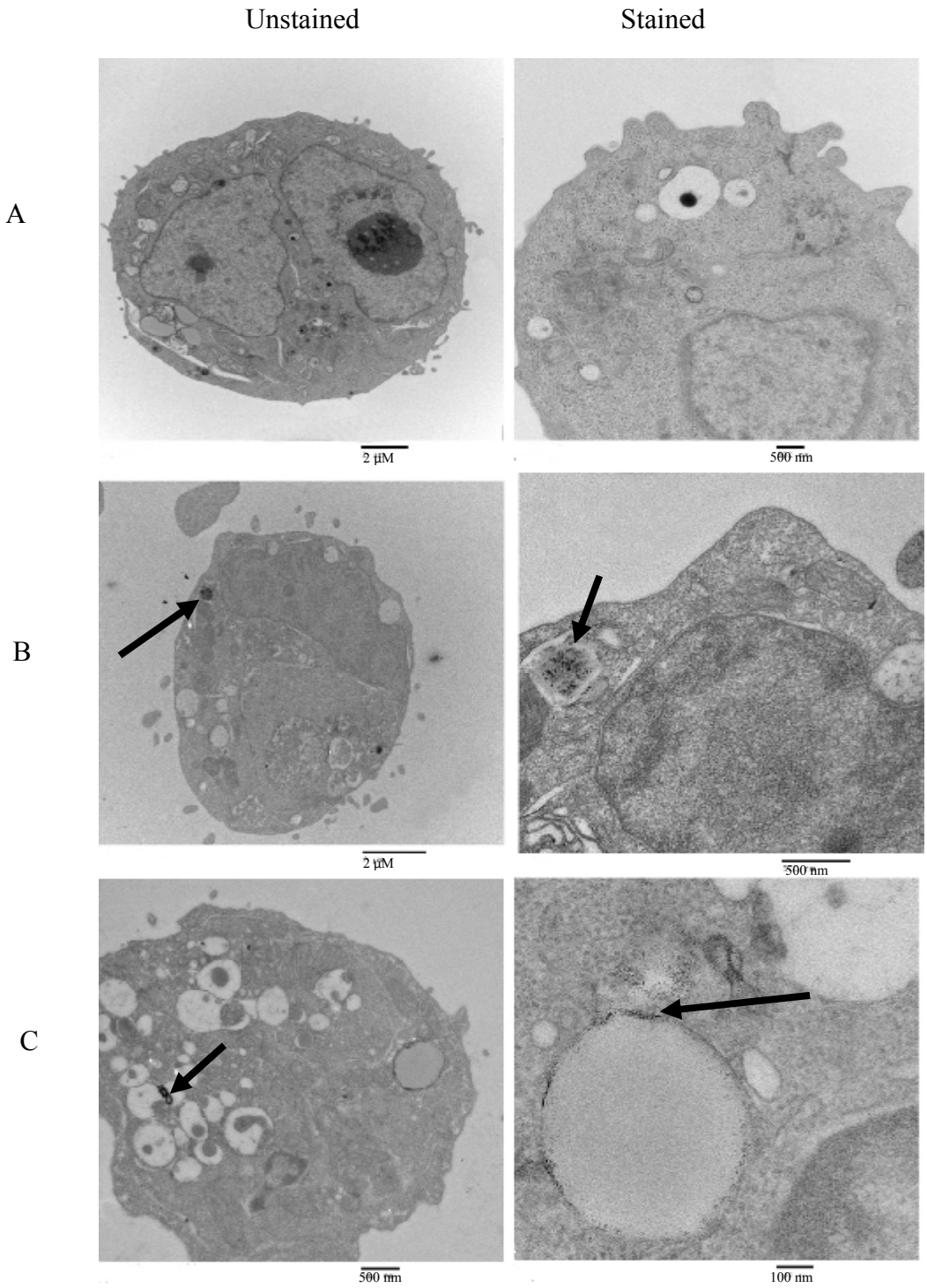

Figure 6.1 TEM images of HL60 cells exposed to A) control; B) positively charged AgNPs (1 µg/ml), 24h; C) $AgNO_3$ (1 µg/ml), 24h. The arrow in B shows the purported AgNPs and in C localisation of silver protein bind to cellular protein.

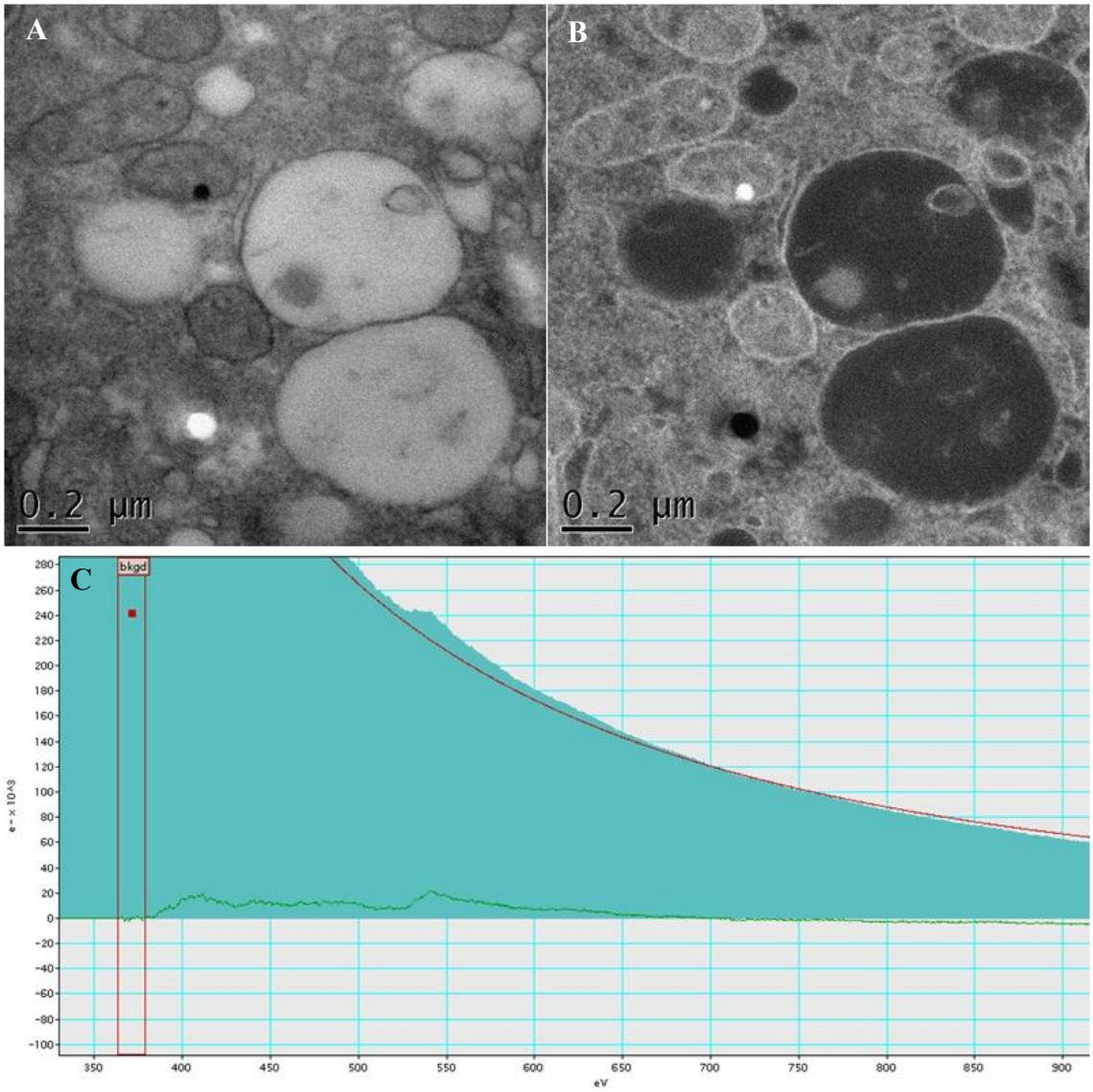

Figure 6.2 A TEM image of HL60 cells treated with $AgNO_3$ (1µg/ml) for 24 h. Bright field image (A); dark field image (B); analysis spectrum by electron energy loss spectroscopy (EELS) (C).

Summary of results of studies of uptake of positively charged AgNPs by HL60 cells

- The morphological appearances of HL60 cells exposed to positively charged AgNPs or $AgNO_3$ were similar to control (Figure 6.1).
- Although the TEM images suggested the presence of NPs within the cell (Fig 6.1 B, C), analysis of the purported AgNPs by EDX did not detect silver.

Uptake of negatively charged AgNPs by HL60 and Jurkat cells

Here, HL60 and Jurkat cells were exposed to negatively charged AgNPs (1 µg/ml or 10 µg/ml) for 10, 30 min or 24h and prepared for TEM followed by elemental analysis by EDX. In contrast to the previous experiment, the cells were fixed with glutaradehyde in sodium cacodylate buffer alone, since the osmium seemed to be producing artefacts that resembled NPs within the cells.

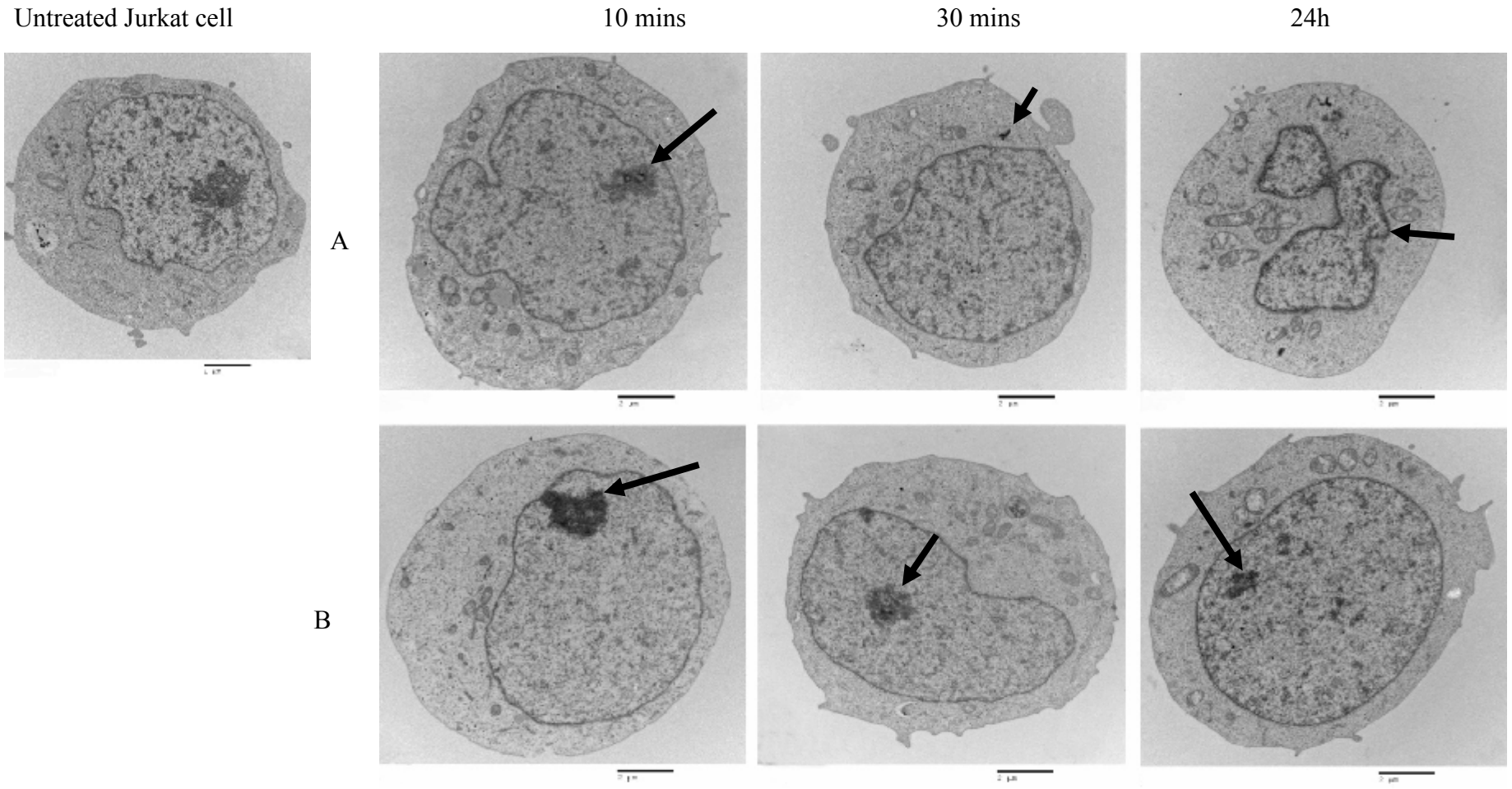

Figure 6.3 TEM images of Jurkat cells exposed to (A) negatively charged AgNPs (1 µg/ml), (B) negatively charged AgNPs (10 µg/ml). The scale bar represents 2 µm. The arrows show the purported AgNPs.

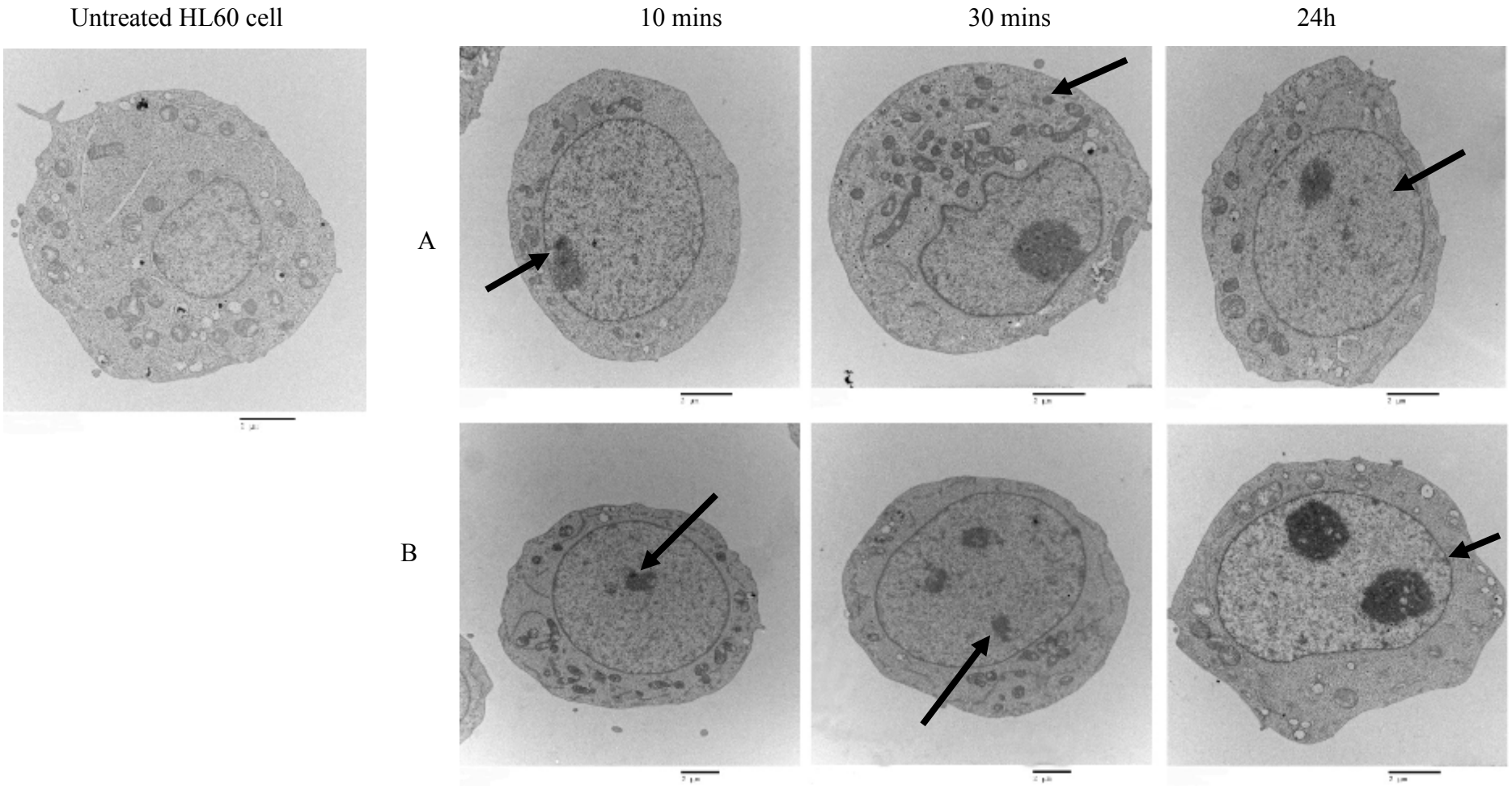

Figure 6.4 TEM images of HL60 cells exposed to (A) negatively charged AgNPs (1 µg/ml), (B) negatively charged AgNPs (10 µg/ml). The scale bar represents 2 µm. The arrows show the purported AgNP.

Summary of results of studies of uptake of negatively charged AgNPs by HL60 and Jurkat cells

- As for exposure to positively charged AgNPs, exposure of Jurkats and HL60s to negatively charged AgNPs did not cause morphological changes to the cells.
- Although the osmium had been removed from the fixing solution, it remained difficult to distinguish between staining artefacts and NPs.

Uptake of negatively charged AgNPs(50 µg/ml, 10 min) by Jurkat cells for 10 mins.

The aim of this experiment was to investigate further whether AgNPs were up taken by cells in culture. In this experiment, Jurkats were exposed to a much higher concentration of negatively charged AgNPs (50 µg/ml) for 10 min (see Methods, Chapter 2). Again, the cells were prepared for imaging by TEM using glutaraldehyde solution without osmium with confirmation of the presence of silver by EDX.

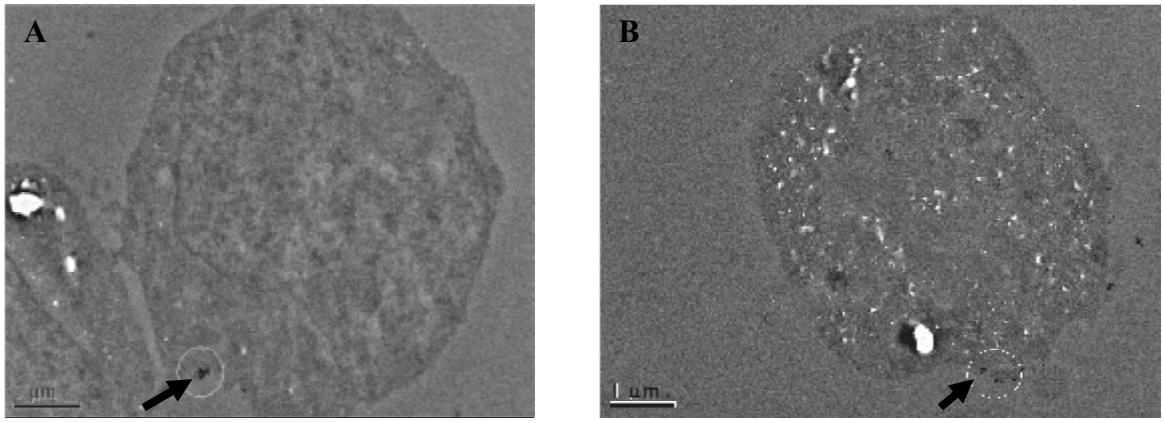

Figure 6.5 TEM images of Jurkat cells exposed to negatively charged AgNPs (50 µg/ml) for 10 min (A and B). The AgNPs appeared to be clustered at the cell membrane (denoted by the circle).

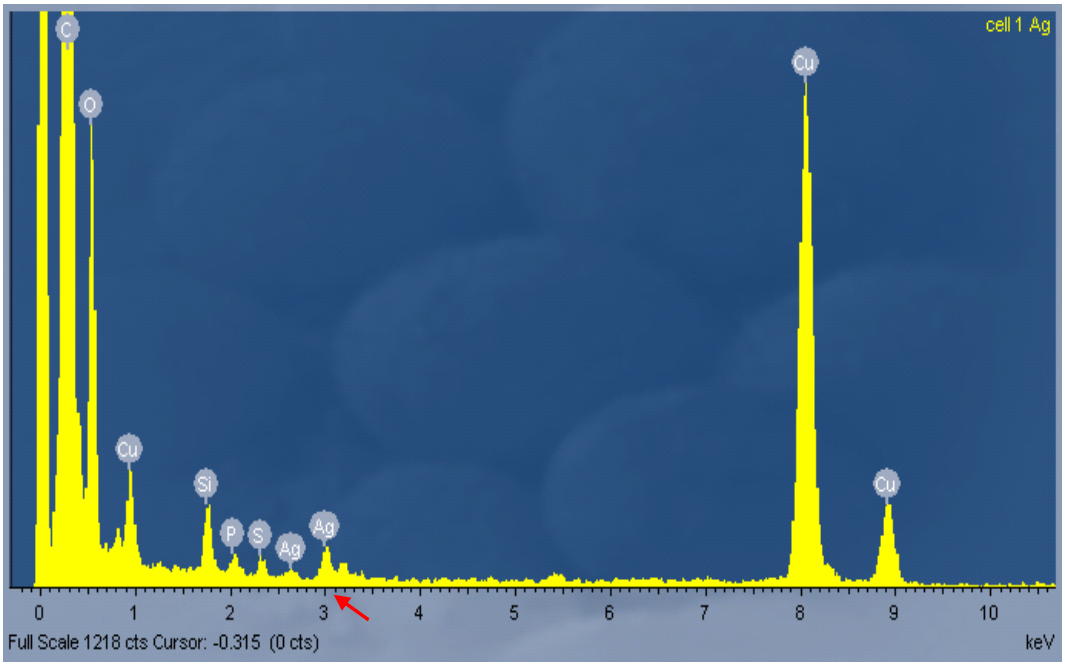

Figure 6.6 An EDX spectrum of Jurkats showing that silver was detected in the cluster of dots within the circle (Figure 6.5). This confirmed that silver was present at the cell membrane.

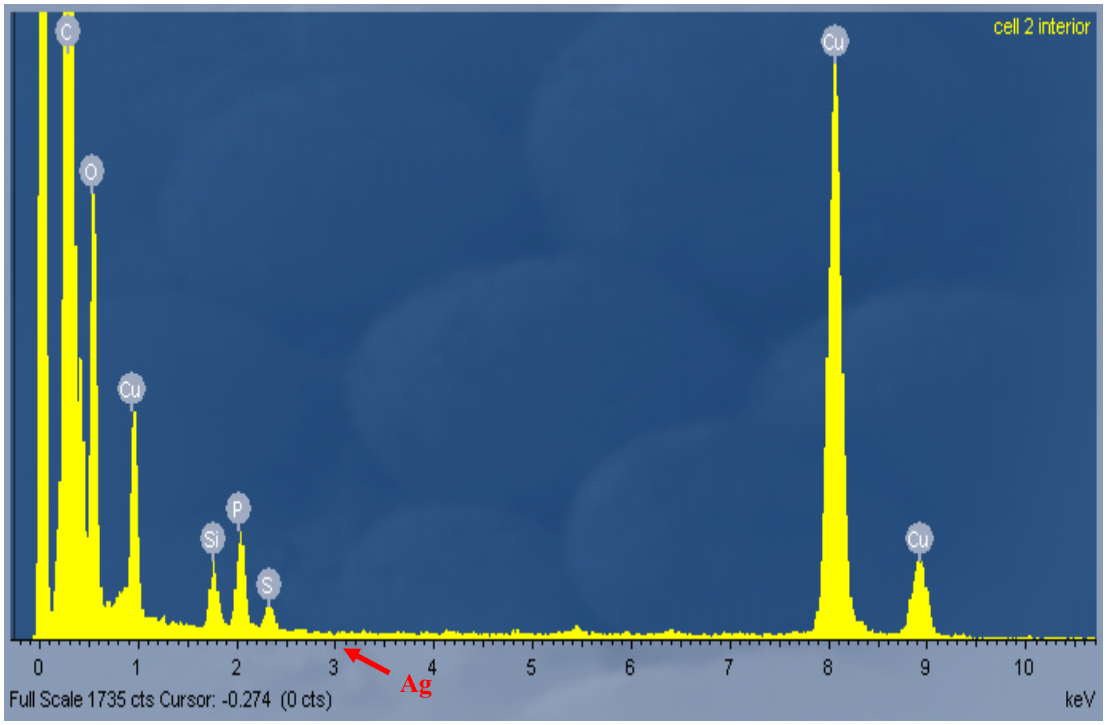

Figure 6.7 A typical EDX spectrum of the intracellular regions Jurkat cells, showing that silver was not detected within the cells shown in figure 6.5.

Summary or results of studies of uptake of negatively charged AgNPs(50 µg/ml, 10 min) by Jurkat cells for 10 mins

- Exposure of Jurkats to negatively charged AgNPs (50 µg/ml), 10 min did not cause morphological changes to the cell.
- The AgNPs were found bound to the cell membrane, but not within the cell.

6.2 Discussion

The aim of this part of the research was to use TEM to investigate cellular localization of AgNPs in HL60s and Jurkats after dosing with up to 50 μg/ml of the NPs for various times. TEM imaging was followed by EDX analysis to confirm that silver was actually present in the purported NPs. It was deemed important to carry out these experiments because, although many papers have now been published in the research area, it is still not known whether the toxicity of AgNPs results from cellular uptake of the NPs, or whether they are bound to the cell membrane and from there release Ag^+ ions for uptake by the cells, or whether a combination of both mechanism is important.

The experiments encountered several problems. First, the relatively low electron density of AgNPs compared to the TEM staining agents, osmium, uranyl acetate and lead citrate, as well as their small size, made it extremely difficult to detect the NPs. Later experiments refined the staining technique so that the osmium could be removed and this resulted in far fewer staining artefacts. It is of concern that several researchers have reported that AgNPs are uptaken by cells, even though osmium staining methods were used and the purported NPs did not undergo EDX elemental analysis to confirm the presence of silver (e.g. Singh et al, 2012; Asharani et al, 2009).

The EDX analysis used may also have lacked the sensitivity to detect silver when the cells were exposed to < 50 μg/ml, as silver was only detected when the concentration of AgNPs was increased. EDX confirmed that the purported AgNPs at the cell membrane of Jurkats actually contained silver. It is unfortunate that time did not permit EDX analysis of HL60s after exposure to the same high concentration of AgNPs and therefore these experiments cannot confirm whether macrophages (such as HL60s) are able to uptake AgNPs as suggested by others (Xia et al, 2006; AshaRani et al, 2009).

CHAPTER 7
GENERAL DISCUSSION

Chapter 7 General discussion

The major findings of this research have been firstly to provide the evidence that the toxicity of AgNPs to cells in culture is likely caused by released Ag^+ ions rather than the uptake of the particle. Importantly this research found using a novel dialysis experiment that Ag^+ ions released from AgNPs, that toxicity was similar to silver nitrate and there was little evidence of cellular internalization of the AgNPs.
Secondly key findings supported the initial hypothesis that cell uptake of AgNPs or Ag^+ ion appeared to differ with respect to cell type and was different for HL60 and Jurkat cells. Finally the hypothesis of altered cellular oxidative stress contributing to silver toxicity and DNA damage was supported by transciptomic studies and a novel effect of silver on SOD1 activity which differed between HL60 and Jurkat cells was described. This research improves our understanding of the mechanism of toxicity of sliver nanoparticles to cells.

This research investigated the toxicity of AgNPs compared to $AgNO_3$ in two human cell types, HL60s (immortalised macrophages) and Jurkats (immortalised T- lymphocytes). At the start of the project, it was hypothesized that HL60 cells would be able to ingest the NPs more efficiently than Jurkats, as macrophages are responsible for particle uptake from the circulation (Cho et al, 2009). It was further hypothesized that HL60s would therefore show more signs of toxicity. In many ways the hypotheses were supported by this research, although more studies are necessary to confirm the findings. To date, the literature is uncertain whether AgNPs themselves are toxic because of their tiny size, or whether they are toxic because they cause "slow release" of silver ions which will result in chronic toxicity by oxidative stress (Chen et al, 2008), or whether both mechanisms are important. Of note, this research supports that both silver ions **and** AgNPs are the source of nano-silver's toxicity.

It was deemed necessary to investigate cellular internalization of the AgNPs because of the potential for particle uptake to influence normal cell function and hence toxicity. Other influential factors in the toxicity of AgNPs are their size and whether the particles are coated with proteins such as FBS in vitro and proteins contained in blood serum in vivo. It has been reported that smaller NPs (<50 nm) are uptaken by cells more efficiently than larger ones since larger particles, which have a relatively smaller surface area to mass ratio, will have less protein adsorbed onto the particle's surface (Chithrani

et al, 2006). The researchers went on to confirm that clathrin-mediated endocytosis was the basis of uptake of AuNPs into HeLa cells, a tumour epithelial cell line. This research investigated both negatively and positively charged AgNPs, both of which had a diameter of about 10 nm, but unfortunately time did not permit investigation of the influence of particle size on toxicity.

Investigation of the mechanisms of cellular uptake of NPs is clearly a very important, but highly complex area of research, which is still in its infancy. This research has supported sparce evidence in the literature (Rothen-Rutishause, 2006; Chithrani and Chan, 2007) that both the charge on the NP and protein adsorption to the surface of the NP drives uptake of AgNPs and that these factors are further influenced by the type of cell being investigated, e.g. macrophages compared to T-lymphocyte cells. During this research project, extensive studies of DNA damage by AgNPs consistently showed that HL60s had more damage than Jurkats, which is in keeping with the macrophage nature of these cells, and this was particularly true for the negatively charged particles. Suresh et al (2010) highlighted the importance of charge on AgNPs in relation to toxicity and reported that negatively charged ones are more toxic because they can bind more efficiently to plasma proteins. It is a valid criticism of this research that EDX analysis to show uptake of AgNPs or Ag^+ ions was not carried out on HL60s following exposure to the higher concentrations of AgNPs. These studies woud determine whether AgNPs were internalized by HL60s for comparison with studies that showed that Jurkats did not internalize the AgNPs, which appeared to be bound to the cell membrane. Internalisation of Ag^+ ions released from the NPs at the cell membrane would likely occur by passive diffusion in Jurkats, leading to toxic effects. However, this could not be confirmed here since EDX analysis cannot detect metal ions or even ions bound to protein.

In argument against HL60s being able to internalize the AgNPs, 1 µg/ml of $AgNO_3$ (6 µM Ag^+ ions), but not the AgNPs at 1 µg/ml (0.03 µM Ag^+ ions) caused both the copper chaperone for SOD1 (CCS) and SOD1 itself to be highly transcriptionally down-regulated. It is entirely possible that CCS and SOD1 would have been down-regulated by less than 6 µM of Ag^+ ions from $AgNO_3$, but this was not investigated in these studies. Later experiments showed a functional decrease in SOD1 activity in HL60s, as well as Jurkats, that were exposed to the lower concentration of AgNPs (0.03 µM Ag^+ ions). Determination of decreased SOD1 at a functional level by low Ag^+ ion

concentrations is an important highlight of this research, since the consequence of this, should it occur *in vivo*, would be increased oxidative stress within the cell. The wide variety of uses of silver today allows human exposure through various routes of entry into the body and it has been estimated that dietary intake of silver is currently about 70-90 μg/day (0.65-0.85 μmol/day) (Drake and Hazelwood, 2005). Of importance for valid risk assessment of nano-Ag, it is likely that exposure is on the increase, given the ever increasing number of products on the market that contain AgNPs (The Woodrow Wilson database for consumer products containing nano-Ag, http://www. nanotechproject.org/ inventories/silver/). Although only a small proportion of nano-Ag entering the body will be bioavailable, recent studies have indicated that AgNPs can accumulate in vital tissues, such as the liver and brain (Kim et al, 2008).
In contrast to HL60s, Jurkats exhibited typical signs of oxidative stress from both $AgNO_3$ and AgNPs. Indeed, Jurkats were much more sensitive than HL60s to loss of cell viability and increased oxidative DNA damage induced by H_2O_2, a model chemical for oxidative toxicity. Glutathione peroxidase (GPx) and SOD2 were highly up-regulated in Jurkats by $AgNO_3$ (6 μM Ag^+ ions), which was not evident in HL60s, although the AgNPs caused less effect on oxidative stress status and DNA damage in Jurkats compared to HL60s. These data should be taken to support the imaging studies, which showed that AgNPs were not internalized by Jurkats.

Another novel finding of this research is that, although SOD1 activity was inhibited in both HL60s and Jurkats, the mechanism underlying this appeared to differ with respect to cell type. As discussed earlier, the size exclusion chromatography experiment showed that SOD1 activity was inhibited in HL60s by a mechanism that did not involve displacement of copper by silver on the Cu/Zn-SOD1 protein. It is possible that AgNPs (or Ag^+ ions) inhibited the copper chaperone for SOD1 (CCS) in HL60s by binding of silver to thiols at the active site of the enzyme, hence preventing delivery of copper to SOD1 and thereby inhibiting its function, as suggested by Lamb et al (2001) (Figure 7.1) and supported here by both the qPCR and size exclusion experiments. In Jurkats, the size exclusion experiment supported inhibition of SOD1 following displacement of copper by silver on the enzyme. Of interest, a proposed mechanism for the bactericidal function of silver is its ability to displace copper on Cu/Zn-ATPase, which effectively shuts down production of ATP causing cell death (Waldron et al, 2009).

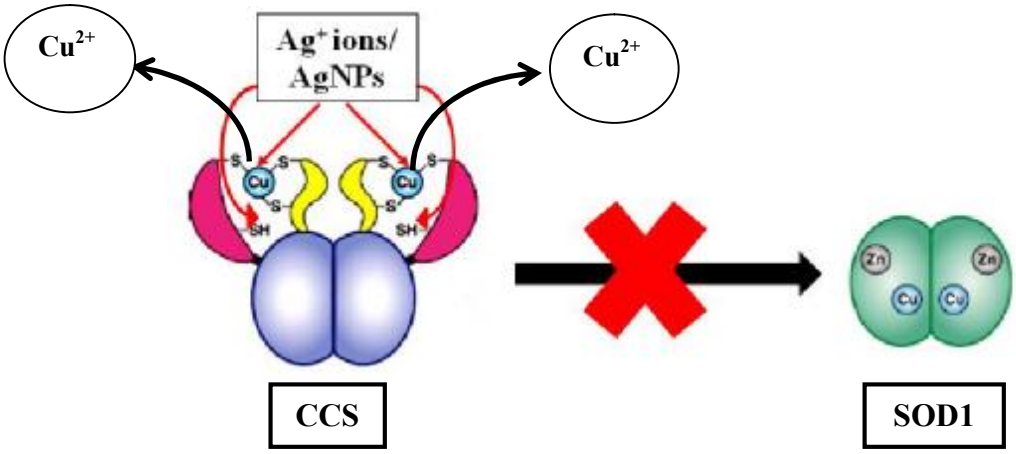

Figure 7.1 Proposed inhibition of the copper chaperone for SOD1 (CCS) by silver in HL60s, so that copper can no longer be taken to SOD1 (adaped from Lamb et al, 2000).

This research suggests that HL60s, but not Jurkats, do internalize AgNPs. It is not unreasonable to suggest that HL60s can ingest AgNPs, since this is one of the endogenous roles of macrophages, and the consequence of this could be an inflammatory response, which is of concern and worthy of consideration in future studies. Such studies should include measurement of increased production of tumour necrosis factor alpha (TNFα), interleukin 1β (IL-1β) and the macrophage inflammatory protein 2 (MIR-2) in HL60s compared to Jurkats following exposure to AgNPs. Of interests, an inflammatory response was seen in lung macrophage cells (NR8383) exposed to AgNPs for 24h after oxidative defense enzymes failed to adequately control escalating production of ROS (Carlson et al, 2008), which reflects the scenario described here for HL60s.

The data presented in this thesis, in context with the recent literature, raises concern that AgNPs may be toxic to man by way of oxidative stress mechanisms, and could lead to pro-mutagenic lesions in DNA. This research also provides evidence that macrophages respond differently to AgNPs compared to T-lymphocytes (Figure 7.2 and 7.3). In contrast to lymphocytes, macrophages may be able to internalize AgNPs, potentially leading to a long lived increase in oxidative stress, which may cause chronic toxicities, including an inflammatory response.

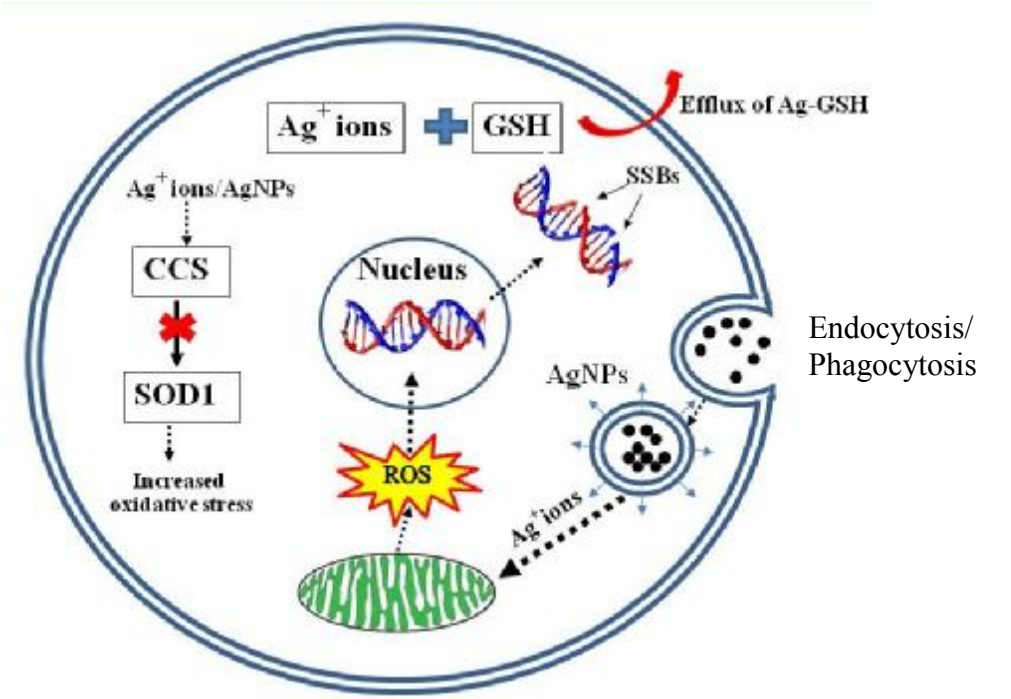

Figure 7.2 A theoretical representation of the toxicity of AgNPs to HL60 cells.

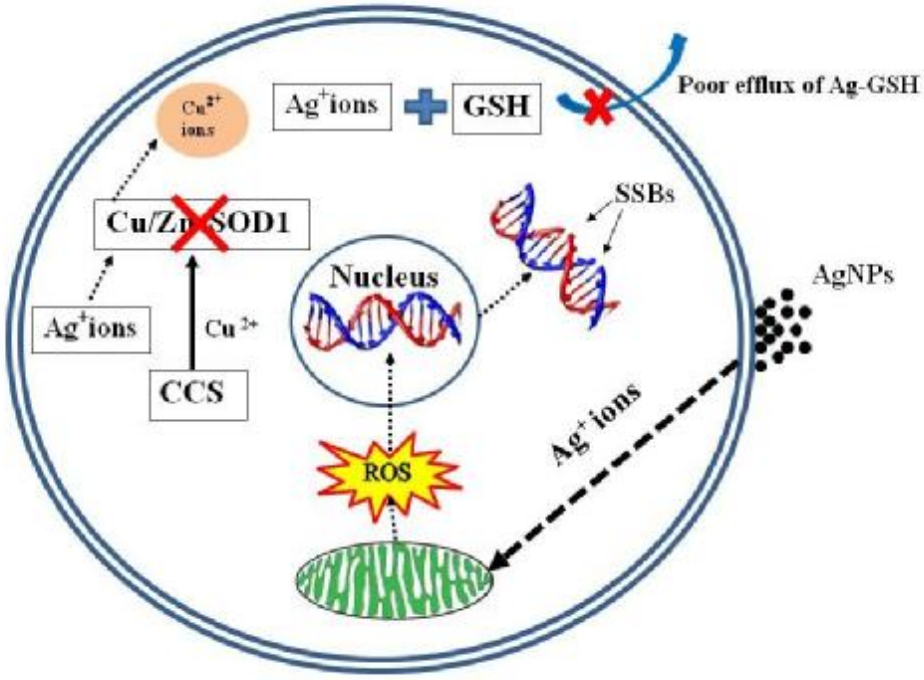

Figure 7.3 A theoretical representation of the toxicity of AgNPs to Jurkat cells.

The results from this research showed a key question to address is if the hazard of the silver nanoparticles can be assessed in the same way as bulk silver which has been considered a nonhazardous element. Generally, the information required for risk assessment is information on the intrinsic hazard of the substance and information on environmental exposure and exposure to human health. The methodology to assess the risks of exposure to nanomaterials needs to be standardised. Currently, The EU Scientific Committee on Emerging and Newly Identified Health Risks (SCENIHR, 2007) stated that the current methodologies used to assess general chemicals are generally likely to be able to identify the hazards associated with the use of nanomaterials, but that modifications are required for the guidance on the assessment of risks. Further detailed in SCENIHR (2009) addressed the main limitations of data contained in high quality exposure and dosimetry documents. This studies focused only on hazard assessment of AgNPs and the results showed AgNPs caused a low level of DNA damage. However, in term of risk assessment of AgNPs still need further study particular in part of exposure assessment. Due to occupational exposure to AgNPs can happen during manufacture and the possibility exist for exposure to products containing AgNPs. The main products posing this possibility are AgNPs contained in foods, consumer products and medical products. The Woodrow Wilson Project on Emerging Nanotechnology reports at least 337 consumer products containing nano-silver on its internet site (Appendix C). The concentration of nano-silver varies between <6 and 10,000 ppm in consumer products; dietary supplements, cosmetics and wound dressings (http://www.nanotechproject.org/inventories/silver/). For the majority of products containing AgNPs on the market, details are not provided about the NP nor are they labeled as products containing AgNPs. Consequently, consumers do not have the opportunity to choose products containing NPs or whether to avoid these products. Because of products containing free NPs having direct human exposure, such as food supplements, are indicated to have high potential exposure, while products in which AgNPs are integrated into materials with indirect human exposure, for example food storage containers, are considered to have low potential exposure. High potential exposure means that there may either be a high probability of exposure, or a probability of high exposure, or both. However, this qualification of high and low potential exposure should have specific interpretation. More information is necessary to carry out valid risk assessments for AgNPs.

Future studies

This research has provided valuable insights about the uptake of AgNPs into cells and potential mechanism underlying the toxicity of these particles. It has also indicated several areas for further research which are necessary to support the data presented here:-

1. To further investigate the mechanism underlying oxidative stress by the AgNPs, which should include determination of mitochondrial function; changes in metallothionein levels and decreases in reduced glutathione.
2. To evaluated the role of inhibition of CCS as a novel mechanism for inhibition of SOD1 by silver.
3. Measurment of inflammatory response markers following dosing with AgNPs.

APPENDIX A

Table 1. The cytotoxicity of silver nitrate to HL60 cells. Cells were exposed to 1, 5 and 10 µg/ml silver nitrate or H_20_2 (positive control) for 4, 24 a d 48 hours

Exposure time	Parameter	HL60 cells				
			Concentration of silver nitrate			50 µM
		Control	1 ug/ml	5 ug/ml	10 ug/ml	H_2O_2
4h	Cell viability (% of control)	100	113.09	87.69	37.40	65.45
	SE	0.03	0.00	0.02	0.00	0.03
24h	Cell viability (% of control)	100	104.68	70.46	43.93	35.29
	SE	0.02	0.01	0.01	0.01	0.02
48h	Cell viability (% of control)	100	111.73	62.22	24.43	0.49
	SE	0.02	0.06	0.03	0.01	0.00

Table 2 The cytotoxicity of silver nitrate to Jurkat cells. Cells were exposed to 1, 5 and 10 µg/ml silver nitrate or H_20_2 (positive control) for 4, 24 and 48 hours

Exposure time	Parameter	Jurkat cells				
			Concentration of silver nitrate			
		Control	1 ug/ml	5 ug/ml	10 ug/ml	50 µM H_2O_2
4h	Cell viability (% of control)	100	68.74	46.20	45.95	61.37
	SE	0.00	0.01	0.01	0.00	0.03
24h	Cell viability (% of control)	100	54.69	42.47	42.97	34.24
	SE	0.00	0.03	0.02	0.00	0.01
48h	Cell viability (% of control)	100	49.92	29.92	29.94	0.32
	SE	0.02	0.03	0.01	0.01	0.00

Table 3 The cytotoxicity of negatively charged AgNPs to HL60 cells. Cells were exposed to 1, 5 and 10 µg/ml silver nitrate or H_20_2 (positive control) for 4, 24 and 48 hours.

Exposure time	Parameter	HL60 cells				
			Concentration of silver nitrate			50 µM H_2O_2
		Control	1 ug/ml	5 ug/ml	10 ug/ml	
4h	Cell viability (% of control)	100	101.61	110.43	104.19	67.65
	SE	0.07	0.04	0.06	0.05	0.04
24h	Cell viability (% of control)	100	96.35	107.64	111.11	26.79
	SE	0.04	0.02	0.11	0.09	0.02
48h	Cell viability (% of control)	100	94.38	99.67	89.91	0.00
	SE	0.10	0.07	0.18	0.04	0.00

Table 4 The cytotoxicity of negatively charged AgNPs to Jurkat cells. Cells were exposed to 1, 5 and 10 µg/ml silver nitrate or H_20_2 (positive control) for 4, 24 and 48 hours.

Exposure time	Parameter	Jurkat cells				
			Concentration of silver nitrate			
		Control	1 ug/ml	5 ug/ml	10 ug/ml	50 µM H_2O_2
4h	Cell viability (% of control)	100	71.30	67.42	88.83	49.47
	SE	0.10	0.34	0.35	0.11	0.04
24h	Cell viability (% of control)	100	94.29	85.03	111.35	22.58
	SE	0.09	0.06	0.40	0.08	0.04
48h	Cell viability (% of control)	100	93.58	85.38	102.11	0.00
	SE	0.15	0.07	0.42	0.07	0.00

Table 5 The cytotoxicity of positively charged AgNPs to HL60 cells. Cells were exposed to 1, 5 and 10 µg/ml silver nitrate or H_20_2 (positive control) for 4, 24 , 48 hours.

Exposure time	Parameter	HL60 cells				
			Concentration of silver nitrate			
		Control	1 ug/ml	5 ug/ml	10 ug/ml	50 µM H_2O_2
4h	Cell viability (% of control)	100	101.61	110.43	104.19	66.64
	SE	0.07	0.04	0.06	0.05	0.02
24h	Cell viability (% of control)	100	96.35	107.64	111.11	26.79
	SE	0.04	0.02	0.11	0.09	0.02
48h	Cell viability (% of control)	100	91.54	97.96	92.53	0.00
	SE	0.09	0.07	0.12	0.07	0.00

Table 6 The cytotoxicity of positively charged AgNPs to Jurkat cells. Cells were exposed to 1, 5 and 10 µg/ml silver nitrate or H_20_2 (positive control) for 4, 24 and 48 hours.

Exposure time	Parameter	Jurkat cells				
			Concentration of silver nitrate			
		Control	1 ug/ml	5 ug/ml	10 ug/ml	50 µM H_2O_2
4h	Cell viability (% of control)	100	103.45	95.96	89.71	63.80
	SE	0.12	0.07	0.34	0.37	0.09
24h	Cell viability (% of control)	100	84.02	85.50	90.19	28.74
	SE	0.04	0.08	0.34	0.40	0.06
48h	Cell viability (% of control)	100	96.63	90.42	102.15	0.00
	SE	0.20	0.03	0.38	0.45	0.00

Table 7 The cytotoxicity of silver nitrate to HL60 cells. Cells were exposed to 0.01, 0.1, 0.5 and 1 µg/ml silver nitrate for 4,24 and 48 hours.

Exposure time	Parameter	HL60 cells				
			Concentration of silver nitrate			
		Control	0.01 µg/ml	0.1 µg/ml	0.5 µg/ml	1 µg/ml
4h	Cell viability (% of control)	100.00	95.77	100.06	99.96	98.50
	SE	0.02	0.01	0.01	0.01	0.01
24h	Cell viability (% of control)	100.00	87.73	88.56	85.15	90.00
	SE	0.07	0.03	0.09	0.13	0.03
48h	Cell viability (% of control)	100.00	97.16	85.18	87.55	87.48
	SE	0.05	0.09	0.02	0.10	0.02

Table 8 The cytotoxicity of silver nitrate to Jurkat cells. Cells were exposed to 0.01, 0.1, 0.5 and 1 µg/ml silver nitrate for 4,24 and 48 hours.

Exposure time	Parameter	Jurkat cells				
			Concentration of silver nitrate			
		Control	0.01 µg/ml	0.1 µg/ml	0.5 µg/ml	1 µg/ml
4h	Cell viability (% of control)	100.00	99.64	95.99	95.41	95.62
	SE	0.04	0.02	0.03	0.02	0.07
24h	Cell viability (% of control)	100.00	101.74	102.23	100.50	98.52
	SE	0.05	0.06	0.03	0.08	0.06
48h	Cell viability (% of control)	100.00	92.18	93.49	92.38	93.28
	SE	0.09	0.07	0.07	0.09	0.08

Table 9 The cytotoxicity of negatively charged AgNPs to HL60 cells. Cells were exposed to 0.01, 0.1, 0.5 and 1 μg/ml for 4,24 and 48 hours.

Exposure time	Parameter	HL60 cells				
			Concentration of negatively charged AgNPs			
		Control	0.01 μg/ml	0.1 μg/ml	0.5 μg/ml	1 μg/ml
4h	Cell viability (% of control)	100.00	103.61	101.11	100.57	100.23
	SE	0.02	0.02	0.05	0.03	0.02
24h	Cell viability (% of control)	100.00	97.90	96.35	92.75	97.09
	SE	0.07	0.04	0.02	0.05	0.09
48h	Cell viability (% of control)	100.00	102.82	99.97	107.75	91.85
	SE	0.05	0.03	0.04	0.01	0.03

Table 10 The cytotoxicity of negatively charged AgNPs to Jurkat cells. Cells were exposed to 0.01, 0.1, 0.5 and 1 µg/ml for 4,24 and 48 hours.

Exposure time	Parameter	Jurkat cells				
			Concentration of negatively charged AgNPs			
		Control	0.01 µg/ml	0.1 µg/ml	0.5 µg/ml	1 µg/ml
4h	Cell viability (% of control)	100.00	92.44	92.44	92.58	99.26
	SE	0.04	0.07	0.07	0.03	0.12
24h	Cell viability (% of control)	100.00	97.46	96.51	98.91	94.12
	SE	0.05	0.05	0.04	0.01	0.01
48h	Cell viability (% of control)	100.00	101.42	109.06	108.96	106.70
	SE	0.09	0.16	0.13	0.10	0.25

Table 11 The cytotoxicity of positively charged AgNPs to HL60 cells. Cells were exposed to 0.01, 0.1, 0.5 and 1 µg/ml for 4,24 and 48 hours.

Exposure time	Parameter	HL60 cells				
			Concentration of positively charged AgNPs			
		Control	0.01 µg/ml	0.1 µg/ml	0.5 µg/ml	1 µg/ml
4h	Cell viability (% of control)	100.00	98.70	99.49	100.23	95.02
	SE	0.02	0.02	0.03	0.03	0.01
24h	Cell viability (% of control)	100.00	93.66	92.34	96.29	90.87
	SE	0.07	0.13	0.14	0.05	0.08
48h	Cell viability (% of control)	100.00	106.44	103.65	99.87	102.14
	SE	0.05	0.10	0.09	0.02	0.02

Table 12 The cytotoxicity of positively charged AgNPs to Jurkat cells. Cells were exposed to 0.01, 0.1, 0.5 and 1 μg/ml for 4,24 and 48 hours.

Exposure time	Parameter	Jurkat cells				
			Concentration of positively charged AgNPs			
		Control	0.01 μg/ml	0.1 μg/ml	0.5 μg/ml	1 μg/ml
4h	Cell viability (% of control)	100.00	91.70	94.31	96.88	91.45
	SE	0.04	0.08	0.04	0.03	0.08
24h	Cell viability (% of control)	100.00	93.73	92.39	95.80	97.68
	SE	0.05	0.08	0.09	0.04	0.02
48h	Cell viability (% of control)	100.00	107.37	111.04	109.25	105.69
	SE	0.09	0.09	0.08	0.08	0.10

APPENDIX B

Table 1 Gene layout of RT^2 Profiler^{TM} PCR Array Human Oxidative Stress and Antioxidant Defense plates (PAHS-065A) (SAbiosciences).

ALB A01	**ALOX12** A02	**ANGPTL7** A03	**AOX1** A04	**APOE** A05	**ATOX1** A06	**BNIP3** A07	**CAT** A08	**CCL5** A09	**CCS** A10	**CSDE1** A11	**CYBA** A12
CYGB B01	**DGKK** B02	**DHCR24** B03	**DUOX1** B04	**DUOX2** B05	**DUSP1** B06	**EPHX2** B07	**EPX** B08	**FOXM1** B09	**GLRX2** B10	**GPR156** B11	**GPX1** B12
GPX2 C01	**GPX3** C02	**GPX4** C03	**GPX5** C04	**GPX6** C05	**GPX7** C06	**GSR** C07	**GSS** C08	**GSTZ1** C09	**GTF2I** C10	**KRT1** C11	**LPO** C12
MBL2 D01	**MGST3** D02	**MPO** D03	**MPV17** D04	**MSRA** D05	**MT3** D06	**MTL5** D07	**NCF1** D08	**NCF2** D09	**NME5** D10	**NOS2** D11	**NOX5** D12
NUDT1 E01	**OXR1** E02	**OXSR1** E03	**PDLIM1** E04	**IPCEF1** E05	**PNKP** E06	**PRDX1** E07	**PRDX2** E08	**PRDX3** E09	**PRDX4** E10	**PRDX5** E11	**PRDX6** E12
PREX1 F01	**PRG3** F02	**PRNP** F03	**PTGS1** F04	**PTGS2** F05	**PXDN** F06	**PXDNL** F07	**RNF7** F08	**SCARA3** F09	**SELS** F10	**SEPP1** F11	**SFTPD** F12
SGK2 G01	**SIRT2** G02	**SOD1** G03	**SOD2** G04	**SOD3** G05	**SRXN1** G06	**STK25** G07	**TPO** G08	**TTN** G09	**TXNDC2** G10	**TXNRD1** G11	**TXNRD2** G12
B2M H01	**HPRT1** H02	**RPL13A** H03	**GAPDH** H04	**ACTB** H05	**HGDC** H06	**RTC** H07	**RTC** H08	**RTC** H09	**PPC** H10	**PPC** H11	**PPC** H12

Table 2 Gene table shows the detail of gene on the PCR array.

Position	Symbol	Description	Gene Name
A01	ALB	Albumin	DKFZp779N1935, PRO0883, PRO0903, PRO1341
A02	ALOX12	Arachidonate 12-lipoxygenase	12-LOX, 12S-LOX, LOG12
A03	ANGPTL7	Angiopoietin-like 7	AngX, CDT6, RP4-647M16.2, dJ647M16.1
A04	AOX1	Aldehyde oxidase 1	AO, AOH1
A05	APOE	Apolipoprotein E	AD2, LDLCQ5, LPG, MGC1571
A06	ATOX1	ATX1 antioxidant protein 1 homolog (yeast)	ATX1, HAH1, MGC138453, MGC138455
A07	BNIP3	BCL2/adenovirus E1B 19kDa interacting protein 3	NIP3
A08	CAT	Catalase	MGC138422, MGC138424
A09	CCL5	Chemokine (C-C motif) ligand 5	D17S136E, MGC17164, RANTES, SCYA5, SISd, TCP228
A10	CCS	Copper chaperone for superoxide dismutase	MGC138260
A11	CSDE1	Cold shock domain containing E1, RNA-binding	D1S155E, DKFZp779B0247, DKFZp779J1455, FLJ26882, RP5-1000E10.3, UNR
A12	CYBA	Cytochrome b-245, alpha polypeptide	p22-PHOX
B01	CYGB	Cytoglobin	HGB, STAP
B02	DGKK	Diacylglycerol kinase, kappa	-
B03	DHCR24	24-dehydrocholesterol reductase	DCE, KIAA0018, Nbla03646, SELADIN1, seladin-1
B04	DUOX1	Dual oxidase 1	LNOX1, MGC138840, MGC138841, NOXEF1, THOX1
B05	DUOX2	Dual oxidase 2	LNOX2, NOXEF2, P138-TOX, TDH6, THOX2
B06	DUSP1	Dual specificity phosphatase 1	CL100, HVH1, MKP-1, MKP1, PTPN10
B07	EPHX2	Epoxide hydrolase 2, cytoplasmic	CEH, SEH
B08	EPX	Eosinophil peroxidase	EPO, EPP, EPX-PEN

Table 2 (Continued)

Position	Symbol	Description	Gene Name
B09	FOXM1	Forkhead box M1	FKHL16, FOXM1B, HFH-11, HFH11, HNF-3, INS-1, MPHOSPH2, MPP-2, MPP2, PIG29, TGT3, TRIDENT
B10	GLRX2	Glutaredoxin 2	GRX2, bA101E13.1
B11	GPR156	G protein-coupled receptor 156	GABABL, MGC142261, PGR28
B12	GPX1	Glutathione peroxidase 1	GSHPX1, MGC14399, MGC88245
C01	GPX2	Glutathione peroxidase 2 (gastrointestinal)	GI-GPx, GPRP, GSHPX-GI, GSHPx-2
C02	GPX3	Glutathione peroxidase 3 (plasma)	GPx-P, GSHPx-3, GSHPx-P
C03	GPX4	Glutathione peroxidase 4 (phospholipid hydroperoxidase)	MCSP, PHGPx, snGPx, snPHGPx
C04	GPX5	Glutathione peroxidase 5 (epididymal androgen-related protein)	-
C05	GPX6	Glutathione peroxidase 6 (olfactory)	GPX5p, GPXP3, GPx-6, GSHPx-6, dJ1186N24, dJ1186N24.1
C06	GPX7	Glutathione peroxidase 7	CL683, FLJ14777, GPX6, GPx-7, GSHPx-7, NPGPx
C07	GSR	Glutathione reductase	MGC78522
C08	GSS	Glutathione synthetase	GSHS, MGC14098
C09	GSTZ1	Glutathione transferase zeta 1	GSTZ1-1, MAAI, MAI, MGC2029
C10	GTF2I	General transcription factor IIi	BAP135, BTKAP1, DIWS, FLJ38776, FLJ56355, GTFII-I, IB291, SPIN, TFII-I, WBS, WBSCR6
C11	KRT1	Keratin 1	CK1, EHK, EHK1, EPPK, K1, KRT1A, NEPPK
C12	LPO	Lactoperoxidase	MGC129990, MGC129991, SPO
D01	MBL2	Mannose-binding lectin (protein C) 2, soluble	COLEC1, HSMBPC, MBL, MBP, MBP-C, MBP1, MGC116832, MGC116833
D02	MGST3	Microsomal glutathione S-transferase 3	GST-III
D03	MPO	Myeloperoxidase	-
D04	MPV17	MpV17 mitochondrial inner membrane protein	MTDPS6, SYM1

Table 2 (Continued)

Position	Symbol	Description	Gene Name
D05	MSRA	Methionine sulfoxide reductase A	PMSR
D06	MT3	Metallothionein 3	GIF, GIFB, GRIF
D07	MTL5	Metallothionein-like 5, testis-specific (tesmin)	CXCDC2, MTLT, TESMIN
D08	NCF1	Neutrophil cytosolic factor 1	FLJ79451, NCF1A, NOXO2, SH3PXD1A, p47phox
D09	NCF2	Neutrophil cytosolic factor 2	FLJ93058, NCF-2, NOXA2, P67-PHOX, P67PHOX
D10	NME5	Non-metastatic cells 5, protein expressed in (nucleoside-diphosphate kinase)	NM23-H5, NM23H5, RSPH23
D11	NOS2	Nitric oxide synthase 2, inducible	HEP-NOS, INOS, NOS, NOS2A
D12	NOX5	NADPH oxidase, EF-hand calcium binding domain 5	MGC149776, MGC149777
E01	NUDT1	Nudix (nucleoside diphosphate linked moiety X)-type motif 1	MTH1
E02	OXR1	Oxidation resistance 1	FLJ10125, FLJ38829, FLJ40849, FLJ41673, FLJ42450, FLJ45656
E03	OXSR1	Oxidative-stress responsive 1	KIAA1101, OSR1
E04	PDLIM1	PDZ and LIM domain 1	CLIM1, CLP-36, CLP36, hCLIM1
E05	IPCEF1	Interaction protein for cytohesin exchange factors 1	KIAA0403, PIP3-E, RP3-402L9.2
E06	PNKP	Polynucleotide kinase 3'-phosphatase	EIEE10, MCSZ, PNK
E07	PRDX1	Peroxiredoxin 1	MSP23, NKEFA, PAG, PAGA, PAGB, PRX1, PRXI, TDPX2
E08	PRDX2	Peroxiredoxin 2	MGC4104, NKEFB, PRP, PRX2, PRXII, TDPX1, TPX1, TSA
E09	PRDX3	Peroxiredoxin 3	AOP-1, AOP1, MER5, MGC104387, MGC24293, PRO1748, SP-22
E10	PRDX4	Peroxiredoxin 4	AOE37-2, PRX-4
E11	PRDX5	Peroxiredoxin 5	ACR1, AOEB166, B166, MGC117264, MGC142283, MGC142285, PLP, PMP20, PRDX6, PRXV
E12	PRDX6	Peroxiredoxin 6	1-Cys, AOP2, KIAA0106, MGC46173, NSGPx, PRX, aiPLA2, p29
F01	PREX1	Phosphatidylinositol-3,4,5-trisphosphate-dependent Rac exchange factor 1	KIAA1415, P-REX1

Table 2 (Continued)

Position	Symbol	Description	Gene Name
F02	PRG3	Proteoglycan 3	MBP2, MBPH, MGC126662, MGC141971
F03	PRNP	Prion protein	ASCR, CD230, CJD, GSS, MGC26679, PRIP, PrP, PrP27-30, PrP33-35C, PrPc, prion
F04	PTGS1	Prostaglandin-endoperoxide synthase 1 (prostaglandin G/H synthase and cyclooxygenase)	COX1, COX3, PCOX1, PGG, HS, PGHS-1, PGHS1, PHS1, PTGHS
F05	PTGS2	Prostaglandin-endoperoxide synthase 2 (prostaglandin G/H synthase and cyclooxygenase)	COX-2, COX2, GRIPGHS, PGG, HS, PGHS-2, PHS-2, hCox-2
F06	PXDN	Peroxidasin homolog (Drosophila)	D2S448, D2S448E, KIAA0230, MG50, PRG2, PXN, VPO
F07	PXDNL	Peroxidasin homolog (Drosophila)-like	FLJ25471, VPO2
F08	RNF7	Ring finger protein 7	CKBBP1, ROC2, SAG
F09	SCARA3	Scavenger receptor class A, member 3	APC7, CSR, CSR1, MSLR1, MSRL1
F10	SELS	Selenoprotein S	ADO15, MGC104346, MGC2553, SBBI8, SEPS1, VIMP
F11	SEPP1	Selenoprotein P, plasma, 1	SELP, SeP
F12	SFTPD	Surfactant protein D	COLEC7, PSP-D, SFTP4, SP-D
G01	SGK2	Serum/glucocorticoid regulated kinase 2	H-SGK2, dJ138B7.2
G02	SIRT2	Sirtuin 2	FLJ35621, FLJ37491, SIR2, SIR2L, SIR2L2
G03	SOD1	Superoxide dismutase 1, soluble	ALS, ALS1, IPOA, SOD, hSod1, homodimer
G04	SOD2	Superoxide dismutase 2, mitochondrial	IPOB, MNSOD, MVCD6
G05	SOD3	Superoxide dismutase 3, extracellular	EC-SOD, MGC20077
G06	SRXN1	Sulfiredoxin 1	C20orf139, FLJ43353, Npn3, SRX1, YKL086W, dJ850E9.2
G07	STK25	Serine/threonine kinase 25	DKFZp686J1430, SOK1, YSK1
G08	TPO	Thyroid peroxidase	MSA, TDH2A, TPX
G09	TTN	Titin	CMD1G, CMH9, CMPD4, DKFZp451N061, EOMFC, FLJ26020, FLJ26409, FLJ32040, FLJ34413, FLJ39564, FLJ43066, HMERF, LGMD2J, TMD

Table 2 (Continued)

Position	Symbol	Description	Gene Name
G10	TXNDC2	Thioredoxin domain containing 2 (spermatozoa)	DKFZp434H0311, MGC35026, SPTRX, SPTRX1
G11	TXNRD1	Thioredoxin reductase 1	GRIM-12, MGC9145, TR, TR1, TRXR1, TXNR
G12	TXNRD2	Thioredoxin reductase 2	SELZ, TR, TR-BETA, TR3, TRXR2
H01	B2M	Beta-2-microglobulin	-
H02	HPRT1	Hypoxanthine phosphoribosyltransferase 1	HGPRT, HPRT
H03	RPL13A	Ribosomal protein L13a	L13A, TSTA1
H04	GAPDH	Glyceraldehyde-3-phosphate dehydrogenase	G3PD, GAPD, MGC88685
H05	ACTB	Actin, beta	PS1TP5BP1
H06	HGDC	Human Genomic DNA Contamination	HIGX1A
H07	RTC	Reverse Transcription Control	RTC
H08	RTC	Reverse Transcription Control	RTC
H09	RTC	Reverse Transcription Control	RTC
H10	PPC	Positive PCR Control	PPC
H11	PPC	Positive PCR Control	PPC
H12	PPC	Positive PCR Control	PPC

APPENDIX C

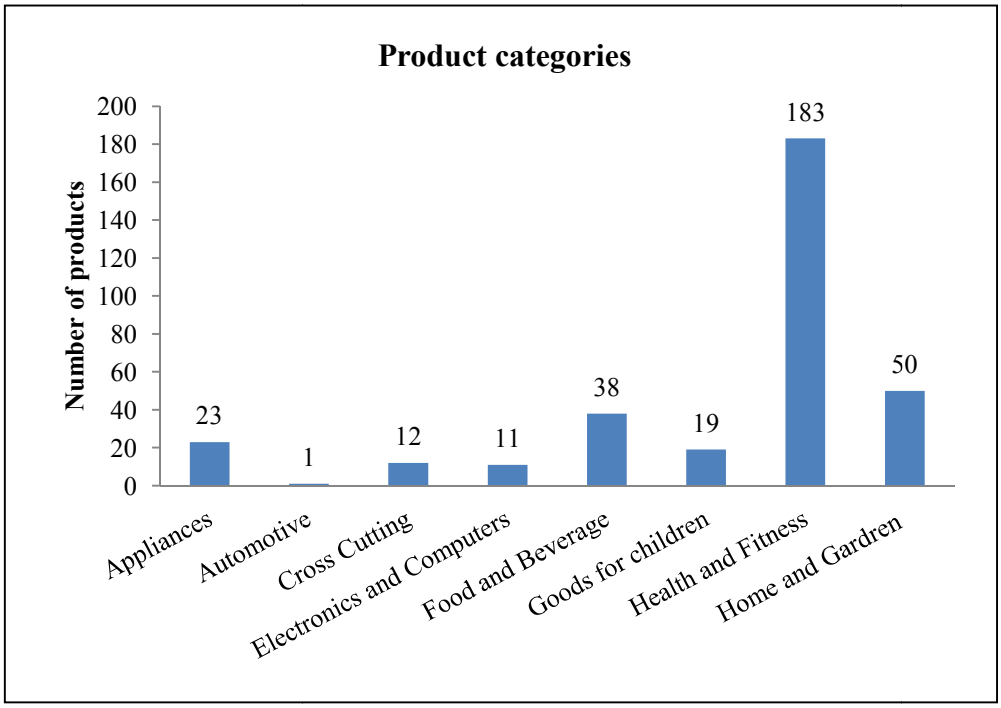

Figure 1 The database of the Nanotechnology project of the Woodrow Wilson International Centre for Scholars (www.nanotechproject.org) shows the silver used in the highest number of different products at this moment, which manufacturers claim is in 377 consumer products were found in August 2012 are in the product categories applianess (23), automotive (1), cross cutting (12), electronics and computers (11) food and beverage (38), goods for children (19), health and fitness (183) and home and gardren (50).

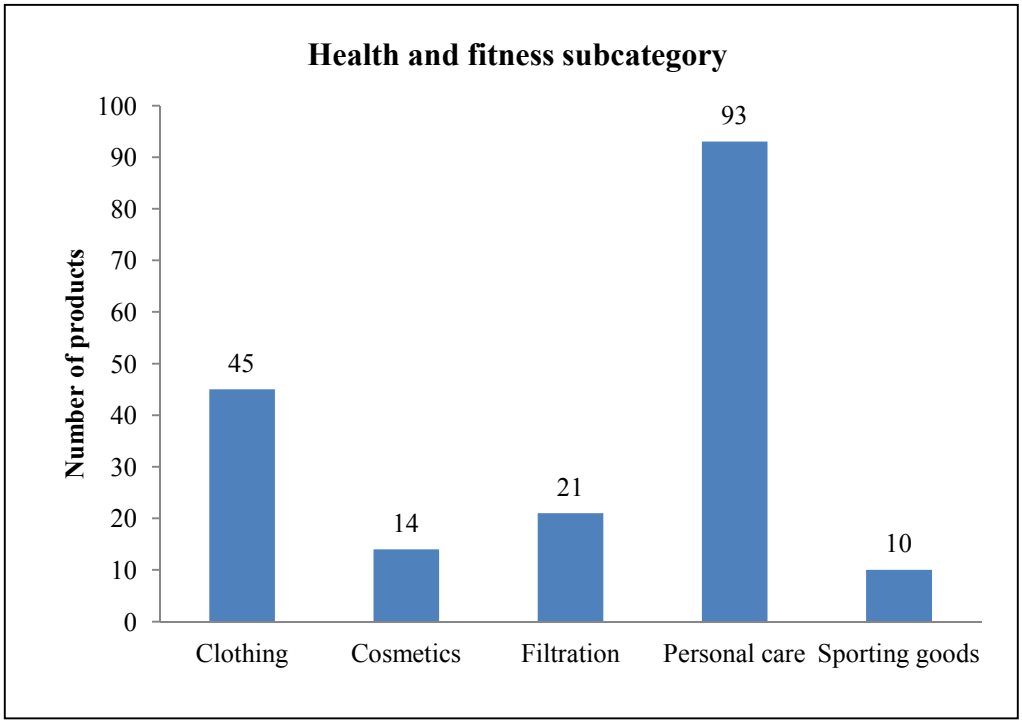

Figure 2 The detail of health and fitness subcategory that show the number of containing silver in the product of clothing (45), cosmetics (14), filtration (21), personal care (93) and sporting goods (10).The Nanotechnology project of the Woodrow Wilson International Centre for Scholars (www.nanotechproject.org).

REFERENCES

References

AHAMED, M., KARNS, M., GOODSON, M., ROWE, J., HUSSAIN, S. M., SCHLAGER, J. J. & HONG, Y. (2008) DNA damage response to different surface chemistry of silver nanoparticles in mammalian cells. *Toxicology and Applied Pharmacology,* 233**,** 404-410.

ALMOFTI, M. R., ICHIKAWA, T., YAMASHITA, K., TERADA, H. & SHINOHARA, Y. (2003) Silver ion induces a cyclosporine A-insensitive permeability transition in rat liver mitochondria and release of apoptogenic cytochrome c. *Journal of Biochemistry,* 134**,** 43-49.

ASHARANI, P. V., MUN, G. L. K., HANDE, M. P. & VALIYAVEETTIL, S. (2009) Cytotoxicity and genotoxicity of silver nanoparticles in human cells. *ACS Nano,* 3**,** 279-290.

ASZ, J., ASZ, D., MOUSHEY, R., SEIGEL, J., MALLORY, S. B. & FOGLIA, R. P. (2006) Treatment of toxic epidermal necrolysis in a pediatric patient with a nanocrystalline silver dressing. *Journal of Pediatric Surgery,* 41**,** e9-e12.

BAKER, C., PRADHAN, A., PAKSTIS, L., POCHAN, D. J. & SHAH, S. I. (2005) Synthesis and antibacterial properties of silver nanoparticles. *Journal of Nanoscience and Nanotechnology,* 5**,** 244-249.

BARROS, j., ABIE, J., BOTTERO, J. Y. AND WIESNER, M. R. (2007). Nanoparticle transport, aggregation, and deposition. *Environmental Nanotechnology*, 231-294.

BARROS, S. P. & OFFENBACHER, S. (2009) Epigenetics: Connecting environment and genotype to phenotype and disease. *Journal of Dental Research,* 88**,** 400-408.

BATARSEH, K. I. (2004) Anomaly and correlation of killing in the therapeutic properties of siliver (I) chelation with glutamic and tartaric acids. *Journal of Antimicrobial Chemotherapy,* 54**,** 546-548.

BENN, T. M. & WESTERHOFF, P. (2008) Nanoparticle silver released into water from commercially available sock fabrics. *Environmental Science and Technology,* 42**,** 4133-4139.

BENN, T., CAVANAGH, B., HRISTOVSKI, K., POSNER, J. D. & WESTERHOFF, P. (2010) The release of nanosilver from consumer products used in the home. *Journal of Environmental Quality,* 39**,** 1875-1882.

BSI Report 2007. PAS 136 Terminology for nanomaterials. http://www. bsi-global.com/en/Standards-and-Publications/Industry-Sectors/ Nanotechnologies/Nano-Downloads/.

BUZEA C., B. I., ROBBIE K. (2007). Nanomaterials and nanopartilces: Sources and toxicity. *Biointerphases* 2, MR17-MR172.

EISSES, J. F., STASSER, J. P., RALLE, M., KAPLAN, J. H. & BLACKBURN, N. J. (2000) Domains I and III of the human copper chaperone for superoxide dismutase interact via a cysteine-bridged dicopper(I) cluster. *Biochemistry,* 39**,** 7337-7342.

BLASER, S. A., SCHERINGER, M., MACLEOD, M. & HUNGERBÜHLER, K. (2008) Estimation of cumulative aquatic exposure and risk due to silver: Contribution of nano-functionalized plastics and textiles. *Science of the Total Environment,* 390**,** 396-409.

BLOKHINA, O., VIROLAINEN, E. & FAGERSTEDT, K. V. (2003) Antioxidants, oxidative damage and oxygen deprivation stress: A review. *Annals of Botany,* 91**,** 179-194.

BRAYDICH-STOLLE, L., HUSSAIN, S., SCHLAGER, J. J. & HOFMANN, M. C. (2005) In vitro cytotoxicity of nanoparticles in mammalian germline stem cells. *Toxicological Sciences,* 88**,** 412-419.

BROWN, D. M., WILSON, M. R., MACNEE, W., STONE, V. & DONALDSON, K. (2001) Size-dependent proinflammatory effects of ultrafine polystyrene particles: A role for surface area and oxidative stress in the enhanced activity of ultrafines. *Toxicology and Applied Pharmacology,* 175**,** 191-199.

BUFFLE, J., WILKINSON, K. J., STOLL, S., FILELLA, M. & ZHANG, J. (1998) A generalized description of aquatic colloidal interactions: The three- culloidal component approach. *Environmental Science and Technology,* 32**,** 2887-2899.

BURD, A., KWOK, C. H., HUNG, S. C., CHAN, H. S., GU, H., LAM, W. K. & HUANG, L. (2007) A comparative study of the cytotoxicity of silver-based dressings in monolayer cell, tissue explant, and animal models. *Wound Repair and Regeneration,* 15**,** 94-104.

CARLSON, C., HUSSEIN, S. M., SCHRAND, A. M., BRAYDICH-STOLLE, L. K., HESS, K. L., JONES, R. L. & SCHLAGER, J. J. (2008) Unique cellular interaction of silver nanoparticles: Size-dependent generation of reactive oxygen species. *Journal of Physical Chemistry B,* 112**,** 13608-13619.

CEDERVALL, T., LYNCH, I., FOY, M., BERGGAÅRD, T., DONNELLY, S. C., CAGNEY, G., LINSE, S. & DAWSON, K. A. (2007) Detailed identification of plasma proteins adsorbed on copolymer nanoparticles. *Angewandte Chemie - International Edition,* 46**,** 5754-5756.

CHA, K., HONG, H. W., CHOI, Y. G., LEE, M. J., PARK, J. H., CHAE, H. K., RYU, G. & MYUNG, H. (2008) Comparison of acute responses of mice livers to short-term exposure to nano-sized or micro-sized silver particles. *Biotechnology Letters,* 30**,** 1893-1899.

CHANG, A. L. S., KHOSRAVI, V. & EGBERT, B. (2006) A case of argyria after colloidal silver ingestion. *Journal of Cutaneous Pathology,* 33**,** 809-811.

CHEN, X. & SCHLUESENER, H. J. (2008) Nanosilver: A nanoproduct in medical application. *Toxicology Letters,* 176**,** 1-12.

CHITHRANI, B. D., GHAZANI, A. A. & CHAN, W. C. W. (2006) Determining the size and shape dependence of gold nanoparticle uptake into mammalian cells. *Nano Letters,* 6**,** 662-668.

CHITHRANI, B. D. & CHAN, W. C. W. (2007) Elucidating the mechanism of cellular uptake and removal of protein-coated gold nanoparticles of different sizes and shapes. *Nano Letters,* 7**,** 1542-1550.

CHO, W. S., CHO, M., JEONG, J., CHOI, M., CHO, H. Y., HAN, B. S., KIM, S. H., KIM, H. O., LIM, Y. T. & CHUNG, B. H. (2009) Acute toxicity and pharmacokinetics of 13㎚ nm-sized PEG-coated gold nanoparticles. *Toxicology and Applied Pharmacology,* 236**,** 16-24.

CHOI, A. O., JU, S. J., DESBARATS, J., LOVRIĆ , J. & MAYSINGER, D. (2007) Quantum dot-induced cell death involves Fas upregulation and lipid peroxidation in human neuroblastoma cells. *Journal of Nanobiotechnology,* 5.

CHURCH D, ELSAYED S, REID O, WINSTON B, LINDASY R. (2006). Burn wound infections. *Clin Microbiol Rev*, 403,434.

CULOTTA, V. C., YANG, M. & O'HALLORAN, T. V. (2006) Activation of superoxide dismutases: Putting the metal to the pedal. *Biochimica et Biophysica Acta - Molecular Cell Research,* 1763**,** 747-758.

DALLAS, P., SHARMA, V. K. & ZBORIL, R. (2011) Silver polymeric nanocomposites as advanced antimicrobial agents: Classification, synthetic paths, applications, and perspectives. *Advances in Colloid and Interface Science,* 166**,** 119-135.

DAY, B. J. (2009) Catalase and glutathione peroxidase mimics. *Biochemical Pharmacology,* 77**,** 285-296.

DEMLING, R. H. & LESLIE DESANTI, M. D. (2002) The rate of re-epithelialization across meshed skin grafts is increased with exposure to silver. *Burns,* 28**,** 264-266.

DRAKE, P. L. & HAZELWOOD, K. J. (2005) Exposure-related health effects of silver and silver compounds: A review. *Annals of Occupational Hygiene,* 49**,** 575-585.

ESTELLER, M. (2006) The necessity of a human epigenome project. *Carcinogenesis,* 27**,** 1121-1125.

EUROPEAN COMMISSION (2011) Commission recommendation of 18 October 2011 on the definition of nanomaterial.Brussels: Office for Official Publications of the European Communities.

FENG, Q. L., WU, J., CHEN, G. Q., CUI, F. Z., KIM, T. N. & KIM, J. O. (2000) A mechanistic study of the antibacterial effect of silver ions on Escherichia coli and Staphylococcus aureus. *Journal of Biomedical Materials Research,* 52**,** 662-668.

FOTAKIS, G. & TIMBRELL, J. A. (2006) In vitro cytotoxicity assays: Comparison of LDH, neutral red, MTT and protein assay in hepatoma cell lines following exposure to cadmium chloride. *Toxicology Letters,* 160**,** 171-177.

FOULKES, E. C. (2000) Transport of toxic heavy metals across cell membranes. *Proceedings of the Society for Experimental Biology and Medicine,* 223**,** 234-240.

GALLAGHER, R., COLLINS, S. & TRUJILLO, J. (1979) Characterization of the continuous, differentiating myeloid cell line (HL-60) from a patient with acute promyelocytic leukemia. *Blood,* 54**,** 713-733.

GRASSIAN, V. H., O'SHAUGHNESSY, P. T., ADAMCAKOVA-DODD, A., PETTIBONE, J. M. & THORNE, P. S. (2007) Inhalation exposure study of Titanium dioxide nanoparticles with a primary particle size of 2 to 5 nm. *Environmental Health Perspectives,* 115**,** 397-402.

GURR, J. R., WANG, A. S. S., CHEN, C. H. & JAN, K. Y. (2005) Ultrafine titanium dioxide particles in the absence of photoactivation can induce oxidative damage to human bronchial epithelial cells. *Toxicology,* 213**,** 66-73.

HAN, X., CORSON, N., WADE-MERCER, P., GELEIN, R., JIANG, J., SAHU, M., BISWAS, P., FINKELSTEIN, J. N., ELDER, A. & OBERDÖRSTER, G. (2012) Assessing the relevance of in vitro studies in nanotoxicology by examining correlations between in vitro and in vivo data. *Toxicology,* 297**,** 1-9.

HARRIS, E. D. (1992) Regulation of antioxidant enzymes. *Journal of Nutrition,* 122**,** 625-626.

HE, D., JONES, A. M., GARG, S., PHAM, A. N. & WAITE, T. D. (2011) Silver nanoparticle-reactive oxygen species interactions: Application of a charging-discharging model. *Journal of Physical Chemistry C,* 115**,** 5461-5468.

HENZLER, T. & STEUDLE, E. (2000) Transport and metabolic degradation of hydrogen peroxide in chara corallina: Model calculations and measurements with the pressure probe suggest transport of h202 across water channels. *Journal of Experimental Botany,* 51**,** 2053-2066.

HSIN, Y. H., CHEN, C. F., HUANG, S., SHIH, T. S., LAI, P. S. & CHUEH, P. J. (2008) The apoptotic effect of nanosilver is mediated by a ROS- and JNK-dependent mechanism involving the mitochondrial pathway in NIH3T3 cells. *Toxicology Letters,* 179**,** 130-139.

HUSSAIN, S. M., HESS, K. L., GEARHART, J. M., GEISS, K. T. & SCHLAGER, J. J. (2005) In vitro toxicity of nanoparticles in BRL 3A rat liver cells. *Toxicology in Vitro,* 19**,** 975-983.

HUSSAIN, S. M., JAVORINA, A. K., SCHRAND, A. M., DUHART, H. M. H. M., ALI, S. F. & SCHLAGER, J. J. (2006) The interaction of manganese nanoparticles with PC-12 cells induces dopamine depletion. *Toxicological Sciences,* 92**,** 456-463.

JI, J. H., JUNG, J. H., KIM, S. S., YOON, J. U., PARK, J. D., CHOI, B. S., CHUNG, Y. H., KWON, I. H., JEONG, J., HAN, B. S., SHIN, J. H., SUNG, J. H., SONG, K. S. & YU, I. J. (2007) Twenty-eight-day inhalation toxicity study of silver nanoparticles in Sprague-Dawley rats. *Inhalation Toxicology,* 19**,** 857-871.

JOHNSTON, H. J., HUTCHISON, G., CHRISTENSEN, F. M., PETERS, S., HANKIN, S. & STONE, V. (2010) A review of the in vivo and in vitro toxicity of silver and gold particulates: Particle attributes and biological mechanisms responsible for the observed toxicity. *Critical Reviews in Toxicology,* 40**,** 328-346.

KARLSSON, H. L., CRONHOLM, P., GUSTAFSSON, J. & MÖLLER, L. (2008) Copper oxide nanoparticles are highly toxic: A comparison between metal oxide nanoparticles and carbon nanotubes. *Chemical Research in Toxicology,* 21**,** 1726-1732.

KIM, J., TAKAHASHI, M., SHIMIZU, T., SHIRASAWA, T., KAJITA, M., KANAYAMA, A. & MIYAMOTO, Y. (2008) Effects of a potent antioxidant, platinum nanoparticle, on the lifespan of Caenorhabditis elegans. *Mechanisms of Ageing and Development,* 129**,** 322-331.

KIM, Y. S., KIM, J. S., CHO, H. S., RHA, D. S., KIM, J. M., PARK, J. D., CHOI, B. S., LIM, R., CHANG, H. K., CHUNG, Y. H., KWON, I. H., JEONG, J., HAN, B. S. & YU, I. J. (2008) Twenty-eight-day oral toxicity, genotoxicity, and gender-related tissue distribution of silver nanoparticles in Sprague-Dawley rats. *Inhalation Toxicology,* 20**,** 575-583.

KIRCHNER, C., LIEDL, T., KUDERA, S., PELLEGRINO, T., JAVIER, A. M., GAUB, H. E., STÖLZLE, S., FERTIG, N. & PARAK, W. J. (2005) Cytotoxicity of colloidal CdSe and CdSe/ZnS nanoparticles. *Nano Letters,* 5**,** 331-338.

KUMAR, R., HOWDLE, S. & MÜNSTEDT, H. (2005) Polyamide/silver antimicrobials: Effect of filler types on the silver ion release. *Journal of Biomedical Materials Research - Part B Applied Biomaterials,* 75**,** 311-319.

LAMB, A. L., TORRES, A. S., O'HALLORAN, T. V. & ROSENZWEIG, A. C. (2001) Heterodimeric structure of superoxide dismutase in complex with its metallochaperone. *Nature Structural Biology,* 8**,** 751-755.

LANSDOWN, A. B. G., SAMPSON, B. & ROWE, A. (2001) Experimental observations in the rat on the influence of cadmium on skin wound repair. *International Journal of Experimental Pathology,* 82**,** 35-41.

LANSDOWN, A. B. G. (2006) Silver in health care: Antimicrobial effects and safety in use. *Current Problems in Dermatology.*

LARESE, F. F., D'AGOSTIN, F., CROSERA, M., ADAMI, G., RENZI, N., BOVENZI, M. & MAINA, G. (2009) Human skin penetration of silver nanoparticles through intact and damaged skin. *Toxicology,* 255**,** 33-37.

LEAPER, D. J. (2006) Silver dressings: Their role in wound management. *International Wound Journal,* 3**,** 282-294+310-311.

Lee, D. H., O'Connor, T. R. and Pfeifer, G. P. (2002). Oxidative DNA damage induced by copper and hydrogen peroxide promotes CGâ†'TT tandem mutations at methylated CpG dinucleotides in nucleotide excision repair-deficient cells. *Nucleic Acids Research* **30**, 3566-3573.

LEE, H. J., YEO, S. Y. & JEONG, S. H. (2003) Antibacterial effect of nanosized silver colloidal solution on textile fabrics. *Journal of Materials Science,* 38**,** 2199-2204.

LESLIE, E. M., HAIMEUR, A. & WAALKES, M. P. (2004) Arsenic transport by the human multidrug resistance protein 1 (MRP1/ABCC1): Evidence that a tri-glutathione conjugate is required. *Journal of Biological Chemistry,* 279**,** 32700-32708.

LESNIAK, W., BLELINSKA, A. U., SUN, K., JANCZAK, K. W., SHI, X., BAKER JR, J. R. & BALOGH, L. P. (2005) Silver/dendrimer nanocomposites as biomarkers: Fabrication, characterization, in vitro toxicity, and intracellular detection. *Nano Letters,* 5**,** 2123-2130.

LI, Z. S., SZCZYPKA, M., LU, Y. P., THIELE, D. J. & REA, P. A. (1996) The yeast cadmium factor protein (YCF1) is a vacuolar glutathione S-conjugate pump. *Journal of Biological Chemistry,* 271**,** 6509-6517.

LIMÓN-PACHECO, J. & GONSEBATT, M. E. (2009) The role of antioxidants and antioxidant-related enzymes in protective responses to environmentally induced oxidative stress. *Mutation Research - Genetic Toxicology and Environmental Mutagenesis,* 674**,** 137-147.

LIN, D. & XING, B. (2007) Phytotoxicity of nanoparticles: Inhibition of seed germination and root growth. *Environmental Pollution,* 150**,** 243-250.

LOK, C. N., HO, C. M., CHEN, R., HE, Q. Y., YU, W. Y., SUN, H., TAM, P. K. H., CHIU, J. F. & CHE, C. M. (2007) Silver nanoparticles: Partial oxidation and antibacterial activities. *Journal of Biological Inorganic Chemistry,* 12**,** 527-534.

MCAULIFFE, M. E. & PERRY, M. J. (2007) Are nanoparticles potential male reproductive toxicants? A literature review. *Nanotoxicology,* 1**,** 204-210.

HÄGGSTRÖM, M (2009) Haematopoiesis [Online]. Available at: http:// en. Wikipedia.org/wiki/Heematopoiesis#References [Accessed: 10 August 2012].

MORONES, J. R., ELECHIGUERRA, J. L., CAMACHO, A., HOLT, K., KOURI, J. B., RAMÍREZ, J. T. & YACAMAN, M. J. (2005) The bactericidal effect of silver nanoparticles. *Nanotechnology,* 16**,** 2346-2353.

MUELLER, N. C. & NOWACK, B. (2008) Exposure modeling of engineered nanoparticles in the environment. *Environmental Science and Technology,* 42**,** 4447-4453.

MURALI MOHAN, Y., LEE, K., PREMKUMAR, T. & GECKELER, K. E. (2007) Hydrogel networks as nanoreactors: A novel approach to silver nanoparticles for antibacterial applications. *Polymer,* 48**,** 158-164.

MURALI MOHAN, Y., LEE, K., PREMKUMAR, T. & GECKELER, K. E. (2007) Hydrogel networks as nanoreactors: A novel approach to silver nanoparticles for antibacterial applications. *Polymer,* 48**,** 158-164.

NAVARRO, E., BAUN, A., BEHRA, R., HARTMANN, N. B., FILSER, J., MIAO, A. J., QUIGG, A., SANTSCHI, P. H. & SIGG, L. (2008) Environmental behavior and ecotoxicity of engineered nanoparticles to algae, plants, and fungi. *Ecotoxicology,* 17**,** 372-386.

NIWA, Y., HIURA, Y., MURAYAMA, T., YOKODE, M. & IWAI, N. (2007) Nano-sized carbon black exposure exacerbates atherosclerosis in LDL-receptor knockout mice. *Circulation Journal,* 71**,** 1157-1161.

NOMIYA, K., YOSHIZAWA, A., TSUKAGOSHI, K., KASUGA, N. C., HIRAKAWA, S. & WATANABE, J. (2004) Synthesis and structural characterization of silver(I), aluminium(III) and cobalt(II) complexes with 4-isopropyltropolone (hinokitiol) showing noteworthy biological activities. Action of silver(I)-oxygen bonding complexes on the antimicrobial activities. *Journal of Inorganic Biochemistry,* 98**,** 46-60.

NOWACK, B. & BUCHELI, T. D. (2007) Occurrence, behavior and effects of nanoparticles in the environment. *Environmental Pollution,* 150**,** 5-22.

OBERDÖRSTER, G., MAYNARD, A., DONALDSON, K., CASTRANOVA, V., FITZPATRICK, J., AUSMAN, K., CARTER, J., KARN, B., KREYLING, W., LAI, D., OLIN, S., MONTEIRO-RIVIERE, N., WARHEIT, D. & YANG, H. (2005) Principles for characterizing the potential human health effects from exposure to nanomaterials: Elements of a screening strategy. *Particle and Fibre Toxicology,* 2.

OBERDÖRSTER, G., OBERDÖRSTER, E. & OBERDÖRSTER, J. (2005) Nanotoxicology: An emerging discipline evolving from studies of ultrafine particles. *Environmental Health Perspectives,* 113**,** 823-839.

OBERDÖRSTER, G., SHARP, Z., ATUDOREI, V., ELDER, A., GELEIN, R., KREYLING, W. & COX, C. (2004) Translocation of inhaled ultrafine particles to the brain. *Inhalation Toxicology,* 16**,** 437-445.

PAL, S., TAK, Y. K. & SONG, J. M. (2007) Does the antibacterial activity of silver nanoparticles depend on the shape of the nanoparticle? A study of the gram-negative bacterium Escherichia coli. *Applied and Environmental Microbiology,* 73**,** 1712-1720.

PANYALA, N. R., PEÑA-MÉNDEZ, E. M. & HAVEL, J. (2008) Silver or silver nanoparticles: A hazardous threat to the environment and human health? *Journal of Applied Biomedicine,* 6**,** 117-129.

PANÁČEK, A., KVÍTEK, L., PRUCEK, R., KOLÁŘ , M., VEČEŘOVÁ, R., PIZÚROVÁ, N., SHARMA, V. K., NEVĚČNÁ, T. & ZBOŘIL, R. (2006) Silver colloid nanoparticles: Synthesis, characterization, and their antibacterial activity. *Journal of Physical Chemistry B,* 110**,** 16248-16253.

PAPAGEORGIOU, I., BROWN, C., SCHINS, R., SINGH, S., NEWSON, R., DAVIS, S., FISHER, J., INGHAM, E. & CASE, C. P. (2007) The effect of nano- and micron-sized particles of cobalt-chromium alloy on human fibroblasts in vitro. *Biomaterials,* 28**,** 2946-2958.

PARK, E. J. & PARK, K. (2009) Oxidative stress and pro-inflammatory responses induced by silica nanoparticles in vivo and in vitro. *Toxicology Letters,* 184**,** 18-25.

PARK, E. J., YI, J., KIM, Y., CHOI, K. & PARK, K. (2010) Silver nanoparticles induce cytotoxicity by a Trojan-horse type mechanism. *Toxicology in Vitro,* 24**,** 872-878.

RAE, T. D., SCHMIDT, P. J., PUFAHL, R. A., CULOTTA, V. C. & O'HALLORAN, T. V. (1999) Undetectable intracellular free copper: The requirement of a copper chaperone for superoxide dismutase. *Science,* 284**,** 805-808.

RAI, M., YADAV, A. & GADE, A. (2009) Silver nanoparticles as a new generation of antimicrobials. *Biotechnology Advances,* 27**,** 76-83.

REJESKI, D. & LEKAS, D. (2008) Nanotechnology field observations: scouting the new industrial west. *Journal of Cleaner Production,* 16**,** 1014-1017.

ROTHEN-RUTISHAUSER, B. M., SCHÜRCH, S., HAENNI, B., KAPP, N. & GEHR, P. (2006) Interaction of fine particles and nanoparticles with red blood cells visualized with advanced microscopic techniques. *Environmental Science and Technology,* 40**,** 4353-4359.

SCANDALIOS, J. G. (2002) The rise of ROS. *Trends in Biochemical Sciences,* 27**,** 483-486.

SCIENTIFIC COMMITTEE ON EMERGING AND NEWLY IDENTIFIED HEALTH RISKS (SCENIHR), EUROPEAN COMMISSION (2006) Modified opinion on the appropriateness of existing methodologies to assess the potential risks associated with engineered and adventitious products of nanotechnologies. Available from: http://ec.europa.eu/health/ph_risk/committees/04_scenihr/docs/scenihr_o_003b.pdf

SCIENTIFIC COMMITTEE ON EMERGING AND NEWLY IDENTIFIED HEALTH RISKS (SCENIHR) (2007) Opinion on the appropriateness of the risk assessment methodology in accordance with the technical guidance documents for new and existing substances for assessing the risks of nanomaterials. Scientific Committee on Emerging and Newly Identified Health Risks. 21–22 June 2007. Accessed from the website: http://ec.europa.eu/health/ph_risk/committees/04_scenihr/docs/scenihr_o_010.pdf.

SCIENTIFIC COMMITTEE ON EMERGING AND NEWLY IDENTIFIED HEALTH RISKS (SCENIHR) (2009) Risk assessment of products of Nanotechnologies. Scientific Committee on Emerging and Newly Identified Health Risks. Opinion

adopted 19 January 2009. Accessed from the website: http://ec.europa.eu/health/ph_risk/committees/04_scenihr/docs/scenihr_o_023.pdf.

SHAHVERDI, A. R., FAKHIMI, A., SHAHVERDI, H. R. & MINAIAN, S. (2007) Synthesis and effect of silver nanoparticles on the antibacterial activity of different antibiotics against Staphylococcus aureus and Escherichia coli. *Nanomedicine: Nanotechnology, Biology, and Medicine,* 3**,** 168-171.

SHI, H., HUDSON, L. G. & LIU, K. J. (2004) Oxidative stress and apoptosis in metal ion-induced carcinogenesis. *Free Radical Biology and Medicine,* 37**,** 582-593.

SHIN, S. H., YE, M. K., KIM, H. S. & KANG, H. S. (2007) The effects of nano-silver on the proliferation and cytokine expression by peripheral blood mononuclear cells. *International Immunopharmacology,* 7**,** 1813-1818.

SKEBO, J. E., GRABINSKI, C. M., SCHRAND, A. M., SCHLAGER, J. J. & HUSSAIN, S. M. (2007) Assessment of metal nanoparticle agglomeration, uptake, and interaction using high-illuminating system. *International Journal of Toxicology,* 26**,** 135-141.

SIBBALD, R. G., BROWNE, A. C., COUTTS, P. & QUEEN, D. (2001) Screening evaluation of an ionized nanocrystalline silver dressing in chronic wound care. *Ostomy/wound management,* 47**,** 38-43.

SILVER, S. (2003) Bacterial silver resistance: Molecular biology and uses and misuses of silver compounds. *FEMS Microbiology Reviews,* 27**,** 341-353.

SINGH, N., MANSHIAN, B., JENKINS, G. J. S., GRIFFITHS, S. M., WILLIAMS, P. M., MAFFEIS, T. G. G., WRIGHT, C. J. & DOAK, S. H. (2009) NanoGenotoxicology: The DNA damaging potential of engineered nanomaterials. *Biomaterials,* 30**,** 3891-3914.

SINGH, R. P. & RAMARAO, P. (2012) Cellular uptake, intracellular trafficking and cytotoxicity of silver nanoparticles. *Toxicology Letters,* 213**,** 249-259.

SLUPPHAUG, G., KAVLI, B. & KROKAN, H. E. (2003) The interacting pathways for prevention and repair of oxidative DNA damage. *Mutation Research - Fundamental and Molecular Mechanisms of Mutagenesis,* 531**,** 231-251.

SUNG, J. H., JI, J. H., YOON, J. U., KIM, D. S., SONG, M. Y., JEONG, J., HAN, B. S., HAN, J. H., CHUNG, Y. H., KIM, J., KIM, T. S., CHANG, H. K., LEE, E. J., LEE, J. H. & YU, I. J. (2008) Lung function changes in Sprague-Dawley rats after prolonged inhalation exposure to silver nanoparticles. *Inhalation Toxicology,* 20**,** 567-574.

SURESH, A. K., PELLETIER, D. A., WANG, W., MOON, J. W., GU, B., MORTENSEN, N. P., ALLISON, D. P., JOY, D. C., PHELPS, T. J. & DOKTYCZ, M. J. (2010) Silver nanocrystallites: Biofabrication using shewanella oneidensis, and an evaluation of their comparative toxicity on gram-negative and gram-positive bacteria. *Environmental Science and Technology,* 44**,** 5210-5215.

TAKENAKA, S., KARG, E., ROTH, C., SCHULZ, H., ZIESENIS, A., HEINZMANN, U., SCHRAMEL, P. & HEYDER, J. (2001) Pulmonary and systemic distribution of inhaled ultrafine silver particles in rats. *Environmental Health Perspectives,* 109**,** 547-551.

TAYLOR, D. A. (2002) Dust in the wind. *Environmental Health Perspectives,* 110**,** A80-A87.

TREDGET, E. E., SHANKOWSKY, H. A., GROENEVELD, A. & BURRELL, R. (1998) A matched-pair, randomized study evaluating the efficacy and safety of acticoat silver-coated dressing for the treatment of burn wounds. *Journal of Burn Care and Rehabilitation,* 19**,** 531-537.

TROP, M., NOVAK, M., RODL, S., HELLBOM, B., KROELL, W. & GOESSLER, W. (2006) Silver-coated dressing acticoat caused raised liver enzymes and argyria-like symptoms in burn patient. *Journal of Trauma - Injury, Infection and Critical Care,* 60**,** 648-652.

UNFRIED, K., ALBRECHT, C., KLOTZ, L. O., VON MIKECZ, A., GRETHER-BECK, S. & SCHINS, R. P. F. (2007) Cellular responses to nanoparticles: Target structures and mechanisms. *Nanotoxicology,* 1**,** 52-71.

VAN VLIET, J., OATES, N. A. & WHITELAW, E. (2007) Epigenetic mechanisms in the context of complex diseases. *Cellular and Molecular Life Sciences,* 64**,** 1531-1538.

VIGNESHWARAN, N., KATHE, A. A., VARADARAJAN, P. V., NACHANE, R. P. & BALASUBRAMANYA, R. H. (2007) Functional finishing of cotton fabrics using silver nanoparticles. *Journal of Nanoscience and Nanotechnology,* 7**,** 1893-1897.

VLACHOU, E., CHIPP, E., SHALE, E., WILSON, Y. T., PAPINI, R. & MOIEMEN, N. S. (2007) The safety of nanocrystalline silver dressings on burns: A study of systemic silver absorption. *Burns,* 33**,** 979-985.

WADHERA, A. & FUNG, M. (2005) Systemic argyria associated with ingestion of colloidal silver. *Dermatology Online Journal,* 11.

WALDRON, K. J., RUTHERFORD, J. C., FORD, D. & ROBINSON, N. J. (2009) Metalloproteins and metal sensing. *Nature,* 460**,** 823-830.

WAN, A. T., CONYERS, R. A. J., COOMBS, C. J. & MASTERTON, J. P. (1991) Determination of silver in blood, urine, and tissues of volunteers and burn patients. *Clinical Chemistry,* 37**,** 1683-1687.

WANG, H., WICK, R. L. & XING, B. (2009) Toxicity of nanoparticulate and bulk ZnO, Al2O3 and TiO2 to the nematode Caenorhabditis elegans. *Environmental Pollution,* 157**,** 1171-1177.

WANG, J. J., SANDERSON, B. J. S. & WANG, H. (2007) Cyto- and genotoxicity of ultrafine TiO2 particles in cultured human lymphoblastoid cells. *Mutation Research - Genetic Toxicology and Environmental Mutagenesis,* 628**,** 99-106.

WARHEIT, D. B., BORM, P. J. A., HENNES, C. & LADEMANN, J. (2007) Testing strategies to establish the safety of nanomaterials: Conclusions of an ECETOC workshop. *Inhalation Toxicology,* 19**,** 631-643.

WIJNHOVEN, S. W. P., PEIJNENBURG, W. J. G. M., HERBERTS, C. A., HAGENS, W. I., OOMEN, A. G., HEUGENS, E. H. W., ROSZEK, B., BISSCHOPS, J., GOSENS, I., VAN DE MEENT, D., DEKKERS, S., DE JONG, W. H., VAN ZIJVERDEN, M., SIPS, A. J. A. M. & GEERTSMA, R. E. (2009) Nano-silver - A review of available data and knowledge gaps in human and environmental risk assessment. *Nanotoxicology,* 3**,** 109-138.

WOODROW WILSON INTERNATIONAL CENTRE FOR SCHOLARS (2007) Project on Emerging Nanotechnologies. Consumer Products Inventory of Nanotechnology Products. Accessed December 2007 from the website: http://www.nanotechproject.org/inventories/consumer/.

WRIGHT, R. O., SCHWARTZ, J., WRIGHT, R. J., BOLLATI, V., TARANTINI, L., PARK, S. K., HU, H., SPARROW, D., VOKONAS, P. & BACCARELLI, A. (2010) Biomarkers of lead exposure and DNA methylation within retrotransposons. *Environmental Health Perspectives,* 118**,** 790-795.

WU, G., FANG, Y. Z., YANG, S., LUPTON, J. R. & TURNER, N. D. (2004) Glutathione Metabolism and Its Implications for Health. *Journal of Nutrition,* 134**,** 489-492.

XIA, T., KOVOCHICH, M., BRANT, J., HOTZE, M., SEMPF, J., OBERLEY, T., SIOUTAS, C., YEH, J. I., WIESNER, M. R. & NEL, A. E. (2006) Comparison of the abilities of ambient and manufactured nanoparticles to induce cellular toxicity according to an oxidative stress paradigm. *Nano Letters,* 6**,** 1794-1807.

ZHENG, Y. G. (2009) Understanding the functions of histone modification enzymes [Online]. Avaiabe at: http:// chemistry.gsu.edu/facuty/Zheng/research.html [Accessed: 19 May 2012]